MODELLING OF GRID CONNECTED GEOGRAPHICALLY DISPERSED PV SYSTEMS FOR POWER SYSTEM STUDIES

Jayaraman Ramachandran

A thesis submitted in partial fulfilment of the requirements
of the Northumbria University
for the degree of Doctor of Philosophy

March 2005

ABSTRACT

The growth of the photovoltaic market indicates that in the near future PV electricity generation may rise to a significant power source. As the proportion of electric power generated from PV systems becomes significant, the effect of these sources on transmission and distribution networks must be considered. This research work has investigated suitable representations of the PV resource and the output power of dispersed PV systems to study the effects of large-scale deployment of PV systems on the grid operation.

The representation of solar radiation is very important since this dictates the output power of PV systems. In this work, the simple and reliable Markov Transition Matrix (MTM) method was selected to generate synthetic horizontal solar radiation data. A single MTM was developed to generate half-hour horizontal solar radiation data for different locations in the UK. Large-scale inclusion of PV systems in the UK electricity supply is expected to take the form of a large number of small, geographically dispersed building integrated PV systems. The study also developed a detailed PV cluster model to represent these dispersed PV systems.

The variation of PV output power may impact the demand and generation balance on the network requiring additional reserve generation to ensure the system security. In this work, the variation of PV output power and the impact on the reserve requirement was analysed for different penetration levels. This is also the first study to analyse the correlation of solar radiation for different locations in the UK in regard to the impact on reserve requirements. Using data from three locations and according to the National Grid Company (NGC) requirements, it was found that PV capacities of 3750 MW could be added to the present network without additional reserve requirements. The additional reserve required is not on the basis of "MW of reserve per MW of PV capacity". Rather it is based on the aggregation of load demand and of PV output from all regions. The reduction in the reserve requirement by forecasting the weather profile of the day was also illustrated. In this case, a PV capacity of 22,500 MW, which can generate a little over 5% of the UK electricity demand, can be added with minimal increase in system cost. Therefore, the variation of PV output power is unlikely to be a threat to the system security.

ACKNOWLEDGEMENTS

I wish to express my sincere gratitude to the director of studies and my supervisor, Professor Nicola M. Pearsall, for her valuable advice, excellent guidance and continuous encouragement throughout my research. I wish to thank her especially for arranging frequent meeting to see my work progress smoothly despite her busy schedule and engagements at several fronts. I wish to extend my sincere gratitude to my second supervisor, Dr. Ghanim A. Putrus, for his valuable comments, continuous encouragement and advice throughout my research.

I wish to express my special thanks to Mrs. Kathleen M. Hynes for her valuable help in solar data collection, administrative works and encouragement throughout my research work. I would like to thank all the other staff in Northumbria Photovoltaics Applications Centre (NPAC) for their helpful attitude and creating a friendly environment conducive for my progress.

I wish to acknowledge the Engineering and Physical Sciences Research Council (EPSRC) for providing financial support. I also want to acknowledge National Grid Company (NGC) and Department of Trade and Industry (DTI) for their additional support in this project. I wish to express my thanks to the project partners from the Electrical Energy and Power Systems Group, The Manchester University, for their useful discussions.

I wish to express my sincere thanks to Meteocontrol GmBh, Augsberg, Germany for providing the solar radiation data.

I would like to thank my wife for her immense patience and understanding. She took care of all the household works, in spite of her busy time with newborn baby. Thanks to my son Haarish for the happiness he brought. Last but not least, thanks to my parents and family members for their love and moral support that made it possible for me to be here.

CONTENTS

LIST OF FIGURES

LIST OF TABLES

NOMENCLATURE

Symbol	*Description*	*Unit*
δ	Declination angle of the day	Degrees
ϕ	Latitude angle of the location	Degrees
ω	Hour angle	Degrees
θ	Angle of incidence	Degrees
β	Tilt angle of PV array	Degrees
γ	Surface azimuth angle	Degrees
ρ	Ground albedo	Dimensionless
η_{10}	Efficiency of the inverter at 10% of nominal rating	%
η_{100}	Efficiency of the inverter at 100% of nominal rating	%
ω_s	Sunset hour angle	Degrees
θ_Z	Zenith angle	Degrees
A	Diode ideality factor	Dimensionless
B	Temperature coefficient of maximum power	$\%/^0C$
C	Short circuit temperature coefficient at current I_{SC}	$\%/^0C$
C_i	i^{th} calculated hourly average tilted radiance value	W/m^2
E_g	Band gap of the material	Volt
G_O	Extraterrestrial radiation on a horizontal surface	W/m^2
G_{SC}	Solar constant	W/m^2
H_O	Daily total radiation on a horizontal surface at the earth's surface	J/m^2
I	Hourly average horizontal radiance on a horizontal surface	W/m^2
I_b	Hourly average beam radiance on a horizontal surface	W/m^2

I_B	Hourly average beam radiance on a tilted surface	W/m^2
I_D	Hourly average diffuse radiance on a horizontal surface	W/m^2
I_d	Diode current	Amp
I_L	Load current	Amp
I_M	Current at the maximum power point	Amp
I_O	Hourly extraterrestrial radiance on a horizontal surface	W/m^2
I_{os}	Saturation current	Amp
I_{osr}	Saturation current at reference condition	Amp
I_P	Photon Current	Amp
I_R	Hourly average ground reflected radiance	W/m^2
I_{ref}	Reference irradiance at standard test condition	W/m^2
I_S	Hourly average sky-diffuse radiance on a tilted surface	W/m^2
I_{SC}	Short circuit current	Amp
I_{Sh}	Ground-shunt current	Amp
I_T	Hourly average tilted radiance	W/m^2
k	Load dependent power loss coefficient of the inverter	Dimensionless
K	Boltzmann's constant	$J/^0K$
k_d	Hourly diffuse fraction	Dimensionless
k_t	Hourly clearness index	Dimensionless
M_i	i^{th} measured hourly average tilted radiance value	W/m^2
n	Day of the year	Dimensionless
N	Total number of observations	Dimensionless
n_{ij}	Number of transition from state I to state j	Dimensionless
P	Ratio of output power to the nominal power of the inverter	Dimensionless

P_{ac}	AC power output from PV system	Watts
P_{dc}	DC power output from PV modules	Watts
P_{ij}	Transition probability from state I to state j	Dimensionless
P_{loss}	Power losses in the inverter	Watts
P_{nom}	Nominal power rating of the inverter	Watts
p_o	Load independent power loss coefficient of the inverter	Dimensionless
q	Electron charge	Coulombs
R	Limiting transition matrix	Dimensionless
R_S	Series resistance of PV cell	Ohm
R_{sh}	Shunt resistance of PV cell	Ohm
T_a	Ambient Temperature	^{0}C or ^{0}K
T_c	Cell temperature	^{0}C or ^{0}K
T_{ref}	Reference Temperature	^{0}C or ^{0}K
V_M	Voltage at the maximum power point	Volt
V_{OC}	Open circuit voltage	Volt

ABBREVATIONS

ARMA	Auto Regressive Moving Average method
BIPV	Building Integrated Photovoltaic
DETR	Department of the Environment, Transport and the Regions
DNO	Distribution Network Operators
DSM	Demand Side Management
DTI	Department of Trade and Industry
EHCS	English House Conditioning Survey
EPSRC	Engineering and Physical Sciences Research Council
EU	European Union
FPSS	Final Plant Scheduling Stage
IEA	International Energy Agency
IGBT	Insulated Gate Bipolar Transistor
LSP	Limiting State Probability
MBE	Mean Bias Error
MC	Multiple Cluster
MOSFET	Metal Oxide Semiconductor Field Effect Transistor
MP	Marginal Probability
MPPT	Maximum Power Point Tracker
MTM	Markov Transition Matrix
NDBS	Non Domestic Building Stock
NFFO	Non Fossil Fuel Obligation
NGC	National Grid Company, UK

NGT	National Grid Transco, UK
NOCT	Nominal Operating Cell Temperature
PCU	Power Conditioning Unit
PV	Photovoltaic
RCEP	Royal Commission on Environmental Pollution
RMBE	Relative Mean Bias Error
RMSE	Root Mean Square Error
RRMSE	Relative Mean Square Error
SCR	Silicon Controlled Rectifiers
SMC	Single Mixed Cluster
STC	Standard Test Conditions
SUC	Single Uniform Cluster
TP	Transition Probability
VOA	Valuation Office Agency of the Inland Revenue
VSA	Valuation Support Application
WHCS	Welsh House Conditioning Survey

1 INTRODUCTION

1.1 PV Systems Background

From heating and lighting to transport, industry and communications, energy is fundamental to almost everything we do. The majority of the electricity consumed in England and Wales is generated by large conventional power plants. The current installed capacity of conventional fossil fuel plants (coal fired and oil fired), combined cycle gas turbine and nuclear power plant was 34 GW, 26 GW and 12 GW respectively in 2003 [1]. A key environmental impact of this energy production and use is the emission of greenhouse gases and the implication for climate changes. Carbon dioxide, considered to be one of the main causes for climate changes, is the most important among the greenhouse gases from electricity generation [1]. The Kyoto protocol target is to reduce the greenhouse gas emission by around 5% of 1990 levels in the period 2008 – 2012. The UK is committed to reduce emission of a basket of 6 green house gases[1] to an average of 12.5% below 1990 levels by the commitment period of 2008 to 2012. The UK government also has a domestic aim of reducing carbon dioxide emissions to 20% below the 1990 levels by 2010 [2].

To fulfil these responsibilities and also to meet the growing energy demand, the UK government has a number of policy instruments available. One of these policies is to promote renewable energy for both diversity and sustainability reasons. The UK government pledged to generate 10% of UK electricity from renewable sources by 2010 and to double renewable sources share of electricity from the 2010 target by 2020 [2]. In their long-term plan, the UK government also has an aim of reducing carbon dioxide emissions by 60% from the current annual carbon dioxide emissions by 2050 [2]. So in the medium to long term, there will be large-scale implementation of renewable energy sources.

Photovoltaic (PV) energy production is one among these renewable sources and is the subject of much interest. PV energy production is silent and an environmentally

[1] The six greenhouse gases are carbon dioxide, methane, nitrous oxide, hydro fluorocarbons, perfluorocarbons, sulphur hexafluoride.

beneficial technology. Photovoltaic energy production transforms sunlight energy (photons) to electricity directly by using photovoltaic cells. PV systems are basically of two different types; stand-alone PV systems and grid connected PV systems. Stand-alone PV systems are generally used in areas that do not have ready access to mains electricity or for low power applications that do not warrant a mains power supply. In this type of system, usually a storage battery is needed. When the solar radiation is high with no or low load, the excess energy produced is used to charge the battery. When there is no or low solar radiation, the load demands are met by discharging the battery in addition to PV output.

In grid connected PV systems, the PV system is connected to the utility grid and the grid serves as an ideal storage component; this means that the PV system usually does not need to include the battery storage. According to the International Energy Agency (IEA) PVPS Task 2, there has been increasing trend for demonstration programmes to focus on grid-connected systems [4]. A schematic diagram of a simple grid-connected PV system is shown in Figure 1-1. A grid connected photovoltaic (PV) system is essentially constituted from an array of PV modules together with one or more inverters. A PV module comprises a number of individual solar cells connected in series or parallel combination. The solar cells convert sunlight directly into DC power output. The inverter is a Power Conditioning Unit (PCU), which, in addition to the conversion of array output to AC, also ensures the optimum utilisation of the PV array and the required power quality and safety for the utility.

Power output from the PV system is affected by many factors such as solar radiation, module operating temperature, shading, mismatch of modules, resistance of wires and cables etc. [3]. PV modules respond almost instantaneously to the variation in solar radiation, so the properties of solar radiation are very important. Solar radiation essentially depends upon the geographical location of the PV system, the PV array tilt angle and orientation. Solar radiation is variable on both a daily and seasonal basis. This causes electricity production of photovoltaic systems to vary correspondingly. When power output from the PV system is high, it supplies the site loads and exports the excess power to the utility grid. If power output is not enough

to meet the site loads, the utility grid supplies the remaining power to meet those loads.

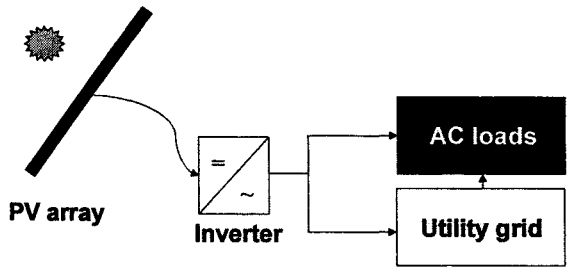

Figure 1-1 Schematic diagram of simple grid-connected PV system

One of the fastest growing sectors of the grid connected photovoltaic market is the building integrated photovoltaic (BIPV) system. In BIPV systems, the PV modules can be integrated in several ways, on a sloped roof, flat roofs and on the façade. This is an ideal application for the use of photovoltaics in an urban environment and takes advantage of the distributed nature of the sunlight and of the electrical load. Some of the benefits of the BIPV system are [5]:

- The electricity is generated at the point of use, so distribution losses and costs of distribution are reduced.
- The system does not require additional land area, since the building surfaces are used to accommodate the PV array.
- There is a possibility of offsetting some of the cost of the PV array by the amount that would have been paid for the building material it has replaced.

In the past few years, several countries have launched programme for building integrated grid connected PV systems. The installed grid connected PV systems in some of these countries are as follows [6]:

- In Germany the total installed grid-connected dispersed PV systems capacity was 380 MW, by the end of December 2003.
- In Japan 778 MW of grid connected PV systems were installed by the end of December 2003.
- In the United States, by the end of December 2003, the installed capacity of grid connected PV systems was 96 MW.

Opportunities for the deployment of photovoltaic technology in northern Europe are increased greatly since the concept of PV integration into buildings [7]. The European Commission White Paper on Renewable Energy Technologies includes a target of 3 GW of photovoltaic systems in the community by 2010 via the installation of 500,000 roofs and facades within Europe [8]. In the UK, the Department of Trade and Industry (DTI) have implemented two field trials to support the development of photovoltaic energy systems and components. The UK Domestic Photovoltaic Systems Field Trial, which is implemented in two phases, consists of 28 projects representing a planned installed capacity of over 750 kWp, over 480 dwellings [9]. The Large-Scale Field Trial (LSFT) is supporting installation of 20 – 100 kWp in a range of public buildings across the UK, which will result in a total capacity of 640 kWp [9]. The DTI, UK launched the Major Demonstration Programme (MDP) on March 2002, with an aim to develop the UK PV industry via the installation of photovoltaic systems on 3,000 houses and 140 commercial buildings. At the midpoint of the MDP program, a total capacity of 5.2 MWp had been approved. [10].

1.2 Project Background

Growth of the PV market indicates that in the near future photovoltaic electricity generation may rise in some countries from its marginal contribution to the public power demand to a more significant power source. The distributed PV generation systems inherently provide some benefits to the utility. They may level the load curve, improve the voltage profile across the power feeder and reduce the loading level of branches and substation transformers etc. Power output of grid connected photovoltaic systems varies rapidly during cloud transients. For low penetration of PV capacity, such fluctuations are not significant when compared to the entire load demand served by other generators in the system. For larger penetration of PV capacity, however, cloud transients may result in significant fluctuations in the power output. This may lead to changes in the characteristics of the load demand to be met by conventional power generators. So rapid fluctuations in the total demand may sometimes require the use of more reserve units, which leads to more operating costs, to keep the systems in balance. PV generation with sudden changes in the power

output may have impact on the grid voltage and stability of the transmission network as the PV penetration level increases. This effect can be reduced by the distributed nature of PV systems.

As the proportion of electric power generated using PV and other renewable energy sources becomes significant, the effect of these sources on the electricity transmission and distribution system must be considered. The integration of a large number of embedded PV generators may have consequences not only on the distribution sector of the electrical supply industry but also on the national transmission and generation systems. The study of the impact of large-scale PV generation on the power system requires suitable representations of the PV resource and the output of PV generators to feed into a model of the grid and to allow investigation of the effects on the power system. So, in recent years, the assessment of the combined power output of geographically distributed PV systems has been the subject of several studies [11-14].

In practice, the large-scale inclusion of PV in the UK electric network is expected to take the form of a large number of small, building integrated systems widely distributed in the urban environment. These systems will represent a variety of sizes, module technologies, array orientation, location, inverter type etc and will be connected to the electricity distribution system at the point of supply to the building on which they are sited. The power output from PV systems mainly depends on solar radiation received by the PV arrays. The power output from PV systems fluctuates due to variation in solar radiation values caused by cloud cover. This cloud cover will not occur in all locations at the same time and hence the power output pattern can be different when combining all PV systems output. Thus, the production patterns of a large ensemble of spatially distributed PV generators are of interest for the assessment of effects on the grid operation.

1.3 Aims and Objectives

The aim of this EPSRC funded project was to study the effects of multiple PV systems on the UK national transmission system. It was carried out in collaboration with the Electrical Energy and Power Systems Group at UMIST. Two PhD students at UMIST have developed the transmission model in terms of both overall supply characteristics and dynamic performance, whilst this research work concentrated on the development of suitable models for PV systems. This work included the development of suitable representations of the PV resource and PV systems for studies in various time frames (hour, half-hour) as well as the aggregation of very large numbers of small, geographically dispersed PV generators. The variation of combined output power from dispersed PV systems and the correlation of solar radiation between different locations were analysed for different time intervals and seasons. This work also analysed the implication of additional reserve generation required, for different PV penetration levels, to keep the system in balance.

The specific aims of the work presented in this thesis are:

- To investigate suitable representations of the PV resource for long term, load flow and dynamic power system studies. This aim is achieved through the following objectives:
    - Generating representative synthetic horizontal solar radiation data for different locations in the UK and for different time periods: hour and half-hour time periods.
    - Translation of horizontal radiation to tilted radiation for different PV systems that vary in tilt angle and orientation.
    - Analysis of the frequency and magnitude of solar radiation fluctuation.

- To propose suitable aggregated models to represent large number of small, geographically dispersed PV systems. This includes both the effects of correlation of the solar resource and a suitable representation of the aggregated power electronic converters. This aim is achieved through the following objectives:

- Development of a PV cluster model to represent very large numbers of small geographically dispersed PV systems. To achieve this, PV system design parameters that may vary for each PV system were identified and methods to represent these parameters have been developed.
- Analysis of sensitivity of PV cluster power output with changes in the system parameters.
- Projection of the system design parameters to the year 2030 in order to analyse the impact of large number of PV systems on the grid.
- Analysis of the frequency and magnitude of power output fluctuation for different time periods: hour, half-hour and minute time periods.
- Analysis of the correlation of solar radiation for different seasons and different time intervals.
- Analysis of the standard deviation of output power fluctuation for different seasons with respect to time of the day for different time intervals.
- Study of the implications for additional reserve requirements for different PV penetration levels by using the combined power output from geographically dispersed PV systems. Factors that affect the reserve requirement in the present UK network and possible strategies that can be used to increase the PV penetration levels with the minimum increase in system cost have been considered.

1.4 Thesis Organisation

In **Chapter 2** the basic theory of photovoltaic systems are explained. PV system components, different types of PV systems, advantages of grid connected BIPV systems and different types of PV inverter are discussed.

Chapter 3 deals with the generation of synthetic horizontal solar radiation values for different locations in the UK using the Markov Transition Matrix (MTM) method. The generation of synthetic solar radiation data for different time periods (hourly and half-hourly periods) is discussed. This chapter also illustrates the validation of

standard methods used to translate the horizontal radiation to tilted radiation values for different PV systems.

Chapter 4 deals with the development of the PV cluster model to represent the geographically dispersed PV systems, which vary in their system parameters like system size, orientation, tilt angle, inverter type and rating. Sensitivity analysis on the assumptions made to represent these parameters is discussed. This chapter also discusses the projection of PV module technologies, inverter efficiencies, dwelling and non-domestic building stock to the year 2030 to allow consideration of the impact of large number of PV systems on the grid.

In **Chapter 5** the fluctuation of solar radiation for a single location and the reduction in fluctuation by aggregating solar radiation values from many locations is discussed. This chapter also discusses the correlation of solar radiation values between different locations for different seasons and time intervals.

For different PV penetration levels, the implications of reserve capacity requirements to keep the system in security are discussed in **Chapter 6.** Factors that may affect the reserve requirement levels in the present UK network condition and the possible changes in the future are discussed. The different strategies that can be used to reduce the reserve requirement levels are also discussed in this chapter.

In **Chapter 7** conclusions from the research project are summarised and further research work is outlined.

1.5 References for Chapter 1

1. "Digest of United Kingdom Energy Statistics 2004", Published by the Stationary Office, Norwich, UK, available at www.dti.gov.uk
2. Energy White Paper, "Our Energy Future – creating low carbon economy", HMSO, 2003, available at www.dti.gov.uk
3. Friedrich Sick and Thomas Erge, "Photovoltaics in Buildings – A Design Handbook for Architects and Engineers", Published by James & James (Science Publishers Ltd.), 1998.

4. U. Jahn, D. Mayer, M. Heidenreich, R. Dhal, S. Castello, L. Clavadetscher, A. Frdich, B. Grimming, W. Nasses, K. Sakuta, T. Sugiura, N. Van der Borg and K. Van Otterdijk, "International Energy Agency PVPS Task 2: Analysis of the operational performance of the IEA database PV systems", 16th European Photovoltaic Solar Energy Conference and Exhibition, Glasgow, UK, Vol. 3, pp. 2673-2677, May 2000, Published by James & James (Science Publishers) Ltd., UK.
5. Mary D. Archer and Robert Hill, "Clean electricity from photovoltaics", Series on Photoconversion of Solar Energy – Vol. 1, Chapter 15, Imperial College Press, London, 2001.
6. "Trends in photovoltaic applications survey report of selected IEA countries between 1992 and 2003", Report IEA-PVPS T1-13: 2004, Published by International Energy Agency, 2004, available at www.iea-pvps.org.
7. A. R. Wilshaw, N. M. Pearsall and R. Hill, "Installation and operation of the first city centre PV monitoring station in the United Kingdom", Solar Energy, Vol. 59, Nos. 1-3, 1997, pp. 19 – 26.
8. "Energy for the Future: Renewable Sources of Energy", White Paper for a community strategy and action plan, HMSO, 1997.
9. James R. Marsh and Gary Shanahan, "The UK's major photovoltaics demonstration programme – progress and trends", 19th European Photovoltaic Solar Energy Conference, Paris, France, Vol.3, June 2004, pp. 2779 – 2782, Proceeding published by WIP – Munich and ETA – Florence.
10. Paul Reed, Martin Brooks, Jim Thornycroft and Kirk Archibald, "Growing a UK PV installer base whilst maintaining quality", 19th European Photovoltaic Solar Energy Conference, Paris, France, Vol.3, June 2004, pp. 3036 – 3039, Proceeding published by WIP – Munich and ETA – Florence.
11. K. Otani, J. Minowa and K. Kurokawa "Study on areal solar irradiance for analysing areally-totalized PV systems", Solar Energy Materials and Solar Cells, Vol. 47, 1997, pp. 281-288.
12. K. Otani, A. Murata, K. Sakuta, J. Minowa and K. Kurokawa, "Statistical smoothing effect of power delivered to utilities by distributed PV systems", 2nd World Conference and Exhibition on Photovoltaic Solar Energy Conversion, Austria, Vol. 3, July 1998, pp. 2530 – 2533, Published by European Commission, Renewable Energies Unit, Ispra.

13. E. Wiemken, H.G. Beyer, W. Heydenreich and K. Kiefer, "Power characteristics of PV ensembles: Experiences from the combined power production of 100 grid connected PV systems distributed over the area of Germany", Solar Energy, Vol. 70, No. 6, 2001, pp. 513-518.
14. A. Murata, and K. Otani, "An analysis of time-dependent spatial distribution of output from very many PV power systems installed on a nation-wide scale in Japan", Solar Energy Materials and Solar Cells, Vol. 47, 1997, pp. 197-202.

2 THEORY OF PHOTOVOLTAIC SYSTEMS

2.1 Renewable Energy Sources

Energy-related problems are most often sustainability problems and environmental problems. Many years ago the sustainability problem that concerns the limited supply of fuel was the main issue. Today's main energy related problem is environmental. One of the most significant problems appears to be that of climate change (so called global warming), a gradual increase in the global average air temperature at the earth's surface. The majority of scientists now believe that global warming is probably taking place, at a rate of around 0.3 ^{0}C per decade [1], and that this is caused by an increase in the concentration of greenhouse gases in the atmosphere. The most significant single component of these greenhouse gas emissions is carbon dioxide released by the burning of fossil fuels. In the UK, the total net declared power system capacity was 76,588 MW in the year 2003 (end December) [2]. Among these coal used for electricity generation in the year 2002 accounted for 32%. About 33% of CO_2 emission released in the UK comes from power stations [2].

Another side effect of burning fossil fuels is acid rain. Some of the gases which are given off when fuels are burned, in particular sulphur dioxide and nitrogen oxides, combine with water in the atmosphere to form sulphuric acid and nitric acid respectively. The result is that any rain which follows is slightly acidic. This acid rain can cause damage to plant life, in some cases seriously affecting the growth of forests, and can erode buildings and corrode metal objects. About 70% of the sulphur dioxide released in the UK comes from power stations [2]. It is mainly from the burning of coal, together with some oil, which contains sulphur in concentrations ranging from 0.5% to 5% per unit volume. In order to overcome these problems, as part of the Kyoto Protocol, the UK government have committed to reducing the emission of a basket of 6 greenhouse gases to an average of 12.5% below 1990 levels by the commitment period of 2008 to 2012.

The present form of the UK network is centralised where electricity is generated by relatively few, very large power stations and distributed throughout the country. There are concerns that these large, vital installations offer potential targets for terrorist or military opponents, which will affect the security of supply [1]. The normal response to such vulnerability is to use many small, dispersed resources to increase the level of protection.

In order to overcome these problems the UK government has programmes to support the usage of renewable energy resources [3]. Energy sources which can be constantly replaced, and are less polluting to the atmosphere, are known as renewable energy sources. Renewable energy sources are much lower energy density than fossil fuels and the generation plants are smaller and geographically dispersed. Renewable energy generators are typically lower than 50 MW in capacity, and they are usually connected to the distribution network [4]. Some of the renewable energy sources are solar energy (photovoltaic, solar thermal), wind, micro-hydro, biomass energy and energy from municipal wastes. The UK government has a target to generate 10% of electricity from renewable energy sources by the year 2010 in order to achieve the commitment to the Kyoto protocol. The European Union (EU) has a target of 12% of energy (22.1% of electricity) from renewables by the year 2010.

In the UK, the Non Fossil Fuel Obligation (NFFO) was initiated in 1990 to boost the amount of renewable generation [3]. Until the year 2000, the NFFO was the main instrument for the renewable generation. Since the year 2000, the UK government has four different policies to increase the generation from renewable energy sources. These are:

- New Renewable Obligation
- Climate Change Levy
- Support Programme for New and Renewable Energy and
- Regional Strategic Approach

In addition to this in October 2001, the European Renewables Directive policy, which aids the member states to achieve their national targets for renewables to reach the overall EU target, was initiated. In the UK, the total installed renewables capacity in the year 2003 was 3,548 MW [2].

Photovoltaic energy production is one among these renewable sources and is the subject of much interest. PV energy production is silent and an environmentally beneficial technology. Photovoltaic energy production transforms sunlight energy to electricity directly by using photovoltaic cells. In normal operation PV systems emit no gaseous or liquid pollutants and no radioactive substances and hence PV systems are not harmful to the environment [1]. PV systems are usually small in size and are geographically dispersed distributed energy sources. Hence the dispersed PV systems provide security and increase the level of protection. The following sections discuss the basic theory of PV system components and different types of PV systems.

2.2 PV Cells

Photovoltaic energy production transforms sunlight energy to electricity directly by using photovoltaic cells. The PV cell consists of a thin piece of semiconductor material. A semiconductor is an element, whose electrical properties lie between conductor and insulator i.e. they are marginally conductive for electricity, under the normal conditions. Through a process called doping a very small amount of impurities are added to the semiconductor, thus creating n-type and p-type layers. The n-type semiconductor doped with an impurity (for example, usually Phosphorous, Arsenic and Antimony are dopants for silicon) such a way that n-type layer has an increased number of electrons. The p-type semiconductor doped with an impurity (for example, usually Boron, Aluminium, Gallium and Indium are dopants for silicon) such a way that the p-type layer has majority of holes.

When the P-type and N-type semiconductor materials are joined, the junction approaches a new thermodynamic equilibrium. This occurs by the flow of electrons from n-type material to p-type material until a voltage difference is established between the two materials. This electric field created in the P-N junction is important for the function of the PV cell [6]. When the p-n junction absorbs light, the energy of the absorbed photons is transferred to the electrons, resulting in the creation of charge carriers that are separated at the junction. The charge carriers in the junction region get accelerated under the electric field create a potential gradient and circulate

as current through an external circuit [5,6,8]. The current is known as the photocurrent (I_P) and the effect is known as the photovoltaic effect. The French physicist Becquerel first discovered this effect in 1830 [5,6].

2.2.1 Types of PV cells

There are different types of PV cells, which are classified, depending upon the type of semiconductor materials used. The major materials are crystalline and thin-film materials, which vary in terms of light absorption, energy conversion, manufacturing technology and cost of production.

Crystalline materials

Single crystal Silicon

The single crystalline silicon (often called mono-crystalline silicon) type of PV cell is the most matured technology used in the PV industry. Single crystal silicon has a uniform molecular structure, which results in a high energy conversion i.e. the ratio of electricity power produced by the cell to the amount of sunlight power available [8,9]. Single crystalline silicon PV cells with 24.7% conversion efficiency have been achieved in the year 2004 [10].

Polycrystalline Silicon

Consisting of small grains of single crystalline silicon, polycrystalline silicon PV cells are less energy efficient than single crystalline silicon. Polycrystalline silicon PV cells with 20.3% conversion efficiency have been achieved in the year 2004 [10]. The average price for a polycrystalline silicon cell is slightly lower than the mono-crystalline silicon.

Gallium Arsenide (GaAs)

A compound semiconductor made of two elements, Gallium (Ga) and Arsenic (As). GaAs has advantages of higher level of light absorption and higher energy conversion efficiency than crystalline silicon. Conversion efficiencies of 25.1% have been achieved [10]. The main disadvantage of GaAs, however, is the high cost. Thus

it is most often used in concentrator systems and space applications where only a small area of GaAs cell is needed [9].

Thin-film materials

In order to lower the cost of PV cell manufacturing, thin-film solar cells are being developed by means of using less material and a faster manufacturing process. However, thin-film materials suffer from lower conversion efficiency due to their non-single crystal structure.

Materials used for thin-film PV cells are given as follows:

Amorphous Silicon (a-Si)

Amorphous silicon is the non-crystalline form of silicon i.e. silicon atoms are disordered in structure. A significant advantage of a-Si is high light absorption, about 40 times higher than that of single crystal silicon. But a-Si has the disadvantages of low cell energy conversion efficiency and efficiency degradation [7]. Amorphous silicon cells with 12.7% conversion efficiency have been achieved [10].

Cadmium Telluride (CdTe)

Polycrystalline semiconductor material made up of cadmium and tellurium, CdTe, has a high level of light absorption. Another advantage is that it is relatively cheap and easy to manufacture. Instability of cell performance is one of the major drawbacks of using CdTe for PV cell. Another disadvantage is that cadmium is a toxic substance, so that even though only a very small amount of cadmium is used in the CdTe cell, extra precautions have to be taken in the manufacturing process [9]. CdTe PV cells with 16.5% conversion efficiency have been achieved [10].

Copper Indium Gallium Diselenide ($CuInGaSe_2$ or CIGS)

A polycrystalline semiconductor of copper, indium, gallium and selenium, CIGS has the highest energy conversion efficient among the thin-film materials. The conversion efficiency comes close to the polycrystalline silicon material conversion efficiency. CIGS PV cells with 18.9% conversion efficiency have been achieved [10]. Being able to deliver such high conversion efficiency without suffering from

the degradation problem, CIGS has demonstrated that thin film PV cells are viable and competitive choice for the solar industry [7,10], although they are still produced at relatively low production volumes.

There are other types of PV multi-junction cells, photochemical cells and concentrator cells that are still considered as at a pre-commercial stage. In the work presented in this thesis, power output from dispersed PV systems is analysed which will be greatly influenced by the commercialised PV cells. Therefore, types of PV cells that are at a pre-commercial stage are out of scope for this thesis.

2.2.2 Equivalent circuit of PV cell

A PV cell can be represented by an equivalent electrical circuit, as shown in Figure 2-1. The PV cell is modelled as an ideal diode in parallel with a light induced current source [11]. The internal losses are represented by the series resistance (R_s) and shunt resistance (R_{sh}). The series resistance (R_s) represents the internal resistance to the current flow, and depends on the junction depth, the impurities and the contact resistance. The shunt resistance (R_{sh}) is inversely related with the leakage current to the ground. In an ideal PV cell, the value of series resistance is zero and the shunt resistance is infinite.

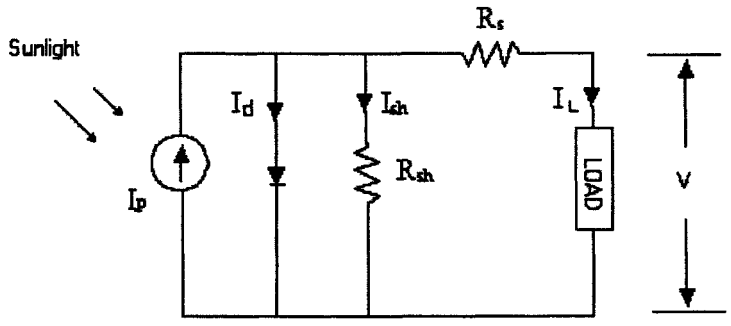

Figure 2-1 Equivalent circuit for PV cell

The current delivered to the load (I_L) equals the photocurrent (I_P) generated by the illumination, less the diode current (I_d) and the ground-shunt current (I_{sh}).
So the current delivered to the load is given by the expression

$$I_L = I_P - I_d - I_{sh} \quad (2.1)$$

The two most important parameters widely used for describing the electrical performance of a PV cell are the short circuit current and the open circuit voltage.

Short-circuit current (Isc):

This is the maximum current that a solar cell can generate, when the voltage across the cell is zero. The short circuit current is a measure that indicates to what extent photons can generate electron-hole pairs. It is directly proportional to the illumination intensity and cell area. The short circuit current increases slightly with increasing temperature.

Open circuit voltage (Voc):

This is the voltage that a solar cell exhibits when no load is connected, i.e. when the current is zero. The open circuit voltage is correlated to the lifetime of the carriers during their diffusion through the material. The more carriers recombine before reaching the contact grid, the lower this voltage. In the ideal case, the open circuit voltage is independent of the cell area. The open circuit voltage is dependent on the cell temperature. The open circuit voltage increases slightly with increasing irradiance.

The electrical parameters, open circuit voltage and short circuit current of a PV cell, vary with the sunlight level and temperature of the PV cell as explained in section 2.2.4. Therefore all electrical performance data for PV cells are referred to the Standard Test Conditions (STC), defined by a temperature of 25^0C, an irradiance of 1000 W/m^2 and a standardised solar spectral distribution of Air Mass 1.5.

The photocurrent (I_P) is given as [12]

$$I_P = \left(I_{SC} + \left(C\left(T_C - T_{ref}\right)\right)\right) I_T / I_{ref} \qquad (2.2)$$

Where,

T_{ref} is the reference temperature (^{0}C)

T_C is the cell temperature (^{0}C)

I_T is the radiance in the plane of the cell (W/m^2)

I_{ref} is the reference radiance at STC (W/m^2)

C is the short-circuit temperature coefficient at I_{SC} (A/^{0}C)

The diode current (I_d) is given as

$$I_d = I_{os}\left[\exp\left(\frac{qV_{OC}}{AKT_C}\right)-1\right] \tag{2.3}$$

Where,

I_{os} is the saturation current of the diode given by

$$I_{os} = I_{osr}\left(\frac{T_C}{T_{ref}}\right)^3 \exp\left(\frac{qE_g}{AK}\left(\frac{1}{T_C}-\frac{1}{T_{ref}}\right)\right) \tag{2.4}$$

q is the electron charge ($1.6\text{x}10^{-19}$ Coulombs)

A is the diode ideality factor

T_C is the cell temperature (^oK)

T_{ref} is the reference temperature (^0K)

K is the Boltzmann constant ($1.38\text{x}10^{-23}$ J/^oK)

E_g is the band gap of the material used (V)

I_{osr} is the saturation current at reference condition (A)

So the current delivered to the load is given as

$$I_L = I_P - I_{os}*\left[\exp\left[\frac{q(V+RsI_L)}{AKT_C}\right]-1\right]-\frac{V+R_sI_L}{R_{sh}} \tag{2.5}$$

2.2.3 I-V curve and power curve

The electrical characteristics of a PV cell can be represented by an I-V curve in which current is plotted as a function of the external voltage. An I-V curve for a PV cell is illustrated in Figure 2-2. The top left of the I-V curve at zero voltage is called the short circuit current (I_{SC}). The bottom right of the I-V curve at zero current is the open circuit voltage (V_{OC}). Power output of the PV cell is the product of the current and voltage. The power plotted against the voltage is known as the power curve. The cell produces no power at zero current or zero voltage, and it produces the maximum power at voltage (V_M) and at current (I_M) at the knee point of the I-V curve.

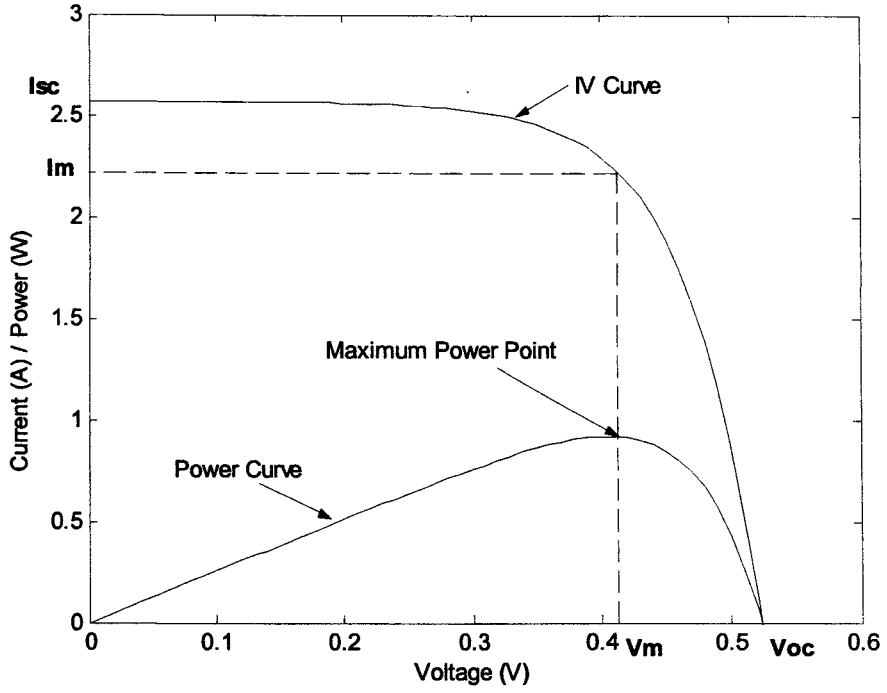

Figure 2-2 Example I-V curve and power curve for a PV cell (Value of I_{SC} and V_{OC} will vary depending on cell details)

Maximum power point (MPP)

The Maximum Power Point is the operating point on the I-V curve where maximum power is produced. In order to achieve this, the resistance of the load has to be adjusted to the I-V characteristics of the solar cell. The effects of two meteorological parameters, irradiance and ambient temperature, complicate this task. The following section explains the change in I-V curve with these parameters.

2.2.4 Effect of irradiance and temperature on I-V curve

Changes in an I-V curve with respect to the irradiance are shown in Figure 2-3. The short circuit current is proportional to the solar irradiance. The open circuit voltage increases slightly with increasing irradiance. The power output of the PV cell is proportional to the irradiance. Changes in an I-V curve with respect to the temperature are shown in Figure 2-4. The short circuit current increases slightly with increasing temperature by approximately 0.07%/C, whereas the open circuit voltage

decreases linearly with increasing temperature. The open circuit voltage decreases with increasing temperature by approximately 0.4%/C for crystalline material and this value is lower for amorphous cells.

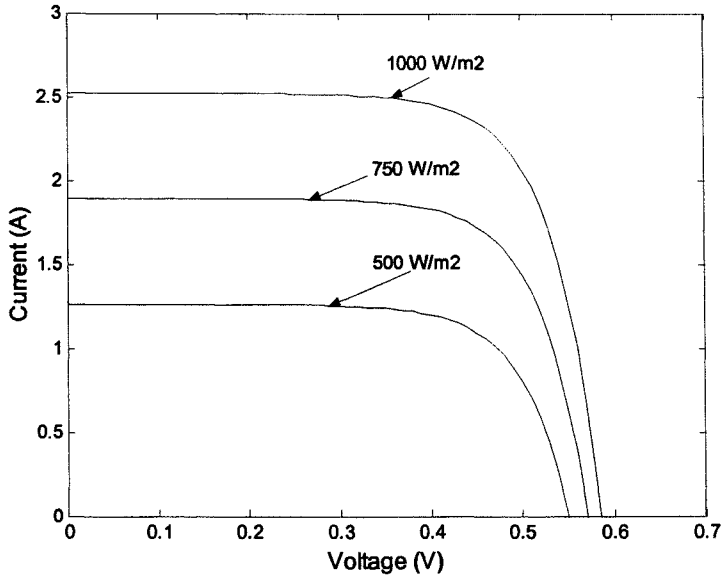

Figure 2-3 Change in I-V curve with change in irradiance at constant temperature

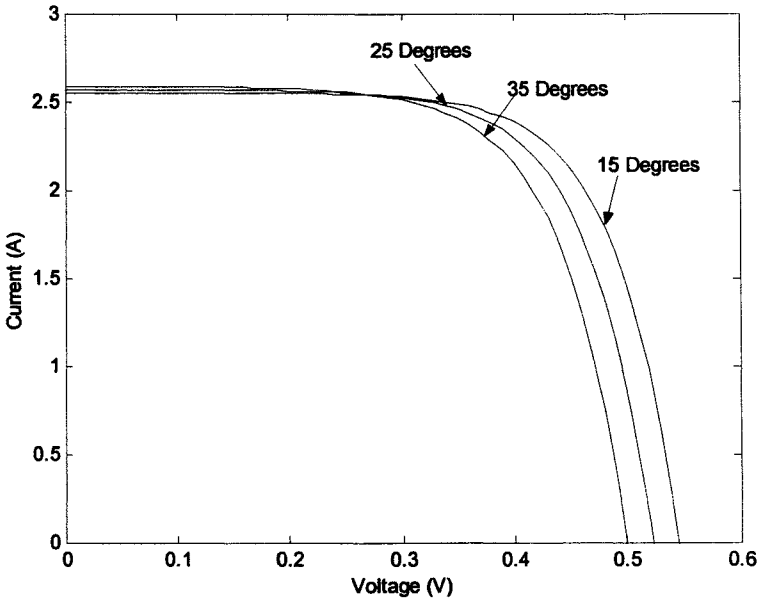

Figure 2-4 Change in I-V curve with change in temperature at constant irradiation

2.3 *PV Generator*

PV cells are not usually operated separately. They are connected in series and/or parallel combinations to form PV modules. In most commercial PV modules, solar cells are connected and placed between a tedlar plate on the bottom and glass on the top. The outermost layer, the cover glass, protects the cells from the environment. It keeps out water, water vapour and gaseous pollutants, which could cause corrosion of PV cells. The cover glass is often tempered to protect the cell from wind damage. A transparent adhesive (EVA sheet) holds the cells in position. Usually PV modules are framed with aluminium or composite materials, which give the mechanical stability for mounting modules in different ways. However, for some building integrated PV systems, modules without frames (called laminates) are often used.

As an example, Figure 2-5 shows the mono-crystalline type PV module, BP585, the product from BP Solar. Ratings of this module at Standard Test Condition are given as [13]:

Nominal Peak Power:	85 Watts
Voltage @ maximum power:	18 V
Current @ maximum power:	4.72 A
Short-circuit current:	5 A
Open-circuit voltage:	22.3 V
Temperature coefficient of voltage:	0.086 V/^{0}C
Temperature coefficient of current:	0.0025 A/^{0}C

The I-V curve of the module and the change in I-V curve of module with temperature is shown in Figure 2-6. These module data were used to calculate the PV system size and output power in the cluster model, explained in Chapter 4. The maximum module efficiency achieved in the year 2004, by each technology are given as [10]:

Single crystal silicon	22.7%
Polycrystalline silicon	15.3%
Amorphous silicon	10.4%
Cadmium Telluride	10.7%
Copper Indium Gallium Diselenide	13.4%

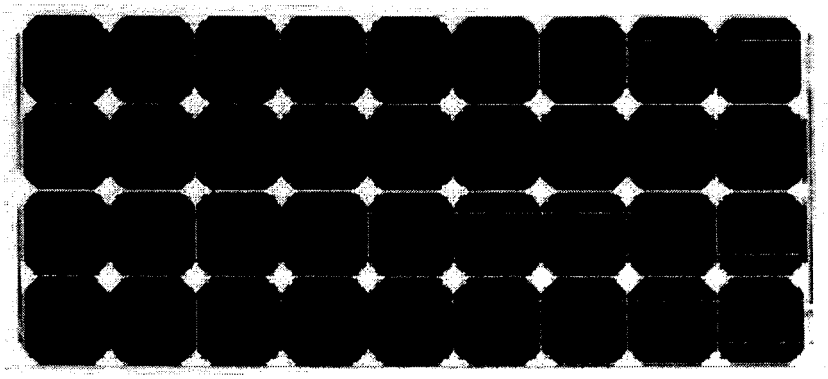

Figure 2-5 Mono-crystalline silicon type PV module (Source: www.bpsolar.com)

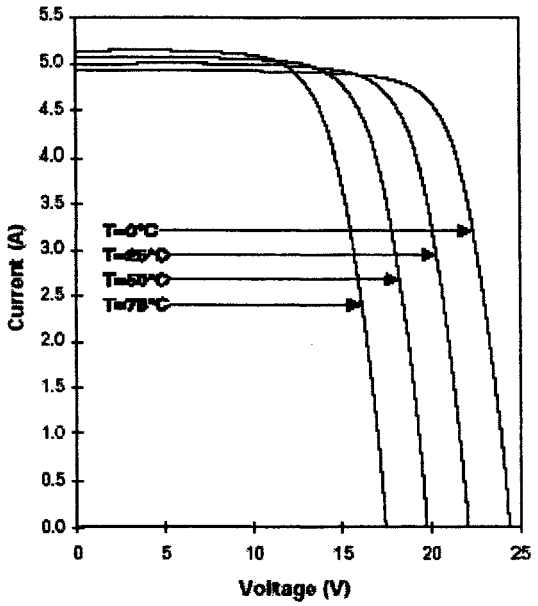

Figure 2-6 I-V curves for the BP585 PV module with change in temperature (Source: www.bpsolar.com)

There are two possible cases in which the PV modules can operate. One is the ideal case where all PV cells are identical and homogeneously illuminated. But in practice there are more chances of cells with different operating conditions. For example a small shadow from a leaf, an antenna pole or an overhead line results in different irradiation levels. This will decrease the output power from the module, due to the fact that the cell with the lowest illumination determines the operating current of the whole string. A partially shaded cell may be forced into a load mode, which can lead to a thermal destruction of the cell and the respective module if not properly

protected. In order to avoid this bypass diodes are used to provide a second current path diverting the current from the shaded cell [5].

The power output of a single module is not sufficient for most of the applications. Therefore, they are connected together so that they form an array, which can generate sufficient power for a particular application. Several modules connected in series are called a string. Several such strings are connected in parallel to achieve the required current level and this is called an array. It is necessary to protect the string cables and modules against the over current. Fuses are used for general over current protection, while blocking diodes prevent current flow into one string from the rest of the PV generator [5]. This operating condition might occur, if a ground fault or short circuit happens in a string. However using modern modules and appropriate cable and wiring methods virtually eliminates the occurrence of such a fault. The final PV array configuration is illustrated in Figure 2-7, where 'n' PV modules are connected in series and 'm' strings are connected in parallel.

The estimation of DC power output from a PV module depends upon the solar radiation and temperature and is explained in Chapter 4. PV module efficiencies for different technologies and the PV module market trends are also discussed in Chapter 4.

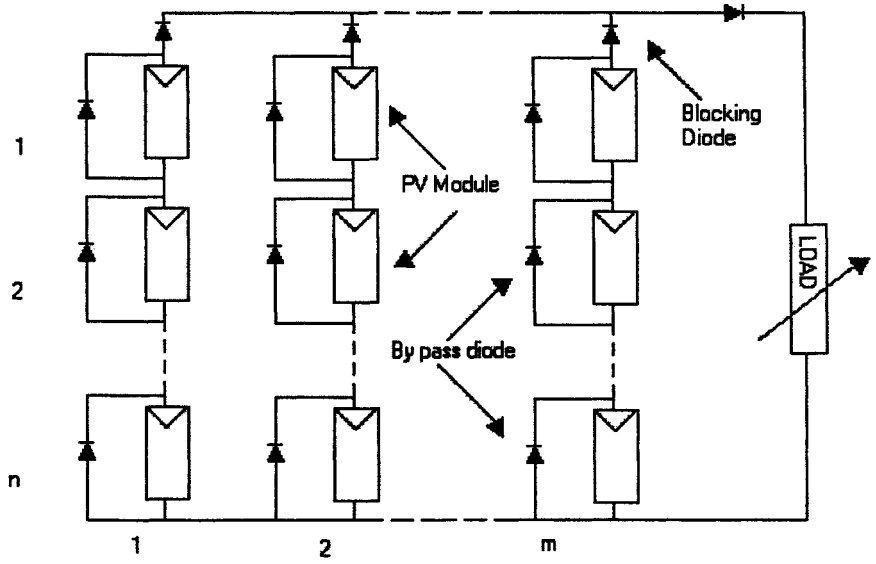

Figure 2-7 PV array configuration

2.4 PV Systems

A PV generator produces a DC power output and depending upon how this DC power used, the photovoltaic systems can be classified into two main groups. They are stand-alone PV systems and grid connected PV systems.

2.4.1 Stand-alone PV systems

Stand-alone PV systems are generally used in areas that do not have ready access to mains electricity or for low power applications that do not warrant a mains power supply. A schematic diagram of a stand-alone PV system is shown in Figure 2-8. In this type of system usually a storage battery is needed. When the solar radiation is high with no or low load, the excess energy produced is used to charge the battery. While there is no or low solar radiation, the loads are met by discharging the battery. Stand-alone PV systems can be highly competitive in the developing countries, and particularly in rural areas where electricity grids are often non-existent. In these countries the use of stand-alone PV systems is growing rapidly for different applications which include PV water pumping, street lighting, PV refrigerators to keep vaccines stored safely in health centres etc. In the UK, stand-alone PV systems are employed for numerous industrial applications including maritime navigation devices, telecommunication equipment devices etc. For some applications, which need AC power, DC power is converted to AC power using DC to AC converters (inverters) [14]. In this work power output from grid-connected PV systems and their impact on the grid are analysed. Therefore stand-alone PV systems are not considered further in this work.

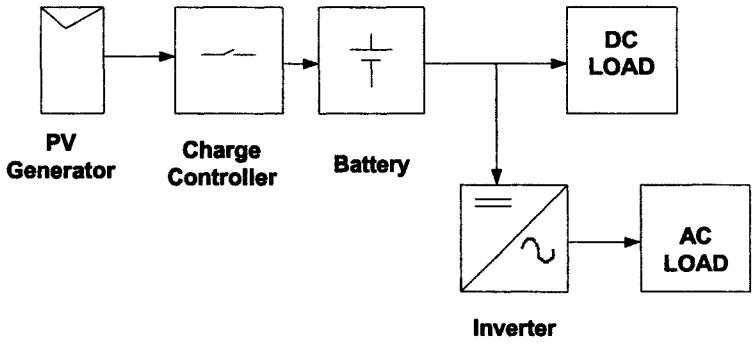

Figure 2-8 Schematic diagram of a standalone PV system

2.4.2 Grid connected PV systems

In grid connected PV systems, PV systems are connected to the utility grid. In this case the grid serves as an ideal storage component, this means the PV system usually does not need to include the battery storage. DC power output from the PV system is converted to AC power and fed to the grid by DC to AC converters. When the solar radiation is high with no or low local load, the excess power is transferred to the grid. When there is no or low solar radiation, the grid will supply the local load. The main area of interest in the UK is grid connected PV systems.

Building Integrated PV (BIPV) systems

Grid connected PV systems are often integrated into buildings and over the last few years the use of photovoltaic systems on buildings has increased substantially in the UK and other countries in the world [14]. In countries like Japan, Germany and USA BIPV systems have increased very significantly in the recent years. The PV modules can be integrated in several different ways: on a sloped roof, flat roofs and in the façade. PV systems on a flat roof or in sloped roofs may be standoff or integral. Standoff is a straightforward mounting method well suited for retrofits. Special mounting elements like hooks or mounting tiles are fixed to the roof. A support structure to which the modules are bolted is fixed to the mounting elements. The integral mounting method uses the PV generator as the building envelope. The modules replace the conventional roof. This method leads to a nicer appearance and cost saving in new buildings. A special design of roof-integrated PV modules is PV tiles, in which pre-wired tiles can be mounted and connected very quickly. Façades are an increasingly popular location for PV generators, since they provide multiple purposes for PV modules. Semitransparent modules may serve for day lighting purposes. PV modules installed in the façades provide shading for the offices behind [8].

The size of the PV system that can be installed on a roof or façade depends upon the building size, suitable area for PV installation, tilt angle and type of PV modules etc. Building stock in the UK and the size of PV system that can be installed are explained in Chapter 4.

Advantages of grid connected BIPV systems

Building Integrated Photovoltaic Systems (BIPV) on domestic houses are connected to the distribution network as single phase at 230V level. BIPV systems on non-domestic buildings (commercial and industrial buildings) are often connected to the network as 3-phase at 415 V level. As the BIPV systems are connected to the distribution network, there are number of advantages for the utility network, which include

- Since generation is close to the consumer load, the amount of power loss through the transmission network is reduced.
- Since the transmission losses are lower, the overall amount of power required to be generated will be reduced.
- The distributed PV generation can meet the consumers' load demand reducing the peak load to be served by the large central power station depending upon the matching of generation and peak load demand.
- Increased fuel diversity.
- Reduced environmental effect.

Because of these advantages to the electricity network and also architectural benefits and economical benefits from PV systems in the built environment there is growing interest in grid connected BIPV systems from utility companies, architects and building engineers.

2.5 Power Conditioning Unit

In almost all types of PV systems, a Power Conditioning Unit (PCU) is required for:

- The optimal operation of the solar generation
- The optimal and safe operation of the connected electrical equipment

Depending upon the application, the following PCU may be needed in a PV system [5]:

- DC to AC converters (Inverters)
- Matching DC/DC Converters
- Charge Controllers

To meet DC loads, it may be necessary to include a DC-DC converter to change the voltage level of the output of the array to that required by the load. It is also usual to include charge control circuitry where the system includes batteries, in order to control the rate of charge and prevent damage to the batteries. When AC loads are to be supplied, an inverter is used as a PCU to convert the DC power output from the PV array to AC power output. So in the case of grid-connected PV systems, the inverter is the Power Conditioning Unit.

2.5.1 Inverter

In grid-connected PV systems, the inverter is used as a Power Conditioning Unit to convert the DC power output from the PV array to AC power output. The grid-connected inverter must integrate smoothly with the electricity supplied by the grid in terms of both voltage and frequency. The inverter ensures that the PV systems power output is fully synchronised with the utility power. The efficiency of the inverter should be high with an average efficiency across its power range generally greater than 92%. The inverter should exhibit high availability [5].

Engineering Recommendations

In order to maintain the power quality and security, in the UK, a PV system connected to the grid through an inverter should follow the Engineering Recommendations. For a system rating less than 16A, connection procedures should comply with the Engineering Recommendations G83/1. If the rating is greater than 16A, requirements should comply with the Engineering Recommendation G59/1. Some of the recommended inverter specifications by Engineering Recommendation G83/1 for the grid connection are [15]:

- It should automatically disconnect the PV system under the utility fault conditions. These include deviation of voltage, frequency etc.
- The allowable over voltage and under voltage levels are 264 Volts (230+14.7%) and 207 Volts (230-10%) respectively. If the limit is violated, the system has to be disconnected within 1.5 seconds.

- The over frequency and under frequency levels are 50.5 Hz (50+1%) and 47 Hz (50-6%) respectively. If the limit is violated, the system has to be disconnected from the utility within 0.5 seconds.
- It should automatically reconnect to the utility after the fault is cleared, and voltage and frequency have remained within the limits for a minimum of 3 minutes.
- The total harmonic distortion of output current should be less than 3% at full load operation.
- The maximum voltage fluctuation and flickering allowed is 4% at full load.
- DC currents entering the distribution system should not exceed 20 mA. To achieve this level, in the Engineering Recommendation G83/1, transformer on the AC side of the inverter is recommended.
- The power factor at rated power can be within the range of 0.95 lagging to 0.95 leading relative to the voltage waveform.
- There should be no shut down if the array power exceeds the rated power. The output of the inverter will be limited to the nominal rating of inverter.
- The inverter should completely switch off at night and it should consume very small power, less than 0.5% of the nominal rating power.

Maximum Power Point Tracker (MPPT)

Since the voltage and current at maximum power point vary with both insolation level and temperature, it is usual to include the control equipment to follow the maximum power point of the array commonly known as Maximum Power Point Tracker (MPPT). The MPPT is an electrical circuit, which can control the effective load resistance of the PV array and thus control the operating point on the I-V characteristic. Often the MPPT operates by checking the power levels on either side of the operating point at regular intervals. If a gain in power is observed in one direction, then the MPPT moves the operating point in that direction until it reaches the maximum value. For grid connected PV systems, the MPPT is often incorporated into the inverter for ease of operation, although it is possible to obtain the MPPT as an independent unit. So the inverter is the Power Conditioning Unit, and, in addition to the conversion of DC to AC power, it ensures the optimum utilisation of PV array using MPPT and power quality and safety to the utility grid.

2.5.2 Inverter topologies

An inverter has to fulfil three main functions in order to feed energy from a PV array into the utility grid [16]:

- To convert PV array output current into AC current
- To shape the output waveform into perfect sinusoidal waveform
- If the array voltage is lower than the grid voltage, the PV array voltage has to be boosted to match the grid voltage.

The way that these three functions are sequenced within an inverter design determines the choice of semiconductors and passive components and consequently leads to various topologies.

Line commutated inverter

Based on drive system technology the first PV inverters at the end of the 1980s were line-commutated inverters. In line-commutated inverters, thyristors (SCR, Silicon Control Rectifier) are used as switching elements, and the line voltage serves to turn off a pair of thyristors in the inverter module when a subsequent pair of thyristors is fired [17,18]. By changing the firing delay time of the thyristors with respect to the zero crossing of the line voltage, the average DC voltage can be controlled such that it matches the array voltage. Any difference between the average DC voltage and array voltage will result in an increasing or decreasing DC current. With proper control of the thyristor firing angle, the PV array can be loaded to its maximum power point. In this type of inverter, the line current will always be lagging the line voltage which results in a poor power factor. The line-commutated inverters may be designed with or without a low frequency transformer in the line side [16]. A line-commutated inverter with transformer on the line side is shown in Figure 2-9. Although these types of inverters are robust, efficient and cheap, their major drawbacks are low power factor, which has to be compensated by drawing reactive power from the grid with special filters as well as high harmonic current in the output current.

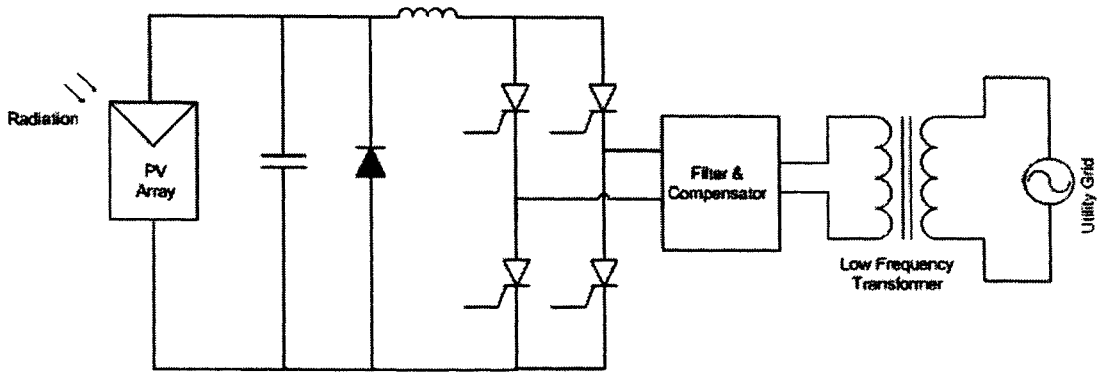

Figure 2-9 Schematic diagram of line commutated inverter

Self-commutated inverter

Due to the rapid developments in the semiconductor device industry, thyristors have been increasingly replaced by MOSFETs and IGBTs, and today PV inverters are mostly self-commutated inverters. The self-commutated inverter consists of a Pulse Width Modulation (PWM) full bridge, mostly using IGBTs or a combination of IGBTs and MOSFETs [16]. A self-commutated inverter with IGBTs as switching elements is shown in Figure 2-10. By alternatively closing pairs of switches a pulse width modulated rectangular voltage can be generated such that the voltage contains both a fundamental (50 Hz) and higher frequency components. The filter blocks high frequency components. Lower harmonic distortion can be achieved by using higher switching frequencies. But switching losses will increase with higher frequencies and overall efficiency will be lower. Self-commutated inverters are line synchronised, they can be easily connected to the grid. This inverter type has the advantage of power factor near to unity.

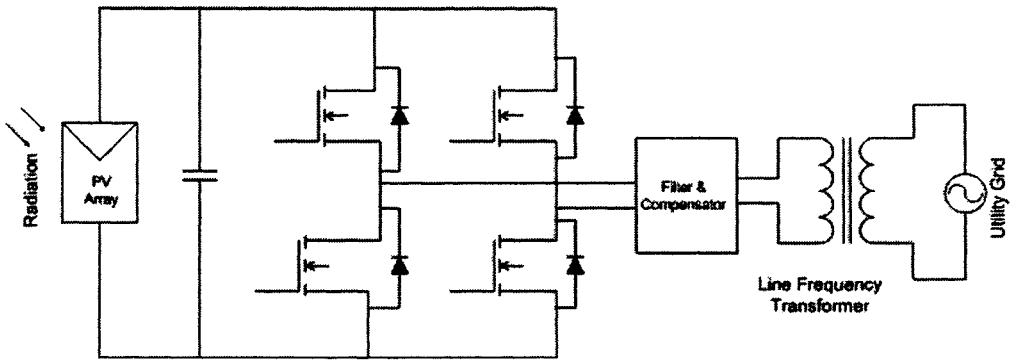

Figure 2-10 Self commutated inverter

Multi stage converters with high frequency transformer

A low frequency transformer in a standard inverter with pulse width modulation is a very heavy and bulky component. When a high frequency transformer (20 kHz) is used, the inverter will be smaller and lighter [16]. This type of inverter needs more additional stages compared with the self commutated inverters. The block diagram given in Figure 2-11 (a) illustrates the operation of a multistage converter. In the first stage, the PV array output is converted to high frequency pulse width modulation voltage which appears at the primary side of the high frequency transformer. At the secondary side, the voltage is rectified and filtered to remove the high frequency components. The output inverter unfolds the rectified current to 50Hz alternating current. A multistage converter with high frequency transformer is shown in Figure 2-11 (b).

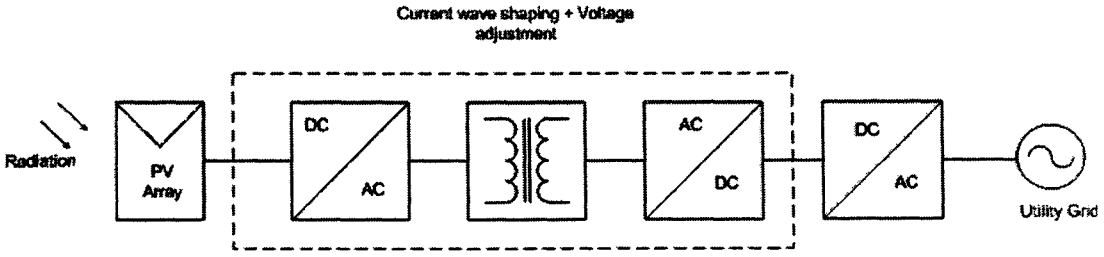

(a) Block Diagram

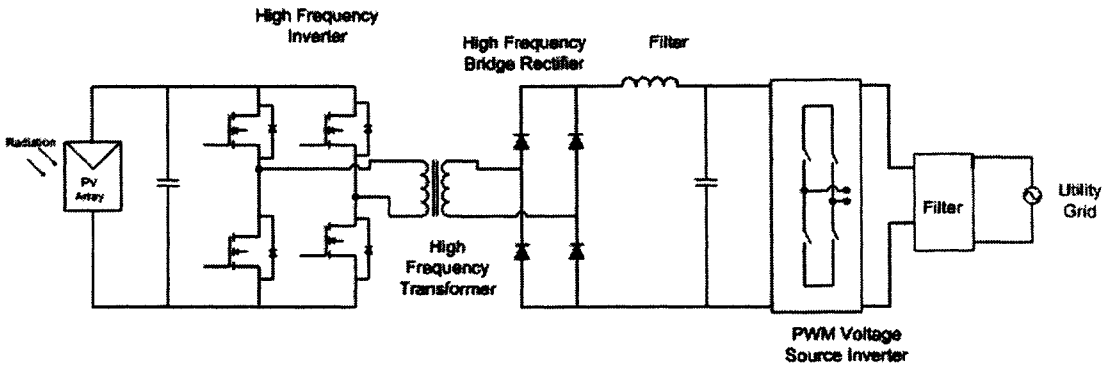

(b) Schematic Diagram

Figure 2-11 Multistage converter with high frequency transformer

Multistage converters without high frequency transformer

In this type of inverter, there is no transformer in order to reduce magnetic components and to increase efficiency. The operation of this type of inverter is

illustrated in Figure 2-12. In the first stage the boost converter is used to boost the low PV voltage, while the shaping and inverting of the output current have to be done in the second stage (inverter & filter). Some of the unique features of these inverters are high efficiency, low no load losses, low harmonic current, low weight and small size. The main disadvantage of these inverters is the high cost per watt [16]. Further disadvantages are the difficult and expensive replacement in case of inverter fault and special safety requirements that may increase the system price.

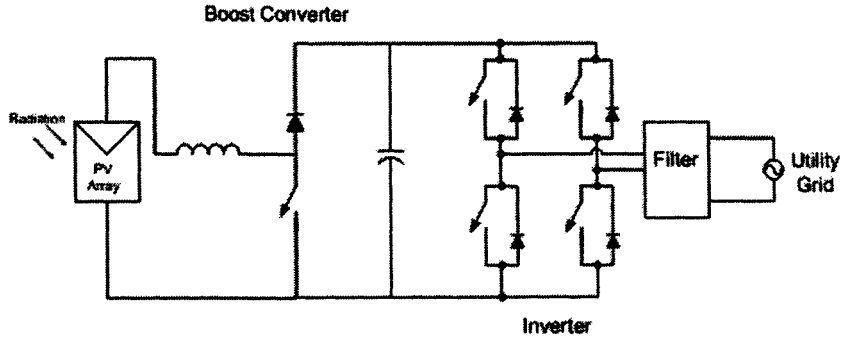

Figure 2-12 Multistage converter without transformer

2.5.3 Evolution of PV inverter concepts

In the grid connected PV systems, the PV module and inverter can be connected in different ways. Depending on this, the inverter configurations can be classified into [16,17]

- Central Inverters
- Module Integrated or Module Oriented Inverters
- String Inverters
- Multi String Inverters

Central inverters

In the central inverter concept, only one inverter is used for the whole PV plant. A schematic diagram for the central inverter concept is shown in Figure 2-13. Line commutated inverter and self-commutated inverter topologies can be used for this concept. Most inverters on the market in the mid 1990s were self commutated or line

commutated central inverters. The disadvantages of all central inverters topologies are:

- Required DC wiring increases cost and decreases safety.
- Shadow from trees or surrounding buildings on a PV module will affect power output from a string. In this inverter concept, there are no means of independently operating sections of the PV array at their maximum power point.
- Due to the large size, a modular, flexible or extensible design is harder.

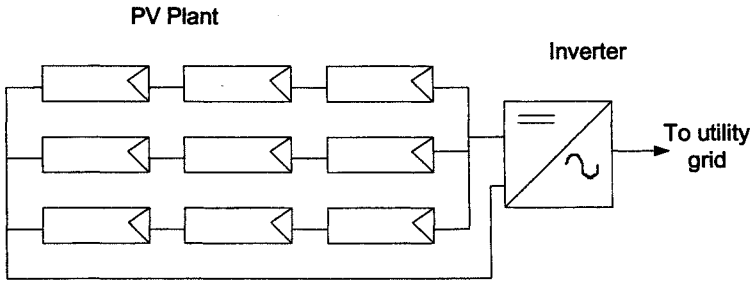

Figure 2-13 Concept of central inverter

Module integrated or module oriented inverters

These inverters are built and operated directly within one or several PV modules. Module integrated inverters provide the highest system flexibility. Because of this configuration, there is no need for DC wiring and each module has its own maximum power point tracking controller. This concept reduces mismatch losses and losses due to shading. Inverter topologies such as self commutated inverter with transformer, multistage inverter with high frequency transformer and multistage inverter without transformer can be used for this concept. Some of the disadvantages are:

- This concept leads to high cost and difficult and expensive replacements of faulty modules and hence it needs more safety requirements.
- Operate in a high temperature environment adjacent to the module.

Because more inverters are used in this concept, it leads to more cost at present. However with mass production of these inverters, the cost of inverters will be reduced. The concept of the module-integrated inverter is illustrated in Figure 2-14.

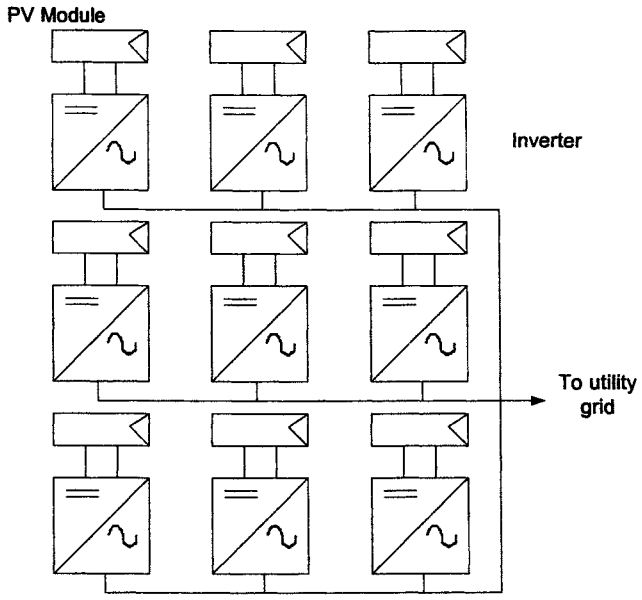

Figure 2-14 Module integrated inverter

String inverters

String inverters are designed for a system configuration of one string of PV modules. The string inverter is capable of combining the advantages of both central and module integrated inverters. A schematic diagram for the string inverter concept is illustrated in Figure 2-15. Various topologies including line-commutated inverters, self-commutated inverters and multistage converters can be used for this concept. The advantages are that string inverters are used in a higher power range, which decreases the price per watt and the system efficiency is higher than in systems with central inverters [16]. The total cost of all string inverters in a system is generally higher than the cost of a central inverter.

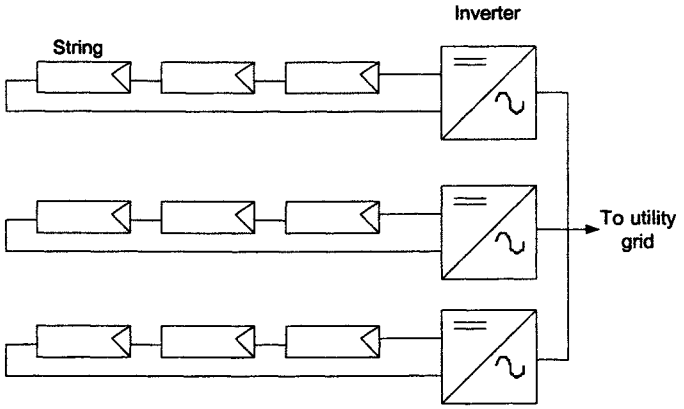

Figure 2-15 Concept of string inverter

Multi string inverters

The multi string inverter is the recent development in the concept. It takes the advantages of the higher energy yield of string inverters with the lower cost of central inverters [16]. Lower power DC-DC converters are connected to individual PV strings. Each PV strings has its own maximum power point tracker which independently optimises the energy output from each PV string. All DC-DC converters are connected via a DC bus through a central inverter to the grid. Multi string inverter concept is illustrated in Figure 2-16.

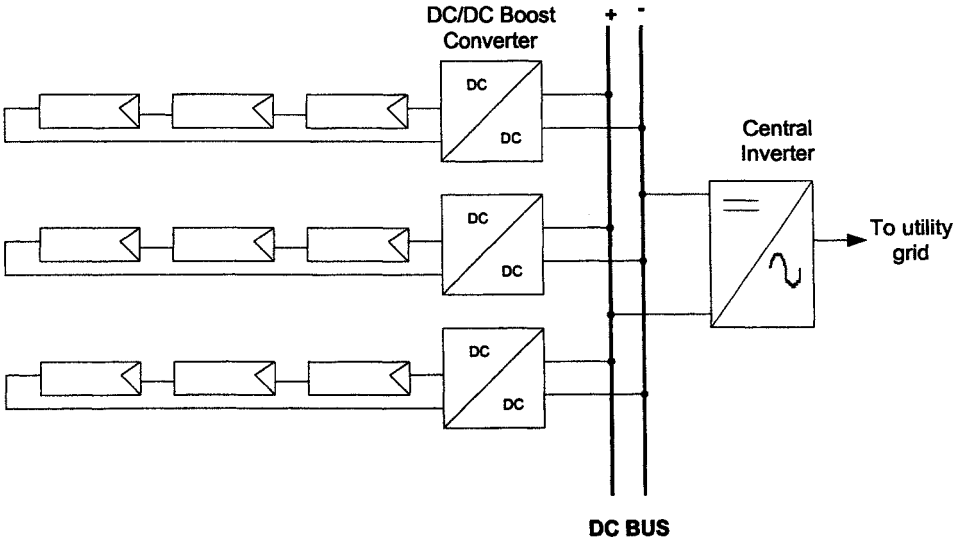

Figure 2-16 Concept of multi string inverter

The market share for each type of inverter topology is discussed in chapter 4. The calculation of inverter losses and AC power output using the efficiency curve of the inverter are also discussed in chapter 4.

2.6 References for Chapter 2

1. Godfrey Boyle, "Renewable Energy – Power for a Sustainable Future", Chapter 1, Oxford University Press in association with the Open University, 1996.
2. "Digest of United Kingdom Energy Statistics 2004", Published by The Stationary Office, Norwich, UK available at www.dti.gov.uk.

3. UK Renewable Energy Policy information available at websites www.dti.gov.uk/energy/renewables and www.restats.org.uk
4. Nick Jenkins, Ron Allan, Peter Crossley, Daniel Kirschen and Goran Strbac, "Embedded Generation", Chapter 1, London: Institution of Electrical Engineers, 2000.
5. Friedrich Sick and Thomas Erge, "Photovoltaics in Buildings – A Design Handbook for Architects and Engineers", Published by James & James (Science Publishers Ltd.), 1998.
6. Mukand R. Patel, "Wind and Solar Power Systems", CRC Press, 1999.
7. The future for renewable energy – Prospects and Directions, EUREC Agency, Published by James and James Ltd., 2002.
8. Mary D. Archer, Robert Hill, "Clean Electricity from Photovoltaics", Series on Photoconversion of Solar Energy – Vol.1, Chapter 1-4, London, Imperial College Press, 2001.
9. L.L. Grigsby, "The Electric Power Engineering Handbook", Chapter 1, CRC Press in cooperation with IEEE Press, 1998.
10. M. A. Green, K. Emery, D. L. King, S. Igari and W. Warta, "Solar cell efficiency tables (Version 25)", Progress in Photovoltaics: Research and Applications, Vol.13, 2005, pp. 49-54.
11. T. Ikegami, T. Maezono, F. Nakanishi, Y. Yamagata and K. Ebihara, "Estimation of equivalent circuit parameters of PV module and its application to optimal operation of PV system", Solar Energy Materials and Solar Cells, Vol. 67, Issues 1-4, pp. 389 – 395, 2001.
12. O. Wasynczuk, "Modeling and dynamic performance of a line-commutated photovoltaic inverter system", IEEE Transaction on Energy Conversion, Vol. 4, No. 3, pp.337 – 343, September 1989.
13. Mono crystalline silicon PV module data sheet obtained from www.bpsolar.com
14. "Trends in photovoltaic applications survey report of selected IEA countries between 1992 and 2003", Report IEA-PVPS T1-13: 2004, Published by International Energy Agency, available at www.iea-pvps.org
15. Engineering Recommendation G83/1 – Recommendation for the connection of small scale embedded generators (up to 16 A per phase) in parallel with public low voltage distribution networks, Electricity Association, UK, 2003.

16. M. Calais, J. Myrzik, T. Spooner and V. G. Agelidis, "Inverters for single-phase grid connected photovoltaic systems - An overview", Proceedings of 33rd annual IEEE Power Electronics Specialist Conference, Vol.4, pp. 1995-2000, 2002.
17. H. Haeberlin, "Evaluation of inverters for grid connected PV-systems from 1989 to 2000", 17th European Photovoltaic Solar Energy Conference, Munich, Germany, Vol. 1, pp. 426 – 430, 2001, Published by WIP – Renewable Energies and ETA Florence.
18. A. T. Veltman, R. Wiecherink, R.J. Burgel, S.W.H. de Haan, E. Widenbeest, S. Cervenka and J. Colin, "Test results of inverters for grid connected photovoltaic systems", 11th E.C. Photovoltaic Solar Energy Conference, Switzerland, 1992, pp. 1175 – 1179, Published by Harwood Acadamic Publishers GmBh Switzerland.

3 Generation of Solar Radiation Data

As explained in Chapter 2, factors which affect the power output from a PV system are solar irradiation, module operating temperature, shading, mismatch of modules in a string and resistance of wires and cables [1]. PV modules respond almost instantaneously to the variation in solar radiation and this causes power output from PV systems to vary correspondingly. To investigate the effect of large-scale adoption of PV systems on the electricity transmission network, the representation of solar radiation is very important since this dictates the power output of PV systems. This chapter discusses the solar radiation properties and explains the needs and methods to generate representative synthetic solar radiation data.

3.1 Solar Radiation Theory

The radiation outside the earth's atmosphere, extraterrestrial radiation, varies due to the apparent motion of the sun, while irregular variation in terrestrial radiation, which occurs inside the earth's atmosphere, is caused by climatic conditions such as cloud cover, atmospheric water vapour content, dust content and ozone content. Several calculations are most conveniently done using normalised radiation levels, that is the ratio of actual radiation level to extraterrestrial radiation [2].

3.1.1 Extraterrestrial radiation

The radiation emitted by the sun and its spatial relationship to the earth results in a nearly constant intensity of solar irradiance at the edge of the earth's atmosphere. However, there are two sources of variation in extraterrestrial radiation. The first is the variation in radiation emitted by the sun. It has been suggested that there are small variations less than ±1.5% with different periodicities and variation related to sunspot activities [2]. The second is the variation of the sun-earth distance, which leads to a variation of extraterrestrial radiation flux in the range ±3%. The dependence of extraterrestrial radiation with time of the year is given as [2]

$$G_{on} = G_{sc}\left(1+0.033\cos\left(\frac{360n}{365}\right)\right) \tag{3.1}$$

G_{on} is the extraterrestrial radiation measured on the plane normal to the radiation on the n^{th} day of the year.

The solar constant (G_{sc}) is the energy from the sun, per unit time, received on a unit area of surface perpendicular to the direction of propagation of the radiation, at mean earth-sun distance, outside of the atmosphere. The World Radiation Centre (WRC) has adopted a value of 1367 W/m^2, with an uncertainty of the order of 1% [2].

Extraterrestrial radiation for a horizontal surface (G_o) at any time between sunrise and sunset is given by

$$Go = Gsc\left(1 + 0.033\cos\left(\frac{360n}{365}\right)\right) * \left(\sin\delta\sin\phi + \cos\phi\cos\delta\cos\omega\right) \tag{3.2}$$

where,

ϕ is the latitude angle

δ is the declination angle, given as

$$\delta = 23.45\sin\left(360\frac{284+n}{365}\right) \tag{3.3}$$

ω is the hour angle, which is the angular displacement of the sun east or west of the local meridian due to rotation of the earth on its axis. The hour angle is zero degrees at solar noon and the angular displacement is 15^0 per hour with respect to solar noon, morning negative, afternoon positive.

The daily total of extraterrestrial irradiation on a horizontal surface, H_o (J/m^2), is obtained by integrating Equation (3.2) over the period from sunrise to sunset, which gives [2]:

$$H_o = \frac{24*3600*G_{sc}}{\pi}\left[1+0.033\cos\left(\frac{360n}{365}\right)\right]*\left[\cos\phi\cos\delta\sin\omega_s + \frac{2\pi\omega_s}{360}\sin\phi\sin\delta\right] \tag{3.4}$$

where ω_s is the sunset hour angle given as

$$\omega_s = \cos^{-1}\left(-\tan\phi\tan\delta\right) \tag{3.5}$$

The hourly total of extraterrestrial irradiation on a horizontal surface, I_o (J/m^2), is obtained [2] by integrating Equation (3.4) for a period defined by hour angles ω_2 and ω_1. Hence

$$I_o = \frac{12*3600*G_{sc}}{\pi}\left[1+0.033\left(\frac{360n}{365}\right)\right]*\left[\cos\phi\cos\delta\left(\sin\omega_2-\sin\omega_1\right)+\frac{2\pi\left(\omega_2-\omega_1\right)}{360}\sin\phi\sin\delta\right] \tag{3.6}$$

3.1.2 Global horizontal radiation

Extraterrestrial radiation at the top of atmosphere reduces as it passes through the earth's atmosphere due to the variability of the weather conditions. As a method of measuring this reduction, clearness index (k_t) is defined as the ratio of global horizontal irradiation (I) to hourly extraterrestrial radiation on a horizontal surface (I_o) [2]. Hence

$$k_t = \frac{I}{I_o} \tag{3.7}$$

The global horizontal radiation (I) consists of two parts namely beam radiation (I_b) and diffuse radiation (I_D). Beam radiation is the solar radiation received from the sun without having been scattered by the atmosphere and diffuse radiation is the solar radiation received from the sun after its direction has been changed, by scattering through the atmosphere.

3.1.3 Tilted radiation

In roof integrated PV systems PV modules can be mounted on sloped roofs or on flat roofs. In the case of PV systems mounted on the sloped roofs, PV modules are usually tilted at the angle of the roof. In flat roofs, PV modules can be integrated in two different ways. One way is for the PV modules can be integrated horizontally to use most of the floor area. This method is not usually followed in practice because of low solar yield and dirt accumulation problems. Another way is for the PV modules to be tilted at an optimum angle to gain the maximum radiation [3] and is the common practice to integrate PV modules in flat roofs. In façade PV systems, PV

modules can be integrated with the façade, in which mostly PV modules are placed vertically. So in most solar energy systems PV arrays are tilted at some angle with respect to the horizontal surface. A crucial input required in the transient simulation of solar energy system is the radiation incident on tilted surfaces. Global radiation on a tilted surface consists of three main components. They are beam radiation, diffuse radiation and ground reflected radiation [2].

The beam radiation component is the direct solar radiation received on the tilted surface.

The diffuse radiation component is the solar radiation received on the tilted surface from the sun after scattering through the atmosphere. The diffuse radiation is composed of three parts; isotropic diffuse, circumsolar diffuse and diffuse from the horizon. The distribution of diffuse radiation over the sky dome is shown in Figure 3-1. The first part is an isotropic part, received uniformly from the entire sky dome. The second part is the circumsolar diffuse, received from forward scattering of solar radiation and concentrated in the part of the sky around the sun. The third part is horizon brightening, concentrated near the horizon, and is most pronounced in clear skies.

Ground reflected radiation is the solar radiation received on the tilted surface after it has been reflected by the ground. The ground reflectance is also referred to as albedo.

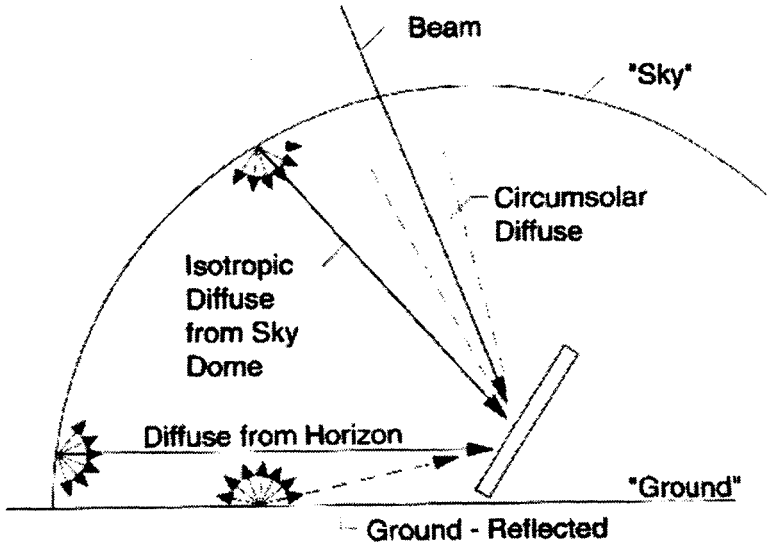

Figure 3-1 Illustration of tilted radiation components (Source: [2])

3.2 Literature Review

Solar radiation is the major factor which affects the power output of PV modules. The global solar radiation shows not only regular yearly or daily variations but also a random behaviour due to weather conditions. It is necessary to use an appropriate data set for the horizontal insolation which can represent both long-term average insolation level and short-term variation. Most available data sets provide either average values or actual measured values. The former does not provide an adequate representation of the level of variation that can be expected in practice, whilst use of the latter would require selection of a particular period of data. The solar radiation data that represent short-term variation for longer time periods are necessary to analyse the impact of PV systems power output on the grid. Generating synthetic radiation values is often the only practical way to obtain solar radiation data that are representative of actual data in terms of short-term variability as well as for longer periods. Generated data that can represent the same statistical features of measured data can be used to study the PV systems power output pattern.

Several methods for the preparation of a representative solar radiation data set have been investigated. Previous attempts to model the solar radiation on horizontal surface have been done in different ways; using sunshine duration [4,5,7,25,26], stochastic methods [8,9,11-19], fuzzy logic method [20] and neural network techniques [21,22,23] each with its own advantages and disadvantages. Some researchers have modelled global solar radiation [4-9, 11-23], beam radiation [10,25] and diffuse radiation [26-31]. Some have investigated the relationship between these radiations [10,25,26,28-31], while others have attempted to model closely allied variables such as clearness index [12-19]. Researchers also used different sampling intervals, such as monthly [4,5,20,21,29], daily [9,10,12,18,22,29] and hourly values [8,13-19,23-31]. A review of these studies and selection of suitable methods to generate the solar radiation data are discussed in the following sections.

3.2.1 Global horizontal radiation models

The first correlation proposed by Angstrom [4] used sunshine duration data to estimate the monthly mean global radiation on a horizontal surface. Prescott [5,6] modified the Angstrom equation in a convenient form. But the Angstrom equation does not consider the effect of latitude and elevation. Gopinathan [7] suggested a model in terms of the latitude, elevation and percentage of possible sunshine. Goh and Tan [8] highlighted the disadvantages of the mathematical model, that the possible short term variations for time periods up to a few days caused by local changes in the weather are not reflected in the models even though such information is essential to the design. They concluded that solar radiation modelling could be improved through the use of stochastic models that account for short-term variation and correlation.

Stochastic models have been used to study stationary and sequential characteristics of series of global radiation. The purpose of some of these studies is to analyse the past data in order to infer statistical properties, which capture the observed empirical regularities of the series, and then use these properties to forecast its future behaviour. This methodology has been used in the study of daily and hourly series of global irradiation. In some of the work conducted, not only solar radiation series are statistically analysed, but also methods that enable generation of synthetic series of irradiation are proposed. The production of synthetic solar radiation sequences mostly has been done using the Auto Regressive and Moving Average (ARMA) method and the Markov Transition Matrix (MTM) method.

Goh and Tan [8] used the ARMA technique to generate an annual sequence of hourly irradiation data for a location in Singapore. Brinkworth [9] applied the ARMA method to model the daily irradiation sequences in the UK. Most of the seasonal variations in the solar radiation are due to the variations in extraterrestrial radiation, which can be accurately predicted. But the atmospheric transparency that depends upon many factors like cloud cover, water vapour content etc is the most difficult part for modelling. This problem can be removed by using the clearness index as a variable, since the clearness index is an indicator of the relative clearness of the

atmosphere. These arguments were recognised early by Liu and Jordan [10] who studied the statistical features of solar radiation, by treating the atmospheric transmittance (also called the clearness index) as the random variable instead of radiation itself.

Klein [11] applied statistical method to generate the solar radiation sequence using the clearness index as a variable. Following this many researchers carried out the production of synthetic daily or hourly solar radiation sequences by the ARMA and MTM methods, using the clearness index as the variable [12-19]. Klein [11] observed that the ARMA model generally suffers from an inability to reproduce some of the basic features of the probability of occurrence of radiation, that is, the probability distribution function for the observed radiation is bimodal while the mathematical nature of ARMA type of models forces it to have a Gaussian distribution. In order to solve this problem, Graham et al. [12] applied the inverse Gaussian mapping method to generate the daily synthetic solar radiation data. The problem of non-Gaussian distribution of the hourly values is accounted for in the Graham et al. [13] model using a function that maps the Gaussian to the beta distribution. The model developed by Graham et al. to generate the hourly synthetic solar radiation data was improved by Aguiar et al. [15]. Mapping techniques in all these models leads to greater complexity.

Researchers have compared the ARMA and MTM methods to generate the hourly solar radiation data [16,17]. Mustacchi et al. [16] generated hourly solar radiation for an Italian location using both ARMA and MTM methods and compared the results obtained from both methods with measured data. Lalaruhk Kamal et al. [17] generated hourly solar radiation for a location in Pakistan using both ARMA and MTM methods and compared the results obtained by both methods with measured data. In both cases, it was found that the MTM method was superior to ARMA methods to generate the solar radiation sequence. Aguiar et al. [18] used the MTM method to generate the daily solar radiation sequence using data from locations in Portugal, Azores Islands, Madeira Islands, Mozambique and France. The model and the matrices that are used in this study to generate the daily solar radiation series proved to be universal. Poggi et al. [19] used the MTM method for generating the hourly solar radiation for a location in France. From these previous studies, it can be

concluded that to generate the solar radiation data, the MTM method is a reliable simulator with the drawback of involving a large number of independent parameters.

Sen [20] applied fuzzy modelling to represent the relations between monthly averages of daily global solar radiation and sunshine duration measurement by a set of fuzzy rules. Many authors have used neural network techniques to generate the global solar radiation [21-24]. Mohandes et al. [21] modelled the monthly mean daily values of global solar radiation using the measured sunshine duration, with the neural network technique. Hontoria et al. [23] used a neural system called Multi Layer Perceptron (MLP) to generate the daily solar radiation series. Zufiria et al. [24] and Hontoria et al. [22] also used the MLP technique to generate the hourly solar radiation data. Even though the neural networks provide good results compared with other methods, in practise selection of appropriate topology as well as training algorithms may become difficult and may need many years of measured data. In this work the MTM method was selected since the MTM method is a simple and reliable method to generate the solar radiation data that can reproduce the basic statistical features of actual data, even with a lower amount of measured data. The MTM method was used to generate the synthetic solar radiation data that can represent the statistical behaviour of actual data. It is worth noting that this method does not predict solar radiation values in real time. In this work the MTM method was chosen for generating the solar radiation for different locations in the UK. This is the first study to generate synthetic solar radiation sequences for the UK, using the MTM method.

3.2.2 Horizontal diffuse radiation models

The knowledge of beam radiation and diffuse radiation on the horizontal surface is important for solar system modelling. Since these data are not measured for most of the sites, often modelling of direct or diffuse radiation is emphasised. There are two types of solar radiation models available in the literature, parametric models and decomposition models. Parametric models require detailed information of atmospheric conditions. Meteorological parameters frequently used as predictors include the type, amount, and distribution of clouds or other observations, such as the fractional sunshine, atmospheric turbidity and perceptible water content [6]. Iqbal

[25] correlated the diffuse and beam radiation with hours of sunshine duration. Gopinathan [26] estimated the diffuse radiation from the sunshine duration. Iqpal [27] developed a model, which takes into account the Rayleigh, ozone, gas, water and aerosol scattering transmittances.

The development of a correlation model to predict the direct or diffuse radiation using the other solar radiation is possible and known as a decomposition model. Decomposition models usually use information only on global radiation to predict the direct or diffuse radiation components. Early work by Liu and Jordan [10] showed a relationship between the global radiation and diffuse radiation on the horizontal surface. The ratio of diffuse horizontal radiation to global horizontal radiation is called the diffuse fraction. Liu and Jordan suggested a unique functional relationship using the clearness index and diffuse fraction. Their original correlation was developed for daily values. Many researchers have developed the diffuse fraction correlation for hourly intervals [28-31].

Orgill and Hollands [28] correlated the hourly diffuse fraction with the hourly clearness index values based on data from Canada. Erbs et al. [29] also developed the relation between the hourly diffuse fraction and hourly clearness index based on data from the United States. They found that the relationship is essentially the same as the relation developed by Orgill and Hollands, even though the data are from different locations. Reindl et al. [30] developed the correlation between the hourly diffuse fraction and hourly clearness index and also they developed the relationship considering other parameters like solar elevation, ambient temperature and relative humidity. Skartveit and Olseth [31] also carried out a similar type of study.

Wong et al. [6] studied different decomposition and parametric models and calculated the diffuse fraction for a location in Hong Kong. Among the decomposition models, they found that the results obtained from the Orgill and Hollands, Erbs and Reindl models with clearness index as variable were almost identical. The Reindl and Skartveit and Olseth models that use clearness index, solar elevation, temperature and humidity as variables, show larger deviation for higher clearness index values and for a lower solar angle. Comparing the parametric and decomposition models, Wong et al. suggested that if the precise atmospheric

information, such as optical properties of clouds, cloud amount, thickness, position and number of layers and turbidity were not available, decomposition models would be a good choice. Since detailed atmospheric information is needed in the parametric model, the decomposition model was chosen. Among the decomposition models, the Erbs model was chosen because of simplicity with good accuracy.

3.2.3 Global tilted radiation models

A crucial input required in the transient simulation of solar energy systems is the radiation incident on tilted surfaces. Tilted radiation values depend upon the tilt angle and orientation of the PV array. Dispersed PV systems will vary in their tilt angles and orientations of PV arrays. Measured tilted radiation data are available for a few sites corresponding to particular tilt angle and orientation. Therefore models are employed to estimate the tilted radiation from the measured global horizontal radiation. In the literature, for evaluating the global radiation on tilted surfaces, the solar radiation is divided into the three components: direct beam radiation, sky diffuse radiation and ground-reflected radiation [2, 32-36]. Modelling of the direct beam and ground reflected components are straightforward but modelling of the diffuse component is difficult. The diffuse component depends upon its distribution over the sky. The distribution depends particularly on the cloud cover and also on the spatial distribution and other atmospheric components. Therefore, modelling of the diffuse component becomes difficult. Models differ generally in their treatment of the sky diffuse component, which is considered as the largest potential source of computational error [2].

Global tilted radiation models can be broadly classified into isotropic and anisotropic models. Liu and Jordan [32] proposed an isotropic model, which is the simplest of tilted surface models. The isotropic model assumes that all of the diffuse radiation is uniformly distributed over the complete sky dome i.e., it is independent of the azimuth and zenith angles. This isotropic model considers only the isotropic diffuse component for the calculation of diffuse radiation on tilted surface. Under completely cloudy skies, the isotropic model becomes a good approximation. As skies become clearer, the validity of the isotropic model deteriorates due to the presence of circumsolar and horizon brightening anisotropic effects.

Since the anisotropic behaviour of circumsolar diffuse radiation becomes more pronounced in the clear skies, Hay et al. [33] developed the anisotropic model, which takes into account the isotropic and the circumsolar components. The authors defined an anisotropic index to weight the circumsolar and isotropic radiation components. Under clear skies, the anisotropic index will be high and the circumsolar diffuse is weighted more heavily than the isotropic diffuse. Under the cloudy skies, anisotropic index goes to zero and all diffuse components are treated as isotropic. In this model the horizon brightening contribution was neglected.

Temps and Coulson [35] improved the Hay model by introducing a correction factor to the isotropic diffuse radiation to include the horizon brightening effects. This correction factor pertains to the clear sky conditions only. Klucher [34] modified this correction factor by a modulating factor to account for cloudiness. This modulating factor forces the anisotropic correction factor to approach unity under cloudy sky conditions so that the model reduces to the isotropic sky model. Perez et al. [36] developed a model which incorporates all three subcomponents to account for circumsolar diffuse, horizon diffuse and isotropic diffuse radiation. The contribution of diffuse radiation from the circumsolar, isotropic and horizon regions is determined by the empirically derived coefficients. The empirical coefficients are derived based on data from France locations. This model was simplified to the Perez2 [37] model, which uses a point source circumsolar region with empirical coefficients derived from US locations.

Attempts have already been made by various investigators to test the applicability of isotropic and anisotropic models for different locations around the world. In some cases anisotropic models are found be superior [38, 40], and in some cases both models are found to give results of similar accuracy [39]. Ma and Iqbal [38] compared the isotropic, Kluchers and Hay models for hourly tilted irradiation calculation using the data recorded at Woodbridge, Canada. Their study showed that the results obtained from isotropic and anisotropic models are similar during summer months and anisotropic models are superior to the isotropic model during the rest of the year for that station. The study showed that the Hay model produced underestimated values but with less error and fewer seasonal effects. Gobinathan

[39] has compared the isotropic and Hay model for estimating the monthly mean daily total irradiation on tilted surfaces for Lesotho in South Africa. He concluded that both the isotropic and anisotropic models are equally accurate. Reindl et al. [40] compared the isotropic model and four anisotropic models for calculating the hourly tilted irradiation values using data from different US locations. This study showed that the isotropic model showed the poorest performance and all the anisotropic models have comparable performance. They showed that the Hay model is simpler to use than Perez models and the study also found that there is no significant degradation of the tilted surface model performance when the diffuse radiation on the horizontal surface is estimated from a diffuse fraction correlation rather than obtained from measurements.

Since anisotropic models are superior to the isotropic model and the Hay model is simpler than other anisotropic models, the anisotropic Hay model was selected in this work to calculate the tilted radiation values. The Hay model requires global horizontal radiation and horizontal diffuse radiation values to calculate the tilted radiation values. Since there is no significant degradation in the performance of the tilted radiation model by using the diffuse radiation estimated from horizontal radiation, in this work the Erbs model was used to calculate the horizontal diffuse radiation from global horizontal radiation.

3.3 Markov Transition Matrix Method

As explained before, to generate the synthetic solar radiation data the simple and reliable MTM method was selected in this work. In this work to generate the synthetic horizontal solar radiation sequence the MTM was constructed, in which the clearness index values were used as a variable. The selected MTM method was used to generate solar radiation data for different locations in the UK and for different time periods: hour and half-hour time periods. The following sections discuss the selected MTM method and the steps followed to generate synthetic solar radiation data for different UK locations.

3.3.1 Markov Process

A stochastic process with the Markov property is known as a Markov process. A stochastic process has the Markov property if the future depends only on the present, not on the past; that is, if the probability distribution of future states of the process depends only upon the current state, and is conditionally independent of the past states. Consider a process that consists of a sequence $X_1, X_2, X_3, \ldots$ with the value of X_n being the state of the system at time n. The conditional distribution of any future state X_{n+1} knowing the past states $X_1, X_2, \ldots X_{n-1}$ and the present data X_n is independent upon the past states and depends only upon the present state. Such a stochastic process is known as a Markov process [43].

If $X_n = i$, the process is in state "i" at time "n", then a fixed probability TP_{ij} exists where the process will undergo a transition into state "j" at time "n+1". The transition probability TP_{ij} which indicates the probability that the system will be in state j given that the system is currently in state i, is given as

$$TP_{ij} = P\left(X_{n+1} = j \mid X_n = i\right) \tag{3.8}$$

Each particular Markov process may be identified with its matrix of transition probabilities called as a Markov Transition Matrix or Transition Probability Matrix. Let MTM denote the matrix of one step transition probabilities TP_{ij}, so that

$$MTM = \begin{bmatrix} TP_{11} & TP_{12} & \ldots & TP_{1n} \\ TP_{21} & TP_{22} & \ldots & TP_{2n} \\ TP_{31} & TP_{32} & \ldots & TP_{3n} \\ \cdot & & & \cdot \\ \cdot & & & \cdot \\ TP_{n1} & TP_{n2} & \ldots & TP_{nn} \end{bmatrix} \tag{3.9}$$

The transition probabilities can be calculated as

$$TP_{ij} = \frac{n_{ij}}{\sum_i n_{ij}} \tag{3.10}$$

Where n_{ij} is the number of transitions from the state i to state j.

3.3.2 Construction of the MTM

The steps involved in the construction of the MTM are:

1. *Determination of the Markov model states*

   The first step in the construction of the MTM is to define the number of states to characterise the Markov model. The clearness index values will vary from zero to one, used as a variable, to be divided into "n" number of states. In previous studies different numbers of states were defined to construct the MTM. Aguiar et al. [18] used a library of 10 matrices, each sized 10x10 to generate the daily solar radiation sequence. Poggi et al. [19] constructed 20x20 transition matrices for each month of a year to generate the hourly solar radiation sequence for a location in France. Mustacchi et al. [16] constructed 25x25 matrices for 12 different locations in Italy to generate the hourly solar radiation sequence. Kamal et al. [17] used four transition matrices of 7x7 size for the four seasons to generate the hourly solar radiation sequence for a location in Pakistan. In this study, instead of using monthly or seasonal matrices, the possibility of using a single yearly MTM to generate the horizontal radiation sequence for different UK locations was analysed. This is due to the low availability of measured data with a short time period. Hence to construct the detailed single matrix, the number of states was taken as 25. The clearness index values were divided into 25 states in steps of 0.04.

2. *Construction of the Markov Transition Matrix*

   The transition probabilities between states are elements of the MTM. The following steps were used to calculate the transition probabilities between states:

   1. For every occurrence of clearness index value, states were numbered from 1 to 25.
   2. Each value in the sequence was placed in its state and a sequence of states obtained like (6,8,9,4...)
   3. Ordered pairs were formed, such as (6,8), (8,9), (9,4), ... by taking all contiguous pairs of states.

4. Each pair is an event and the number of occurrences of each event was calculated and the Transition Number Matrix was obtained.
5. The Transition Number Matrix was normalised to unity for each row by using the total number of events in the row resulted the Markov Transition Matrix.

3.3.3 Testing of the MTM

The quality of the Markov Transition Matrix can be analysed by checking the equilibrium or Ergodic property [16,19]. The procedure to test the equilibrium property of the MTM is explained as follows:

By raising the Markov Transition Matrix (MTM) to a high power "n", $\lim_{n\to\infty} MTM^n = R$, a new matrix called a Limiting Transition Matrix would be obtained.

Let $R = \begin{bmatrix} r_{11} & r_{12} & \dots & r_{1n} \\ r_{21} & r_{22} & \dots & r_{2n} \\ . & & & . \\ . & & & . \\ r_{n1} & r_{n2} & \dots & r_{nn} \end{bmatrix}$ is the Limiting Transition Matrix. Then

(a) The sum of all elements in each row should be equal to 1, given as $\sum_{j=1}^{n} r_{ij} = 1$.

(b) All the rows in the Limiting Transition Matrix should be equal and given as $r_{1j} = r_{2j} = \dots = r_{nj}$ for all j = 1, 2, ...n.

(c) If the Limiting Transition Matrix occurs, there should be a unique vector $r = [r_{1j}, r_{2j}, \dots r_{nj}]$ with the condition that $r.MTM = r$

If these conditions exist then the equilibrium or ergodic property of the MTM is proved.

The Limiting Transition Matrix represents the probability that a process in state "i" will be in state "j" after "n" transitions. After a large number of transitions, the Limiting State Probabilities (LSP), given as r_j (j = 1,2...n), represents the probability

of finding the system in state "j", which is known as the Marginal Probability (MP). The MP can also be calculated from the measured data, using the following equation

$$MP_j = \frac{n_j}{\sum_j n_j} \tag{3.11}$$

where n_j is the number of occurrences in state j.

3.3.4 Procedure for generating the global horizontal radiation data

This section explains the procedure to generate the hourly global horizontal radiation data. The MTM and marginal probability values were used to generate the horizontal solar radiation data. Using the marginal probability values the first hour of the day was generated and the following hours of the day were generated using the transition probabilities.

For any day, a sequence of k_t values was generated using the following procedure. The state of the first hour of the day was selected by using the following steps:

1. A random number (ε) between 0 and 1 was chosen.
2. Elements of marginal probabilities were added until their sum was greater than the random number. $\varepsilon \leq \sum_{x=1}^{i} MP_x$
3. Thus the state of the first hour of the day was chosen as "i".

The state of the following hours of the day was selected by using the following steps:

1. The state of the first hour of the day "i" was selected as explained.
2. The next random number (ε') between 0 and 1 was chosen.
3. Elements of transition probabilities in the row "i" were added until their sum was greater than the random number. $\varepsilon' \leq \sum_{x=1}^{j} TP_{ix}$
4. Thus the state of the second hour of the day was selected as "j".
5. The procedure was repeated for other hours until the sunset of the day.

Once the sequence of the states was generated, the corresponding clearness index values were generated by the mid-value or random value method (explained in the section 3.4.2). The generated clearness index values were multiplied by the

corresponding extraterrestrial radiation values to calculate the horizontal radiation values.

3.4 Generation of Hourly Horizontal Radiation for Single Location

3.4.1 Data acquisition

In order to investigate the Markov Transition Matrix method for generating the horizontal solar radiation, data from the Northumberland Building PV system were used. Northumberland Building is on the main city centre campus of Northumbria University in Newcastle upon Tyne which has a latitude of 54^0 59' N and longitude of 1^0 37' W. Hereafter this location will be identified as North East 1. The Northumberland Building PV system is a 39.5 kWp PV façade system. The PV façade comprises a total of 465 BP585 crystalline silicon PV modules, with 15 modules connected in each string and 31 strings connected in parallel [44]. The PV arrays are south east oriented, with the surface azimuth angle of -16.5^0. The measured global horizontal radiation data recorded for every minute for the year 1997 to 2001 were used to construct the MTM. In this study, the clearness index values were used as a variable. From the measured minute global horizontal radiation the hourly global horizontal radiation and hence the hourly clearness index values were calculated.

3.4.2 Investigation of different MTM methods

The generation of hourly horizontal solar radiation using the MTM method has been investigated previously, where the MTM was constructed for each month [19] or each season [17] or yearly [16]. In this study four different MTM methods were investigated to generate the horizontal radiation data for the UK. They are

- *Yearly Instantaneous MTM Method*

  Hourly instantaneous data were used to construct the MTM. All the five years data were used to construct a single MTM called yearly instantaneous MTM.

This MTM was used to generate instantaneous global horizontal radiation sequences.

- *Monthly Instantaneous MTM Method*

Hourly instantaneous data were used to construct the MTM. In this method, the corresponding data from each month from all the years were used to generate 12 monthly instantaneous MTMs. These 12 monthly instantaneous MTMs were used to generate instantaneous global horizontal radiation sequences.

- *Yearly Average MTM Method*

Five years of hourly averaged data were used to construct a single MTM called yearly average MTM. This MTM was used to generate hourly average global horizontal radiation data.

- *Monthly Average MTM Method*

Hourly averaged data were used to construct the MTM. Corresponding data from each month for all the five years were used to generate 12 monthly average MTMs. These 12 monthly average MTMs were used to generate average global horizontal radiation sequences.

In all these methods, after the construction of MTMs, the equilibrium of the matrices (Ergodic property) was tested. By the procedure explained in the previous section the state of each hour in the day was generated. After selecting the states of hours, the clearness index values were selected by the following two different methods.

- *Mid-Value Method*

In this case the clearness index value was chosen as the middle value of the selected interval. For example if the selected state is 1, where the interval is 0 – 0.04, the clearness index value was chosen as 0.02.

- *Random Value Method*

In this case the clearness index value was chosen as a random number in the selected interval. For example if the selected state is 1, where the interval is 0 – 0.04, the clearness index was chosen as a random value between 0 and 0.04.

The selected clearness index values for each hour were multiplied by the corresponding extraterrestrial radiation values to get global horizontal radiation values. The following sections explain the results obtained from the investigated methods.

3.4.3 Results from yearly instantaneous MTM method

The measured minute global horizontal radiation data were stored in an Excel sheet. A Macro was written to convert the minute data to hourly instantaneous data. Using these data the hourly clearness index values were calculated. The clearness index values were divided into 25 states, in intervals of 0.04, and the Transition Number Matrix was constructed (See Appendix A). The transition probability values were calculated for all events and the yearly instantaneous MTM was constructed (Provided in Appendix A)[2].

After the construction of the MTM, the equilibrium of the matrix was tested. When the matrix was raised to the power 35, the elements in each row of the matrix became equal, resulted in a Limiting Transition Matrix (See Appendix A) and hence the equilibrium of the matrix was proved. Limiting State Probabilities (LSP) from the Limiting Transition Matrix and Marginal Probabilities from measured data (Refer to Appendix A) were compared and plotted as shown in Figure 3-2. The comparison between Limiting State Probabilities and Marginal Probabilities were not well established for most of the states and particularly for low and high order states. However the constructed MTM can be used for generating the instantaneous horizontal solar radiation data since the equilibrium of the matrix was proved.

Using the procedure explained before, the states for each hour were selected. Once the states were selected the clearness index values were generated by mid-value method or random value method. For the first hour, the selected state was 10 corresponding to the interval 0.36-0.4. By the mid-value method, the middle value of the interval 0.38 was selected. By the random value method a random number between 0.36 and 0.4 was selected.

[2] MTMs for several cases are provided for reference in Appendix A.

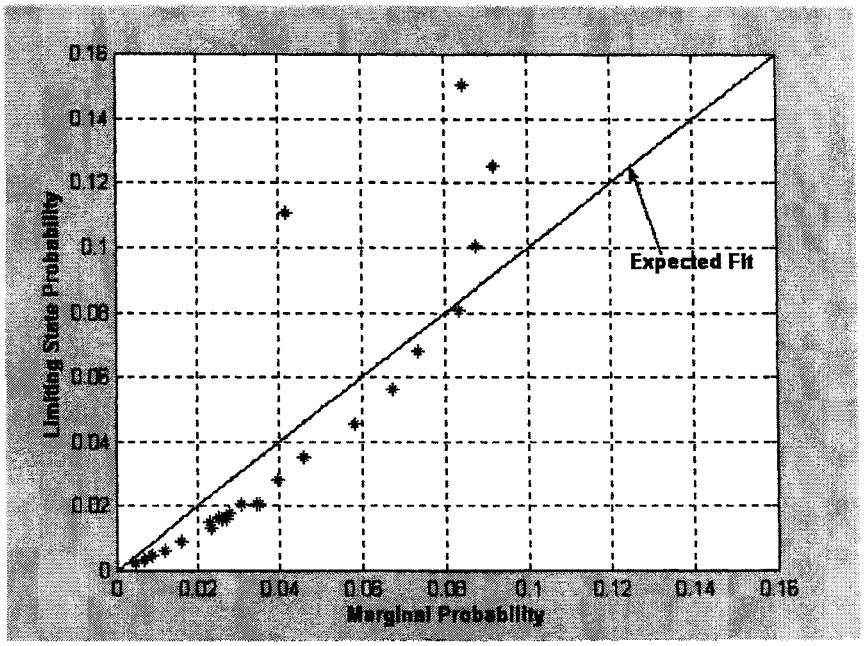

Figure 3-2 Comparison between MP and LSP from yearly instantaneous MTM

The selected clearness index values were multiplied by the corresponding extraterrestrial radiation values to get the hourly instantaneous horizontal radiation values. When a higher accuracy was needed it could be necessary to repeat the procedure until a sequence that will lie within the desired limit of accuracy. In this analysis the procedure was repeated until the daily total irradiation values were within the error limit, which was set as ±1%. An m-file was created to construct the MTM and to generate the synthetic radiation data using the MATLAB package.

Hourly instantaneous horizontal radiation data were generated for the North East 1 location, using the yearly instantaneous MTM, for the year 1996[3]. Latitude, longitude and daily total irradiation values were given as input. Hourly instantaneous radiation values were generated by both the mid-value and random value methods and compared with the measured data. In the literature, the statistical quantities Mean Bias Error (MBE), Root Mean Square Error (RMSE), Relative Mean Bias Error (RMBE) and Relative Root Mean Square Error (RRMSE) values were used to compare the generated and measured data [19]. MBE, RMSE, RMBE and RRMSE are defined in equations (3.12) to (3.15).

[3] Measured data for the year 1996 were not used to construct the MTM.

$$MBE = \frac{1}{N}\sum_{i=1}^{n}(M_i - C_i) \tag{3.12}$$

$$RMSE = \sqrt{\frac{1}{N}\sum_{i=1}^{n}(M_i - C_i)^2} \tag{3.13}$$

$$RMBE = \frac{1}{N}\sum_{i=1}^{n}\left(\frac{(M_i - C_i)}{M_i}\right) \tag{3.14}$$

$$RRMSE = \sqrt{\frac{1}{N}\sum_{i=1}^{n}\left(\frac{(M_i - C_i)^2}{M_i^2}\right)} \tag{3.15}$$

Where,

N is the number of observations made

M_i is the measured data and

C_i is the generated data

Poggi et al. [19] used these quantities to compare the daily total irradiation values. In this work, the radiation sequence was generated until the daily total irradiation values with in the error limit and hence hourly radiation values were compared. As explained before, the MTM method can generate a solar radiation sequence that represents the statistical behaviour of actual data in long term but not to predict the solar radiation values in real time. Hence there will be a difference between the measured and generated data. When the measured hourly radiation values were low, RMBE and RRMSE produced very high values and hence these are not useful comparison parameters. The MBE and RMSE quantities were used in this work to compare the generated and measured hourly radiation values. The RMSE indicates the accuracy of the model; the lower the RMSE, the more accurate is the model. The MBE value explains whether the generated data are overestimated or underestimated compared with measured data. The correlation coefficient value between generated and measured horizontal radiation data was also calculated. The statistical comparison results are given in Table 3-1. It can be observed that there is no significant difference in the results obtained from mid-value method and random value method.

The occurrences of clearness index values in each interval from the simulated data were compared with measured data and the result is shown in Figure 3-3. From this result it is observed that the simulated data by both mid-value and random value methods have a higher number of occurrences in the first state compared with the measured data. The number of occurrences in the high states (clearness index values greater than 0.76) is more in the simulated data compared with measured data. It is also observed that there is no significant difference between the mid-value and random value methods.

Table 3-1 Statistical comparison results for the yearly instantaneous MTM method

Methods	RMSE (W/m^2)	MBE (W/m^2)	Correlation Coefficient
Mid-Value Method	160	-0.02	77.1%
Random Value Method	159	-0.01	77.4%

3.4.4 Results from monthly instantaneous MTM method

In this method the hourly instantaneous clearness index values from the corresponding months were used to construct the monthly instantaneous MTMs. As an example, data from June months in 1997-2001 were used to construct the June instantaneous MTM (provided in Appendix A). Similarly for all months the MTMs were constructed and the equilibrium of matrices was tested and proved. The comparison between Limiting State Probabilities and Marginal Probabilities were not well established for all states and particularly in low and high states, which is similar to the yearly instantaneous MTM results (Appendix A). The instantaneous solar radiation data for the year 1996[4] were generated using 12 monthly MTMs.

[4] Measured data for the year 1996 were not used to construct the MTMs.

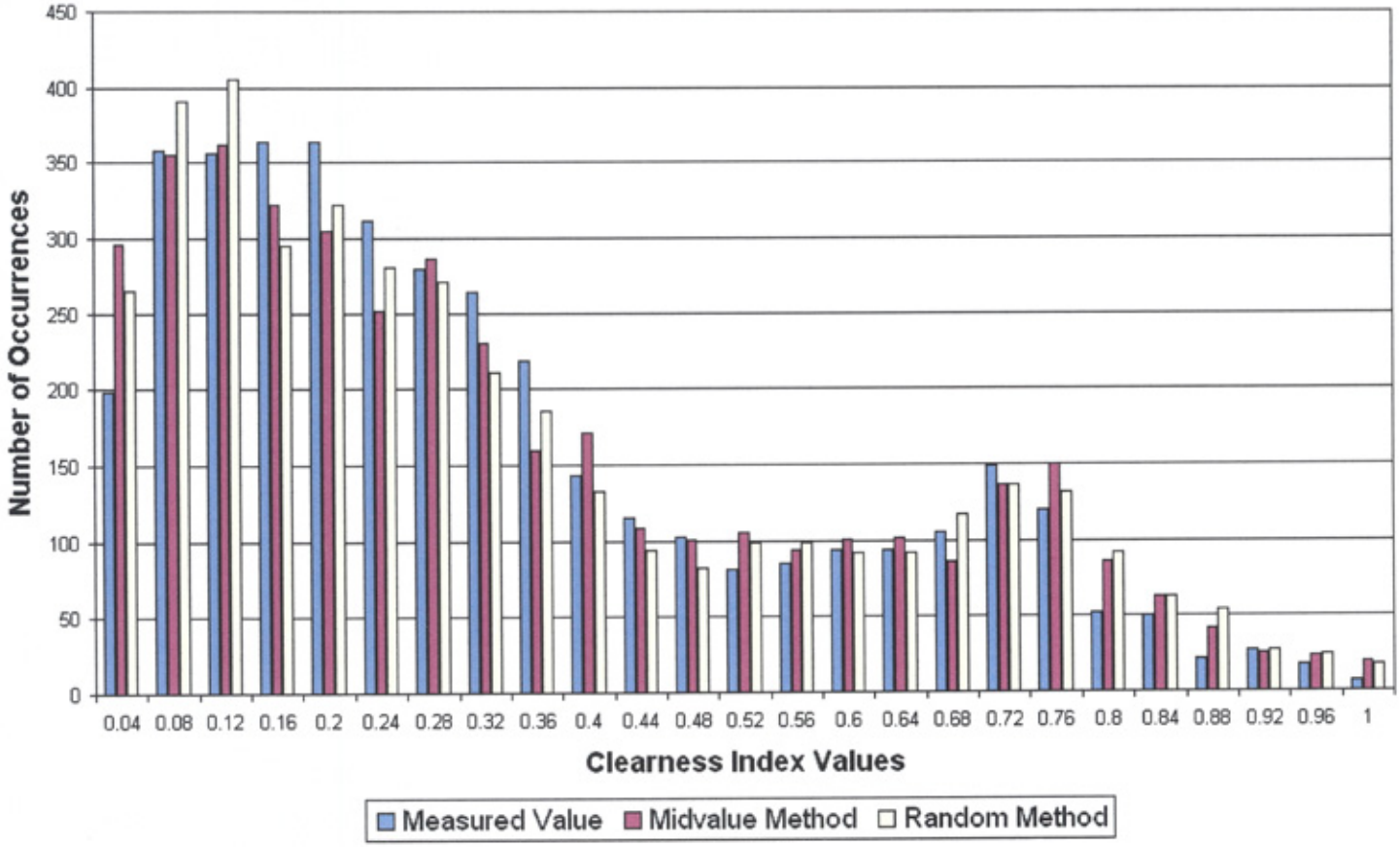

Figure 3-3 Comparison of clearness index occurrences between the generated series, obtained from the yearly instantaneous MTM, with measured series for the North East 1 location

The statistical comparisons between the simulated and measured data were calculated and results are given in Table 3-2. The RMSE and correlation coefficient values are similar to the results obtained from the yearly instantaneous MTM method. The MBE value is positive in the case of the mid-value method indicating the measured values are higher than simulated data whereas the MBE value is negative in the case of the random value method. The occurrences of clearness index value in each interval from the simulated data were compared with measured data as shown in Figure 3-4. From this result it is observed that the simulated data have more occurrences in the first state and in high states compared with measured data. In general these results are similar to the results obtained for the yearly instantaneous MTM method. It is observed that there is no improvement in results obtained by using 12 monthly instantaneous MTMs compared with single yearly instantaneous MTM results.

Table 3-2 Statistical comparison results for the monthly instantaneous MTM method

Method	RMSE (W/m^2)	MBE (W/m^2)	Correlation Coefficient
Mid-Value Method	158	0.02	77.6%
Random Value Method	159	-0.06	77.4%

3.4.5 Results from yearly average MTM method

In this method instead of using hourly instantaneous data, hourly average data were used. Measured minute global horizontal radiation data were stored in an Excel sheet. A macro was written to convert the minute data to hourly average data. Using these data the hourly clearness index values were calculated. The clearness index values were divided into 25 states, in intervals of 0.04, and the Transition Number Matrix was constructed (Appendix A). The Transition Number Matrix was used to calculate the transition probabilities and from these values the yearly average MTM was constructed (Appendix A). In the yearly average MTM, the value of elements along and close to the diagonal are high and also the transition to distant states are rare events. The probability of transition to distant states is higher in the yearly instantaneous MTM compared with yearly average MTM.

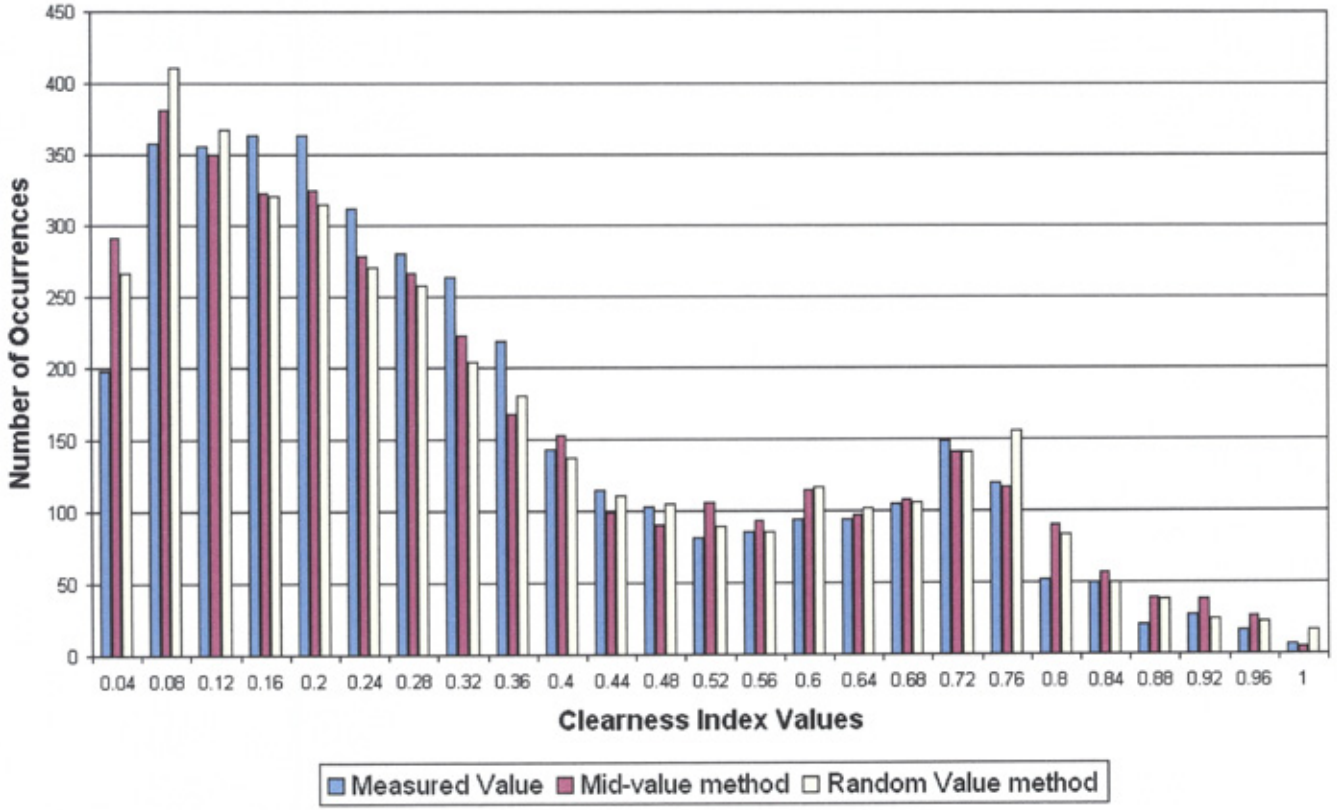

Figure 3-4 Comparison of clearness index occurrences in the generated series, obtained by the monthly instantaneous MTM method, with measured series for the North East 1 location

After the construction of the MTM the equilibrium of the matrix was tested. When the matrix was raised to the power 57, the elements in each row of the matrix became equal resulted a Limiting Transition Matrix (Appendix A). Limiting State Probabilities (LSP) from the Limiting Transition Matrix and Marginal Probabilities from the measured data were compared and plotted in Figure 3-5. A good agreement between these quantities is observed, which confirms that any row of the Limiting Transition Matrix gives the state probabilities. Thus the ergodic property of the MTM is well illustrated in this case compared with the yearly instantaneous MTM.

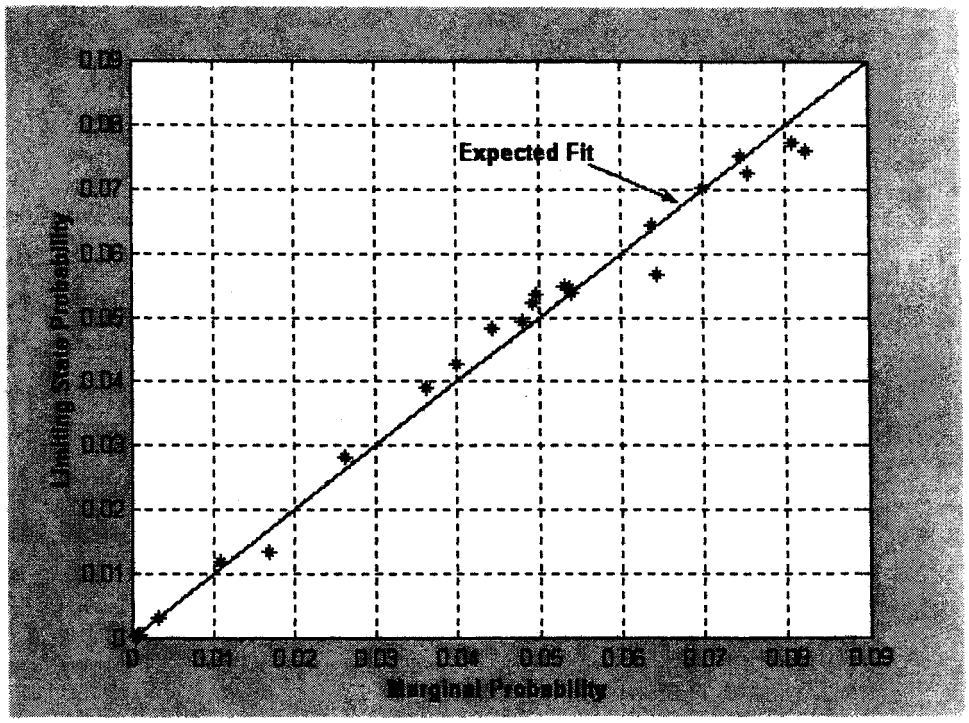

Figure 3-5 Comparison between MP and LSP from the yearly average MTM

Hourly average horizontal radiation data were generated for the North East 1 location, using the yearly average MTM, for the year 1996. The measured data for the year 1996 were not used for the construction of the MTM. Latitude, longitude and daily total irradiation values were given as input. Hourly averaged radiation values were generated by both mid-value method and random value method. Generated data were compared with measured data and the statistical comparison results are given in Table 3-3. From these results it was observed that the RMSE values obtained from the yearly average MTM method was lower compared with results obtained from the yearly instantaneous MTM method. In contrast, the

correlation coefficient values between measured and simulated data from the yearly average MTM method was higher compared with results obtained from the yearly instantaneous MTM method. In this method, the MBE values obtained from both mid-value and random value methods were low and positive. The occurrences of clearness index value in each interval from the simulated data were compared with measured data and the comparison result is shown in Figure 3-6. The simulated data by both mid-value and random value methods showed good agreement with measured data. These results indicate that the generated hourly average values have very good fit with measured data.

Table 3-3 Statistical comparison results for the yearly average MTM method

Method	RMSE (W/m^2)	MBE (W/m^2)	Correlation Coefficient
Mid-Value Method	104	0.04	88.3%
Random Value Method	104	0.04	88.2%

3.4.6 Results from monthly average MTM method

In this method the hourly average data from the corresponding months were used to construct the monthly average MTMs. The monthly average MTM constructed for June is given in Table 3-4. From this matrix it can be observed that the transition probabilities of all the elements corresponding to the rows 24^{th} and 25^{th} were zero. Similarly in many monthly average MTMs, all the elements in the high states were zero. The transition to distant states is low in the hourly average data and hence the elements in high states were zero, whereas it was possible to construct the monthly instantaneous MTM since the transition to distant states occurred in the instantaneous data. It may be possible to construct monthly average MTMs with more data and it may be used to generate the synthetic solar radiation data that is representative of actual data. However with less data available, the single yearly average MTM was able to generate representative synthetic data. Hence it will be the simple solution to use a single matrix to generate solar radiation data instead of using 12 matrices. Therefore, it was decided to use the yearly average MTM method to generate the synthetic solar radiation data.

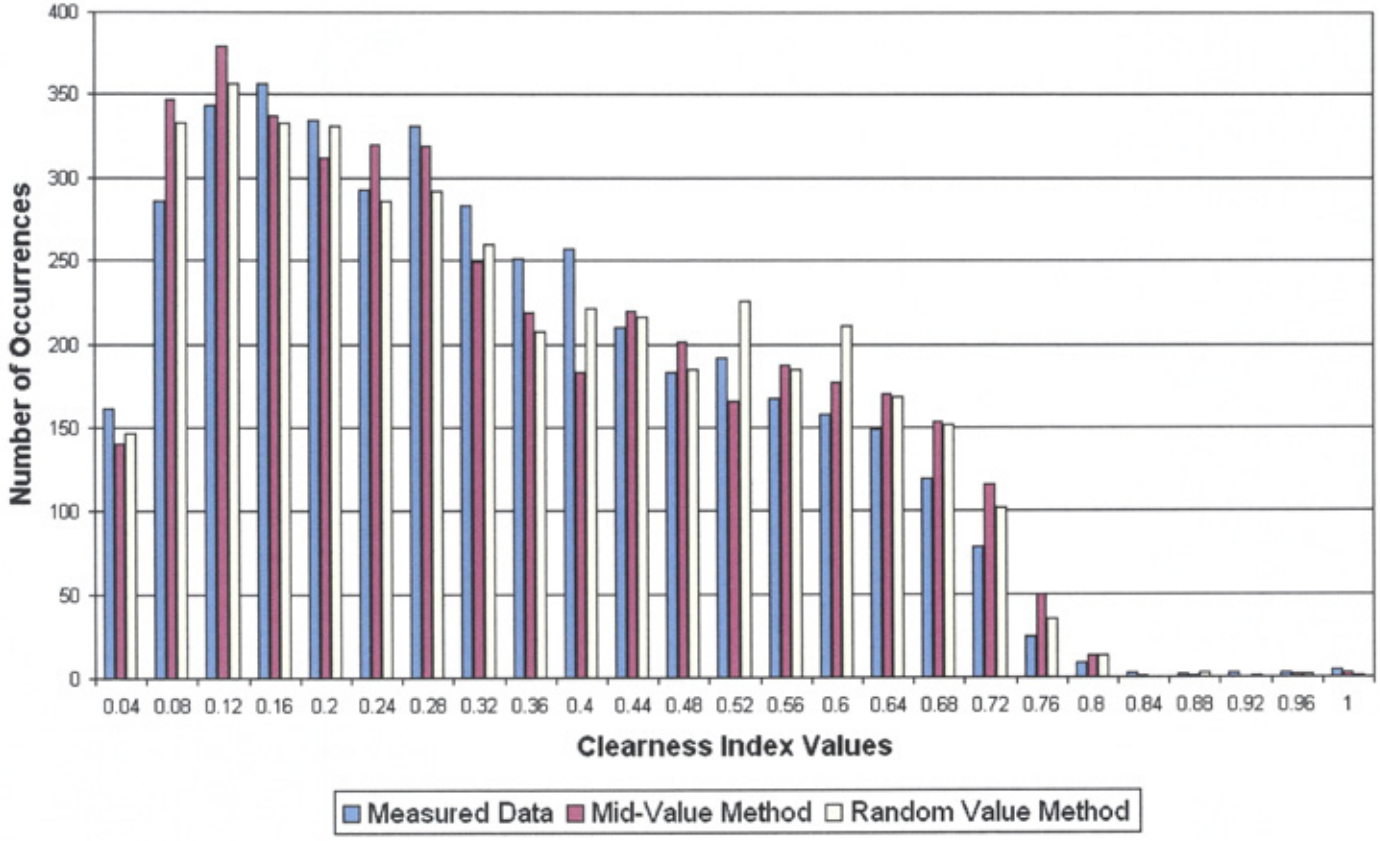

Figure 3-6 Comparison of clearness index occurrences in the generated series, obtained by yearly average MTM method, with measured series for the North East 1 location

Table 3-4 June month average Markov Transition Matrix

	State 1	State 2	State 3	State 4	State 5	State 6	State 7	State 8	State 9	State 10	State 11	State 12	State 13	State 14	State 15	State 16	State 17	State 18	State 19	State 20	State 21	State 22	State 23	State 24	State 25
State 1	0.3684	0.2632	0.1579	0.0526	0.0000	0.0526	0.0526	0.0000	0.0000	0.0000	0.0000	0.0000	0.0000	0.0000	0.0526	0.0000	0.0000	0.0000	0.0000	0.0000	0.0000	0.0000	0.0000	0.0000	0.0000
State 2	0.1023	0.3295	0.3068	0.1477	0.0682	0.0114	0.0114	0.0114	0.0000	0.0000	0.0000	0.0000	0.0000	0.0000	0.0000	0.0000	0.0000	0.0000	0.0000	0.0000	0.0114	0.0000	0.0000	0.0000	0.0000
State 3	0.0099	0.1824	0.3705	0.2235	0.1118	0.0412	0.0235	0.0118	0.0059	0.0000	0.0000	0.0099	0.0059	0.0099	0.0000	0.0000	0.0000	0.0000	0.0000	0.0000	0.0000	0.0059	0.0000	0.0000	0.0000
State 4	0.0054	0.0591	0.1720	0.2742	0.1989	0.1183	0.0860	0.0376	0.0161	0.0000	0.0054	0.0054	0.0000	0.0215	0.0000	0.0000	0.0000	0.0000	0.0000	0.0000	0.0000	0.0000	0.0000	0.0000	0.0000
State 5	0.0000	0.0339	0.0960	0.1977	0.1525	0.1582	0.1356	0.0678	0.0339	0.0339	0.0339	0.0169	0.0169	0.0000	0.0000	0.0000	0.0000	0.0000	0.0113	0.0056	0.0000	0.0000	0.0000	0.0000	0.0056	0.0000
State 6	0.0068	0.0000	0.0520	0.0925	0.1850	0.1603	0.0925	0.1445	0.0694	0.0405	0.0578	0.0520	0.0231	0.0116	0.0058	0.0058	0.0116	0.0000	0.0000	0.0000	0.0000	0.0000	0.0000	0.0000	0.0000	0.0000
State 7	0.0000	0.0069	0.0270	0.0676	0.1486	0.1351	0.1081	0.1081	0.1419	0.0405	0.0811	0.0270	0.0743	0.0135	0.0068	0.0135	0.0000	0.0000	0.0000	0.0000	0.0000	0.0000	0.0000	0.0000	0.0000	0.0000
State 8	0.0000	0.0000	0.0357	0.0357	0.0595	0.1488	0.1190	0.1429	0.1250	0.0952	0.0536	0.0536	0.0119	0.0417	0.0179	0.0179	0.0238	0.0119	0.0000	0.0000	0.0000	0.0000	0.0060	0.0000	0.0000	0.0000
State 9	0.0000	0.0000	0.0352	0.0423	0.0563	0.0704	0.1056	0.1408	0.1972	0.0634	0.0775	0.0563	0.0634	0.0423	0.0352	0.0000	0.0141	0.0000	0.0000	0.0000	0.0000	0.0000	0.0000	0.0000	0.0000	0.0000
State 10	0.0000	0.0084	0.0084	0.0168	0.0168	0.0840	0.0840	0.1261	0.0672	0.1176	0.1008	0.1176	0.0588	0.0504	0.0588	0.0252	0.0252	0.0168	0.0084	0.0084	0.0000	0.0000	0.0000	0.0000	0.0000	0.0000
State 11	0.0000	0.0076	0.0076	0.0000	0.0229	0.0382	0.0763	0.1069	0.1221	0.1298	0.0916	0.0992	0.0992	0.0534	0.0382	0.0534	0.0000	0.0305	0.0153	0.0076	0.0000	0.0000	0.0000	0.0000	0.0000	0.0000
State 12	0.0000	0.0000	0.0090	0.0090	0.0270	0.0180	0.0360	0.0450	0.0811	0.0811	0.1351	0.1261	0.0811	0.1081	0.0721	0.0450	0.0541	0.0360	0.0090	0.0270	0.0000	0.0000	0.0000	0.0000	0.0000	0.0000
State 13	0.0000	0.0000	0.0000	0.0086	0.0172	0.0345	0.0431	0.0776	0.0776	0.1379	0.0862	0.0603	0.1207	0.0862	0.1034	0.0603	0.0345	0.0172	0.0172	0.0172	0.0000	0.0000	0.0000	0.0000	0.0000	0.0000
State 14	0.0000	0.0000	0.0000	0.0000	0.0222	0.0111	0.0333	0.0667	0.0222	0.1000	0.1444	0.1222	0.0889	0.0667	0.1111	0.0556	0.0778	0.0444	0.0333	0.0000	0.0000	0.0000	0.0000	0.0000	0.0000	0.0000
State 15	0.0000	0.0000	0.0000	0.0000	0.0112	0.0337	0.0112	0.0225	0.0225	0.0449	0.0562	0.1236	0.1573	0.0899	0.1011	0.1348	0.1124	0.0674	0.0112	0.0000	0.0000	0.0000	0.0000	0.0000	0.0000	0.0000
State 16	0.0000	0.0000	0.0000	0.0000	0.0118	0.0236	0.0000	0.0588	0.0118	0.0353	0.0471	0.0000	0.1176	0.1294	0.1647	0.1059	0.1765	0.0588	0.0235	0.0235	0.0118	0.0000	0.0000	0.0000	0.0000	0.0000
State 17	0.0000	0.0000	0.0000	0.0000	0.0000	0.0103	0.0103	0.0103	0.0309	0.0309	0.0515	0.0206	0.0722	0.0515	0.0928	0.2062	0.1546	0.1856	0.0619	0.0103	0.0000	0.0000	0.0000	0.0000	0.0000	0.0000
State 18	0.0000	0.0000	0.0000	0.0000	0.0000	0.0000	0.0000	0.0000	0.0192	0.0385	0.0288	0.0192	0.0192	0.0385	0.0192	0.0769	0.2596	0.3942	0.0769	0.0096	0.0000	0.0000	0.0000	0.0000	0.0000	0.0000
State 19	0.0000	0.0000	0.0000	0.0000	0.0000	0.0000	0.0000	0.0000	0.0000	0.0364	0.0364	0.0364	0.0364	0.0000	0.0364	0.0364	0.0909	0.2727	0.4182	0.0000	0.0000	0.0000	0.0000	0.0000	0.0000	0.0000
State 20	0.0000	0.0000	0.0000	0.0000	0.0000	0.0000	0.0000	0.0000	0.0667	0.0000	0.0000	0.1333	0.1333	0.0667	0.0000	0.0667	0.0667	0.0000	0.2667	0.2000	0.0000	0.0000	0.0000	0.0000	0.0000	0.0000
State 21	0.0000	0.0000	0.0000	0.0000	0.0000	0.0000	0.0000	0.0000	0.0000	0.0000	0.0000	0.0000	0.0000	0.0000	0.0000	0.0000	0.0000	0.0000	0.0000	0.5000	0.5000	0.0000	0.0000	0.0000	0.0000	0.0000
State 22	0.0000	0.0000	0.0000	0.0000	0.0000	0.0000	0.0000	0.0000	0.0000	0.0000	0.0000	0.0000	0.0000	0.0000	0.0000	0.0000	0.0000	0.0000	0.0000	0.0000	0.0000	0.0000	0.0000	0.0000	0.0000	0.0000
State 23	0.0000	0.0000	0.0000	0.0000	0.0000	0.0000	0.0000	0.0000	0.0000	0.0000	0.0000	0.0000	0.0000	0.0000	0.0000	0.0000	0.0000	0.0000	0.0000	0.0000	0.0000	0.0000	0.0000	0.0000	0.0000	0.0000
State 24	0.0000	0.0000	0.0000	0.0000	0.0000	0.0000	0.0000	0.0000	0.0000	0.0000	0.0000	0.0000	0.0000	0.0000	0.0000	0.0000	0.0000	0.0000	0.0000	0.0000	0.0000	0.0000	0.0000	0.0000	0.0000	0.0000
State 25	0.0000	0.0000	0.0000	0.0000	0.0000	0.0000	0.0000	0.0000	0.0000	0.0000	0.0000	0.0000	0.0000	0.0000	0.0000	0.0000	0.0000	0.0000	0.0000	0.0000	0.0000	0.0000	0.0000	0.0000	0.0000	0.0000

3.4.7 Discussion

The generation of instantaneous and average horizontal solar radiation data using monthly and yearly MTM methods was investigated. The RMSE values between the measured and generated data were higher with the instantaneous MTM methods compared with the average MTM method. The correlation coefficient between the generated and measured data was higher with the average MTM method compared with the instantaneous MTM methods. The comparison between Limiting State Probabilities with Marginal Probabilities gave good fit in the case of the average MTM method. In the case of both yearly and monthly instantaneous MTM methods, the comparison between Limiting State Probabilities and Marginal Probabilities was not well established. The occurrences of clearness index value were well established in the case of the average MTM method compared with instantaneous MTM methods. Based on these results, it was decided to generate the hourly average horizontal solar radiation data rather than instantaneous data.

RMSE, MBE and correlation coefficient values obtained from the yearly instantaneous MTM and monthly instantaneous MTM methods were almost the same. Also the number of clearness index occurrences was similar in both methods and there was no considerable advantage in using the monthly MTM method. In the case of average MTM methods, even with five years of data the monthly average MTM was not able to produce the robust matrix. It was possible to construct a robust yearly average MTM with the five years of data. So instead of using 12 monthly MTMs, a single yearly MTM can be used to generate the solar radiation data.

Comparing mid-value method and random value method results, there was no considerable advantage to favour one over the other. But some times when the selected state was 1, the random value method produced very low radiation values. For an example in the generation of instantaneous data using the yearly instantaneous MTM the selected state was 1 at 11:00 and the random value method produced the clearness index value as 0.00022. This value resulted in the horizontal irradiation value of 0.05 W/m^2 that was very low value. Also the standard deviation of clearness index values was almost the same for each state. So the mid-value method was

chosen to select the clearness index values. From these results it was decided to generate the solar radiation data using the yearly average MTM method and mid-value method to select the clearness index values.

In order to study the dynamic performance of a transmission network, the fluctuation of solar radiation is important. To analyse this behaviour the fluctuation of solar radiation from one hour to the next was calculated for the simulated data obtained by using the yearly average MTM. The fluctuation magnitude was divided into intervals of 50W in step width. The fluctuation magnitude and the numbers of occurrence in each interval were calculated. The same procedure was repeated for the measured data and compared. The results are given in Figure 3-7, which show an excellent agreement between the measured and simulated data. Simulated data have slightly more number of occurrences for the fluctuation magnitude below ±25W, but the general shape of the curve is very similar across the whole range of values. From this it is observed that the MTM could produce the horizontal solar radiation data, which is representative of variation as well as absolute values.

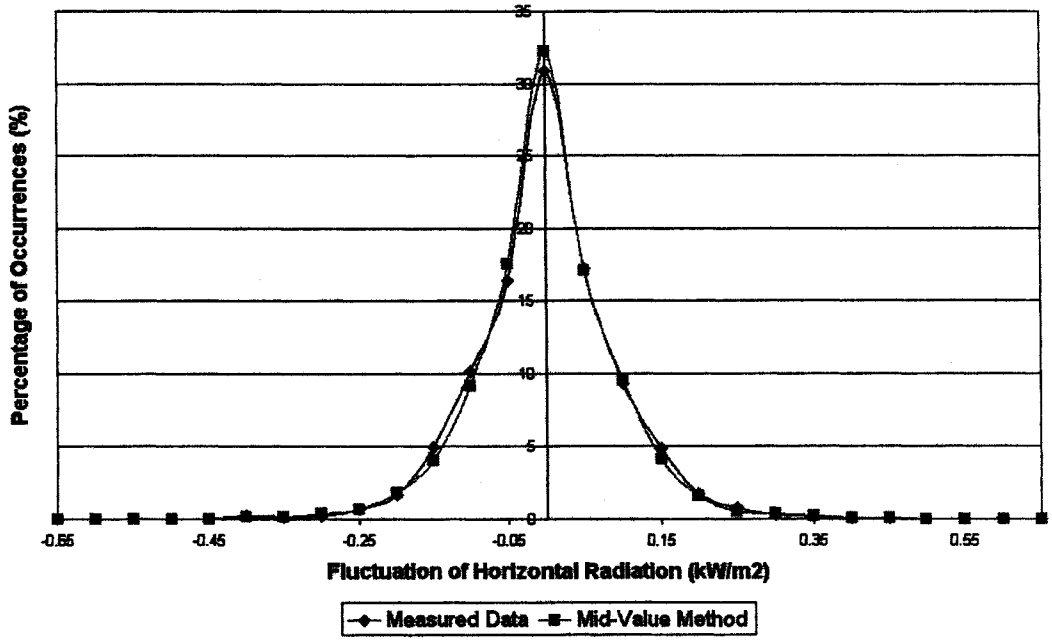

Figure 3-7 Comparison of horizontal radiation fluctuation in generated series, obtained from yearly average MTM method, with measured series for the North East 1 location

3.5 *Generation of Hourly Horizontal Solar Radiation Data for Different Locations*

In order to investigate the effect of geographically dispersed PV systems at different positions on the grid, it is necessary to consider solar data for different UK locations. Mustacchi et al. [16] developed a Markov Transition Matrix for each location to generate solar radiation data for 12 Italian locations. In the work presented in this thesis the possibility of using a single yearly MTM, constructed by using measured data from four different UK locations, to generate the solar radiation for these four locations was analysed. The following sections discuss the use of a single yearly average MTM to generate the horizontal irradiation data for these locations.

3.5.1 Data acquisition

The measured data from three more locations across the UK, a location in the West Midlands region (identified as West Midlands 1), a location in the London region (London 1) and a second location in the North East region (North East 2), were included with the North East 1 data to form a single yearly MTM. The West Midlands 1 PV system is 1.02 kWp and is connected to an 850W SMA inverter. The system is located at a latitude of 52^0 19'N and a longitude of 1^0 34'W. The measured global horizontal radiation data from November 2000 to June 2002 were used for this analysis. The London 1 PV system is 2.2 kWp located at a latitude of 51^0 32' N and a longitude of 0^0 02' W. The measured global horizontal irradiation data from November 2000 to May 2002 were used for this analysis. North East 2 PV system is 73 kWp located at Doxford International Business Park [45], which has a latitude of 54^0 52' N and a longitude of $1^0$26' W. The measured horizontal radiation data from November 1998 and the year 1999 (January to October) were used in this analysis.

3.5.2 Yearly average UK MTM

Using data from all these four locations the single yearly average UK MTM was constructed (Appendix A). Once the MTM was constructed the equilibrium of the

matrix was tested. When the MTM was raised to power 60, all rows in the MTM became equal and hence the equilibrium of the MTM was proved. From this, the Limiting State Probability values were obtained (Appendix A) and compared with the Marginal Probability values obtained from the measured data as shown in Figure 3-8, which shows a good fit between these values. After this test the single yearly average UK MTM was used to generate the synthetic solar radiation sequence for different locations.

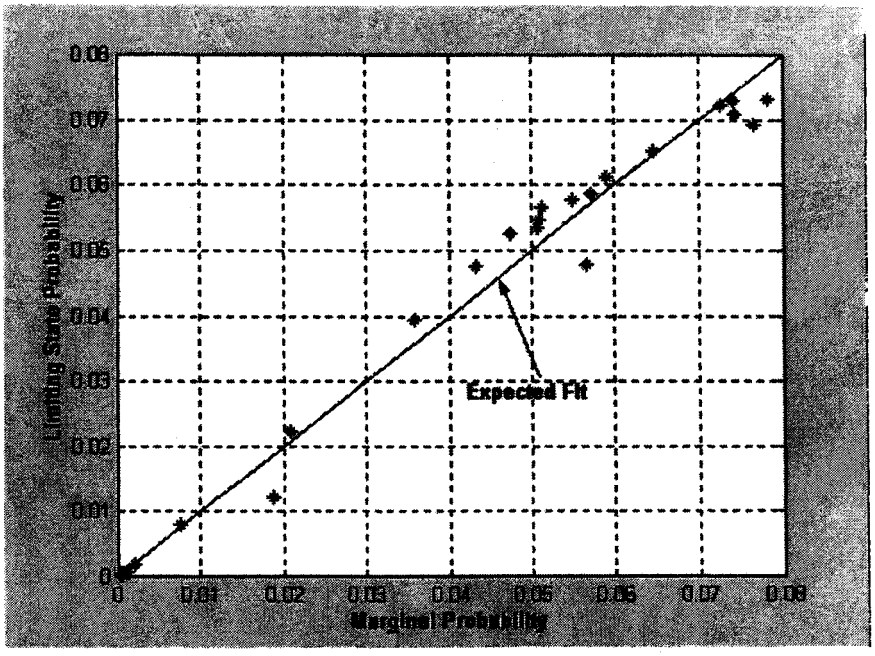

Figure 3-8 Comparison between MP and LSP from the yearly average UK MTM

3.5.3 Results for the London 1 location

The yearly average UK MTM was used to generate hourly averaged global horizontal radiation data for the London 1 location for the year 2001. Latitude, longitude and daily total irradiation values were given as input. The simulated hourly data and measured data for few days in January and June are shown in Figure 3-9 and Figure 3-10 respectively to show the results obtained for different seasons. The MBE and RMSE error values between the two series were calculated as –0.07 W/m^2 and 106 W/m^2 respectively. These error values are slightly higher compared with

results obtained for generation of solar radiation for the North East 1 location using the yearly average MTM. The correlation coefficient value between the series was calculated as 89.5%. The number of clearness index value occurrences from the generated series was compared with measured series and is shown in Figure 3-11.

The number of occurrences in low states (1 & 2) from the generated data was less compared with measured data. The number of occurrences in high states (17^{th} to 21^{st}) was more in the generated data compared with measured data. In all other states the number of occurrences from the simulated data has good fit with measured data. The fluctuation of generated solar radiation values was compared with measured data and is shown in Figure 3-12. The generated data has more number of occurrences when the fluctuation magnitude was $\pm 25 W/m^2$ compared with the measured data. When the fluctuation magnitude was 75 to 175 W/m^2, the number of occurrences in the simulated data was slightly low compared with measured data. However, the general shape of the curve is similar across the whole range of values.

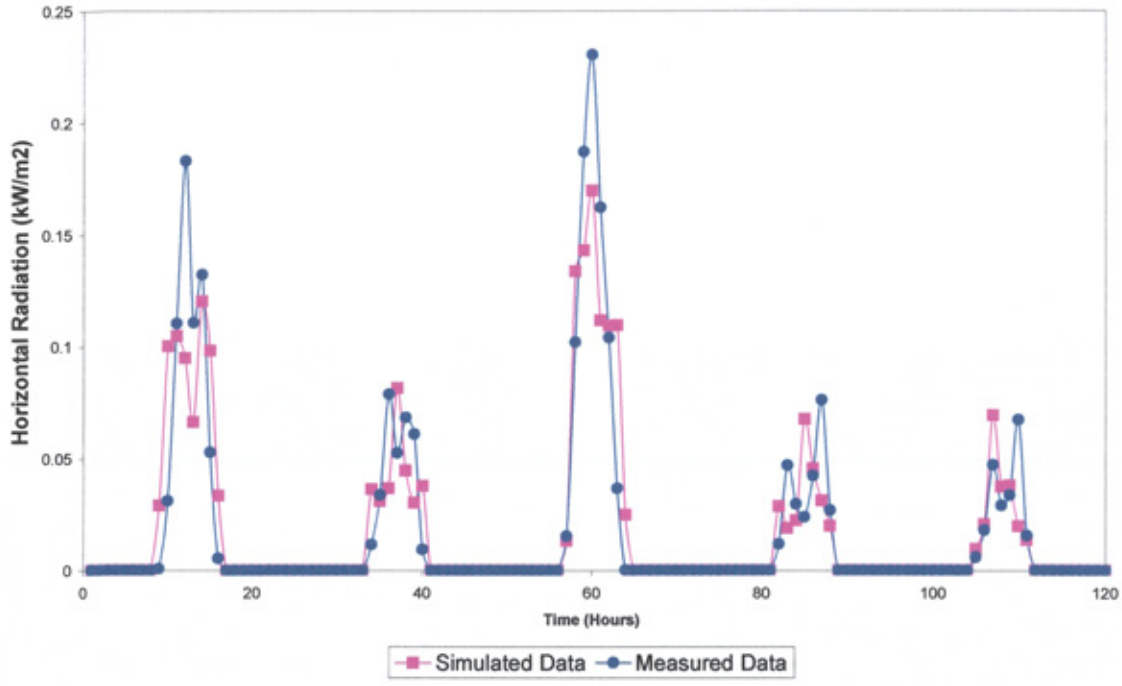

Figure 3-9 Comparison between measured and generated hourly horizontal radiation data for January, for the London 1 location

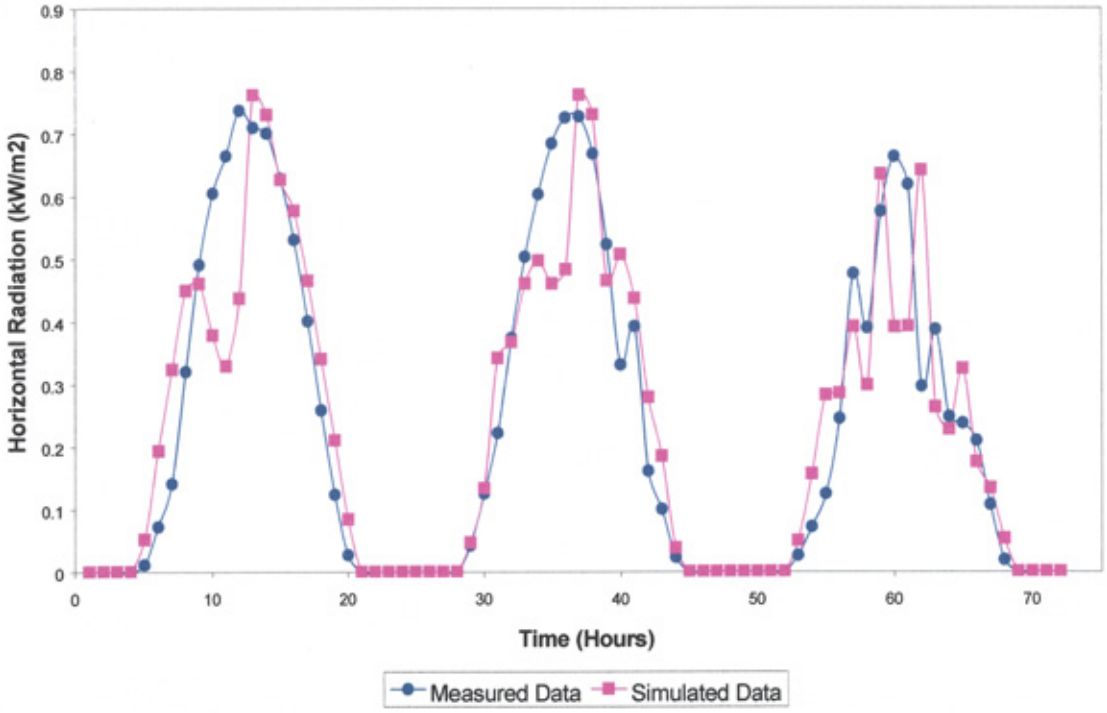

Figure 3-10 Comparison between measured and generated hourly horizontal radiation data for June, for the London 1 location

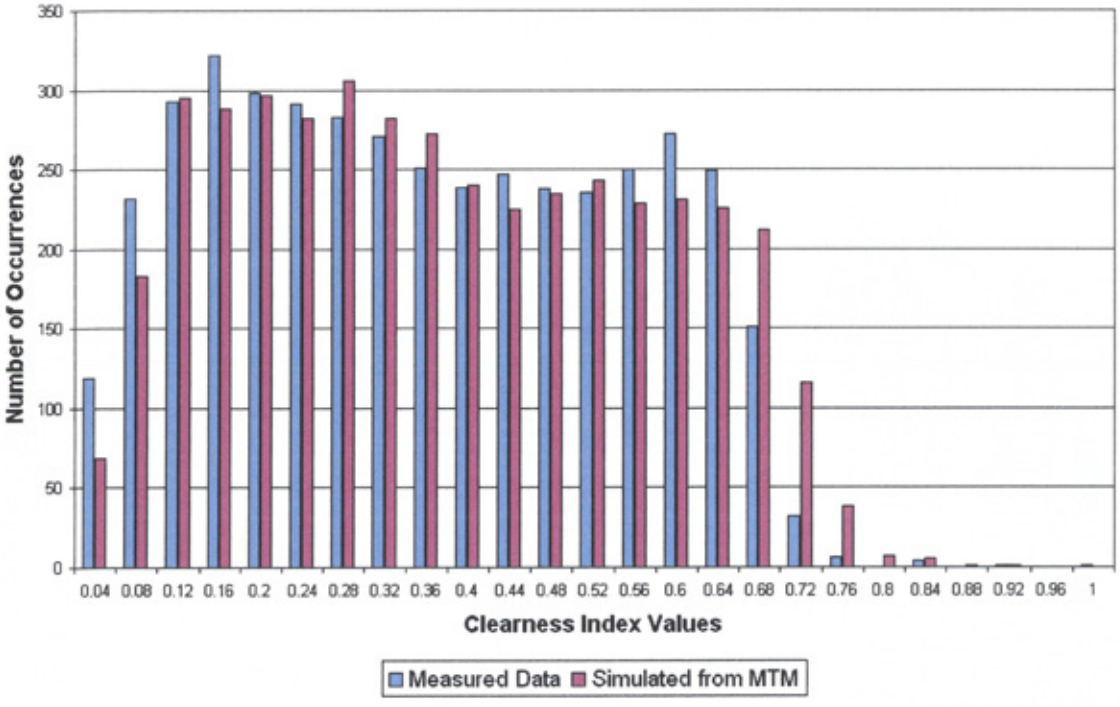

Figure 3-11 Comparison of clearness index occurrences in the generated series, obtained by yearly average UK MTM, with measured series for the London 1 location

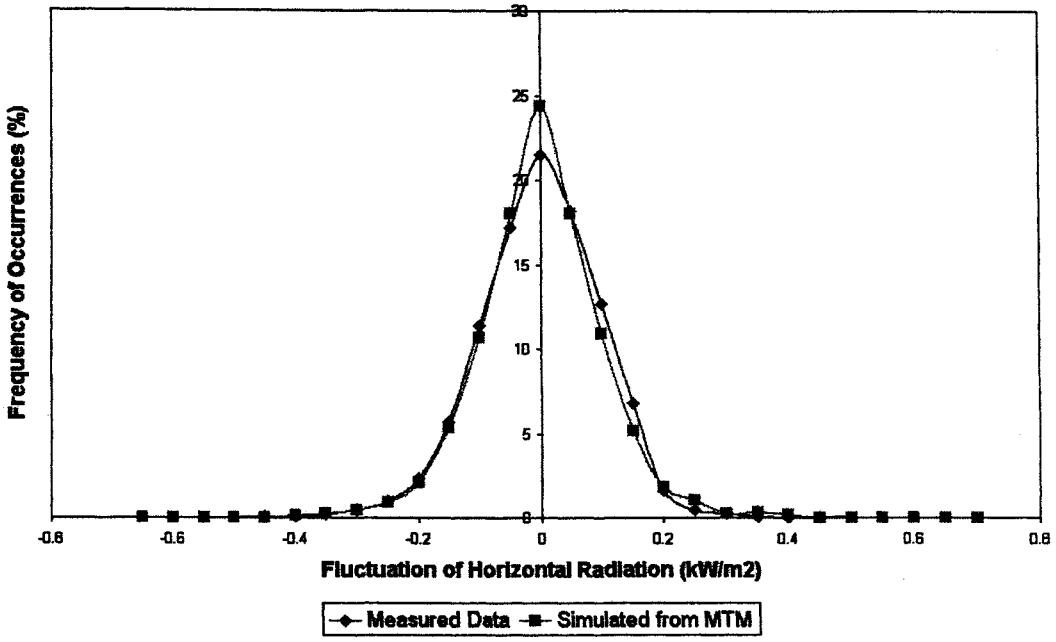

Figure 3-12 Comparison of horizontal radiation fluctuation in the generated series, obtained by using yearly average UK MTM, with measured series for the London 1 location

3.5.4 Results for the West Midlands 1 location

Similarly hourly averaged solar radiation data were generated for the West Midlands 1 location for the year 2001 using the yearly average UK MTM. Generated series and measured series for few days in January and June are shown in Figure 3-13 and Figure 3-14 respectively to show the seasonal variation. The MBE and RMSE error values between the two series were calculated as 0.01 W/m^2 and 105 W/m^2 respectively. The number of occurrences of clearness index values from the generated series was compared with the measured series and is shown in Figure 3-15. The number of occurrences in high states (17^{th} to 20^{th}) was more in the generated series compared with measured series. However, the generated series showed good agreement with measured data in the middle sector where over 85% of the data points occurs. The fluctuation of generated solar radiation behaviour was also compared with measured data and is shown in Figure 3-16. The generated data has slightly high number of occurrences when the fluctuation magnitude was $\pm 25 W/m^2$

compared with measured data. In general the number of occurrences from the simulated data has good fit with measured data across the whole range of values.

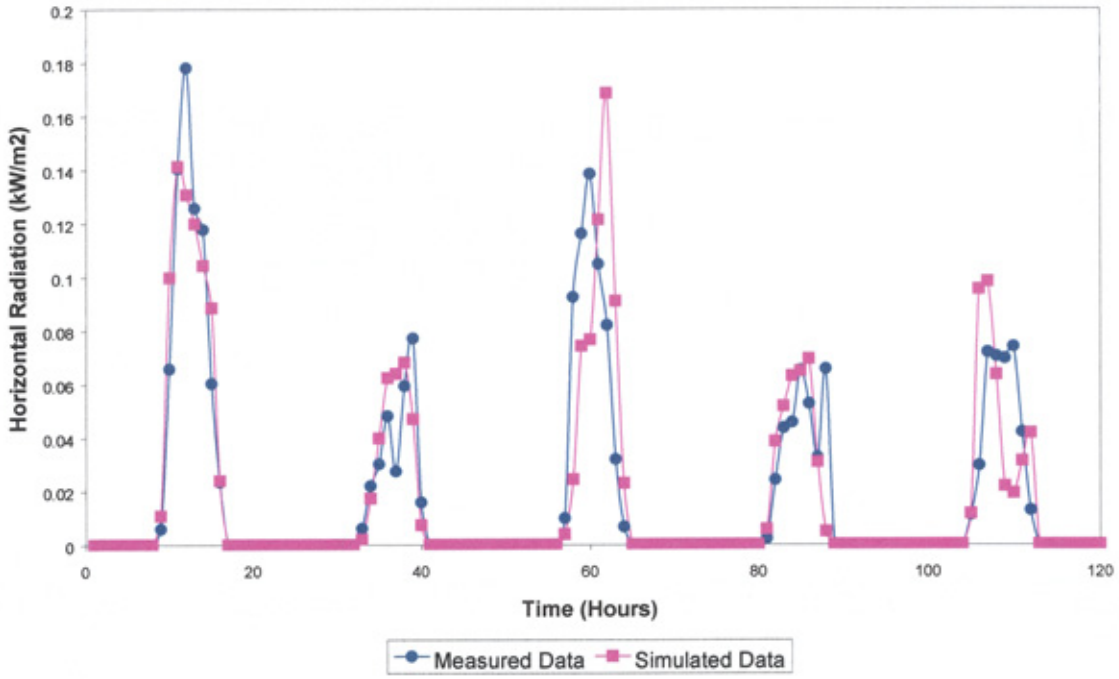

Figure 3-13 Comparison between measured and generated hourly horizontal radiation data for January, for the West Midlands 1 location

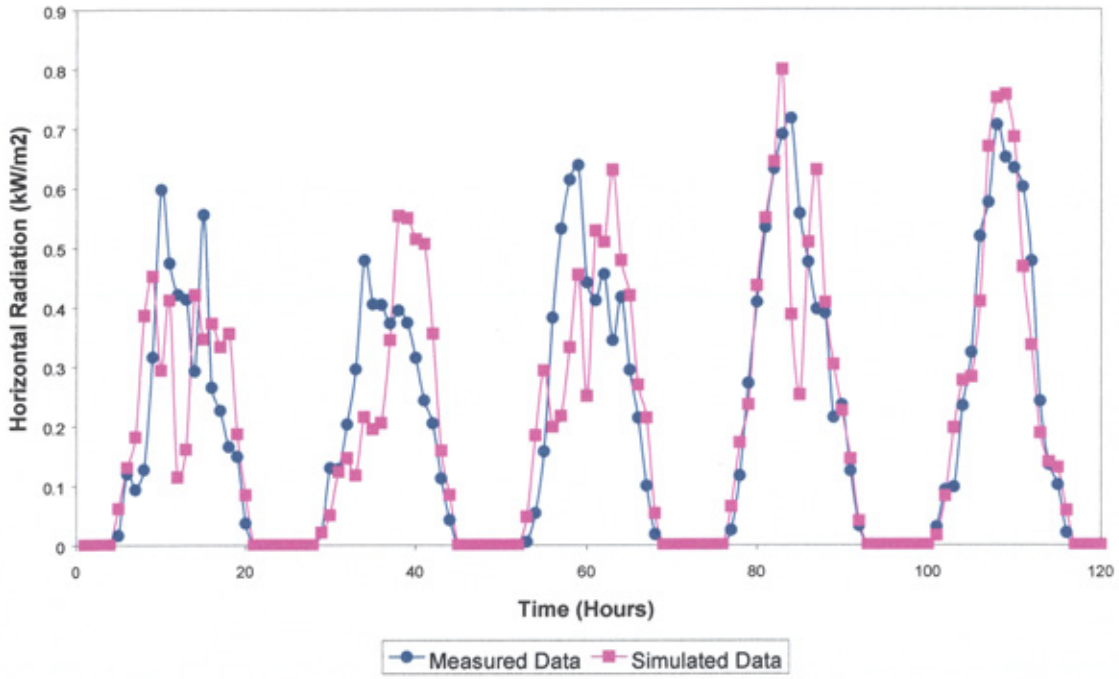

Figure 3-14 Comparison between measured and generated hourly horizontal radiation data for June, for the West Midlands 1 location

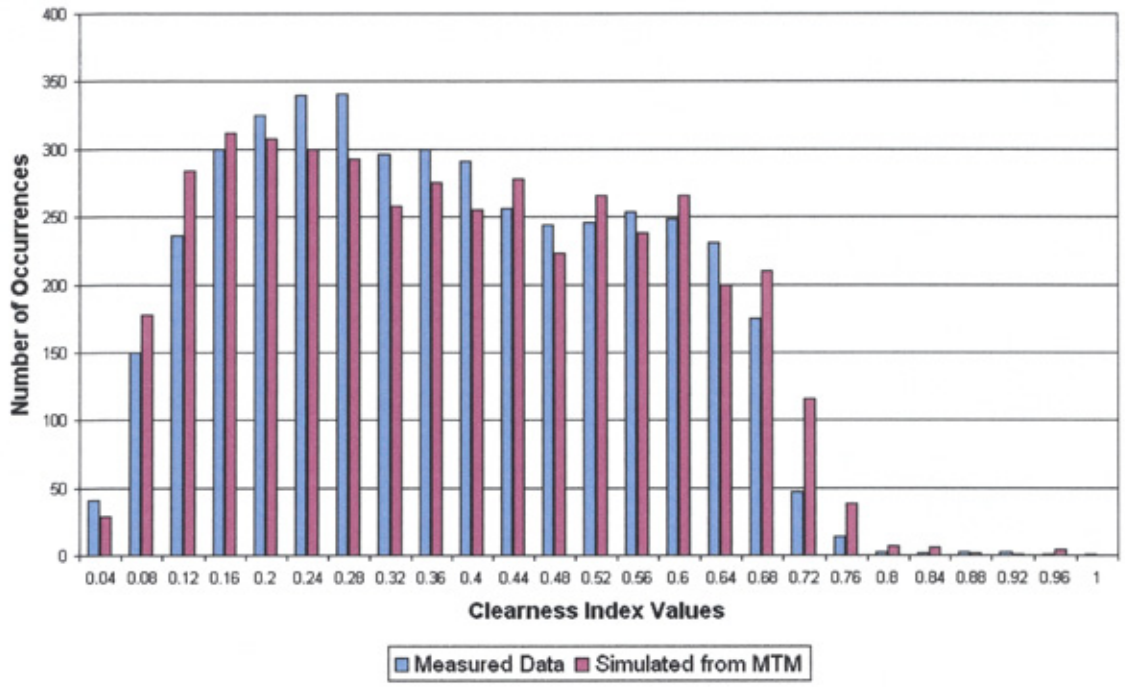

Figure 3-15 Comparison of clearness index occurrences in the generated series, obtained by yearly average UK MTM, with measured series for the West Midlands 1 location

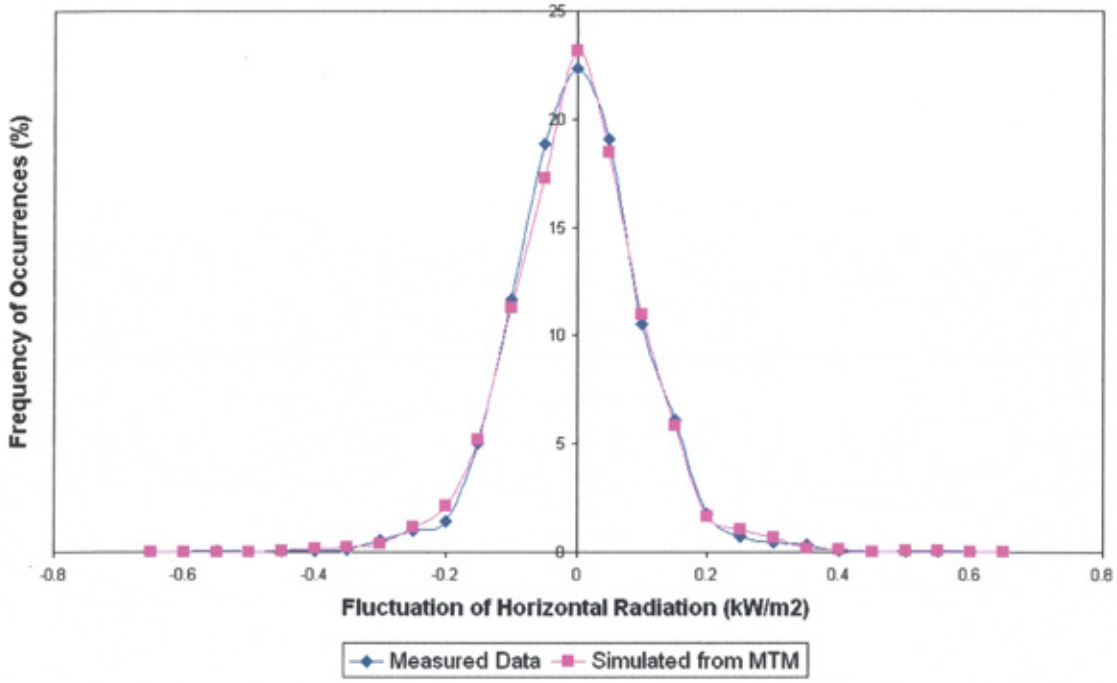

Figure 3-16 Comparison of horizontal radiation fluctuation in the generated series, obtained by using yearly average UK MTM, with measured series for the West Midlands 1 location

3.5.5 Discussion

Solar radiation data for different locations in the UK is required to study the effect of dispersed PV systems on the grid. Because of the scarcity of measured data, a single yearly average UK MTM was constructed by using data from four different locations in the UK. The compatibility of the constructed MTM to generate horizontal radiation data for these locations was verified. The constructed MTM was derived from the clearness index values, which dictates the transition of cloud from one hour to the next, whereas the weather pattern of the day was identified by the daily total irradiation values. So even though the weather pattern of two different locations was different a single yearly MTM that represents the cloud transition can be used to generate the solar data for both the locations. In this work the daily total irradiation values for each location is given as input and the correlation of irradiation values between sites is not considered. The correlation of solar radiation values for different locations is discussed in Chapter 5.

From these results it was observed that the generated series have good fit with measured series in terms of error values, correlation coefficient value, frequency of occurrences of clearness index values and power fluctuation pattern. It is worth to note that this matrix was constructed by using eight years of data, where around 6 years of data were from the North-east England locations. So it may be possible to have a still more robust matrix with many other locations data added with these data. It is clear that using single yearly UK MTM is a simpler solution than the construction of a new matrix for each location considered, not least because of the scarcity of suitable measured data.

3.6 Generation of Half-hour Solar Radiation Data

To analyse the impact of PV systems on power systems, knowledge of sub-hourly solar radiation is useful. For example half-hour power output is necessary to study the impact of PV systems on power systems economics, as defined by the grid group. So the analysis was extended to study the possibility of using the MTM method to generate half-hour horizontal radiation data. The following sections explain the

generation of half-hour solar radiation data by using the single yearly half-hour average UK MTM method and results that have been obtained.

3.6.1 Yearly half-hour average UK MTM

Measured horizontal radiation data from the North East 1, London 1, West Midlands 1 and North East 2 locations were used in this analysis. The measured data were stored in an Excel sheet and a Macro was written to convert it into half-hour average data. From the half-hour horizontal radiation data half-hour clearness index values were calculated. These values were used to construct the yearly half-hour average UK MTM (Appendix A). Once the matrix was constructed the equilibrium property of the matrix was tested (Appendix A). Limiting state probabilities obtained from the matrix were compared with Marginal Probability values calculated from measured data as shown in Figure 3-17. Limiting State Probabilities gave good fit with Marginal Probability and it proves that the equilibrium of matrix was well established.

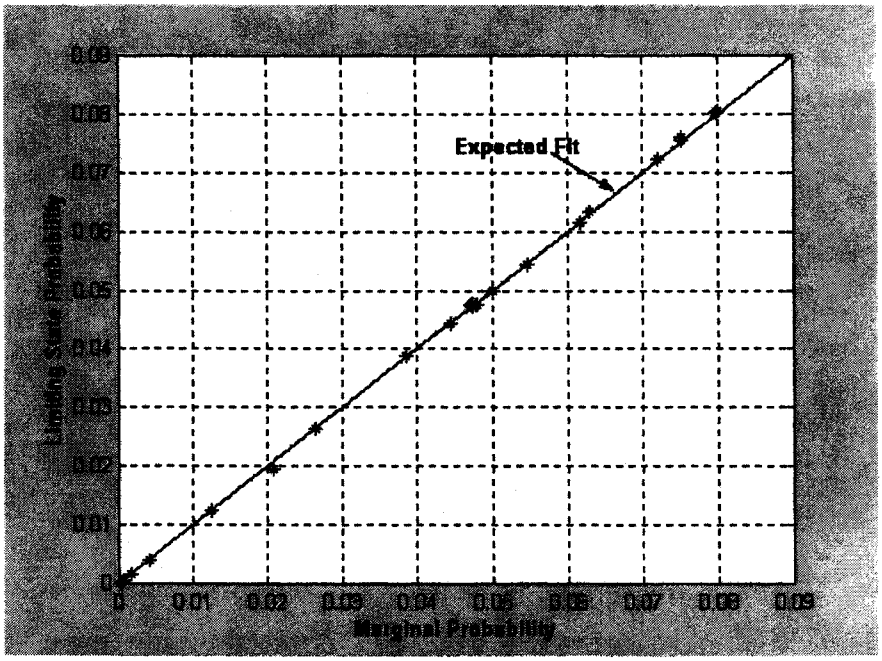

Figure 3-17 Comparison between MP and LSP from the yearly half-hour average UK MTM

3.6.2 Results

The constructed yearly half-hour average UK MTM was used to generate half-hour horizontal radiation data for the London 1 location. Figure 3-18 and Figure 3-19 show the comparison of generated and measured series for few days in January and June that represent the results obtained for different seasons. The MBE and RMSE error values between the two series were calculated as –0.02 W/m^2 and 124 W/m^2 respectively. The RMSE value was higher compared with the result obtained for hourly horizontal radiation generation. The correlation coefficient between the two series was calculated as 86.8%. The correlation coefficient value obtained in the generation of half-hour radiation is lower compared with the hourly radiation generation. The number of clearness index value occurrences from generated series was compared with measured series and is shown in Figure 3-20. The number of occurrences in high states (17th to 20th) was more in the generated series compared with measured series. In all other states the generated series showed good agreement with measured series.

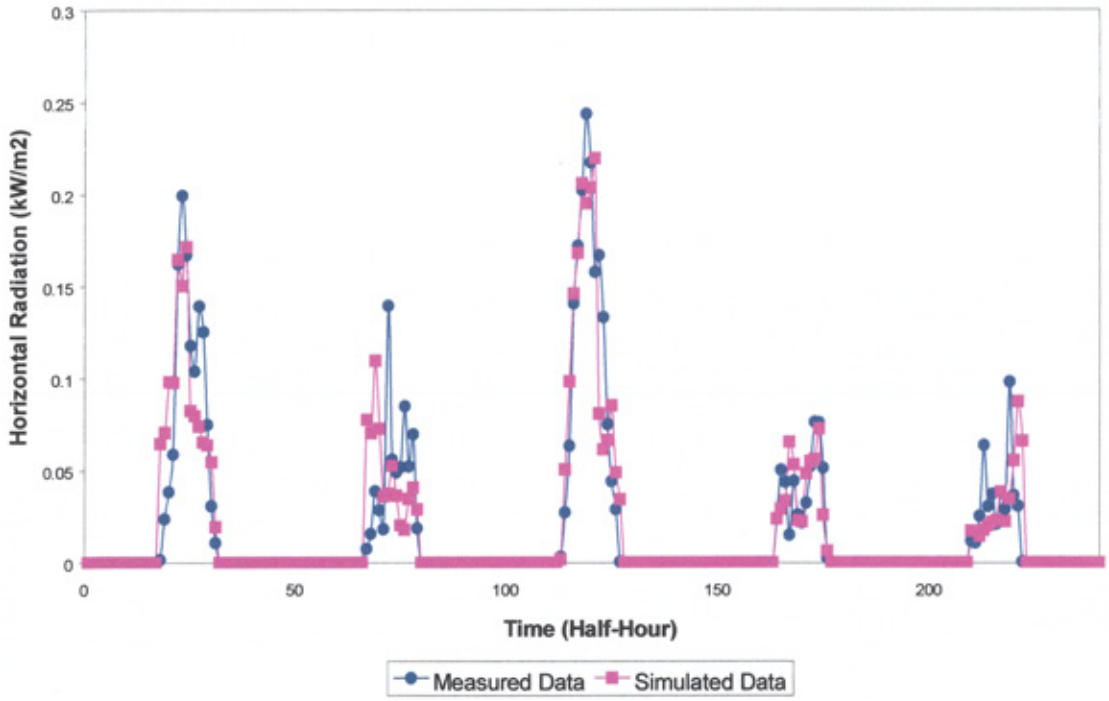

Figure 3-18 Comparison of simulated and measured half-hour horizontal radiation data for the London 1 location, for January

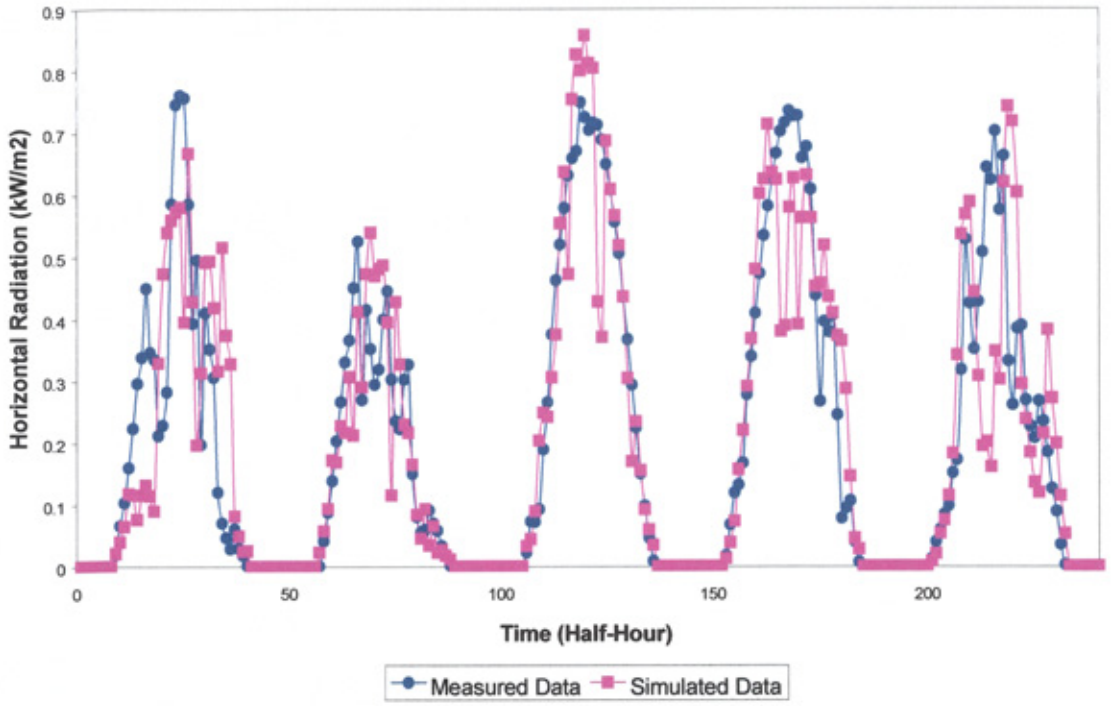

Figure 3-19 Comparison of measured and simulated half-hour radiation data for the London 1 location, for July

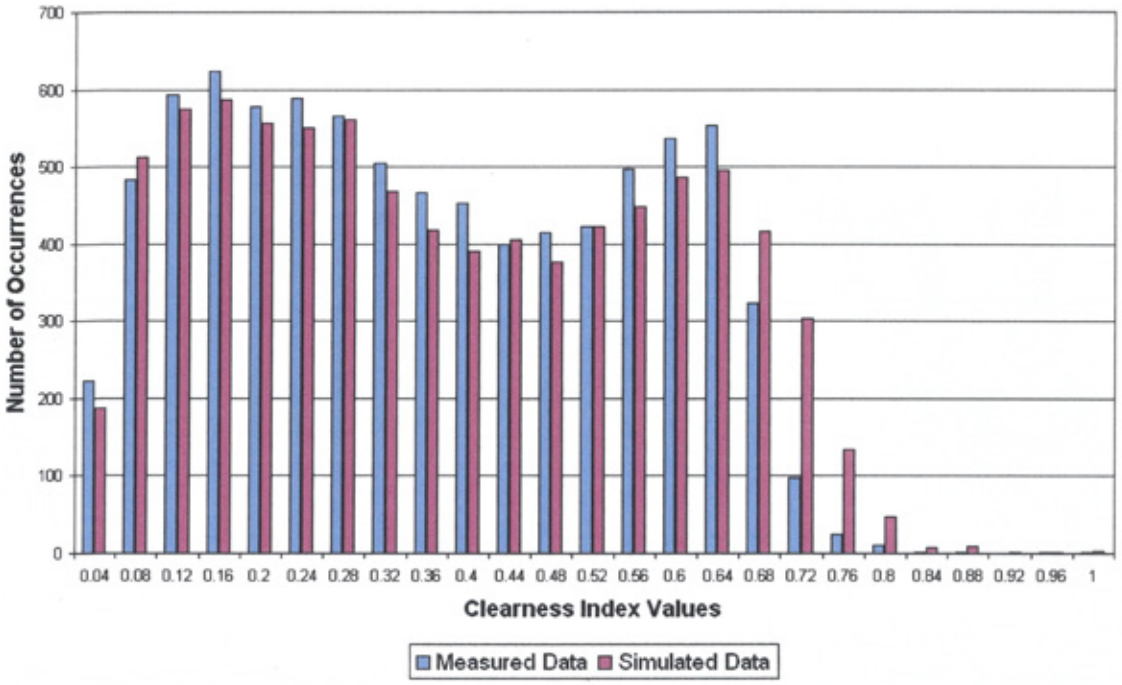

Figure 3-20 Comparison of half-hour clearness index occurrences for the London 1 location

The fluctuation of generated solar radiation behaviour was compared with measured data and is shown in Figure 3-21. In the generated data there was a higher number of occurrences when the fluctuation magnitude was ±25W/m^2 and a lower number of occurrences when the fluctuation magnitude was 25W/m^2 to 75 W/m^2 compared with measured data. The general shape of the curve is similar across the whole range of values and only a small difference between the measured and simulated data was observed.

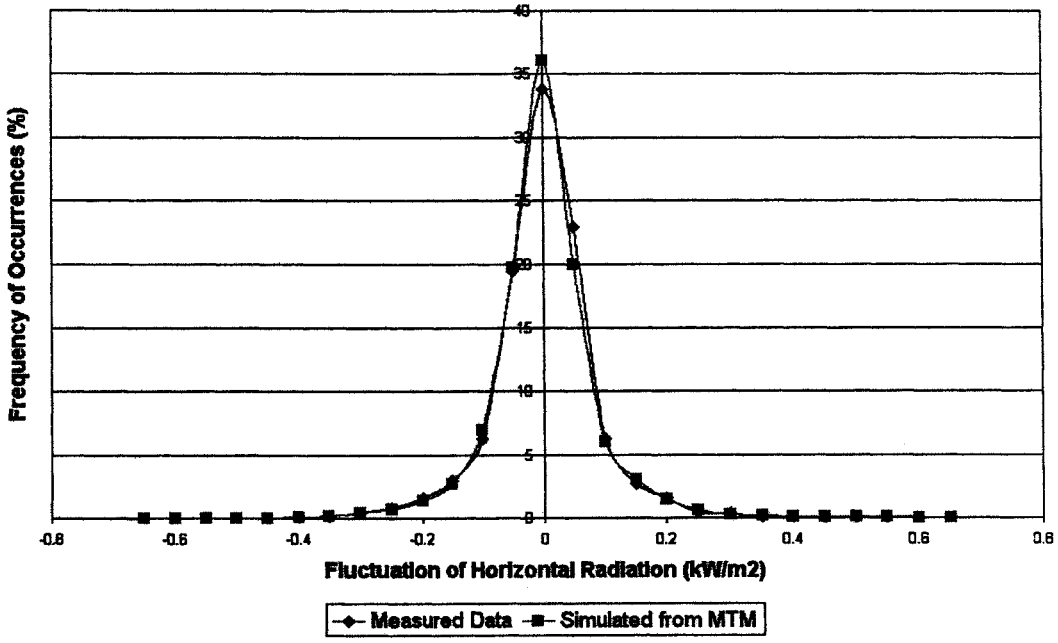

Figure 3-21 Comparison of half-hour horizontal radiation fluctuation for the London 1 location

Similarly half-hour horizontal radiation data were generated for the West Midlands 1 location. Figure 3-22 and Figure 3-23 show the comparison of generated and measured series for a few days in January and July which represent the results obtained for different seasons. The MBE and RMSE error values between the two series were calculated as –0.19 W/m^2 and 122 W/m^2 respectively. The correlation coefficient between the two series was calculated as 86.5%. These values are similar to the results obtained in generation of half-hour radiation data for the London 1 location. In this case also the RMSE value was greater and the correlation coefficient value was lower compared with results obtained in generation of hourly radiation.

The number of occurrences of clearness index values from the generated series was compared with measured series and is shown in Figure 3-24. The numbers of occurrence in the high states (18^{th} to 20^{th}) was more in the generated series compared with the measured series. However, the generated series showed good agreement in the middle sector. The fluctuation of generated solar radiation behaviour was compared with measured data and is shown in Figure 3-25. The general shape of the curve is similar across the whole range of values and there were only very small differences between the measured and simulated data.

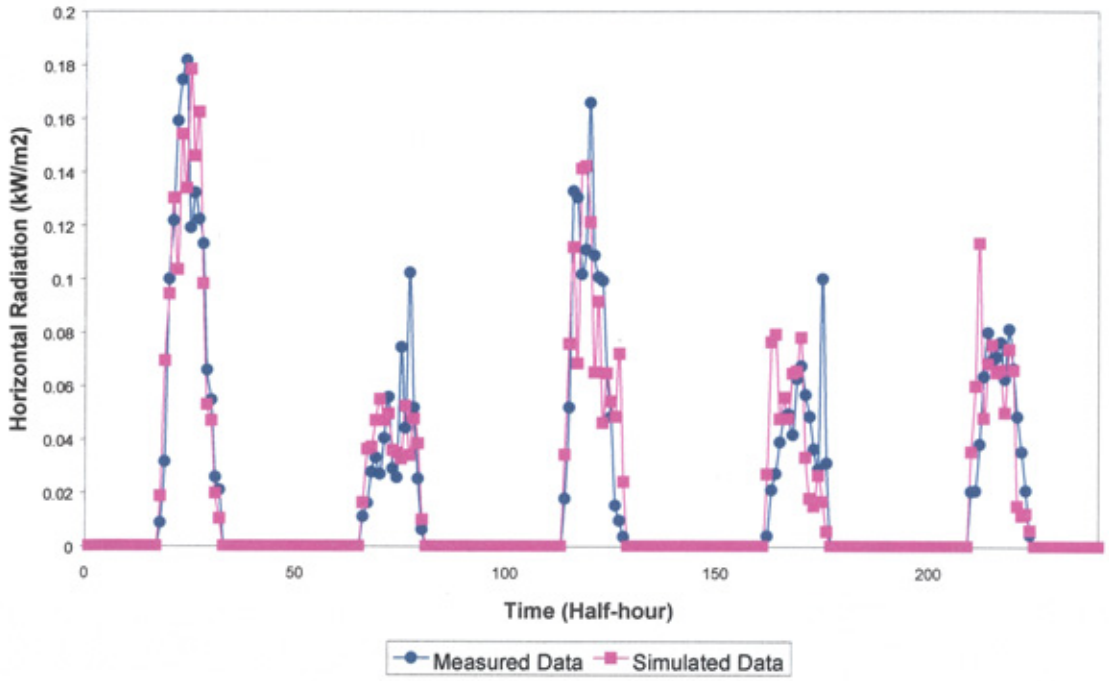

Figure 3-22 Comparison of simulated and measured half-hour horizontal radiation data for the West Midlands 1 location, for January

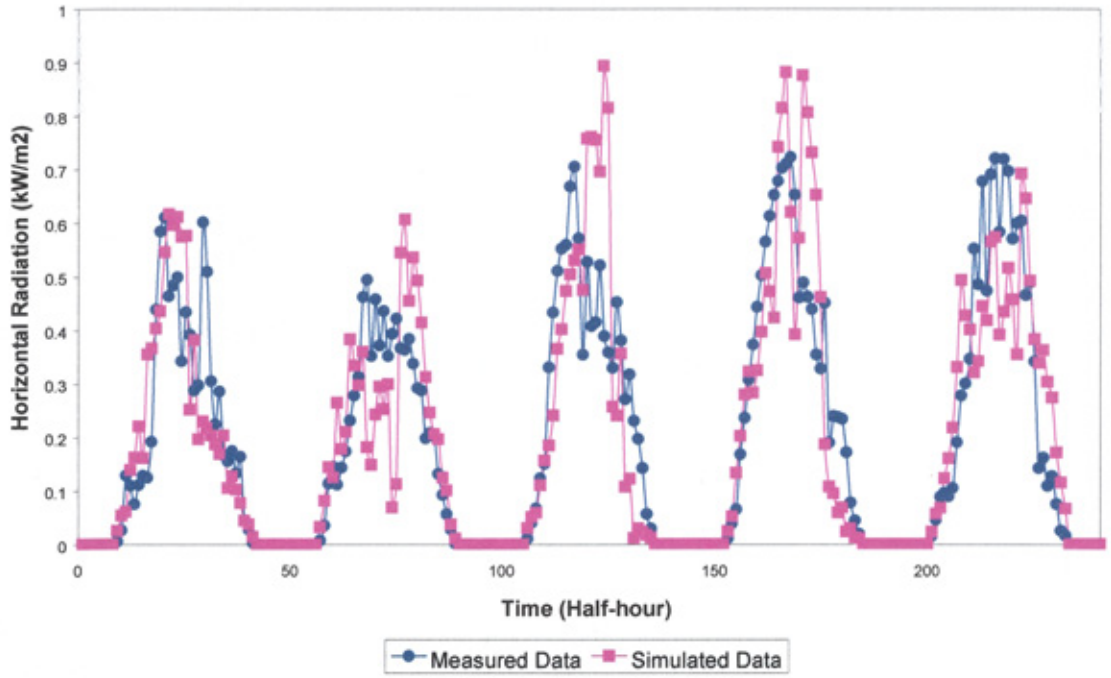

Figure 3-23 Comparison of measured and simulated half-hour horizontal radiation data for the West Midlands 1 location, for July

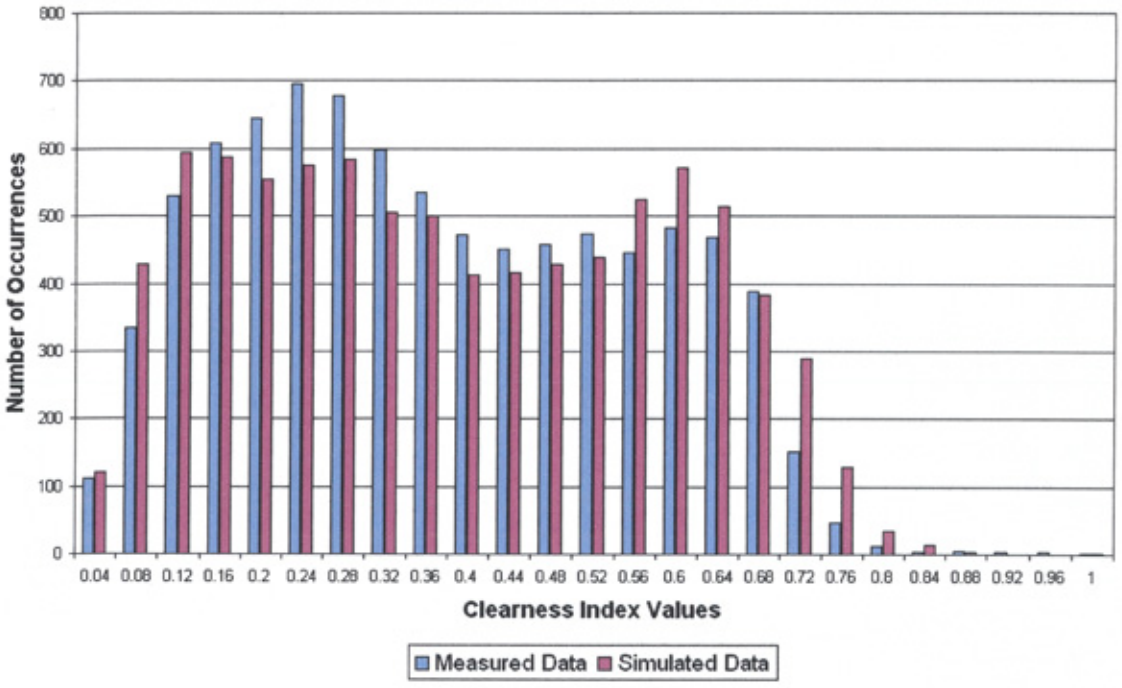

Figure 3-24 Comparison of half-hour clearness index occurrences for the West Midlands 1 location

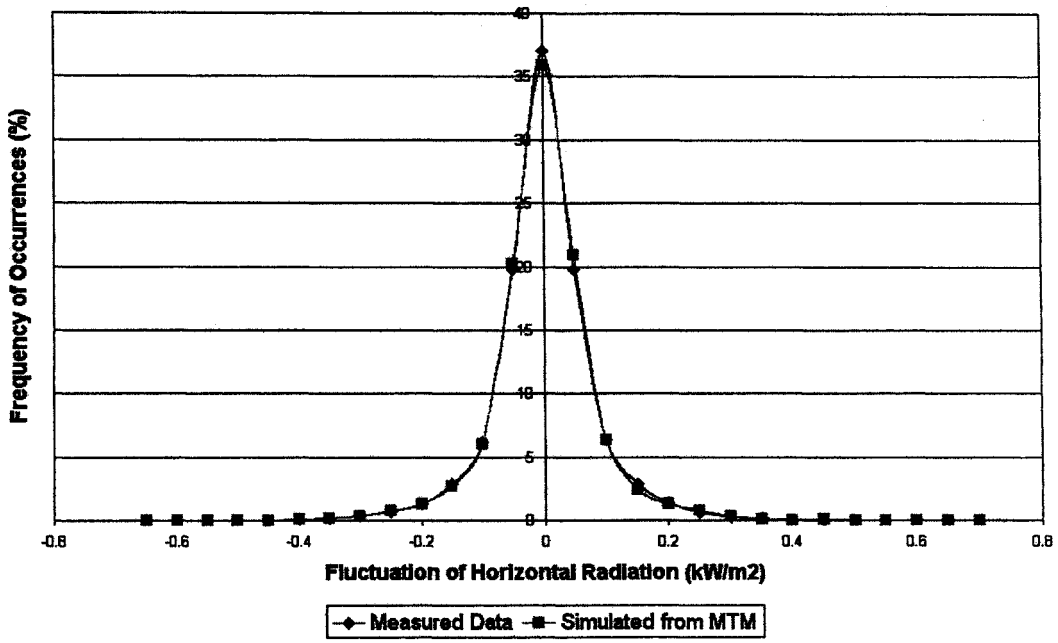

Figure 3-25 Comparison of half-hour horizontal radiation fluctuation for the West Midlands 1 location

3.6.3 Discussion

To study the economics and dynamics of power systems, the half-hour power output data is useful. In order to study the half-hour power output from PV systems, half-hour solar radiation data is necessary. The ability of the single yearly average MTM to generate the hourly solar radiation for different locations was proved. So the analysis was extended to the generation of half-hour solar radiation data.

The single yearly half-hour UK MTM was capable of producing the half-hour solar radiation data for different locations in the UK. The MP and LSP gave a very good fit compared with the hourly average data. The RMSE values were higher in the generation of half-hour solar radiation data compared with hourly solar radiation data generation. The generated series has a higher number of occurrences in high states compared with the measured data. However, the generated series gave good agreement in the middle sector where most of the data points occur. From these results it was decided to use the single yearly MTM to generate half-hourly solar radiation data for different locations in the UK.

3.7 Tilted Radiation Model

In most of the PV systems PV arrays are tilted at an angle with respect to the horizontal surface. The amount of radiation incident on the tilted surface is an important parameter to study the power output from a PV system. As explained before, since the measured tilted radiation data are available only for few systems it is necessary to use a model to translate horizontal radiation to tilted radiation for PV systems with any tilt angle and orientation. In this work the Hay model was selected to calculate the tilted radiation values from horizontal radiation data. This section discusses the Hay model and the validation of the Hay model for different PV systems that vary in their tilt angles and orientations.

Global tilted radiation (I_T) consists of three main components given as [33,38]

$$I_T = I_B + I_S + I_R$$

Where,

I_B is the beam radiation on the tilted surface

I_S is the sky-diffuse radiation on the tilted surface

I_R is the ground reflected radiation on the tilted surface

The geometrical relationship between a plane of any particular orientation relative to the earth at any time and the incoming beam solar radiation, that is, the position of the sun relative to that plane, can be described in terms of several angles [2]. Some of the angles are illustrated in Figure 3-26.

According to the Hay model, the hourly beam radiation on a tilted surface is given as

$$I_B = (I - I_D)\frac{\cos\theta}{\cos\theta_Z}$$

Where,

I is the hourly global horizontal radiation

I_D is hourly diffuse radiation on the horizontal surface

θ is the angle of incidence and

θ_Z is the zenith angle

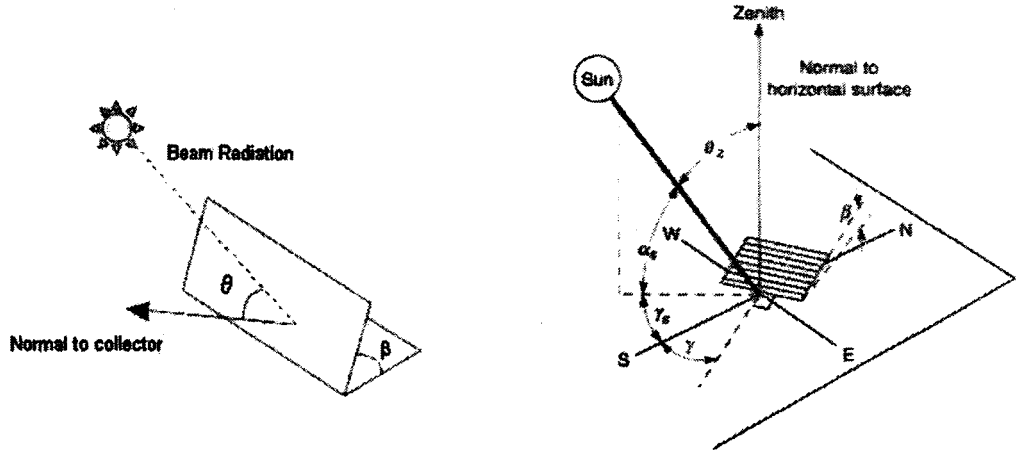

(a) Representation of the angle of incidence (θ)

(b) Representation of zenith angle (θ_z)

Figure 3-26 Representation of a tilted surface, the angle of incidence, zenith angle and related angles (Source: [2])

The angle of incidence (θ) is defined as

$$\cos\theta = \sin\delta\sin\phi\cos\beta - \sin\delta\cos\phi\sin\beta\cos\gamma + \cos\delta\cos\phi\cos\beta\cos\omega + \cos\delta\sin\phi\sin\beta\cos\gamma\cos\omega + \cos\delta\sin\beta\sin\gamma\sin\omega$$

Where,

ϕ is latitude angle of the location

ω is the hour angle

δ is the declination angle

γ is the surface azimuth angle, the deviation of the projection on a horizontal plane of the normal to the surface from the local meridian, with zero south, east negative and west positive

β is the tilt angle

The zenith angle (θ_Z) is defined as

$$\cos\theta z = \cos\phi\cos\delta\cos\omega + \sin\phi\sin\delta$$

If the angle of incidence or zenith angle is equal to or greater than 90^0, the beam radiation will be negative, which is not practical. For an angle of incidence greater than 86^0 there are higher errors in calculating the clearness index values and hence there are more errors in calculating direct radiation values. In this study whenever the angle of incidence or zenith angle was greater than 86^0, the corresponding beam radiation on the tilted surface was considered as zero[5].

Hourly ground reflected radiation (I_R) is given as

$$I_R = I\rho\frac{(1-\cos\beta)}{2}$$

Where,

ρ is the ground reflectance or albedo.

In general it is not possible to calculate the reflected energy term in detail, to account for buildings, trees, etc the changing solar radiation incident on them, and their changing reflectances. The standard procedure is to assume that there is one surface, a horizontal, diffusely reflecting ground. In this study, the ground reflectance was assumed as 0.2 [2].

In order to model the sky diffuse radiation on a tilted surface, the Hay model considers the isotropic and circumsolar components. Hourly sky diffuse radiation on a tilted surface is given as

$$I_S = I_D\left\{\frac{(I-I_D)}{Io}\frac{\cos\theta}{\cos\theta z}+\left[\frac{1+\cos\beta}{2}\right]\left[1-\frac{(I-I_D)}{Io}\right]\right\}$$

In order to calculate the hourly global tilted radiation, hourly diffuse radiation on the horizontal surface data is necessary. The empirical Erbs model was chosen from the literature survey to calculate the horizontal diffuse radiation from global horizontal radiation. In this model the hourly diffuse fraction (k_d) is correlated with hourly clearness index values (k_t). The hourly diffuse fraction (k_d) is given as

$$k_d = 1.0 - 0.09k_t \qquad for\ k_t \le 0.22$$

$$k_d = 0.9511 - 0.1604k_t + 4.388k_t^2 - 16.638k_t^3 + 12.336k_t^4 \qquad for\ 0.22 < k_t \le 0.8$$

$$k_d = 0.165 \qquad for\ k_t > 0.8$$

[5] Also the sun is not a point source

The hourly diffuse horizontal radiation can be calculated by multiplying the hourly diffuse fraction and hourly global horizontal radiation.

3.7.1 Validation of the Hay model

Horizontal diffuse radiation values were calculated from measured global horizontal radiation data using the Erbs model. Measured global horizontal radiation and calculated horizontal diffuse radiation data were used to calculate the global tilted radiation values. To validate the Hay model, the calculated tilted radiation values were compared with measured tilted radiation data. The model was validated on the basis of statistical error test. As explained in section 3.4.3 among different statistical parameters MBE and RMSE [37,38,39] were used for the comparison. RMSE indicates the accuracy of the model; the lower the RMSE, the more accurate is the model. A positive MBE indicates the overestimation of the calculated values while a negative MBE indicates an underestimation of the calculated values.

3.7.2 Results for hourly tilted radiation

In order to validate the Hay model, data from the Northumberland Building PV system were used. In this system PV arrays are tilted at an angle of 65^0 to the horizontal surface and southeast oriented with the surface azimuth angle of -16.5^0. The measured hourly radiation data for the year 1999 were used to calculate the hourly tilted radiation values. The MATLAB package was used and a M-file was created for this calculation. The input parameters are latitude, longitude, measured horizontal radiation, tilt angle and azimuth angle.

The calculated tilted radiation values were compared with measured tilted radiation values. Measured tilted radiation values are plotted against the calculated values for summer months as shown in Figure 3-27 and Figure 3-28, for a winter month in Figure 3-29 and for a autumn month in Figure 3-30. These figures illustrate the seasonal variation in the accuracy of calculating tilted radiation values. It can be

observed that the calculated values have very good fit with measured values in summer months compared with other months.

The statistical results, MBE and RMSE values were calculated for each month and are given in Table 3-5. The RMSE values are low for summer months and high for winter months. For summer periods the MBE values were very low compared with winter months. From these results it was observed that there was a good agreement between the measured and calculated values for all except winter months. The error is high for winter months because more errors occur in finding the diffuse radiation for winter months and also the method provides unreasonable clearness index values when the sun elevation is very low.

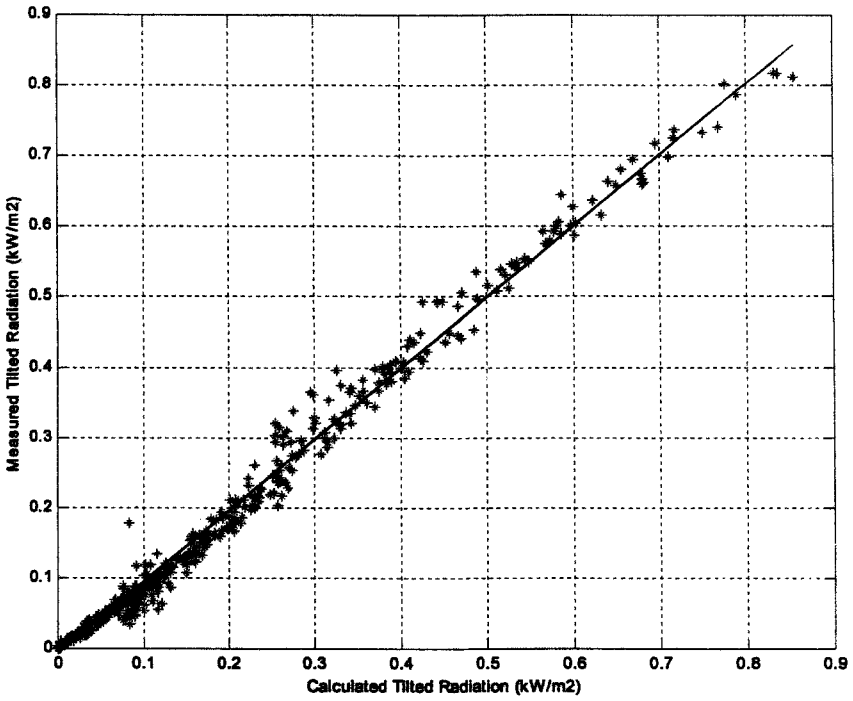

Figure 3-27 Hourly tilted radiation result for the North East 1 location for June 1999

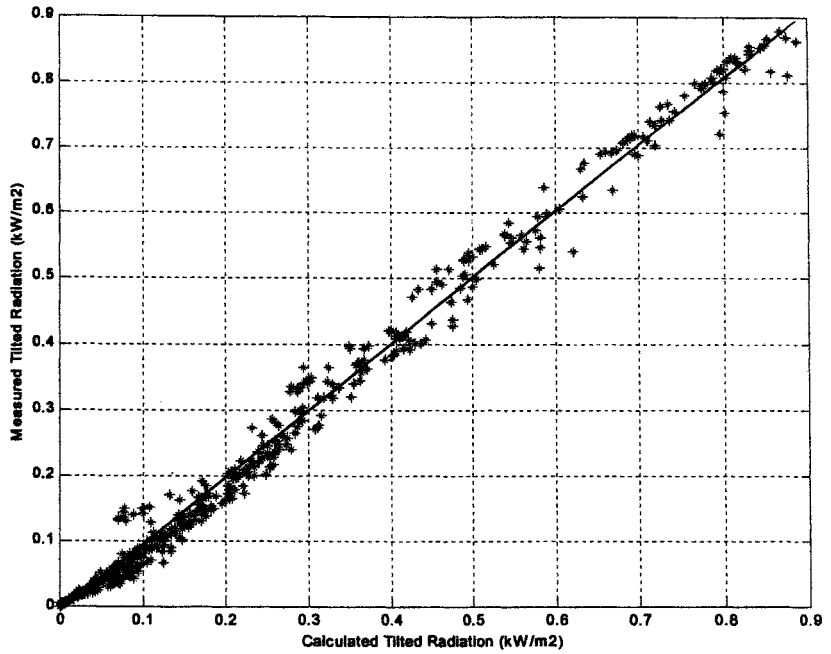

Figure 3-28 Hourly tilted radiation result for the North East 1 location for July 1999

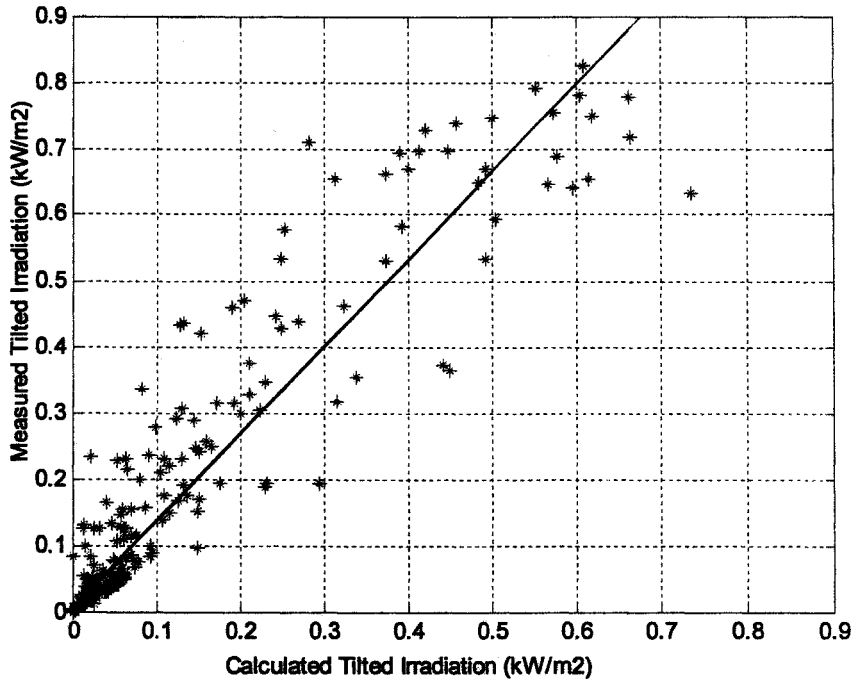

Figure 3-29 Hourly tilted radiation result for the North East 1 location for January 1999

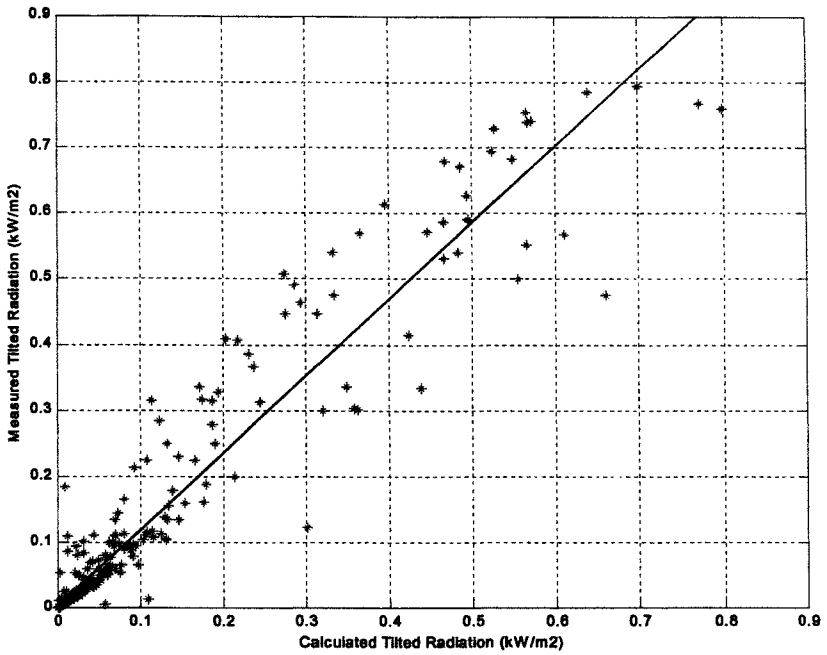

Figure 3-30 Hourly tilted radiation result for the North East 1 location for November 1999

Table 3-5 Statistical comparison of hourly tilted radiation results for the North East 1 location, using the year 1999 data

Month	MBE (kW/m^2)	RMSE (kW/m^2)
January	-0.0573	0.1091
February	-0.0508	0.0911
March	-0.0171	0.0496
April	-0.0130	0.0368
May	-0.0023	0.0276
June	0.0066	0.0205
July	0.0046	0.0245
August	-0.0048	0.0287
September	-0.0221	0.0503
October	-0.0263	0.0621
November	-0.0292	0.0721
December	-0.0592	0.1229

In order to validate the selected Hay model for different orientations and tilt angles, data from two more systems were used. One PV system is located at West Midlands 1, in which PV arrays are tilted at an angle of 35^0 to the horizontal surface and are south oriented i.e., the azimuth angle is 0^0. Another PV system is located at London 1, in which the PV arrays are tilted at an angle of 30^0 to the horizontal surface. The PV arrays are southwest oriented with an azimuth angle of 64^0. Measured minute horizontal and tilted radiation data are available for these systems. The minute horizontal radiation data recorded for the year 2001 were used to calculate hourly horizontal radiation. Hourly horizontal radiation data were used to calculate the hourly tilted radiation and were compared with the measured hourly tilted radiation data. The statistical comparison results are given in Table 3-6 and Table 3-7.

Table 3-6 Statistical comparison of hourly tilted radiation results for the West Midlands 1 location data, for the year 2001

Month	MBE (kW/m^2)	RMSE (kW/m^2)
January	-0.0415	0.0688
February	-0.0216	0.0553
March	-0.0169	0.0421
April	-0.0130	0.0368
May	-0.0159	0.0539
June	-0.0172	0.0501
July	-0.0129	0.0424
August	-0.0216	0.0539
September	-0.0178	0.0468
October	-0.0307	0.0540
November	-0.0302	0.0555
December	-0.0410	0.0686

Table 3-7 Statistical comparison of hourly tilted radiation results for the London 1 location data, for the year 2001

Month	MBE (kW/m^2)	RMSE (kW/m^2)
January	0.0053	0.0383
February	0.0070	0.0402
March	0.0027	0.0230
April	0.0026	0.0329
May	0.0047	0.0335
June	0.0056	0.0333
July	0.0015	0.0346
August	-0.0024	0.0339
September	-0.0009	0.0406
October	-0.0029	0.0381
November	-0.0001	0.0338
December	0.0085	0.0484

The RMSE values obtained for all three systems are plotted in Figure 3-31. From these results it can be observed that for all cases the RMSE values are low in summer months and high in winter months. The MBE values obtained for all three systems are plotted in Figure 3-32. The model overestimated the values in some cases and underestimated the values in some other cases. It can be observed that the MBE values are low for summer months and high for winter months. From the RMSE and MBE values it was observed that there was a good agreement between the measured and calculated values for all months except winter months. These error values were high in the winter season particularly for systems with high tilt angle. Also it can be observed that results have less seasonal effect when tilt angles are small (30^0 & 35^0) compared with when the tilt angle is high (65^0).

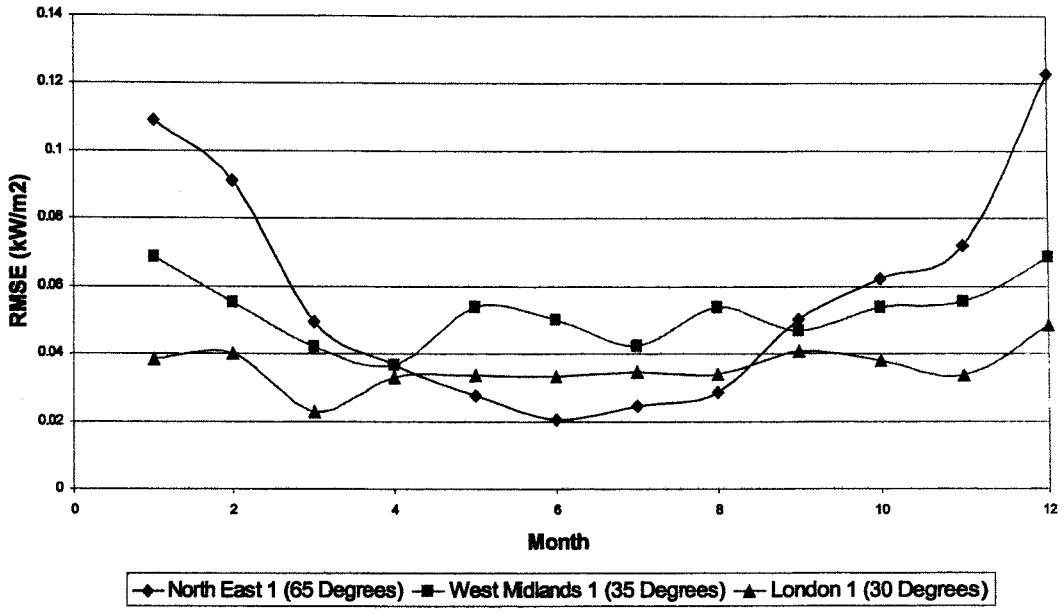

Figure 3-31 Comparison of hourly tilted radiation results for different PV systems

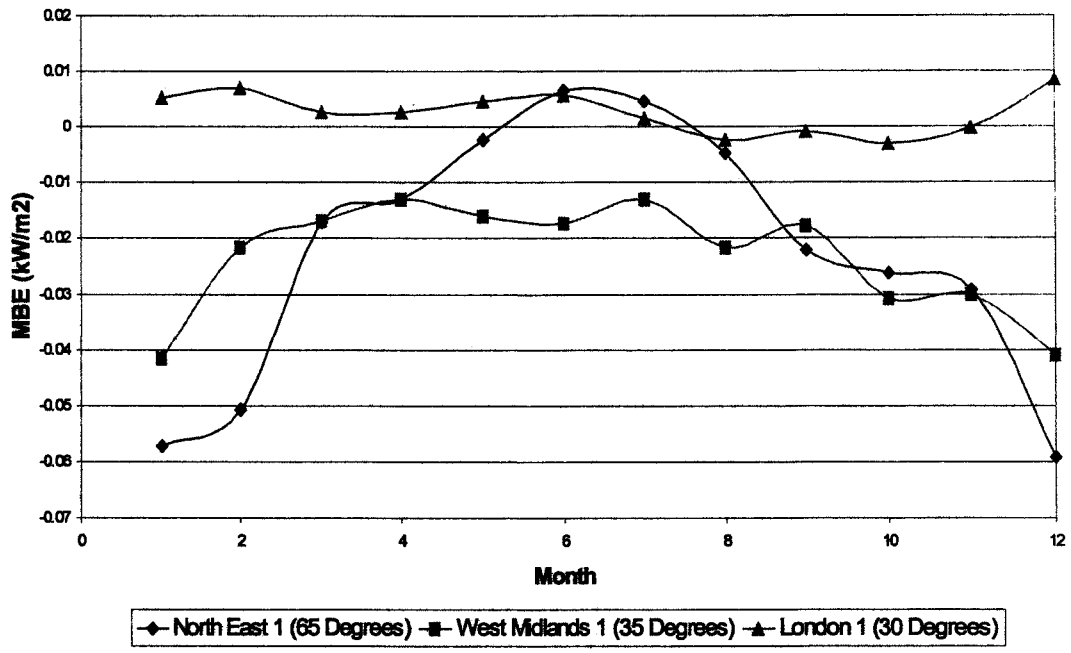

Figure 3-32 Comparison of MBE results from hourly tilted radiation results for different PV systems

3.7.3 Results for half-hour tilted radiation

Similar to the previous analysis, the validation of the Hay model to calculate half-hourly tilted radiation was carried out for the North East 1 location. Measured values are plotted against the calculated values for February and May in Figure 3-33 and Figure 3-34. These figures represent the seasonal variation in accuracy of calculating the tilted radiation values. The statistical comparison results are shown in Table 3-8. Similarly half-hour tilted radiation values were calculated for the West Midlands 1 and London 1 PV systems. The statistical comparison results are given in Table 3-9 and Table 3-10. RMSE values obtained for all three systems are plotted in Figure 3-35. The RMSE values are low for summer months and high for winter months. The MBE values obtained from all three systems are plotted in Figure 3-36. The MBE values are low for summer months and high for winter months.

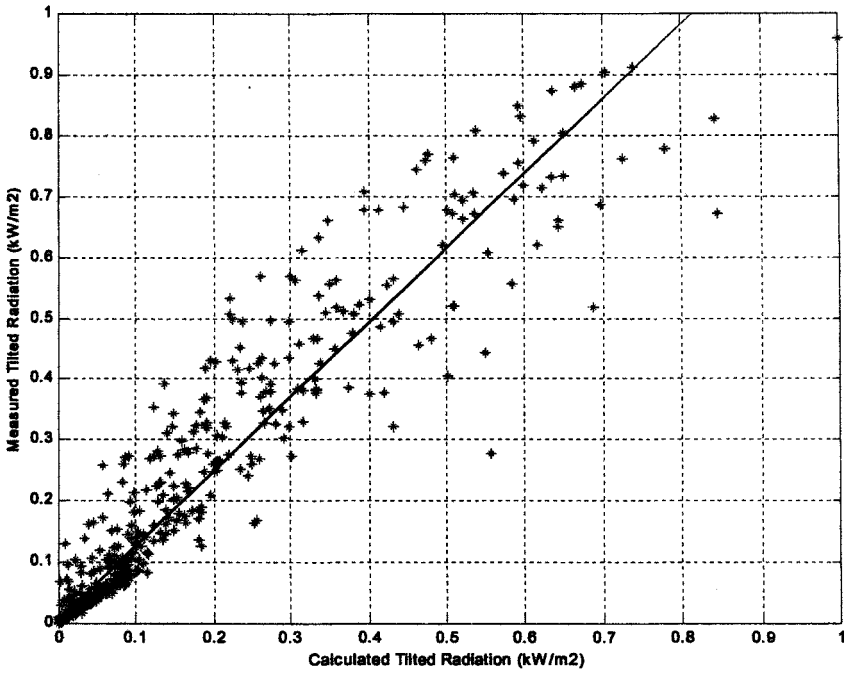

Figure 3-33 Half-hourly tilted radiation result for the North East 1 location, for February 1998

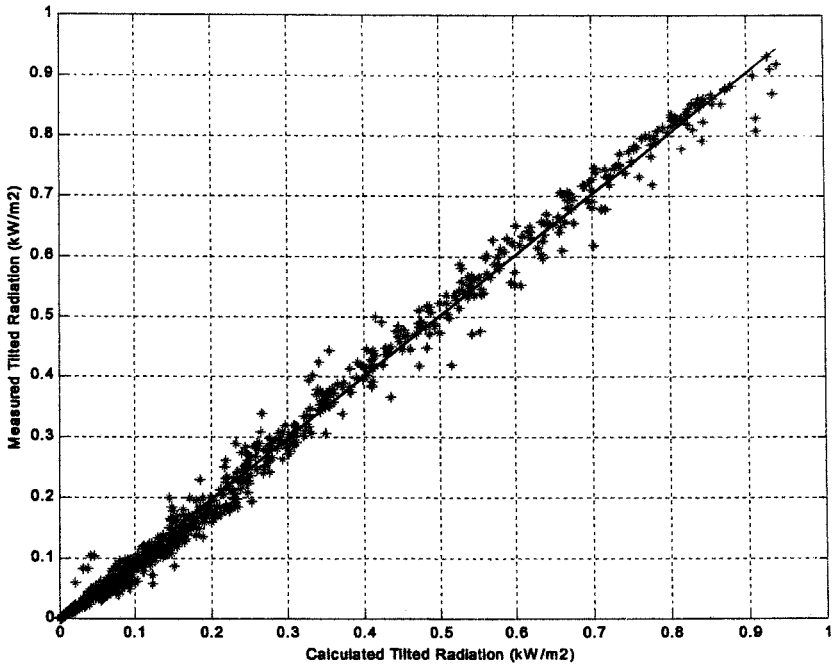

Figure 3-34 Half-hourly tilted radiation result for the North East 1 location, for May 1998

Table 3-8 Statistical comparison of half-hourly tilted radiation results for the North East 1 location, year 1998

Month	MBE (kW/m^2)	RMSE (kW/m^2)
January	-0.0409	0.0933
February	-0.0468	0.0946
March	-0.0254	0.0694
April	-0.0031	0.0291
May	0.0034	0.0207
June	0.0086	0.0201
July	0.0089	0.0223
August	-0.0006	0.0263
September	-0.0055	0.0356
October	-0.0343	0.0794
November	-0.0437	0.0962
December	-0.0397	0.0905

Table 3-9 Statistical comparison of half-hourly tilted radiation results for the West Midlands 1 location, year 2001

Month	MBE (kW/m^2)	RMSE (kW/m^2)
January	-0.0401	0.0697
February	-0.0185	0.0573
March	-0.0139	0.0428
April	-0.0120	0.0357
May	-0.0158	0.0499
June	-0.0165	0.0459
July	-0.0123	0.0406
August	-0.0207	0.0524
September	-0.0153	0.0470
October	-0.0265	0.0526
November	-0.0254	0.0560
December	-0.0450	0.0757

Table 3-10 Statistical comparison of half-hour tilted radiation results for the London 1 location, year 2001

Month	MBE (kW/m^2)	RMSE (kW/m^2)
January	0.0029	0.0337
February	0.0072	0.0387
March	0.0009	0.0197
April	0.0012	0.0277
May	-0.0012	0.0320
June	0.0013	0.0315
July	-0.0026	0.0337
August	-0.0068	0.0351
September	-0.0029	0.0330
October	-0.0031	0.0418
November	-0.0016	0.0260
December	0.0023	0.0376

These results are similar to the hourly tilted radiation results. The RMSE and MBE results indicate that calculated values from the Hay model and measured values have good fit for all months except winter months. During the winter season the error values were high particularly for the system with high tilt angle. During the winter season the RMSE values are higher for system with high tilt angle (65^0) compared with systems with low tilt angle PV systems (30^0 and 35^0).

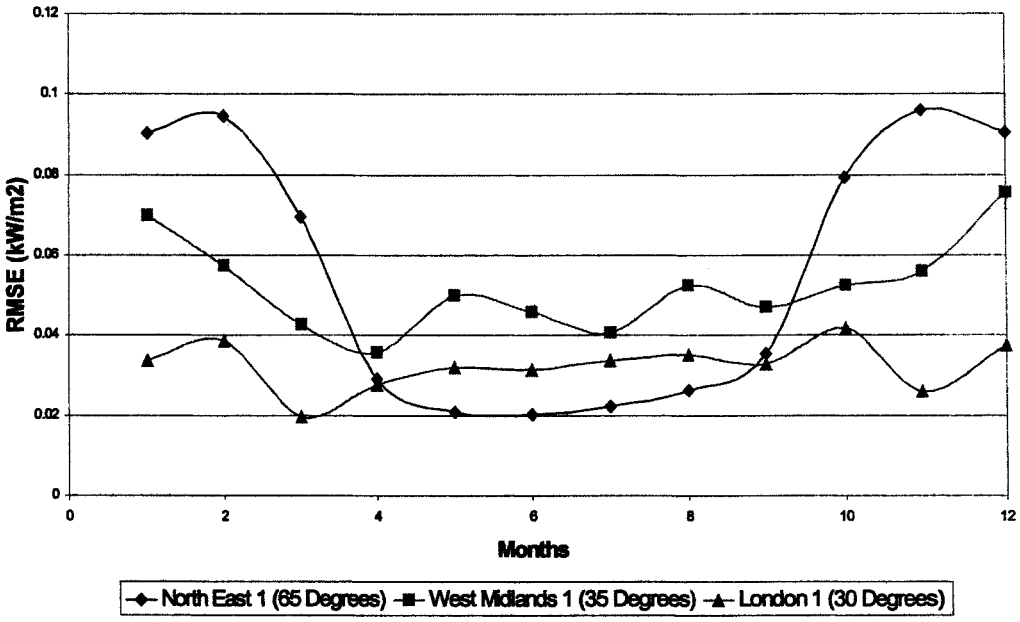

Figure 3-35 Comparison of RMSE values from half-hour tilted radiation results

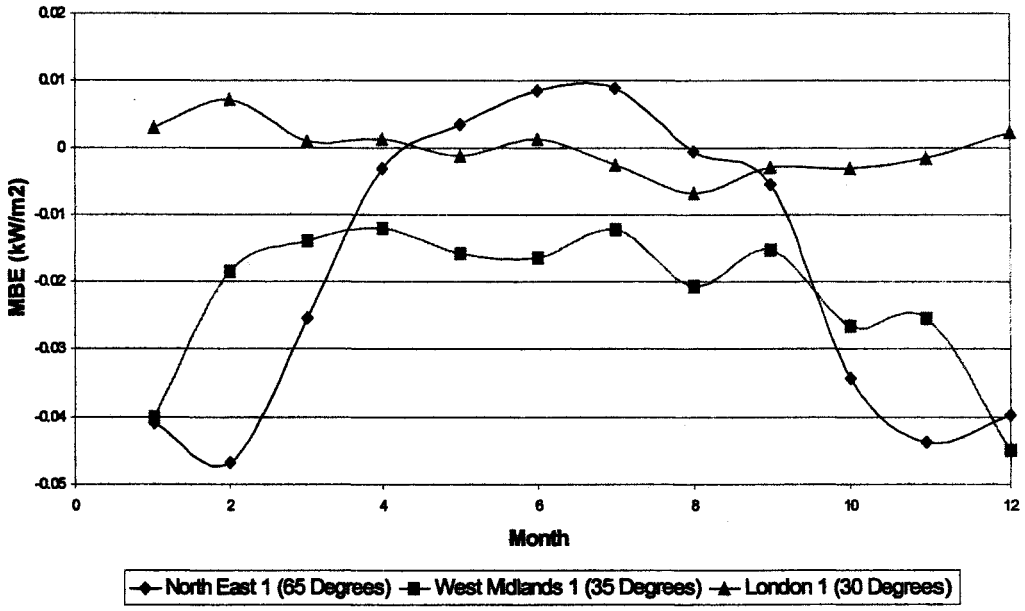

Figure 3-36 Comparison of MBE values from half-hour tilted radiation results

3.7.4 Discussion on tilted radiation results

The power output from a PV system depends upon the solar radiation received by the PV array and that depends upon the tilt angle and orientation of the PV array. The geographically dispersed PV systems will vary in their tilt angles and orientations. The measured tilted radiation values are available for a few PV systems that correspond to particular tilt angles and orientations. Therefore it was necessary to use a model to translate horizontal radiation to tilted radiation values. From the literature survey the Hay model was selected to calculate the tilted radiation values. The Erbs model was chosen to calculate the horizontal diffuse radiation values from global horizontal radiation values. The selected model was validated for different PV systems, which varies in their tilt angles, orientations and locations.

From this analysis it was found that the RMSE values were low for summer months and high for winter months. The MBE values indicate that the model overestimates in some cases and underestimates in some other cases. The MBE values were low for summer months and high for winter months. These results indicated that the calculated tilted radiation values from the selected Hay model gave good fit with measured tilted radiation values for all months except winter months. During the winter season the error values were high particularly for the system with high tilt angle. From these results it can be concluded that the selected Hay model can be used to translate the horizontal radiation to tilted radiation values for PV arrays with any tilt angles and orientations.

3.8 Discussion on Results

In order to analyse the power output from geographically dispersed PV systems the solar radiation data at different locations are needed. The horizontal solar radiation data were generated for different locations in the UK using the MTM method. From this study it was found that the MTM method is capable of producing horizontal solar radiation data which is representative of actual data in terms of the fluctuation as well as the absolute values. The Hay model was selected to calculate the tilted radiation values and validated for different PV systems.

The next step followed was to combine the MTM method and Hay model to generate the solar radiation data. Steps followed to validate the simulated data are illustrated in Figure 3-37. Hourly horizontal radiation data were generated for the West Midlands 1 location using the MTM method. These generated data were used to calculate the hourly tilted radiation values using the Hay model. Calculated tilted radiation values were stored in an Excel sheet. A Macro was written to calculate the daily tilted irradiation values and compared with measured daily tilted irradiation values and is shown in Figure 3-38. The analysis was also carried out for the London 1 location and the comparison result is shown in Figure 3-39. The statistical comparison results between the measured and simulated daily tilted irradiation values are given in Table 3-11.

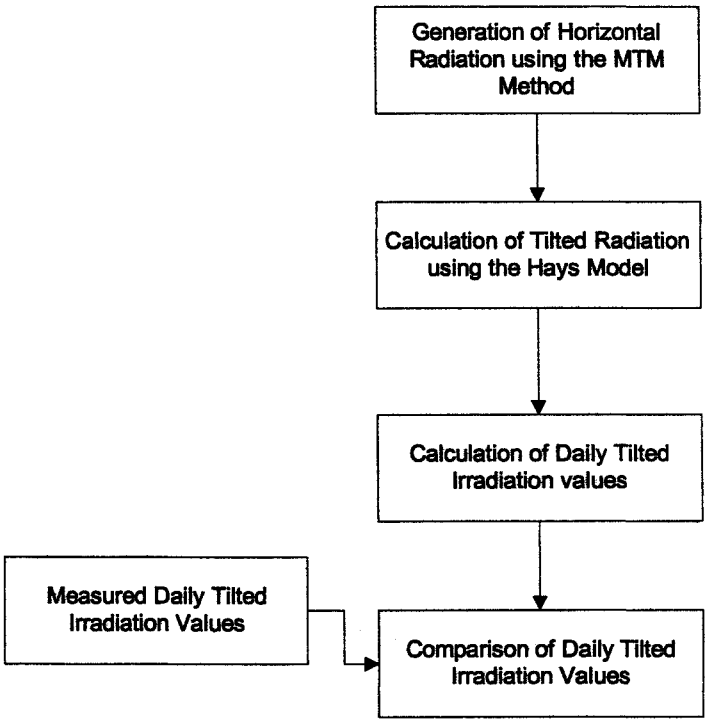

Figure 3-37 Illustration of validation of the simulated data

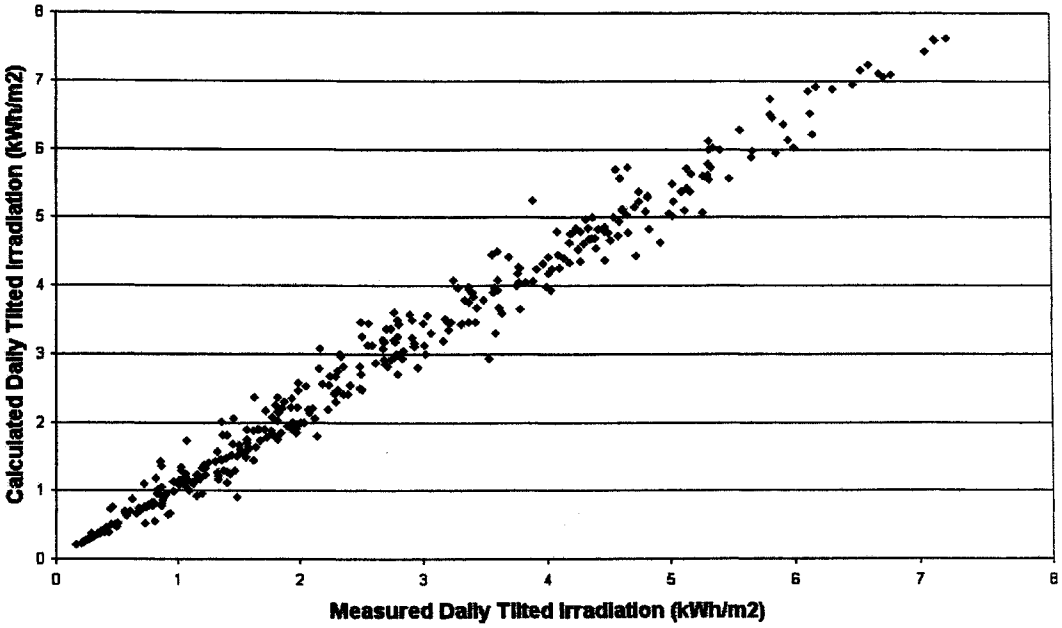

Figure 3-38 Comparison of daily total of hourly tilted irradiation for the West Midlands 1 location

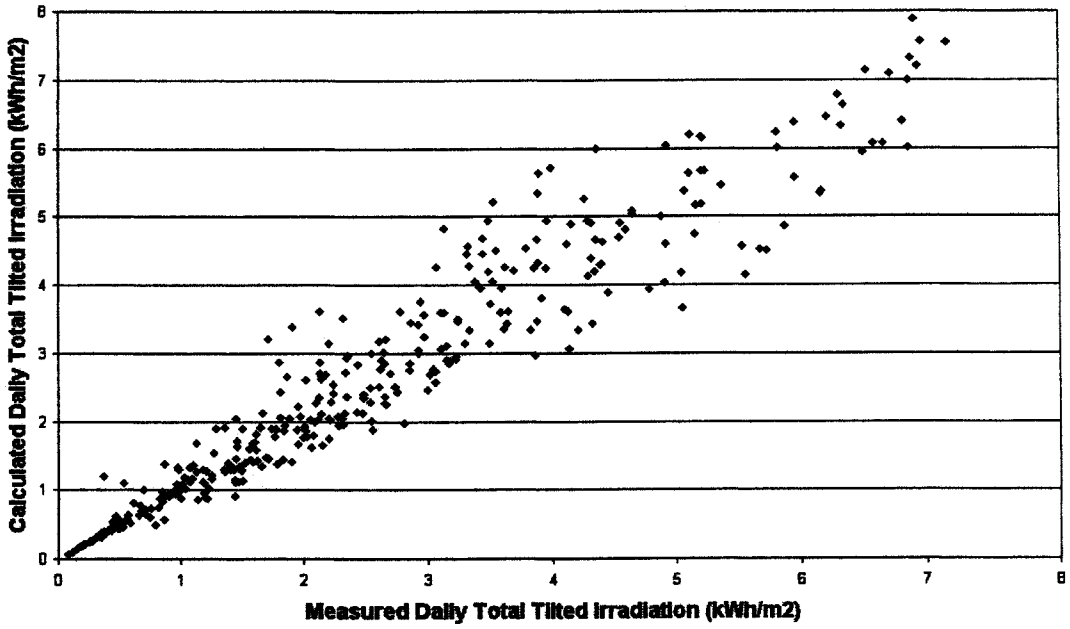

Figure 3-39 Comparison of daily total of hourly tilted irradiation for the London 1 location

Table 3-11 Statistical comparison of daily total hourly tilted irradiation data

Location	MBE (kWh/m^2)	RMSE (kWh/m^2)	RMBE	RRMSE	Correlation Coefficient
West Midlands 1	0.2389	0.3695	0.0940	0.1630	0.9904
London 1	-0.094	0.5056	-0.0096	0.1716	0.9627

Similarly the analysis was carried out for the West Midlands 1 and London 1 locations with half-hour solar radiation generation. The comparison results are shown in Figure 3-40 and Figure 3-41. The statistical comparison results are given in Table 3-12.

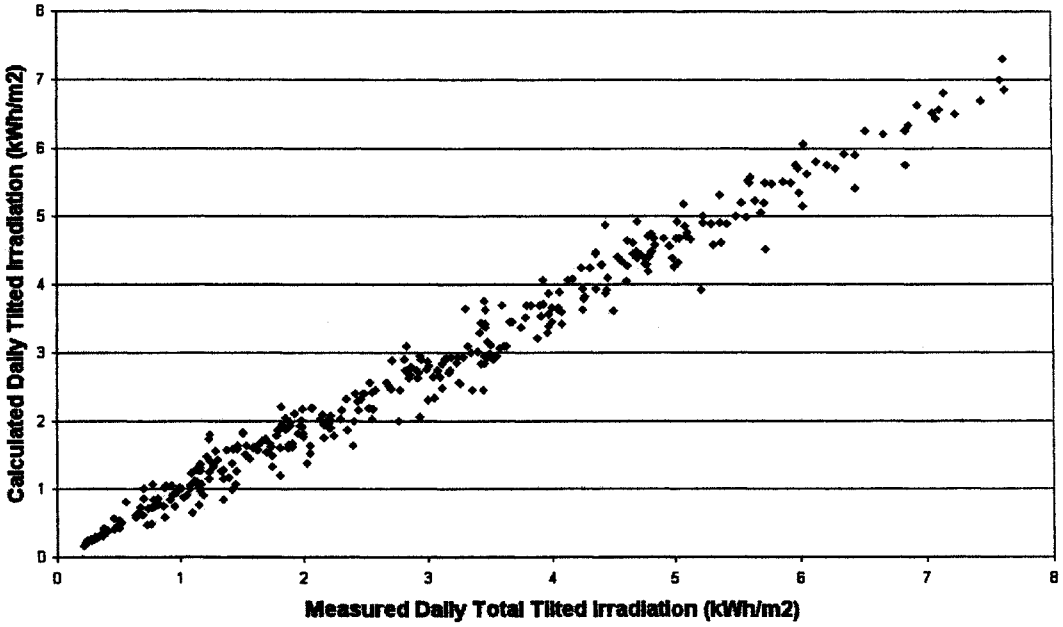

Figure 3-40 Comparison of daily total of half-hour tilted irradiation for the West Midlands 1 location

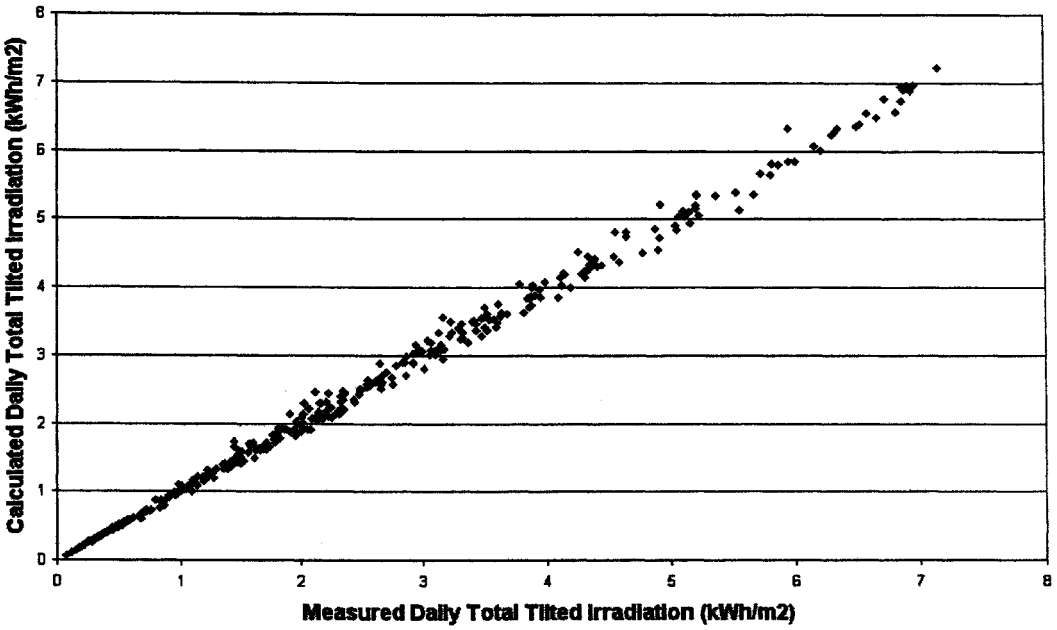

Figure 3-41 Comparison of daily total of half-hour tilted irradiation for the London 1 location

Table 3-12 Statistical comparison of daily total half-hour tilted irradiation data

Location	MBE (kWh/m^2)	RMSE (kWh/m^2)	RMBE	RRMSE	Correlation Coefficient
West Midlands 1	-0.2117	0.3619	-0.0607	0.1316	0.9903
London 1	-0.0070	0.1065	0.0006	0.0435	0.9982

From these results it can be observed that the calculated values gave good fit with measured values. The correlation coefficient values between the two series were always greater than 96%. These results indicate that from the selected models the representative solar radiation data can be generated. For the given daily total horizontal irradiation values the representative hourly or half-hourly horizontal radiation values can be generated from the MTM method. From the generated horizontal radiation values tilted radiation values for PV systems with different tilt angle and orientation can be calculated using the selected Hay model. These tilted

radiation data can be used to analyse the power output from geographically dispersed PV systems. The methods to represent the geographically dispersed PV systems and the calculation of power output from these systems are discussed in the next chapter.

3.9 References for Chapter 3

1. Photovoltaics in Buildings, A design Handbook for Architects and Engineers, Solar Heating & Cooling Programme, Task 16, International Energy Agency, Paris, France, 1996.
2. Duffie and Beckman, "Solar Engineering of Thermal Processes", Chapters 1 and 2, Second Edition, 1991, A Wiley- Inter science Publication.
3. Potential for Building Integrated Photovoltaics, Photovoltaic Power System Programme, Technical Report IEA-PVPS T7-4: 2002, Published by International Energy Agency.
4. A. Angstrom, "Solar and terrestrial radiation", Quarterly Journal of Royal Meteorological Society, 50, pp.121-125, 1924.
5. A. Prescott, "Evaporation from a water surface in relation to solar radiation", Trans. Roy. Soc. Austr., 64, pp.114-118, 1940.
6. C.T. Wong, "Solar radiation model", Applied Energy, Vol.69, pp.191-224, 2001.
7. K.K. Gopinathan, "A general formula for computing the coefficients of the correlation connecting global radiation to sunshine duration", Solar Energy, Vol. 41, No.6, pp.499-502, 1988.
8. T. N. Goh and K.J. Tan, "Stochastic modelling and forecasting of solar radiation data", Solar Energy, Vol.19, pp.755-757, 1977.
9. B.J. Brinkworth, "Autocorrelation and stochastic modelling of insolation sequences", Solar Energy, Vol.19, pp.343-347, 1977.
10. B.Y.H. Liu and R.C. Jordan, "The interrelationship and characteristic distributions of direct, diffuse and total solar radiation", Solar Energy, Vol.4, pp.1-19, 1960.
11. S.A. Klein, "A design procedure for solar heating systems", Solar Energy, Vol.19, pp. 325-329, 1976.

12. V.A. Graham, K.G.T. Hollands and T.E. Unny, "A time series model for K_t with application to global synthetic weather generation", Solar Energy, Vol.40, No.2, pp.83-92, 1988.
13. V.A. Graham and K.G.T. Hollands, "A method to generate synthetic hourly solar radiation globally", Solar Energy, Vol.44, No.6, pp.333-341, 1990.
14. R. Aguiar and M. Collares – Pereira, "Statistical properties of hourly global radiation", Solar Energy, Vol.48, No.3, pp.157-167, 1992.
15. R. Aguiar and M. Collares – Pereira, "TAG: A time-dependent, Autoregressive, Gaussian model for generating synthetic hourly radiation", Solar Energy, Vol.49, No.3, pp.167-174, 1992.
16. Carlo Mustacchi, Vincenzo Cena and Massimo Rocchi, "Stochastic simulation of hourly global radiation sequences", Solar Energy, Vol.23, pp.47-51, 1979.
17. Lalarukh Kamal, Yasmin Zahra Jafri, "Stochastic modelling and generation of synthetic sequences of hourly global solar irradiation at Quetta, Pakistan", Renewable Energy, Vol.18, pp.565-572, 1999.
18. R. Aguiar, M. Collares – Pereira and J.P. Conde, "Simple procedure for generating sequence of daily radiation values using a library of Markov Transition Matrices", Solar Energy, Vol.40, No.3, pp.269-279, 1988.
19. P. Poggi, G. Notton, M. Muselli and A. Louche, "Stochastic study of hourly total solar radiation in Corsica using a Markov model", International Journal of Climatology, Vol.20, pp.1843-1860, 2000.
20. Zekai Sen, "Fuzzy algorithm for estimation of solar irradiation from sunshine duration", Solar Energy, Vol.63, No.1, pp.39-49, 1998.
21. M. Mohendas, S. Rehman and T.O. Halawani, "Estimation of global solar radiation using artificial neural networks", Renewable Energy, Vol.14, Nos.1-4, pp.179-184, 1998.
22. L. Hontoria, J. Riesco, J. Aguilera and P. Zufiria, "Application of neural networks in the solar irradiation field: Obtainment of solar irradiation maps", 16th European Photovoltaic Solar Energy Conference, 1-5 May 2000, Glasgow, UK, Vol. 3, pp. 2359 – 2542, Published by James and James (Science Publishers) Ltd., UK.
23. L. Hontoria, J. Riesco, J. Aguilera and P. Zufiria, "Statistical study of solar irradiation data generated by the neural net Multilayer Perceptron", 16th

European Photovoltaic Solar Energy Conference, 1-5 May 2000, Glasgow, UK, Vol. 1, pp. 214 – 217, Published by James and James (Science Publishers) Ltd., UK.

24. P.J. Zufiria, A. Vazquez, J. Riesco, J. Aguilera and L. Hontoria, "A neural network approach for generating solar irradiation artificial series", Proceeding of the IWANN'99, Alicante, 4-5 June, 1999.
25. M. Iqbal, "Correlation of average diffuse and beam radiation with hours of bright sunshine", Solar Energy, Vol.23, pp.169-173, 1979.
26. K.K. Gopinathan, "Estimation of hourly global and diffuse solar radiation from hourly sunshine duration", Solar Energy, Vol.48, No.1, pp.3-5, 1992.
27. M. Iqbal, "An Introduction to Solar Radiation", Toronto: Academic Press, 1983.
28. J.F. Orgill and K.G.T. Hollands, "Correlation equation for hourly diffuse radiation on a horizontal surface", Solar Energy, Vol.19, pp.357-359, 1977.
29. D.G. Erbs, S.A. Klein and J.A. Duffie, "Estimation of the diffuse radiation fraction for hourly, daily and monthly-average global radiation", Solar Energy, Vol.28, No.4, pp.293-302, 1982.
30. D.T. Reindl, W.A. Beckman and J.A. Duffie, "Diffuse fraction correlations", Solar Energy, Vol.45, No.1, pp.1-7, 1990.
31. A. Skartveit, J.A. Olseth, "A model for the diffuse fraction of hourly global radiation", Solar Energy, Vol.38, No.4, pp.271-274, 1987.
32. B.Y. Liu and R.C. Jordan, "Daily insolation on surfaces tilted towards the equator", Trans ASHRAE, Vol.67, pp.526-541, 1962.
33. J.E. Hay and J.A. Davies, "Calculation of the solar radiation on an inclined Surface", Proceedings of the First Canadian Solar Radiation Data Workshop, Toronoto, pp.59-72, 1980.
34. T.M. Klucher, "Evaluation of models to predict insolation on tilted surfaces", Solar Energy, Vol.23, pp.111-114, 1979.
35. R.C.Temps, K.L. Coulson, "Solar radiation incident upon slopes of different orientations", Solar Energy, Vol.19, pp.179-184, 1977.
36. R. Perez, "An anisotropic model for the diffuse radiation incident on slopes of different orientations", Proceedings of ASES, Minneapolis, pp.883-888, 1983.

37. R. Perez, "A new simplified version of the Perez diffuse irradiation model for tilted surfaces", Solar Energy, Vol.39, No.3, pp221-231, 1987.
38. C.C.Y. Ma, M. Iqbal, "Statistical comparisons of models for estimating solar radiation on inclined surfaces", Solar Energy, Vol.31, pp313-317, 1983.
39. K.K. Gopinathan, "Solar radiation on inclined surfaces", Solar Energy, Vol.45, No.1, pp19-25, 1990.
40. D.T. Reindl, W.A. Beckman and J.A. Duffie, "Evaluation of hourly tilted surface radiation models", Solar Energy, Vol.45, No.1, pp9-17, 1990.
41. J. Remund, E. Salvisberg and S. Kunz, "On the generation of hourly shortwave radiation data on tilted surfaces", Solar Energy, Vol. 62, No. 5, pp 331-344, 1998.
42. L. Mora-Lopez and M. Sidrach-De- Cardona, "Multiplicative ARMA models to generate hourly series of global irradiation", Solar Energy, Vol. 63, No. 5, pp. 283-291, 1998.
43. Ronald A. Howard, "Dynamic Probabilistic Systems, Volume 1: Markov Models", Chapter 1, 1971, John Wiley & Sons, Inc., New York.
44. N.M. Pearsall, A.R. Wilshaw and F.C. Crick, "The first year of operation of the Northumberland Building photovoltaic façade", 4th International Conference on Solar Energy in Architecture and Urban Planning, Berlin, March 1996, pp. 599-602, Published by H.S. Stephens & Associates, Bedford, UK.
45. D. Lloyd Jones, C. Matson and N.M. Pearsall, "The solar office: A solar powered building with a comprehensive energy strategy", 2nd World Conference on Photovoltaic Solar Energy Conversion, Vienna, Austria, July 1998, Vol. 3, pp. 2559 – 2562, Published by European Commission, Renewable Energies Unit, Ispra.

4 DEVELOPMENT OF PV CLUSTER MODEL

Large-scale inclusion of PV systems in the UK electricity supply is expected to take the form of a large number of small, geographically dispersed building integrated PV systems. These systems will vary in their design parameters like system size, type of PV module, array orientation, tilt angle, location of the system, inverter type and inverter rating etc. For example the PV system parameters of system size, tilt angle and orientation depend upon the building envelope in which the PV system is integrated. Moreover these PV systems will be connected to different points of the grid. The solar radiation at different grid points will be different and hence the output power from dispersed PV systems will be different. So the combined output power from geographically dispersed PV systems would not be a simple aggregation of the single optimised PV system. Murata et al. [1] investigated the output power from very many PV systems installed on a nation-wide scale in Japan, using solar radiation for different locations. But in their study it was assumed that 3 kW south oriented PV systems are installed on house roofs. In the work presented in thesis a detailed study on modelling the large-scale geographically dispersed PV systems was carried out for the UK. This chapter explains the steps that have been taken to develop a PV cluster model to represent the large number of small, geographically dispersed PV systems. To develop the PV cluster model, the UK domestic and non-domestic building stock, PV module technologies and inverter technologies were used. This chapter explains the methods followed to estimate the combined output power from geographically dispersed PV systems. The sensitivity of PV output power with changes in the system design parameters are also analysed in this chapter. This chapter also discusses the possible changes in domestic and non-domestic building stock, PV module technologies and inverter technologies for the year 2030 to analyse the impact of large-scale PV systems on the grid.

4.1 Types of Cluster

Due to the complexity in developing the PV cluster model that represents geographically dispersed PV systems, step-by-step procedures have been followed.

In this work modelling of a PV cluster model was carried out in three steps. These are

- ***Modelling of single PV system***

  This is the first step to represent the single PV system. In this step, a method to calculate the DC and AC output power from a single PV system is analysed for the specified system design parameters.

- ***Modelling of Single Mixed Cluster***

  The Single Mixed Cluster (SMC) is considered to be equivalent to a large number of PV systems of varying size, system design and feeding to a single point of the grid model. So in this model the variation of system size, tilt angle, orientation, PV module technologies, inverter topologies and inverter rating were taken into account. For the SMC modelling the insolation level is assumed to be identical for all PV systems in the cluster.

- ***Modelling of Multiple Cluster***

  The Multiple Cluster (MC) consists of a combination of several single clusters feeding in at different points of the grid model and is used to consider the effect of location of the feed-in point and interaction of clusters. This cluster model considers different insolation levels across the geographical area.

In the following sections the methods followed to model these clusters are discussed and steps followed to estimate the output power from geographically dispersed PV systems are also discussed.

4.2 Modelling of Single PV System

The DC output power from PV arrays depends upon the tilted radiation, PV module efficiency and ambient temperature. The AC output power from a PV system also depends upon the inverter efficiency. The following sections explain the methods used to calculate the DC power and AC output power from a PV system for the specified system design parameters.

4.2.1 DC output power calculation

Factors which affect the output power of PV modules are the solar radiation, module operating temperature, shading, mismatch of modules in a string, resistance of wires and cables etc. [2]. A simple and widely used expression for estimating the DC output power of PV modules using the maximum power temperature coefficient parameter is given as [3,4]

$$P_{dc} = P_{ref} * \left(\frac{I_T}{I_{ref}}\right) * [1 + B(T_c - T_{ref})] \quad (4.1)$$

where,

I_T is the tilted radiance (kW/m^2)

P_{ref} is the maximum output power of the PV module at reference condition (kW)

I_{ref} is the radiance at reference condition (kW/m^2)

B is the temperature coefficient of maximum power (-0.045/ ^{0}C for crystalline silicon)

T_{ref} is the reference temperature (^{0}C) and

T_c is the cell temperature (^{0}C)

Cells in an illuminated module operate at a higher temperature than the ambient temperature. The cell temperature, T_c is given as [3,4]

$$T_c = T_a + \varsigma G_a \quad (4.2)$$

where,

T_a is ambient temperature (^{0}C) and

ς is a function of the Nominal Operating Cell Temperature (NOCT). NOCT is an indicator of difference between ambient and cell temperature and is measured under defined operating conditions of ambient temperature of 20^{0}C, solar irradiation of 0.8 kW/m^2, and wind speed of 1m/s [5] with the modules mounted on an open framework.

Whitaker et al. [3] investigated the power temperature coefficient for different operating conditions and showed that temperature coefficients can be considered constant over the normal range of operating conditions. Therefore equation 4.1 can be used to calculate the DC output power from BIPV systems.

4.2.2 AC output power calculation

The AC output power of a PV system (P_{ac}) also depends on the inverter efficiency for which instantaneous values depend on the ratio between output power (P_{ac}) and nominal power of the inverter (P_{nom}). Schmid et al. [6] proposed the method of calculating inverter efficiency as a function of AC output power. Other researchers [4,7] also used this relation to find the AC output power of PV systems.

According to this method, losses in the inverter (P_{loss}) are classified as load independent and load dependent losses given by:

$$P_{loss} = (p_0 + kp^2)P_{nom} \tag{4.3}$$

where,

p_o is the load independent loss coefficient

k is the load dependent loss coefficient and

p is the ratio of output power to the nominal power of the inverter (P_{ac}/P_{nom}).

AC power produced is given by

$$P_{ac} = P_{dc} - \left[p_0 + k\left(\frac{P_{ac}}{P_{nom}}\right)^2 \right] P_{nom} \tag{4.4}$$

Parameters p_o and k are calculated from the efficiency curve of the inverter as

$$p_0 = \frac{1}{99}\left(\frac{10}{\eta_{10}} - \frac{1}{\eta_{100}} - 9\right) \tag{4.5}$$

$$k = \frac{1}{\eta_{100}} - p_0 - 1 \tag{4.6}$$

Where

η_{10} is the efficiency at 10% of nominal rating and

η_{100} is the efficiency at 100% of nominal rating.

4.2.3 Output power from a single PV system

In order to model the output power from a PV system, a 3kW PV system with BP585F PV modules [8] was assumed. The nominal rating of each module is 85 Watts and the efficiency of PV module is 14%. Nominal Operating Cell Temperature (NOCT) of these modules is 47±2 °C [8]. The tilt angle of PV arrays were assumed as 65° to the horizontal and southeast oriented with an azimuth angle of -16.5^0. The selected tilt angle and orientation values correspond to the Northumberland Building PV system values. These values were selected in order to check the calculated values directly against the measured values. This PV system was assumed to have a multistage type inverter with high frequency transformer, Sunny Boy 2500 [9]. The nominal rating of the inverter is 2.2 kW and the maximum output power is 2.5 kW.

As explained in Chapter 3, using the MTM method hourly horizontal solar radiation data was generated for a London location (latitude of 51.63^0N and longitude of 0.03^0W), from daily total irradiation values. The Hay model was used to calculate the hourly tilted radiation from the horizontal radiation values for the assumed tilt angle and orientation. The DC output power from PV array was calculated using equations 4.1 and 4.2. The AC output power from the PV system was calculated by using equations 4.3 to 4.6. Although in practice an inverter can usually sustain an output slightly higher than its nominal rating for a limited time period, in this work it was assumed that AC output power from the inverter will not exceed the nominal rating of the inverter.

If a cluster consists of 1000 such 3kW PV systems, which are identical, output power from the cluster will be 1000 times the output power of a 3 kW PV system. The AC output power from a PV cluster, 3MW capacity (1000 identical 3 kW PV systems), was calculated for June and is shown in Figure 4-1. Similarly, using solar radiation data from North East 1 and West Midlands 1 locations, the output power for a PV cluster of 3 MW in each region was calculated. These output values were provided to the UMIST group to analyse fluctuation of PV output power and their impact on the reserve requirement (Refer to Chapter 6). But in practice PV systems will vary in

their design parameters such as tilt angle, orientation etc. The methods to represent the variation in system design parameters are analysed in the next section.

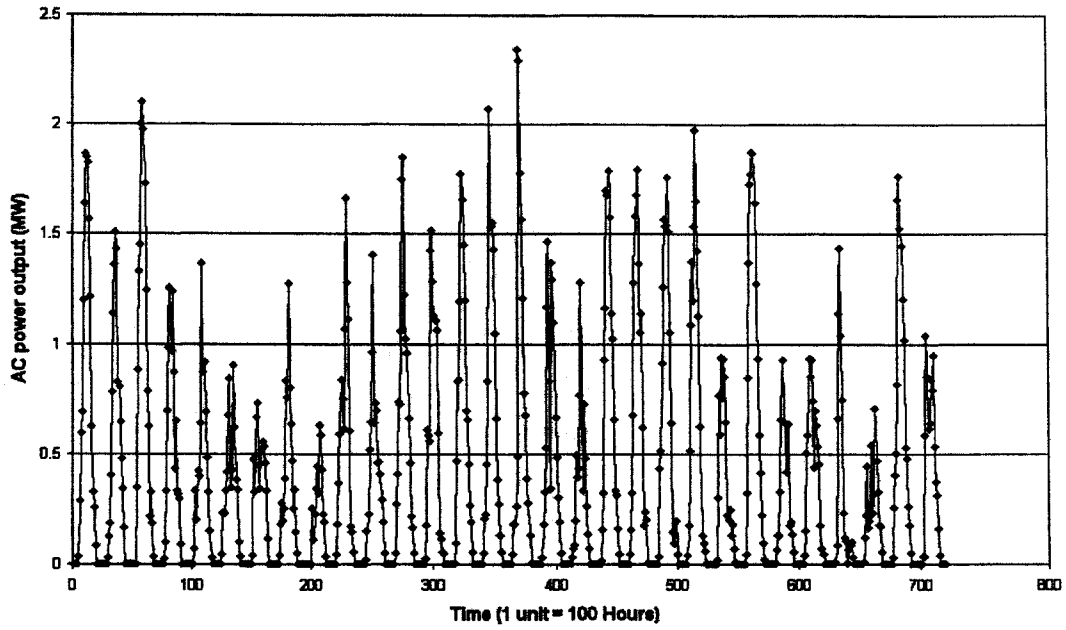

Figure 4-1 Output power from a PV cluster, capacity of 3 MW (1000 identical PV systems), for June

4.3 Modelling of Single Mixed Cluster (SMC)

As explained in the previous section, the dispersed PV systems will vary in their design such as system size, PV module technology, orientation, tilt angle, inverter type and inverter rating etc. and these are taken into consideration in the SMC modelling. The flow chart shown in Figure 4-2 illustrates the concept of the single mixed cluster modelling. PV systems will vary in their system size, orientation, inverter type etc called as **parameters**. Each parameter can be classified into different **groups**, for example the system size can be classified into groups A, B, C. The percentage of PV systems in each group is defined as x%, y% and z% respectively. Similarly the orientation can be classified into groups I, II, III. The percentage of PV systems in each group is defined as a%, b% and c% respectively. PV systems with system size "A" and orientation "I" is a one possible combination called as a ***category***. The percentage of PV systems in the A-I category is the multiplication of x% and a%. The total number of PV systems in the A-I category is

(x%*a%*total number of PV systems). Building data and the assumed percentage of buildings with PV were used to estimate the total number of PV systems in the SMC.

The output power from a PV system in "A-I category" can be calculated as explained in the previous section. These values are multiplied by the total number of PV systems in the "A-I category" to estimate the output power from all PV systems in this category. This can be repeated for different categories and the sum of output power from all categories will be the output power from the SMC. The total number of categories is the number of possible combinations like A-I, A-II, B-I, B-II and so on. The percentage of PV systems in each category can be calculated by multiplying the percentage of each group in that category.

By this approach, the model can be used to study the output power from dispersed PV systems which can be analysed for different scenarios. For example

- The number of groups in each parameter and the percentage of PV systems in each group can be modified easily and the output power from SMC can be studied for different cases.
- The percentage of buildings with PV can be adjusted easily to study the output power from PV systems for different penetration levels.

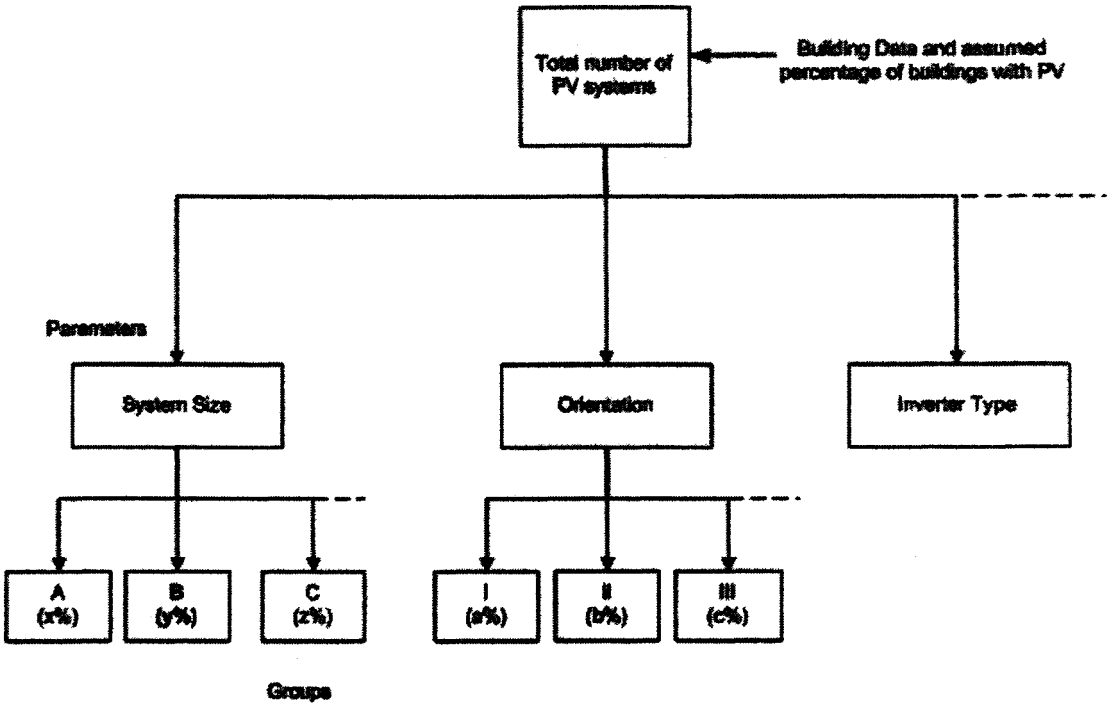

Figure 4-2 Illustration of the Single Mixed Cluster modelling

In order to develop the SMC, PV systems are classified into three types. They are

- Domestic PV systems
- Commercial PV systems and
- Industrial PV systems

Output power from the SMC is the addition of output power from domestic, commercial and industrial PV systems. The methods to represent these systems and the estimation of output power from the SMC are discussed in the following sections.

4.4 Modelling of Domestic PV Systems

The PV system shown in Figure 4-3 is an example of PV system installed on domestic house. The capacity of this PV system is 1.53 kWp and it uses mono-crystalline silicon type PV modules. PV arrays are tilted at an angle of 22^0 and they are south oriented. These design parameters may be different for each domestic PV system. For example parameters like PV system size and tilt angle and orientation of PV arrays depend upon the building envelopes, which may vary from one house to another.

Figure 4-3 Domestic PV System (Source: PV Systems Ltd.)

Therefore system parameters which vary within the domestic PV systems are identified as

- PV system size which depends upon the roof area and PV module technology
- Tilt angle of PV array that depends upon roof type
- Orientation of PV array that depends upon the building orientation

- Inverter type that depends upon the inverter market and
- Inverter rating that depends upon the PV system capacity

Methods to represent these parameters in the domestic PV systems modelling are discussed in the following sections.

4.4.1 Dwellings data

To define the total number of domestic PV systems in the SMC, the dwelling stock for England and Wales and an assumed percentage of dwellings with PV were used. For this purpose data on the dwelling stock for England and Wales were collected and this is discussed in this section. According to the government statistical release on dwelling stock [10,11] the total number of dwellings for the year 2000 in each region of England is given in Table 4-1. Not all the dwelling stock is currently in use and hence there are vacant properties [10]. These buildings are vacant due to some repair work or property to let or for sale. In these type of buildings the chances for PV installation is low and hence the total number of vacant dwellings was deducted from the total dwelling stock. In the occupied dwelling stock there are also unfit dwellings for human habitation [10], classified as having unsatisfactory facilities for preparation and cooking of food or problems with structural stability, ventilation, disrepair, dampness etc. In these buildings lacking primary facilities, the opportunity for PV installation is low, so the number of unfit dwellings was also deducted from the total occupied dwellings.

The Department of the Environment Transport and Regions (DETR) conducts the survey on English house conditions, once every five years. The surveys provide a major source of information for the development and monitoring of housing polices. The English House Conditioning Survey (EHCS) 1996, is the seventh in the five year series undertaken by the DETR [10,12]. According to the EHCS 1996, the percentage of vacant dwellings in each region is given in Table 4-1. According to the EHCS 1996, the percentage of unfit dwellings in occupied dwellings for the whole England stock is 6.1%. For all regions this value was used to calculate the number of unfit dwellings since regionally separated data are not available. From these data, the number of dwellings in which PV systems can be installed was calculated and results are given in Table 4-2.

Table 4-1 Dwelling stock for England

Region	Dwelling Stock	Percentage of Vacant (%)	Occupied Dwellings
North East	1,127,000	4	1,081,920
Yorkshire and Humber	2,144,000	5	2,036,800
North West	2,956,000	4	2,837,760
East Midlands	1,776,000	3	1,722,720
West Midlands	2,206,000	5	2,095,700
South West	2,128,000	5	2,021,600
Eastern	2,285,000	3	2,216,450
South East	3,333,000	3	3,233,010
London	3,054,000	4	2,931,840

Table 4-2 Number of fit dwellings for England

Region	Occupied Dwellings	Unfit Dwelling	Dwellings Fit
North East	1,081,920	6.1%	1,015,923
Yorkshire and Humber	2,036,800		1,912,555
North West	2,837,760		2,664,657
East Midlands	1,722,720		1,617,634
West Midlands	2,095,700		1,967,862
South West	2,021,600		1,898,282
Eastern	2,216,450		2,081,247
South East	3,233,010		3,035,796
London	2,931,840		2,752,998

Dwelling stock includes both houses and flats. Due to the multiple occupancy behaviour in flats, there will be PV system ownership problem. In this analysis it was assumed that PV systems would be installed only on houses. However there are example PV systems installed in flats. In the domestic PV system model the changes can be easily incorporated to include PV systems on flats. According to the EHCS 1996 the percentage of houses and flats for each region is given in Table 4-3 [10,12]. From these data the number of houses that are fit, in which PV systems can be installed, was calculated.

Table 4-3 Percentage of houses and flats in the dwelling stock

Region	Dwellings Fit	Percentage of Houses (%)	Percentage of Flats (%)	House Stock Fit
North East	1,015,923	85.5	14.5	868,614
Yorkshire and Humber	1,912,555	85.5	14.5	1,635,235
North West	2,664,657	88.1	11.9	2,347,562
East Midlands	1,617,634	90.3	9.7	1,460,724
West Midlands	1,967,862	84.2	15.8	1,656,940
South West	1,898,282	84.8	15.2	1,609,743
Eastern	2,081,247	84.9	15.1	1,766,978
South East	3,035,796	82.2	17.8	2,495,425
London	2,752,998	52.7	47.3	1,450,830

Similar analysis was carried out for Wales. Dwelling stock for Wales in the year 2000 was 1,267,000 [11]. According to the Welsh house statistics [13] the occupied dwellings were 1,157,300. The percentage of unfit dwellings in the occupied dwellings was 8.5% [13,14] and hence the number of dwellings that were fit was 1,058,930. In this dwelling stock the percentage of houses is 90% [10,12]. So the number of houses that are fit, where the PV installation could be possible, was calculated as 953037. In these calculations the number of houses was rounded up to the nearest whole number.

4.4.2 Size of domestic PV systems

PV systems on domestic houses are usually installed on roofs. Due to the shading, aesthetic and vandalism problems it is not practical to install PV systems on the wall. The capacity of a PV system that can be installed on a house depends upon the floor area, tilt angle of the roof, suitable roof area that can be used for PV installation and PV module technology. Steps used to calculate the capacity of PV systems that can be installed on a domestic house are illustrated in Figure 4-4.

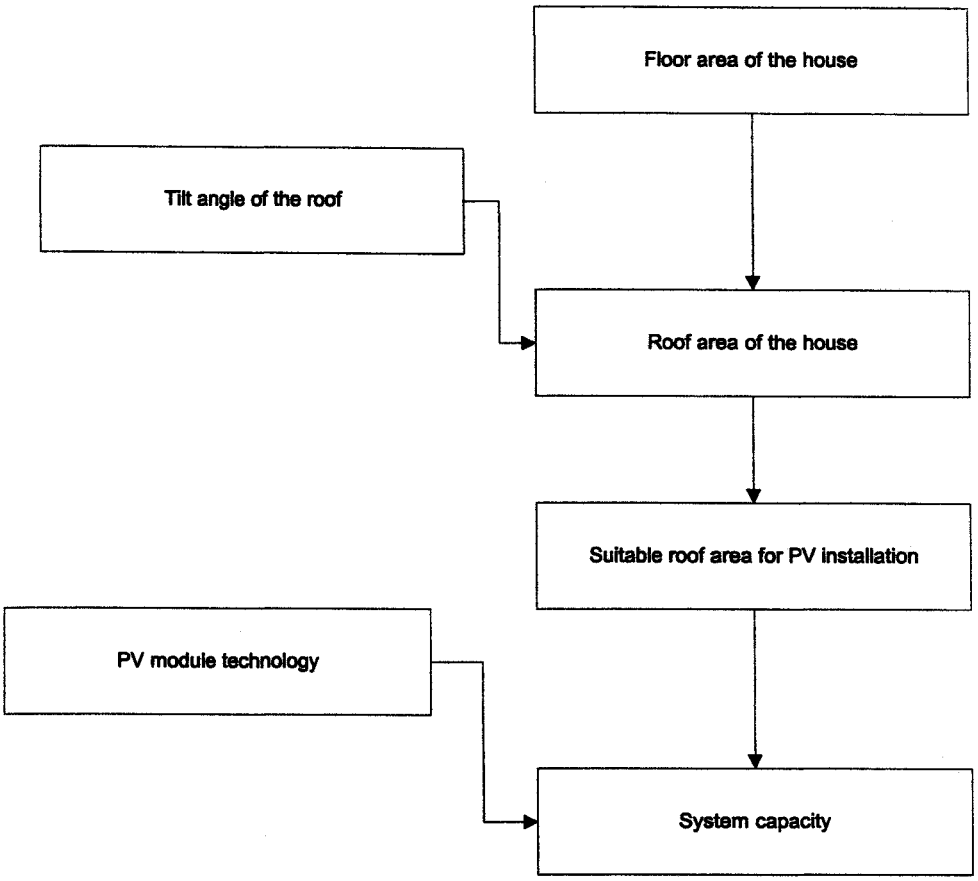

Figure 4-4 Illustration of PV system capacity calculation

House floor area

The size of PV systems that can be installed on a domestic house depends upon the floor area of the house. To represent this parameter houses are classified into four different groups depending upon the number of bedrooms. They are one bedroom, two bedrooms, three bedrooms and four or more bedroom houses. The percentage of each bedroom group data and their mean floor area data for England were collected from the EHCS 1996 [10,12] and are given in Table 4-4.

Table 4-4 Mean floor area by number of bedrooms

Number of Bed Rooms	Percentage	Mean Floor Area (m^2)
One Bedroom	3.1	52
Two Bedrooms	23.7	66
Three Bedrooms	52.1	84
Four & above Bedrooms	19.2	130

Roof type and tilt angle

The roof area of a house is the ratio of floor area to the cosine of the roof's tilt angle. In the case of flat roof, the roof area is equal to floor area. So in order to calculate the roof area, the roof type and tilt angle data for the UK domestic houses are necessary. To define the roof type, data regarding the type of roof materials used for roofing in England houses were collected from the EHCS 1991 [15]. The percentage of dwellings with different type of roof covering materials is given in Table 4-5.

Table 4-5 Percentage of dwellings by roof covering materials

Roofing Materials	Percentage
Natural Slate	18.2
Asbestos Cement Slate	4.2
Clay Tile	22.7
Concrete Tile	50.6
Asphalt	1.5
Felt	1.8
Glass/Metal	0.5
No predominant roof covering	0.6

Bitumen Felt, Mastic Asphalt, Single-ply systems and Bitumen/Asphalt tiles and sheeting are some of the flat roof materials [16]. Percentage of dwellings with these roof materials is around 5%. So it was assumed that 5% of the dwellings would have flat roofs. The remaining 95% of dwellings would have inclined roofs. In the inclined roof type, concrete tiles, clay tiles and natural slate tiles are predominant roof covering materials because the life period of these types of materials is high [16].

There are two main principles concerning the best use of flat roofs. These are [17]:

- Best yield can be obtained by having the PV arrays at an optimum tilt angle.
- Most roof area can be used by horizontal integration of the PV modules and this method is not a usual practice. Also, in general, the minimum tilt angle of 15^0 to the horizontal is recommended to allow the rain to wash dust off the array [18].

Therefore in this analysis it is assumed that PV arrays on flat roofs are tilted at an optimum angle to get the best yield. For the UK the optimum tilt angle is 30^0 to 40^0 for south oriented PV arrays [18], depending upon locations. In this work an average tilt angle of 35^0 is chosen for flat roof PV systems.

The tilt angle for the inclined roofs were selected by the following steps:
For the natural slate the minimum pitch recommended is 20^0 [16] and the average tilt angle for the slate roofs is 25^0. Hence it is expected that the tilt angle for most of the slate type roofs will be 25^0 to 30^0. The percentage of dwellings with natural slate and cement slate type roof materials is 22%. In this work, the tilt angle for 15% of dwellings with slate roof was considered as 25^0 and tilt angle for the remaining 7% of dwellings with slate roof was considered as 30^0.

Clay tiles can be used on a variety of roof shapes, the main limitation being a minimum pitch of 35^0 for plain tiles. However, interlocking products are available which allow minimum pitch of 22.5^0. Concrete plain tiles can be used down to roof pitches of 35^0. From these data it can be concluded that tilt angle of the dwellings with clay and concrete tiles will be in the range of 25^0 to 40^0 and tilt angle for most of the dwellings will be 35^0. The percentages of dwellings with clay tile and concrete tile type roofs are 23% and 50% respectively. In this 15% of dwellings were assumed to have a tilt angle of 40^0, 40% of dwellings were assumed to have a tilt angle of 35^0 and 8% of the dwellings were assumed to have a tilt angle of 30^0.

From these data the tilt angle parameter was classified into 5 groups and the percentage of houses in each group for England is given in Table 4-6. This classification was used to represent the tilt angle parameter in the domestic PV systems.

Table 4-6 Percentage of houses by tilt angle

Tilt angle	Percentage of Houses
Flat roof – 35 Degrees	5%
25 Degrees	15%
30 Degrees	25%
35 Degrees	40%
40 Degrees	15%

Suitable roof area and PV capacity

The roof area can be calculated from the house floor area and roof tilt angle data. From the available roof area, only certain area can be used for PV installation because of the obstruction due to construction, shading etc. For an example in the

UK because of the chimney construction on the roof, some part cannot be used for PV installation. The International Energy Agency (IEA) technical report PVPS-T7 [17] analysed and compared existing BIPV potential estimation and case studies carried out for different IEA countries. This report developed the rule-of-thumb for the determination of BIPV potential for the selected IEA countries. According to this IEA report the solar-architecturally suitable roof area for the inclined roof area was calculated through the following steps.

- 10% of roof area was assumed unsuitable due to the roof constructions like ventilation and chimney construction etc. After deducting this unsuitable area, the percentage of suitable roof area is 90%.
- In this suitable area 10% of area was unsuitable part due to the shading from surrounding buildings or vegetation effect. After neglecting this the suitable roof area is 81%.
- In this suitable area the unsuitable part of roof area due to the historical restrictions is 10%. After neglecting this the architecturally suitable roof area is 72.9%
- In the architecturally suitable area the roof area that is not suitable due to low solar yield should be deducted. In the IEA report two different criteria were analysed to select the solar suitable area. One is roof area that can receive 90% or more of annual solar yield. Another criterion is roof area that can receive 80% or more annual solar yield. The unsuitable roof area is 75 % due to the low solar yield when subject to the criterion of 90% of annual solar yield. The unsuitable area due to the solar yield is 50% with subject to the criterion of 80% of annual solar yield.

From these values it was found that for an inclined roof, almost 40% of roof area could be used for PV installation with criterion of 80% solar yield [17]. If 90% solar yield is applied, the suitable area for PV installation will be reduced to almost 20%. If all architecturally suitable areas are used, the suitable area will be almost doubled. In this analysis for inclined roofs the suitability factor was taken as 20% with the criterion of 90% solar yield. For flat roofs, the unsuitable roof part due to obstacles is 20%. In the remaining 80% of suitable area, 45% of roof area is accounted for the spacing between PV arrays. Therefore, for flat roofs the suitable roof area was considered as 44% of total roof area (80% * 55%), considering 20% for obstacle and

45% for spacing between PV arrays [17]. Using these suitable factor values the roof areas that are suitable for PV installation was calculated.

PV system size depends upon the suitable roof area and type of PV modules used. In this analysis mono-crystalline type PV modules, which had a market share of 33% in 2003, were used to calculate the system size. This provides the highest output power per unit area and hence would have the highest impact on the network. Nominal rating of the mono-crystalline PV module, BP585F, is 85 Watts and the area of a single module is $0.63m^2$ [8]. PV system size for a one-bedroom house with an inclined roof of 35^0 was calculated from the following steps.

- The mean floor area for a one-bedroom house is $52m^2$.
- For an inclined roof of 35^0 tilt angle, the roof area is $(52 / \text{Cos}(35)) = 63.48\ m^2$.
- The suitable factor for an inclined roof is 20%. Therefore the suitable roof area which can be used for PV system installation is $0.2*63.48\ m^2 = 12.7\ m^2$.
- PV system size using the BP585F PV module is = (12.7/0.63)*0.085 kW =1.7kW.

Similarly, the size of PV systems for each bedroom group with inclined roof of 35^0 was calculated and results are given in Table 4-7.

Table 4-7 Domestic PV system size for 35^0 inclined roof by bedroom type

Bedroom Size	Floor Area (m^2)	Roof Area (m^2)	Suitable Roof Area (m^2)	System Size (kW)
One Bedroom	52	63.48	12.69	1.7
Two Bedrooms	66	80.57	16.11	2.2
Three Bedrooms	84	102.55	20.51	2.8
Four & more Bedrooms	130	158.70	31.74	4.3

The PV system size that can be installed on a one-bedroom house with a flat roof was calculated using the following steps:

- The mean floor area for a one-bedroom house is $52m^2$.
- For the flat roof types the roof area is equal to mean floor area.

- The suitable factor for flat roof is 44%. Therefore the suitable roof area which can be used for PV system installation is 0.44*52 m^2 = 22.88 m^2.
- PV system size using the BP585F PV module is (22.88/0.63)*0.085 kW = 3.09kW.

Similarly the size of PV systems for each bedroom group with a flat roof was calculated and results are given in Table 4-8.

Table 4-8 Domestic PV system size for flat roof by bedroom type

Bedroom Size	Floor Area (m^2)	Roof Area (m^2)	Suitable Roof Area (m^2)	System Size (kW)
One Bedroom	52	52	22.88	3.1
Two Bedrooms	66	66	29.04	3.9
Three Bedrooms	84	84	36.96	5.0
Four & more Bedrooms	130	130	57.2	7.7

This method can be applied to any combination of bedroom groups and tilt angle groups. In this analysis it was assumed that there are no financial constraints on the PV system size selection. The bedroom size classifications and tilt angle classifications for Welsh houses were considered to be the same as for English houses.

4.4.3 Orientation

In this analysis, the suitable roof area was calculated with the criterion of 90% solar yield. In order to achieve this it was assumed that PV systems would be installed within the range of $\pm 45^0$ east or west of south. The orientation parameter was classified into five groups. They are

- South oriented – Azimuth angle of 0^0
- South - southwest oriented – Azimuth angle of 22.5^0
- Southwest oriented – Azimuth angle of 45^0
- South - southeast oriented – Azimuth angle of -22.5^0
- Southeast oriented – Azimuth angle of -45^0

Details about the orientation of houses are not available, therefore the percentage of houses in each group was assumed as 20% at first instance.

4.4.4 Inverter type

There are many PV inverter types available in the market, which are discussed in Chapter 2. They are mainly classified into

- Line Commutated Inverter
- Self commutated Inverter – With Line Frequency Transformer
- Multistage Converter – With High Frequency Transformer
- Multistage Converter – Without Transformer

Calais et al. [19] studied the inverter topologies and their market share in Germany. The market shares for each type of inverter topology in Germany, for the year 2002, are given in Figure 4-5. According to the Department of Trade & Industry (DTI) UK guide for the installation of PV systems [20] and the recent Engineering Recommendation G83 report, the inverter should have separation between DC and AC using an isolating transformer. In the report published by DTI on grid connected PV systems [21] it was concluded that the hazard of the DC component (within the limit specified) from small PV systems for the local distribution transformer seems to be negligible and therefore a general requirement for isolation transformers for PV inverters was not justified. So, in future the transformerless inverter could become a normal practice. In this work, in the first instance, the percentage of PV systems in each group was assumed as

- Self Commutated With Line Frequency Transformer 50%
- Self Commutated Without Transformer 25%
- Self Commutated With High Frequency Transformer 25%

4.4.5 Inverter rating

Figure 4-6 shows the inverter efficiency curves for two different inverter ratings of 30 kW and 40 kW. The efficiency of the 30 kW inverter is higher in the low power range and lower in the high power range compared with the 40 kW inverter. If the duration of peak irradiance levels is low, the 30 kW inverter may produce more energy than 40 kW inverter.

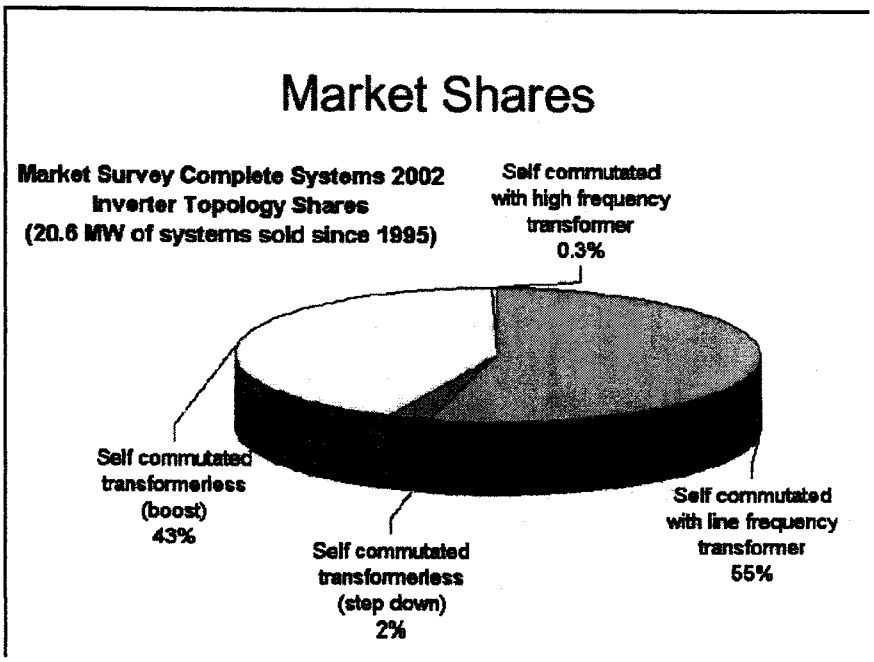

Figure 4-5 Inverter market in Germany, by topology for the year 2002 (Source Reference [19])

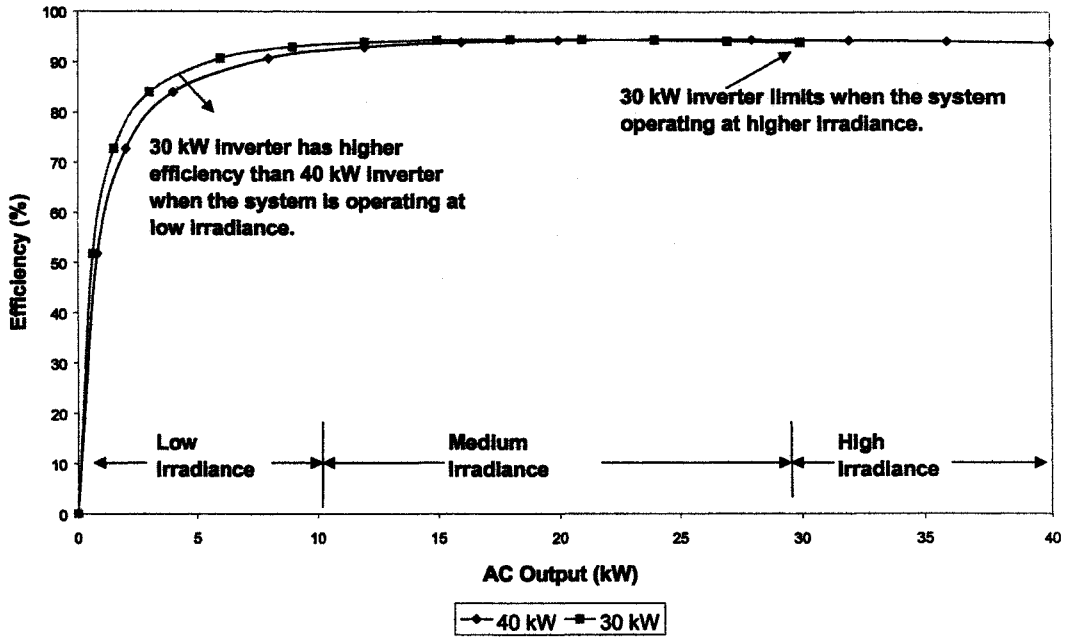

Figure 4-6 Comparison of inverter efficiency curves for 30 kW and 40 kW ratings

For places like the UK where the duration of peak irradiance levels are relatively low, selecting the optimal size inverter will increase the energy output. By selecting the optimal size, the additional energy generated leads to saving in running cost and a

reduction in inverter rating which also leads to saving in capital cost. Hence in grid connected PV systems selecting an inverter rating lower than the PV system rating usually leads to better economy where the duration of peak irradiance values is limited [22,24]. So in practice inverter rating may be lower than PV system rating or it may be equal to the PV system rating.

The optimal size of the inverter will vary depending upon the inverter topology. For the UK, the optimal size of the inverter for different inverter topologies was evaluated using the grid connected 39.5 kWp photovoltaic PV façade on Northumberland Building as an example [24]. Measured in-plane irradiance and ambient temperature were used to calculate the DC output power of the system. For a selected inverter, the loss parameters were calculated from the efficiency curve and hence AC output power of the inverter was calculated. When input DC power is less than load independent losses, the inverter shuts down and the output is zero. The maximum output of the inverter is restricted to the nominal rating of the inverter in this analysis, although in practice an inverter can usually sustain an output slightly higher than its rating for a limited period. The inverter energy efficiency has been calculated as a function of the ratio of the nominal rating of the inverter to the PV array capacity [7,23] as shown in Figure 4-7. The ratio that gives the maximum energy efficiency was selected as the optimal ratio, from which the optimal size of the inverter was calculated [24]. The same procedure was repeated for different types of inverters.

PV inverters can be broadly classified into three main groups. They are:

- Group A –Line Commutated Inverters
- Group B – Single Stage Inverters
- Group C – Multi-stage Converters
    - Group C1- Multi-stage Converters with high frequency transformer
    - Group C2 – Multi-stage Converters without high frequency transformer

Two inverters of the same Group B were used in this analysis named as B(1) and B(2). The characteristics of the inverters [9,25-27] studied and their optimal ratios are shown in Table 4-9.

Table 4-9 Characteristics of the inverters studied and their optimal ratio

Inverter Group	Group A	Group B		Group C	
	A	B (1)	B (2)	C1	C2
Manufacturer	SMA	SIEMENS	SMA	MASTERVOLT	SMA
Type	PV-WR-T40	SINVERT	SUNNY CENTRAL	SUNMASTER 130S	SUNNY BOY 2000
Switching Component	Thyristor	IGBT	IGBT		
Nominal Rating	40 kW	40kW	40 kW	0.11 kW	1.8kW
Transformer	LF	LF	LF	HF	No
η_{10}	81.5%	84%	89%	81%	92.5%
η_{100}	92%	94%	93%	91%	96%
Optimal Ratio	0.725	0.75	0.775	0.725	0.8

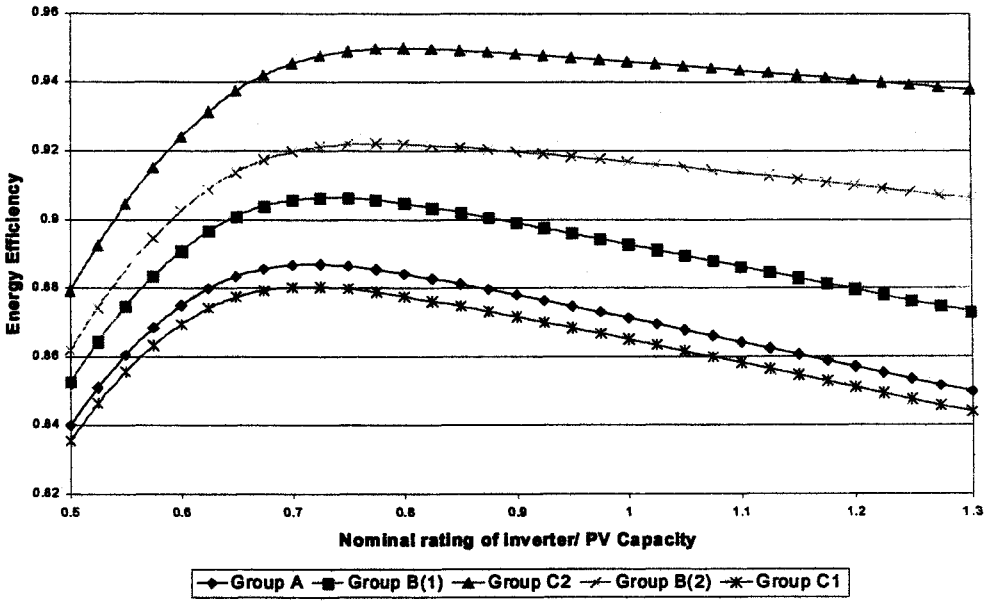

Figure 4-7 Energy efficiency curves for studied inverters

The Northumberland Building PV system is a commercial PV system, with a tilt angle of 65 degrees and an orientation of 16.5^0 south-east. Most of the residential PV systems in the UK are likely to have a tilt angle in the range of 25^0 to 40^0. Therefore the optimal size of an inverter for a system with a PV array at 35^0 tilt angle and south oriented was calculated and results are shown in Table 4-10. The changes in optimal

size of the inverter with respect to the changes in tilt angle were observed as small [4,24]. From these results the optimal size for each inverter group was selected and are given in Table 4-11. Since the optimal size of the inverter leads to saving in energy and cost [4,24], it would be expected that most of the PV systems would have the optimal inverter size. In this analysis, it was assumed that 80% of PV systems would have an inverter rating lower than PV system size and 20% of PV systems would have an inverter rating equal to the PV system size.

Table 4-10 Optimal ratio for a system with PV arrays 35^0 tilt and south oriented

Inverter	Group A	Group B (1)	Group C2	Group B (2)	Group C1
Optimal Ratio	0.75	0.75	0.825	0.8	0.725

Table 4-11 Optimal ratio for the chosen inverter groups

Inverter Type	Percentage (%)	Optimal Ratio
Self Commutated With Line Frequency Transformer (Group B)	50	0.75
Self Commutated Without Transformer (Group C2)	25	0.825
Self Commutated With High Frequency Transformer (Group C1)	25	0.725

The flowchart shown in Figure 4-8 represents the methods developed to represent the domestic PV systems. Parameters that vary within the cluster, different groups in each parameter and the percentage of each category are illustrated in the flowchart. Similar to the domestic PV systems modelling, the non-domestic PV system modelling was carried out and is explained in the following sections.

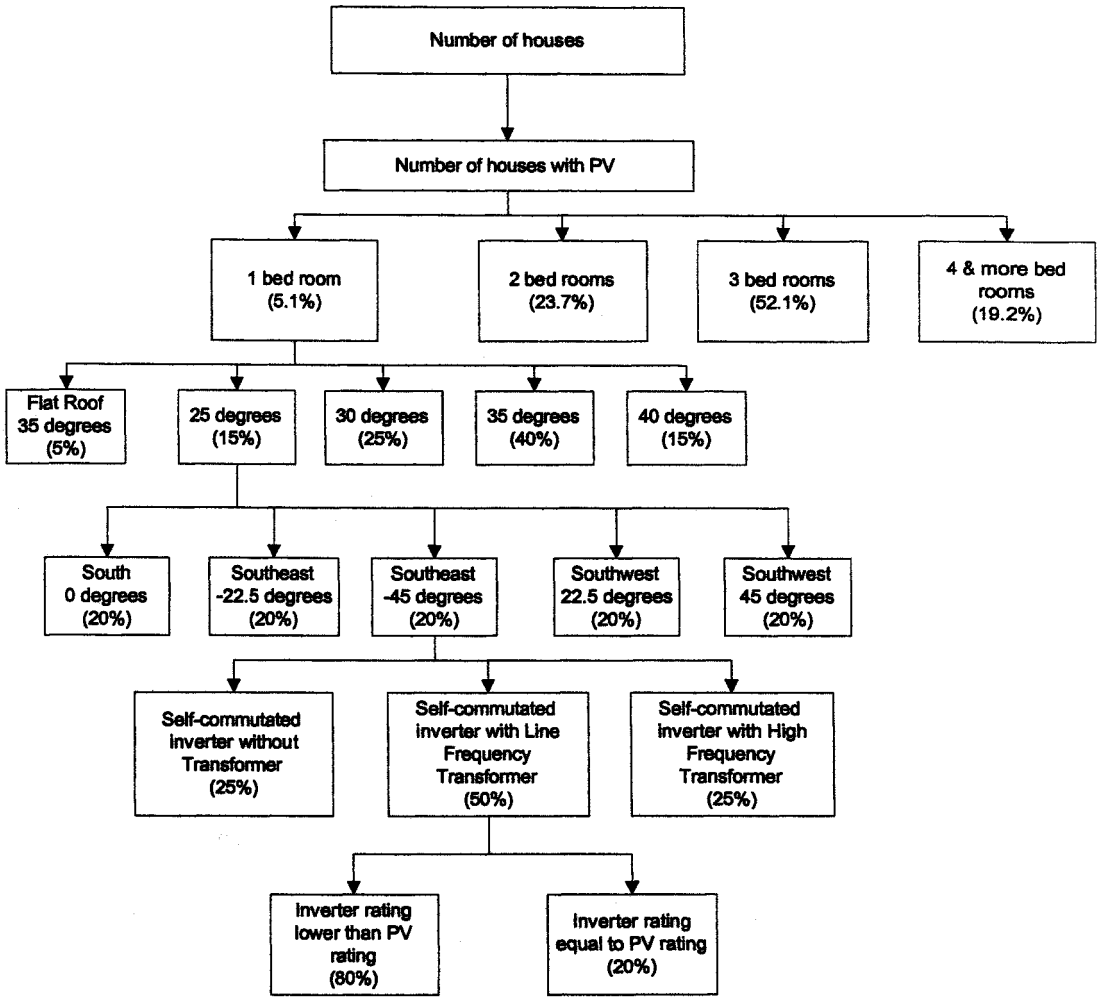

Figure 4-8 Representation of domestic PV systems modelling

4.5 Modelling of Non-domestic PV Systems

The commercial and industrial PV systems are together considered as non-domestic PV systems. PV systems can be installed on either the roof or wall of the non-domestic buildings. Therefore modelling of non-domestic PV systems is divided into two cases: the modelling of non-domestic roof PV systems and the modelling of non-domestic façade PV systems. Similar to the domestic PV systems modelling, methods to represent parameters that vary within non-domestic PV systems were developed. The following sections discuss the development of models to represent the non-domestic roof and non-domestic façade PV systems.

4.5.1 Non-domestic building data

To estimate the number of non-domestic PV systems, the non-domestic building stock data and an assumed percentage of buildings with PV were used. For this purpose non-domestic buildings data were collected for England and Wales. The main source for non-domestic building stock detail is the Valuation Office Agency (VOA) of the Inland Revenue (the UK taxation agency), who makes detailed surveys of the majority of non-domestic buildings in order to calculate the commercial rates [10,28]. Individually rated properties are known as hereditaments and these form the basic unit of data. Generally, a hereditament corresponds to an extent of contiguous or adjacent space appropriate for a single occupant. Most are either individual building, groups of buildings or parts of buildings. However some are just land, for example open-air car parks, storage and various kinds of sports grounds. Some are neither building nor land at all, for example advertising rights. A large office or mixed-use commercial building will, if shared between several tenants or owner, consist of several hereditaments. For example, a flower stall or newspaper kiosk in an office building can constitute a separate hereditament. Conversely a single large hereditament may be comprised of many distinct buildings, for example a large factory on a single site [10,28].

The only types of non-domestic property exempt from rates are churches and other places of worship, agricultural lands and buildings. Crown properties i.e., defence establishments, prison and various other central government buildings were exempted until the year 2000. But they are now liable for business rates. There were around 1.7 million rateable non-domestic hereditaments in England and Wales in the year 2000 [10,29,30]. The non-domestic hereditaments can be classified as bulk classes and non-bulk classes. The bulk classes comprise 1.3 million hereditaments, which include shops, offices, factories and warehouses. The non-bulk classes comprise 0.4 million hereditaments, which include hotels, public houses, schools, hospitals, libraries and leisure premises amongst others. Floor space data are only systematically available for the 1.3 million hereditaments in the bulk classes from the Valuation Support Application (VSA) database developed by the VOA.

The Global Atmosphere Division of the UK Department of the Environment, as part of its research on climate change developed a database of energy use in the non-domestic building stock [29,30]. The report details give the whole non-domestic building stock for England and Wales, which includes mainly the bulk class details from the VSA database and the non-bulk class details from a wide variety of sources [29,30]. This non-domestic building stock data accounts for over 90% of the stock by floor area [30]. In this report, the Non Domestic Building Stock (NDBS) is divided into 14 inference activity groups [30,31] and six major built form groups (see Appendix B for more details). Non-domestic premises were divided into eight different size groups.

The number of premises and the mean floor area in each activity group in eight different size distributions are given in the NDBS report (Appendix B). It may not be possible to install PV systems in some types of non-domestic buildings. Therefore the chances for PV installation in the non-domestic buildings were analysed. In the activity group of churches and buildings used for worship, because of the traditional value of these buildings, chances for PV installation are very small. So buildings under the churches activity group were neglected in this analysis. In the retail and clubs activity groups, when the size of the building is small, they are most possibly in the basement or lower floor of a building. Because of the shading, aesthetic and vandalism problems the possibilities of PV installation on these buildings are very low. So the buildings in the retail and club activity groups with the size band lower than 300 m^2 were also neglected in this analysis. After neglecting these premises, the mean floor area for non-domestic buildings in each size band was calculated and results are given in Table 4-12. The percentage of premises in each size band category was calculated and is also given in the table.

Similar to the domestic PV system modelling, in the non-domestic modelling the vacant properties were also deducted from the total building stock because chances for PV installation in these buildings are low. From the Non-Domestic Building Energy Fact File report, the percentage of non-domestic vacant buildings was calculated as 8% [32]. Using this value the number of premises occupied was calculated as 927720 that have potential for PV installations.

Table 4-12 Mean floor area by premises size band

Premises Size band (m^2)	Number of Premises	Total Floor Area (m^2)	Mean Floor Area (m^2)	Percentage (%)
0-30	77333	1692041	22	7.67
30-100	242473	17910161	74	24.05
100-300	276932	55319429	200	27.46
300-1000	288792	167062049	578	28.64
1000-3000	85725	158277696	1846	8.50
3k-10k	29974	169884983	5668	2.97
10k-30k	6174	103406904	16822	0.61
30k-100k	1011	58842407	58202	0.10

4.5.2 Modelling of non-domestic roof PV systems

The PV system shown in Figure 4-9 is an example of a PV system for a non-domestic roof. The capacity of the PV system is 19 kW and it is installed on the flat roof of a petrol filling station.

Figure 4-9 Example of non-domestic roof PV system (Source www.pv-uk.org.uk)

The design parameters in non-domestic buildings will also vary depending upon the building envelope. System parameters that may vary in each non-domestic PV roof systems were identified as:

- PV system capacity that depends upon the roof area and PV module technology

- Tilt angle of the roof that depends upon the roof type
- Orientation of PV array that depends upon the building orientation
- Inverter type that depends upon the inverter market
- Inverter rating that depends upon the PV system capacity

Methods to represent these parameters are explained in this section.

Non-domestic PV system capacity

Steps involved in modelling the non-domestic roof PV systems capacity are illustrated in Figure 4-10. The PV system capacity depends upon the roof area of the building. The suitable roof area for PV installation depends upon the roof type and PV module technology. The following sections discuss the methods followed to represent these parameters.

Roof plan area

The floor area represents the net floor area in all the storeys but the premise has only one roof. In the UK, about 56% of total floor area is not directly below a roof i.e., floors covered by other storeys [32]. In order to model the PV roof systems, it is necessary to know how the floor area relates to the roof area. In the NDBS project the floor area, roof plan area (floor area covered by roof), type of roof and tilt angle of the roof for non-domestic premises were analysed [30,32,33]. A study was carried out from very detailed surveys made in four English towns: Manchester, Swindon, Tamworth and Bury St Edmunds. These locations represent different ranges of population size, widely spread geographical location and none is dominated by a single industry. In all, 3400 premises comprising around 4 km^2 of floor space and covering a wide range of building types were surveyed. Most of the steps in the inference process are based on correlations between the relevant attributes of buildings, as observed in data deriving from very detailed surveys made in four English towns.

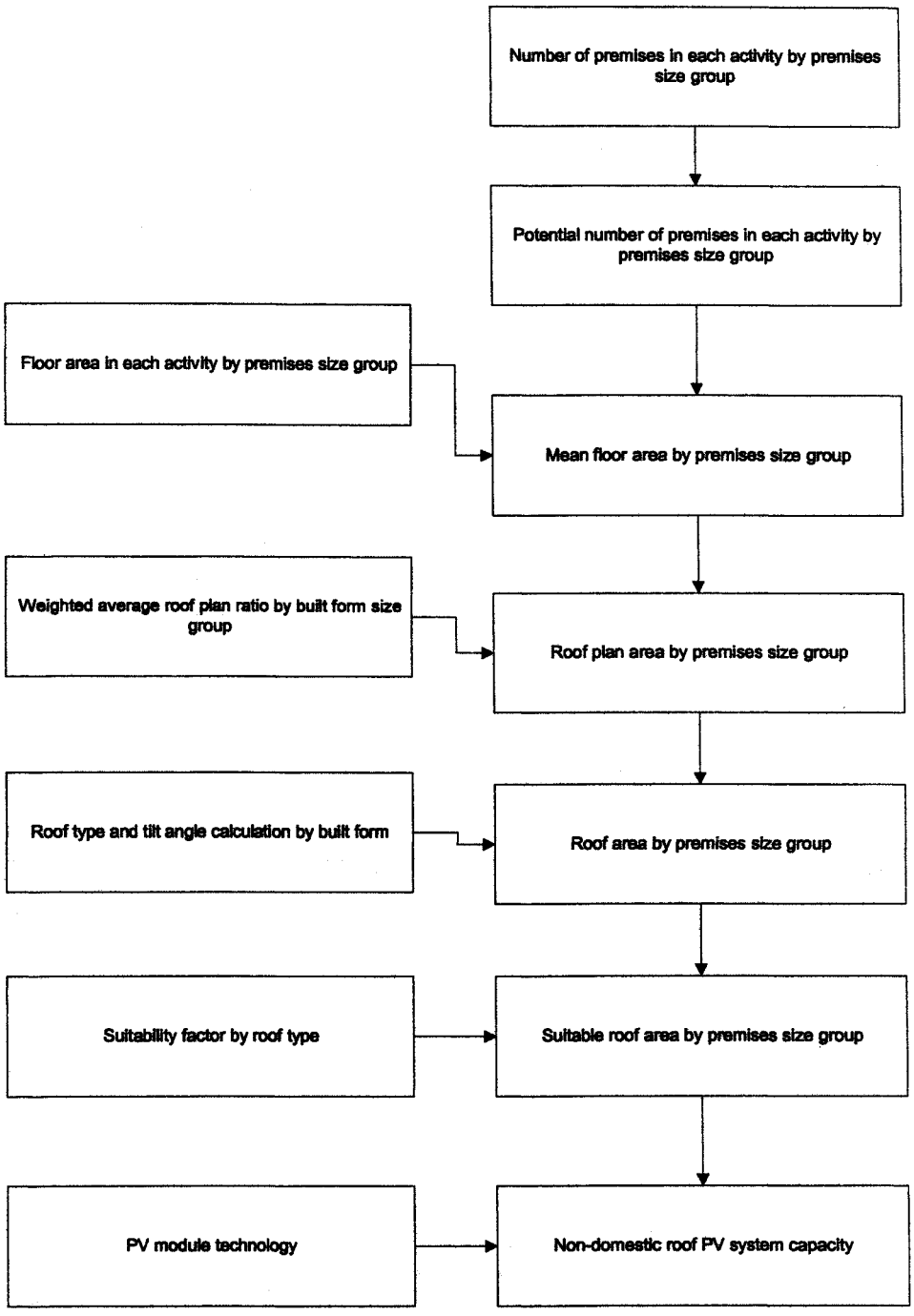

Figure 4-10 Flow chart to illustrate the non-domestic roof PV system capacity calculation

From this NDBS report the ratio of roof plan area to floor area by built form, for each built form size band, was obtained. Among these different built forms, the circulation (CIRC) built form relates to forms serving the purposes of circulation attached to the outsides of primary forms like circulation towers, walkways, bridges

etc. The other (MISC) built form contains mostly minor parasitic forms and small single room forms, but also includes open-plan car parking, which can account for significant areas of floor space in certain building types. These two types of built forms have a low chance for PV installation. For an example the open-plan car parking in MISC built form is the just the land area without any building. Similarly walkways in the CIRC built form are attached structures and not the main building area. Therefore in this analysis, these built forms were neglected.

After neglecting these built forms, the ratio of roof plan area to floor area by built form in each size band is given in Table 4-13. The floor area by built form in each size band is given in Table 4-14. These values were used to calculate the weighted average ratio of roof plan area to floor area. For an example the roof plan ratio for the 0-30 m^2 size band CSX built form is 0.81 and the floor area is 251629 m^2. The total floor area for the 0-30 m^2 size band is 3942628 m^2. The weighted ratio is calculated as $0.81*\left(\frac{251629}{3942628}\right) = 0.05$.

Similarly the weighted ratio was calculated for all the built forms and an average value for all built form was calculated as weighted average roof ratio. The weighted average roof plan ratio for all size bands is shown in Table 4-15. These values were used to calculate the floor area covered by the roof, in bands relating to the size of the premises.

Table 4-13 Ratio of roof plan area by built form size group

Size Band (m^2)	CSX	CDOX	OSX	HALL	EX
0-30	0.81	0.7	0.97	1	0.92
30-100	0.7	0.62	0.96	0.94	0.86
100-300	0.54	0.51	0.94	0.9	0.72
300-1000	0.42	0.4	0.9	0.74	0.65
1000-3000	0.32	0.31	0.86	0.66	0.6
3k – 10k	0.23	0.22	0.83	0.62	
10k – 30k	0.14	0.15	0.8	0.6	
30k-100k	0.1	0.12			

Table 4-14 Floor area (m^2) by built form size group

Size Band (m^2)	CSX	CDOX	OSX	HALL	EX	All
0-30	251629	587	128616	28672	3533124	3942628
30-100	9649735	192045	4518965	701282	3856979	18919006
100-300	50333137	1676360	15657168	7538980	1307833	76513478
300-1000	85087336	14612521	60300583	8667986	241111	168909537
1000-3000	69700931	47865902	63611971	4139866	347078	185665748
3k – 10k	68396140	66946115	60314709	246871	0	195903835
10k – 30k	15351012	28504984	23640204	1808109	0	69304309
30k-100k	19975614	2945227	0	0	0	22920841

Table 4-15 Weighted average roof plan ratio

Size Band (m^2)	CSX	CDOX	OSX	HALL	EX	Average
0-30	0.05	0.00	0.03	0.01	0.82	0.92
30-100	0.36	0.01	0.23	0.03	0.18	0.80
100-300	0.36	0.01	0.19	0.09	0.01	0.66
300-1000	0.21	0.03	0.32	0.04	0.00	0.61
1000-3000	0.12	0.08	0.29	0.01	0.00	0.51
3k – 10k	0.08	0.08	0.26	0.00	0.00	0.41
10k – 30k	0.03	0.06	0.27	0.02	0.00	0.38
30k-100k	0.09	0.02	0.00	0.00	0.00	0.10

Roof type

The classification of roof types by geometry, slope and material were discussed in the NDBS report [30,31]. Different roof types in the non-domestic building stock are given in Table 4-16. The "other" type includes barrel vaults, domes, conical roofs and roofs with multiple geometries. In non-domestic building stock, the dominant roof type is the flat roof which accounts for around 42% of roof plan area. The percentage of each roof type in different built form groups is given in Table 4-17. The total floor area for each built form was used to calculate the weighted average percentage of each roof type and results are given in Table 4-18. In the non-domestic buildings flat roof types are predominant over other roof types. The following section explains the method to represent the tilt angle for each roof type.

Table 4-16 Roof types in the non-domestic building stock

Geometry	Slope	Material
Flat	0 degrees	Felt/ Asphalt
Flat	0-20 degrees	Lightweight
Mono pitch	Any	Lightweight
Mono pitch	Any	Tiles and Slates
Double pitch	Any	Felt/ Asphalt
Double pitch	> 20 degree	Tiles and Slates
Double pitch	0-20 degree	Lightweight
Double pitch	20-45 degree	Lightweight
Mansard	Any	Any
Monitor	Any	Lightweight
Other	Any	Any

Table 4-17 Percentage of roof type in each built form

Roof Type	CSX	CDOX	OSX	HALL	MIS
Flat: Felt/Asphalt	48.3	63.5	10.9	12.1	35.1
Flat: Lightweight	1.5	1.6	3.4	5.6	2.8
Mono pitch: Lightweight	0.6	0	3.3	0.5	7.6
Mono pitch: Tiles and Slates	1.4	0.6	0.4	1.9	1.5
Double pitch: Felt/Asphalt	0.6	0.4	0.4	1.1	0.5
Double pitch: Tiles and Slates	29.7	14.9	5.6	32	6.1
Double pitch: 0-20 degrees	0.9	0.9	19.5	2.5	0.9
Double pitch: 20-45 degrees	2.8	1	32.1	4.1	3.5
Mansard	1.7	2	0	3.5	0.7
Monitor	0		9.4		
Other	12.5	15	14.9	36.7	41.3

Table 4-18 Weighted percentage of roof type

Roof Type	CSX	CDOX	OSX	HALL	EX	Percentage
Flat: Felt/Asphalt	19.5	13.1	3.1	0.4	0.6	38.9
Flat: Lightweight	0.6	0.3	1.0	0.2	0.0	2.3
Mono pitch: Lightweight	0.2	0.0	1.0	0.0	0.2	1.8
Mono pitch: Tiles and Slates	0.6	0.1	0.1	0.1	0.2	1.1
Double pitch: Felt/Asphalt	0.2	0.1	0.1	0.0	0.0	0.5
Double pitch: Tiles and Slates	12.0	3.1	1.6	0.9	0.1	18.1
Double pitch: 0-20 degrees	0.4	0.2	5.6	0.1	0.0	6.3
Double pitch: 20-45 degrees	1.1	0.2	9.3	0.1	0.1	11.0
Mansard	0.7	0.4	0.0	0.1	0.0	1.2
Monitor	0.0	0.0	2.7	0.0	0.0	2.7
Other	5.0	3.1	4.3	1.1	0.1	15.9

Monitor, Mansard and Other types are more complex in their geometries and hence the chances for having PV systems are lower. So these types of roof were neglected in this analysis. After neglecting these roof types the percentages of non-domestic premises with different roof types were calculated and given as:

- Flat roof type: 51%
- Inclined roof type: 49%
    - Mono pitch: 3%
    - Double pitch: 46%

Roof slope

This section explains the steps that have been followed to define the tilt angle for each roof type and the percentage of non-domestic premises in each category.

Flat Roof

In the non-domestic buildings the main type of roof is the flat roof. As discussed in the domestic PV systems modelling it was assumed that PV systems in flat roofs were tilted at an optimum angle for the best yield. For the UK the optimum tilt angle is 30^0 to 40^0 for the south oriented PV arrays [18]. In this work an average angle of 35^0 was chosen as the tilt angle for the PV arrays in the flat roof.

Inclined Roof

In the NDBS project, in order to calculate roof surface area for the mono pitch roof type with slope 'Any' in Table 4-16, the tilt angle was assumed as 25^0. In this work also the tilt angle for PV arrays in the mono pitch type roofs was assumed as 25^0. Among the 46% of buildings with a double pitch roof it was assumed that 12% of buildings had a 25^0 tilt angle, 20% of buildings had a 30^0 tilt angle and 14% of buildings had a 35^0 tilt angle.

From these, the percentage of different roof types and corresponding tilt angle values were derived for the non-domestic roof PV systems. These results, given in Table 4-19 were used to represent roof type and tilt angle for non-domestic buildings. The following section explains the calculation of PV system capacity from the roof type and tilt angle data.

Table 4-19 Assumed percentage of roof type and tilt angle

Roof Type	Tilt Angle (Degrees)	Percentage (%)
Flat	35	51
Mono Pitch/ Double Pitch	25	15
Double Pitch	35	14
Double Pitch	30	20

Roof surface area & PV capacity

Flat Roof

For flat roof types the roof surface area is equal to the roof plan area. Suitability factor for the flat roof is 0.44 and this value was used to calculate the suitable roof area for PV installation [17]. The capacities of PV systems that can be installed in the non-domestic flat roofs in each size band were calculated using the BP585F PV modules data and results are given in Table 4-20.

Table 4-20 PV System capacity on non-domestic flat roof

Premises Size Band (m^2)	Roof Plan Ratio	Mean Floor Area (m^2)	Roof Plan Area (m^2)	Suitable Area (m^2)	System Capacity (kW)
0-30	0.92	22	20.13	8.86	1.2
30-100	0.8	74	59.41	26.14	3.5
100-300	0.66	200	131.95	58.06	7.8
300-1000	0.61	578	350.49	154.21	20.8
1000-3000	0.51	1846	942.45	414.68	56.0
3000-10000	0.41	5668	2334.09	1027.00	138.6
10000-30000	0.38	16822	6413.30	2821.85	380.7
30000-100000	0.10	58202	5969.77	2626.70	354.4

Inclined Roofs

For inclined roofs the roof surface area was calculated by dividing the roof plan area by the cosine of tilt angle. The suitability factor for inclined roofs is 0.2. This value was used to calculate the roof area which can be used for PV installation. The capacities of PV systems that can be installed in the non-domestic inclined roofs in each size band were calculated using the BP585F PV modules data. Table 4-21 shows the system capacity for each size band premises with an inclined roof tilted at

an angle of 35^0. Similarly for different roof types and tilt angle combination PV systems capacity on non-domestic buildings can be calculated.

Table 4-21 PV systems capacity on non-domestic 35^0 tilt roof

Premises Size Band (m^2)	Roof Plan Ratio	Mean Floor Area (m^2)	Roof Plan Area (m^2)	Roof Surface Area (m^2)	Suitable Area (m^2)	System Capacity (kW)
0-30	0.92	22	20.13	24.58	4.92	0.7
30-100	0.8	74	59.41	72.52	14.50	2.0
100-300	0.66	200	131.95	161.07	32.21	4.4
300-1000	0.61	578	350.49	427.84	85.57	11.5
1000-3000	0.51	1846	942.45	1150.46	230.09	31.0
3000-10000	0.41	5668	2334.09	2849.23	569.85	76.9
10000-30000	0.38	16822	6413.30	7828.74	1565.75	211.3
30000-100000	0.10	58202	5969.77	7287.32	1457.46	196.6

The steps that have been followed to model the non-domestic roof PV systems are shown in Figure 4-11. Parameters that vary within non-domestic roof PV systems, different groups in each parameter and the percentage of PV systems in each category are illustrated in this flow chart. The representation of parameters orientation, inverter type and inverter rating for the non-domestic buildings were considered the same as for the domestic PV systems modelling.

4.5.3 Modelling of non-domestic façade PV systems

The PV system shown in Figure 4-12 is an example of a non-domestic façade PV system. System parameters that will vary within the non-domestic façade systems were identified as:

- PV system size that depends on the wall area, suitable wall area for PV installation and PV module technology
- Orientation of PV array that depends on the building orientation
- Inverter type that depends upon the inverter market
- Inverter rating that depends upon the PV system capacity

In most of the PV façade systems, the PV arrays are placed vertically and hence the tilt angle for PV façade systems was assumed to be 90^0. The following section explains the steps that have been followed to model non-domestic façade PV systems.

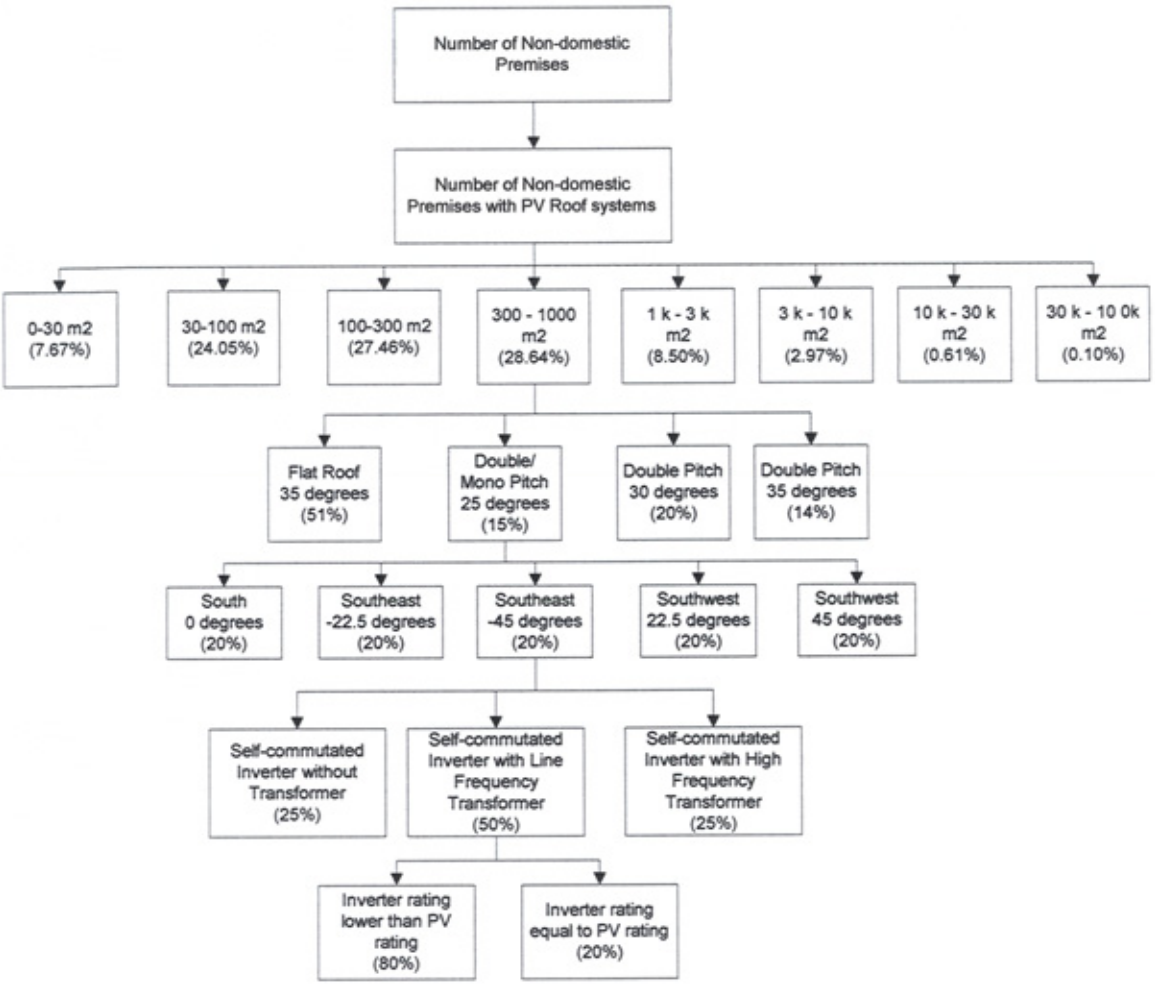

Figure 4-11 Flow chart for non-domestic roof PV systems modelling

Figure 4-12 Northumberland Building PV façade system at Northumbria University, Newcastle upon Tyne

Exposed wall area

The exposed wall ratio by built form, in built form size band was collected from the Non Domestic Building Stock (NDBS) report. As explained before in the non-domestic roof PV systems modelling, CIRC and MISC built forms were neglected. After neglecting these built forms the exposed wall ratio by built form, in built form size band is given in Table 4-22. The weighted average values of exposed wall ratio by size band were calculated and results are given in Table 4-23. These values were used to calculate the exposed wall area from the mean floor area.

Table 4-22 Exposed wall ratio by built form size group

Size Band (m^2)	CSX	CDOX	OSX	HALL	EX
0-30	1.8	2.6	2.4	2.3	1.9
30-100	1.2	0.9	1.2	1.5	1.4
100-300	0.9	0.6	1	0.9	1
300-1000	0.7	0.5	0.8	0.7	0.6
1000-3000	0.6	0.4	0.5	0.5	
3000-10000	0.5	0.4	0.4	0.4	
10k – 30k	0.4	0.3	0.3	0.3	
30k – 100k	0.3	0.2			

Table 4-23 Weighted average exposed wall ratio

Size Band (m^2)	CSX	CDOX	OSX	HALL	EX	Average
0-30	0.11	0.00	0.08	0.02	1.70	1.91
30-100	0.61	0.01	0.29	0.06	0.29	1.25
100-300	0.59	0.01	0.20	0.09	0.02	0.92
300-1000	0.35	0.04	0.29	0.04	0.00	0.72
1000-3000	0.23	0.10	0.17	0.01	0.00	0.51
3000-10000	0.17	0.14	0.12	0.00	0.00	0.43
10k – 30k	0.09	0.12	0.10	0.01	0.00	0.32
30k – 100k	0.26	0.03	0.00	0.00	0.00	0.29

Suitable wall area & PV capacity

The exposed wall ratio data and suitability factor for façade PV installation values were used to define the PV façade system capacity. According to the rule of thumb developed by the IEA report [17] the architectural unsuitable wall area is 80% and hence architectural suitable area is 20%. In this the wall area that can receive considerable solar energy is 50%. Therefore the solar-architectural suitable wall area

is estimated as 10% i.e., if the wall area is 1.5 m^2 then suitable wall area is 0.15 m^2. This value is as an average for high-rise residential buildings, commercial and industrial buildings. According to the IEA report this value is higher for commercial and industrial buildings given as 0.2 m^2 that represents 13.3% of total wall area. In this work the commercial and industrial PV façade systems were considered and hence the suitability factor for the façade is considered as 15%. This suitability factor was used to calculate the suitable wall area. As explained in the domestic PV systems modelling the BP 585F PV module data were used to calculate the façade PV systems capacity. The premises with floor area less than 300 m^2 are likely to have less number of storeys. Due to the shading, façade suitability and vandalism problems, installation of PV façade systems in low storey buildings is lower. Therefore in this analysis these premises were neglected for PV façade installation. After neglecting these premises the percentage of non-domestic buildings by size band and their PV façade system capacity was calculated and results are given in Table 4-24.

Table 4-24 PV system capacity for non-domestic façade systems

Premises Size Band (m^2)	Exposed Wall Ratio	Mean Floor Area (m^2)	Exposed Wall Area (m^2)	Suitable Wall Area (m^2)	System Capacity (kW)	Percentage (%)
300-1000	0.72	578	415	62.27	8.4	70.15
1000-3000	0.51	1846	943	141.45	19.1	20.82
3k-10k	0.43	5668	2465	369.76	49.9	7.28
10k – 30k	0.32	16822	5419	812.88	109.7	1.49
30k – 100k	0.29	58202	16713	2506.91	338.2	0.25

The methods that have been used to represent the non-domestic PV façade systems are illustrated in Figure 4-13. The representation of the parameters of orientation, inverter type and inverter rating were assumed to be the same as the domestic PV systems modelling.

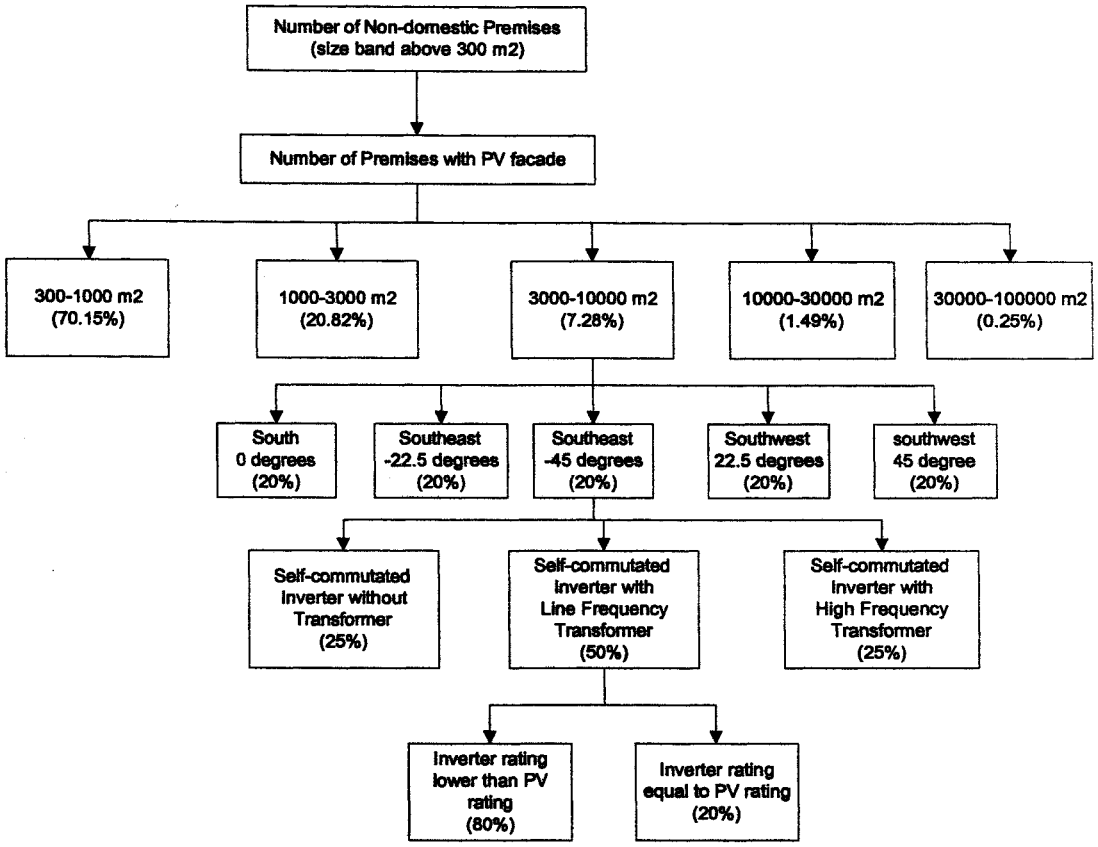

Figure 4-13 Flow chart for non-domestic façade systems modelling

4.6 Output power from SMC

The DC output power from PV systems depends upon the tilted radiation, PV module efficiency and cell temperature as given by equation 4.1. The DC output power also depends upon the losses due to dirt in modules, shading losses, mismatch of PV array and ohmic losses due to installation of wires, cables etc. In this study the typical values for losses due to dirt in modules, mismatch of PV array and DC installation are considered as 1.5%, 3% and 3% respectively. These percentages of losses are subtracted from the DC power calculated from equation 4.1 and the resulting DC output power will be the input to inverter. The shading loss in a PV system depends upon the surrounding building elements and vegetation etc. The shading loss also depends upon the time and season. In this study, the shading loss is neglected and hence this analysis considers low loss systems. The low loss systems

considered in the analysis provide the highest output power and hence would have the highest impact on the grid.

The AC output power from PV systems also depends upon the inverter efficiency. The efficiency values were used to calculate the losses in the inverter (using equation 4.3) and the AC output power was calculated using equation 4.4. For the self-commutated inverter with line frequency transformer type, the SMA Sunny Central inverter was selected. The efficiency at 10% nominal rating of the inverter is 89% and the efficiency at 100% nominal rating of the inverter is 93%. For the self-commutated inverter with high frequency transformer type, the Mastervolt Sunmaster 130s inverter was selected. The efficiency at 10% nominal rating of the inverter is 81% and the efficiency at 100% nominal rating of the inverter is 91%. For the self-commutated inverter without transformer type, the SMA Sunny Boy 2000 inverter was selected. The efficiency at 10% nominal rating of the inverter is 92.5% and efficiency at 100% nominal rating of the inverter is 96%.

It was assumed that in the total England and Wales building stock 2% of houses have PV systems, 1% of non-domestic premises have PV systems on the roof and 1% of non-domestic premises have PV façade systems and this represents the total PV capacity of 1157 MW. In the SMC modelling a total of 1950 different categories of PV system designs were used. As an example, the total output power from these PV systems was calculated using measured half-hour horizontal radiation for the London 1 location. From these output power values, the energy output was calculated and it represents an average annual energy output of 802 kWh/kW of PV capacity from domestic PV systems, which is typical for a well defined PV system in the UK. Similarly an average annual energy output was calculated for non-domestic PV roof systems as 802 kWh/kW of PV capacity and 571 kWh/kW of PV capacity for non-domestic façade PV systems. The output power from domestic and non-domestic PV systems were added to estimate the output power from the SMC. The output power from the SMC for each half hour is shown in Figure 4-14. It can be observed that, as expected, the output power is higher for summer season than winter season. However, the peak values occurred in both the winter and summer seasons.

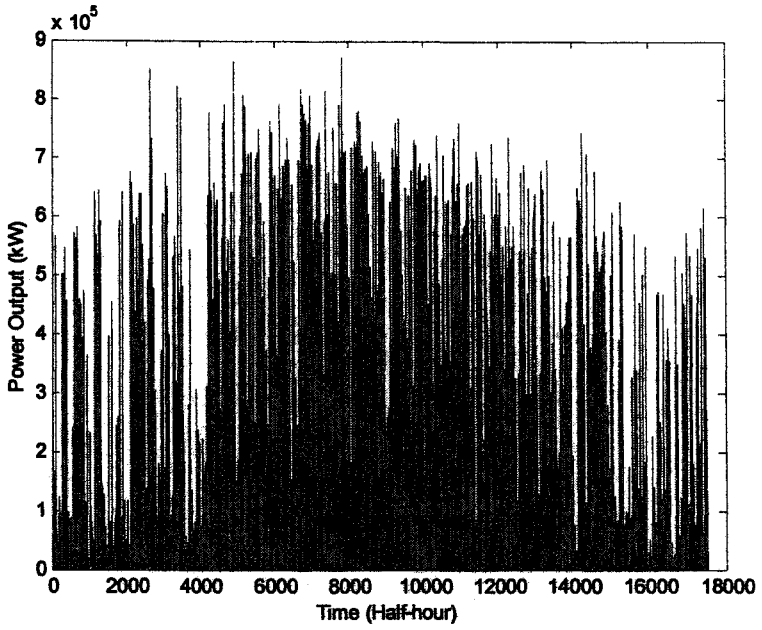

Figure 4-14 Output power from the SMC

The Performance Ratio (PR) of a PV system, which is the ratio of actual PV energy produced to the theoretical available energy that can be produced, was calculated. Jahn et al. [42] investigated the performance ratio of 334 grid connected PV systems in IEA countries. According to this study for PV systems installed in 1983 – 1995 the average PR for all systems is 0.66 and the maximum PR is about 0.7. For PV systems installed in 1996 – 2002 the average PR for all systems is 0.7 and the maximum PR is about 0.8. It can be observed that the performance ratio values are increasing in the recent years. In this analysis the calculated PR values for PV systems in the SMC range from 0.76 to 0.86. These values are higher compared with the PR of present PV systems because low loss systems were considered in this analysis.

4.7 Sensitivity Analysis

Sensitivity analysis was carried out to find the change in output power from the cluster with changes in representing the system design parameters. Sensitivity analysis was carried out for a change in the following parameters: orientation, tilt angle, inverter type and inverter rating. At first the sensitivity analysis was carried out for a single system and then it was extended to the SMC modelling. The

following sections explain the procedure followed in the sensitivity analysis and the results that were obtained.

4.7.1 Sensitivity analysis for a single system

As a first step the sensitivity analysis was carried out for a single PV system. For this analysis a single PV system on the roof of a three-bedroom domestic house was considered. Measured half-hour horizontal irradiation for the London 1 location was used for this analysis. The PV system was assumed to have an inverter of multistage converter type with transformer. The nominal rating of the inverter was assumed to have the optimal size. For different tilt angles and orientations the energy output (kWh/kW capacity) was calculated and results are shown in Figure 4-15. The maximum energy output was obtained when the PV arrays are tilted at an angle of 35^0 and south oriented[6]. By taking this value as a reference the change in energy output for different possibilities was calculated and results are given in Table 4-25. This result is similar to the IEA findings on changes in the percentage of energy capture with orientation and tilt angle for European locations as shown in Figure 4-16.

When the PV system was assumed to be south oriented (azimuth angle is zero) the change in energy output was calculated with changes in the tilt angle. The maximum reduction in energy output of 0.76% was obtained when the tilt angle was 25^0. So the change in energy output with changes in the tilt angle from 25^0 to 40^0 is small. Similarly when the PV system was assumed to have 35^0 tilted PV arrays the change in energy output with changes in azimuth angle was calculated. The maximum reduction in energy output of 5.94% was obtained when the azimuth angle changed from south to southeast of -45^0. The change in energy output was higher with changes in the azimuth angles compared with changes in the tilt angle.

[6] The analysis was carried out for only tilt angles 25, 30, 35 and 40 degrees. So tilt angle 35 degrees was optimum among these values.

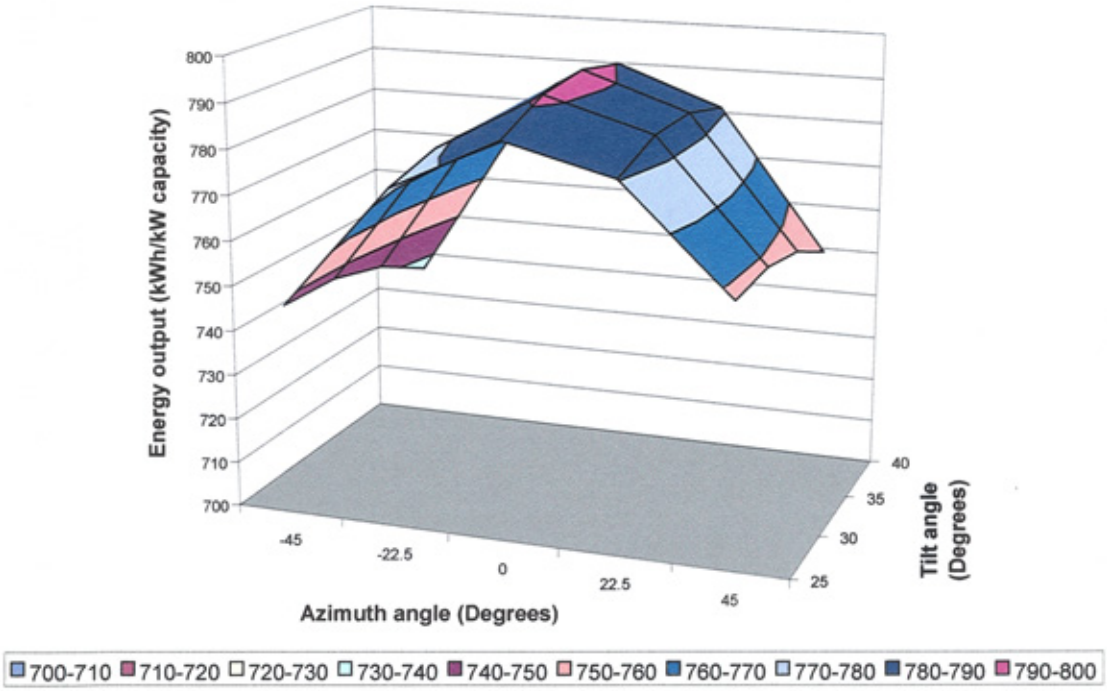

Figure 4-15 Energy output for different tilt angles and azimuth angles

Table 4-25 Change in energy output with respect to tilt angle and orientation

Change in Energy Output (%)					
	Azimuth angle -45^0	-22.5^0	0^0	22.5^0	45^0
Tilt angle 25^0	-5.48	-2.17	-0.76	-1.49	-4.24
30^0	-5.52	-1.75	-0.15	-0.99	-4.16
35^0	-5.94	-1.78	0	-0.96	-4.49
40^0	-6.74	-2.23	-0.33	-1.39	-5.24

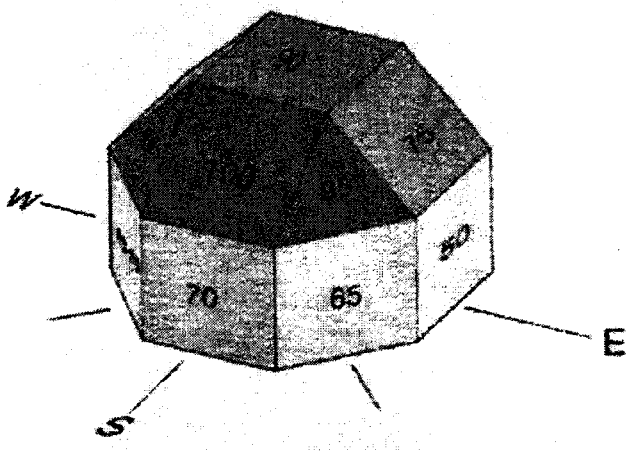

Figure 4-16 Effect of orientation on energy output for Europe locations (Source: www.demosite.ch)

4.7.2 Sensitivity analysis for SMC

In order to carry out the sensitivity analysis for the SMC modelling different cases were defined for each parameter. For each parameter an extreme case was defined to study the maximum possible change in output power pattern with change in representing the parameter. The following sections explain the different cases defined and the change in energy output and the fluctuation of output power from the SMC.

Selected cases

For the parameter of orientation, two different cases were defined. In case 1, it was assumed that 20% of PV systems were in each group.

- 20% of PV systems south oriented with azimuth angle of 0^0
- 20% of PV systems southeast oriented with azimuth angle of -22.5^0
- 20% of PV systems southeast oriented with azimuth angle of -45^0
- 20% of PV systems southwest oriented with azimuth angle of -22.5^0
- 20% of PV systems southwest oriented with azimuth angle of -45^0

In case 2 an extreme condition was assumed where all PV systems are south oriented.

- 100% of PV systems south oriented with azimuth angle of 0^0

For the parameter of tilt angle, two different cases were defined. In the modelling of domestic PV systems, tilt angle was assumed as

- 5% of PV systems in flat roof with assumed tilt angle of 35^0
- 15% of PV systems in inclined roof with tilt angle 25^0
- 25% of PV systems in inclined roof with tilt angle 30^0
- 40% of PV systems in inclined roof with tilt angle 35^0
- 15% of PV systems in inclined roof with tilt angle 40^0

This assumption was considered as case 1. For case 2, the tilt angle was assumed as

- 5% of PV systems in the flat roof with assumed tilt angle of 35^0
- 95% of PV systems in the inclined roof with tilt angle 35^0

In the modelling of non-domestic roof PV systems, tilt angle was assumed as

- 51% of PV systems in flat roof with assumed tilt angle of 35^0
- 15% of PV systems in inclined roof with tilt angle 25^0
- 20% of PV systems in inclined roof with tilt angle 30^0
- 14% of PV systems in inclined roof with tilt angle 35^0

This assumption was considered as case 1. For case 2 the tilt angle was assumed as

- 51% of PV systems in flat roof with assumed tilt angle of 35^0
- 49% of PV systems in inclined roof with tilt angle 35^0

In modelling of non-domestic façade PV systems, tilt angle was assumed as 90^0 for both cases, since mostly the façade PV systems are expected to have vertical PV arrays.

For the parameter of inverter type, case 1 was assumed as

- 50% of PV systems with self commutated inverter with line frequency transformer
- 25% of PV systems with self commutated inverter with high frequency transformer
- 25% of PV systems with self commutated inverter without transformer

In case 2, it was assumed that

- 50% of PV systems with self commutated inverter with line frequency transformer
- 50% of PV systems with self commutated inverter with high frequency transformer

An extreme condition was assumed in the case 3, in which

- 100% of PV systems with self-commutated inverter with line frequency transformer

For the parameter of inverter rating it was assumed as

- 80% of PV systems with optimal inverter size
- 20% of PV systems with inverter size equal to the PV system size

From the cases defined for each parameter, the sensitivity was analysed for 12 possible combinations.

Energy output from SMC

Measured half-hourly horizontal radiation data from the London location was used for this analysis. The total number of houses in England and Wales is 16,293,691 after neglecting the vacant and unfit dwellings. In this analysis 2% of houses were assumed to have PV systems and the capacity of PV systems was calculated as 954 MW. The total number of non-domestic premises in England and Wales is 927,720 after neglecting the vacant premises. In this analysis 1% of non-domestic premises were assumed to have PV systems on the roofs, which results in the capacity of 144 MW. 1% of non-domestic premises (378720) were assumed to have PV systems on the façade, which results in the capacity of 59 MW. Energy output (kWh/kW capacity) for each case was calculated and results are given in Table 4-26.

Table 4-26 Energy output from the SMC for 12 different cases

Number of Possibilities	Tilt angle	Orientation	Inverter Type	Energy (kWh/kW Capacity)
1	Case 1	Case 1	Case 1	789.78
2	Case 1	Case 1	Case 2	774.21
3	Case 1	Case 1	Case 3	793.77
4	Case 1	Case 2	Case 1	811.01
5	Case 1	Case 2	Case 2	795.46
6	Case 1	Case 2	Case 3	814.99
7	Case 2	Case 1	Case 1	790.50
8	Case 2	Case 1	Case 2	774.90
9	Case 2	Case 1	Case 3	794.47
10	Case 2	Case 2	Case 1	812.53
11	Case 2	Case 2	Case 2	796.93
12	Case 2	Case 2	Case 3	816.49

Energy output (kW/kW capacity) was compared for different inverter type cases. The base case is when tilt angle and orientation parameters are assumed as case 1. For the inverter type case 1, the energy output in the base case was 789.78kWh/kW capacity. When the orientation was changed from case 1 to case 2, the energy output increased by 2.68%. When the tilt angle was changed from case 1 to case 2, the energy output was increased by very small percentage of 0.09%. The main reasons for the very low change in energy output are:

- Tilt angle of the non-domestic façade PV systems were assumed as 90^0 in both cases
- 51% of non-domestic PV systems in flat roof with tilt angle of 35^0 and 14% of non-domestic roof PV systems in inclined roof with tilt angle of 35^0 remain the same in both cases
- 5% of domestic PV systems in flat roof with tilt angle of 35^0 and 40% of domestic PV systems in inclined roofs with tilt angle of 35^0 remain the same in both cases.
- Another important factor is as explained in the sensitivity analysis for a single PV system, there will be very small change in energy output with change in tilt angle.

When both the tilt angle and orientation parameters were changed from case 1 to case 2, the change in energy output was 2.88%. Similar results were obtained for other inverter type cases.

Among the different inverter type cases, case 2 gave less energy output. The energy output was reduced by 1.84% in the inverter type case 2 comparing with the inverter type case 1. Because case 2 considers 50% of self-commutated inverters with high frequency transformer that has less efficiency compared with other type of inverters. Comparing the inverter type case 1 with case 3 the energy output was increased by 0.44% because case 1 considers inverters with low efficiency. The comparison results are shown in Figure 4-17.

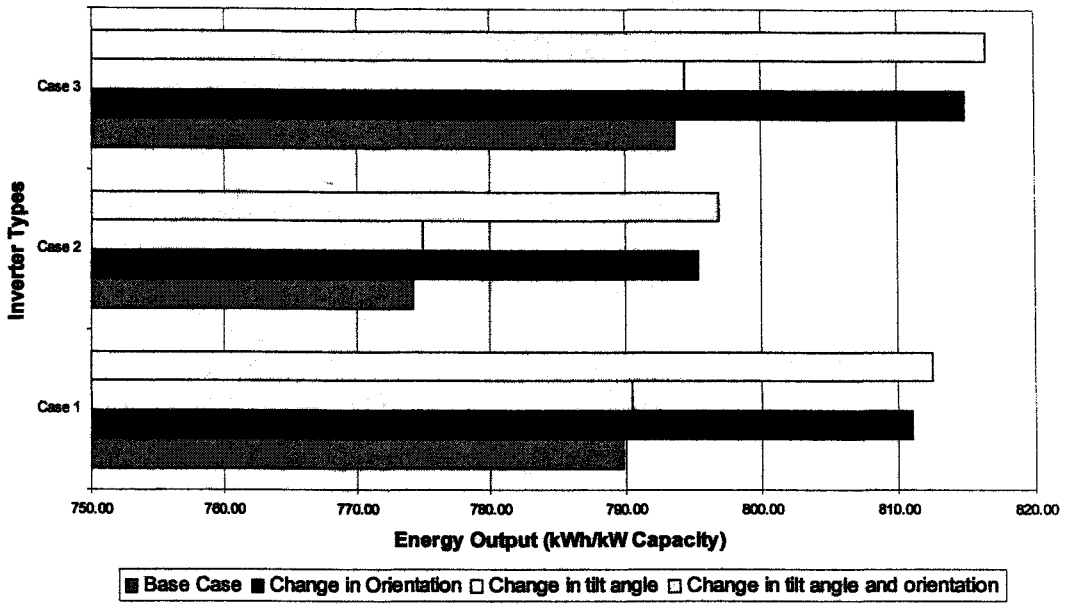

Figure 4-17 Energy output from the SMC when 80% of PV systems with optimal inverter size

In the previous analysis it was assumed that 80% of PV systems had the optimal size of inverter and 20% of PV systems had an inverter rating equal to the system size. The same analysis was carried out for the case when all PV systems in the cluster have the optimal size of the inverter. Energy output was higher by a small percentage of 0.24 compared with the previous case. The same analysis was also repeated for the case when all PV systems in the cluster had an inverter rating equal to the PV system size. There was a reduction in energy output compared with the previous cases. The maximum decrease in energy output was 1.2%, comparing with the case when all PV systems with optimal size inverter. Energy outputs for the 12 different possibilities, for different inverter rating are shown in Figure 4-18.

Output power fluctuation

Since the fluctuation of output power is an important factor for power system dynamic performance, it is important to study the change in output power fluctuation behaviour with changes in the assumptions made in modelling the SMC. The power fluctuation behaviour was studied for the 12 different cases that are selected. In this analysis it was assumed that 80% of PV systems would have inverter with the optimal size.

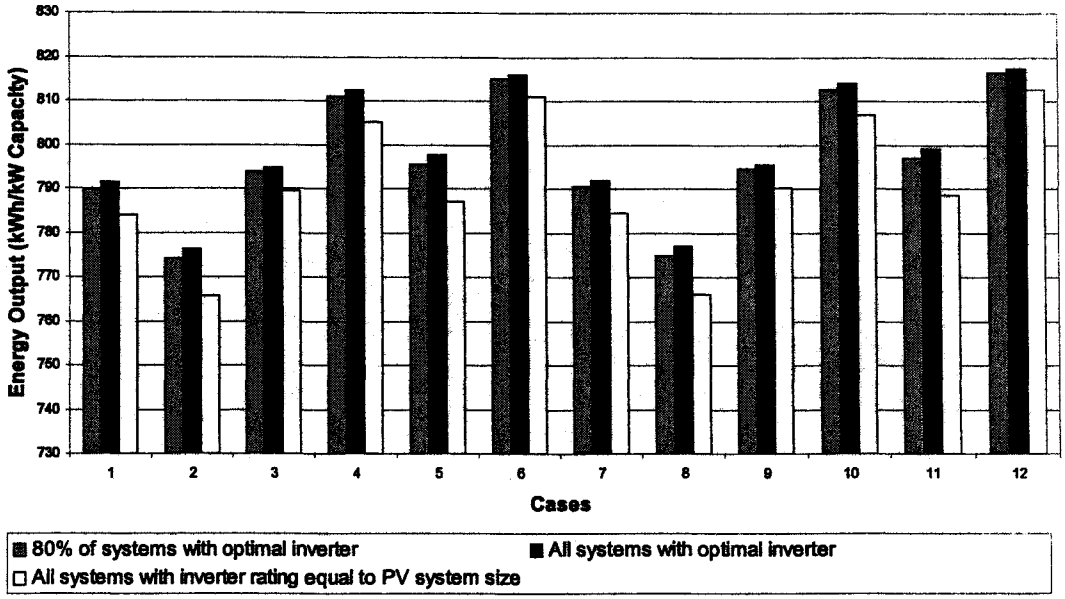

Figure 4-18 Comparison of energy output from the SMC for 12 different cases with changes in inverter ratings

The base case assumes the parameters tilt angle, orientation, and inverter type are as in case 1. The magnitude of output power fluctuation and the frequency of occurrence from one half-hour to the next were calculated for the base case. When the orientation was changed from case 1 to case 2, there was a slightly higher number of occurrences in higher magnitude of power fluctuation compared with the base case. When the tilt angle was changed from case 1 to case 2, there were no considerable changes in the power fluctuation pattern. These results are illustrated in Figure 4-19. The magnitude of the output power fluctuation and the frequency of occurrences were calculated for different inverter type cases and shown in Figure 4-20. The inverter type case 1 consists of 25% of transformerless inverter that have the highest efficiency compared with other inverters. These inverters can produce output power even for low irradiation levels while the output power from other inverters was zero. Hence there was a very small increase in the number of occurrences for fluctuation magnitude ±2.5% of PV capacity in case 1 compared with other cases. In general the change in power fluctuation pattern with change in inverter types is very low.

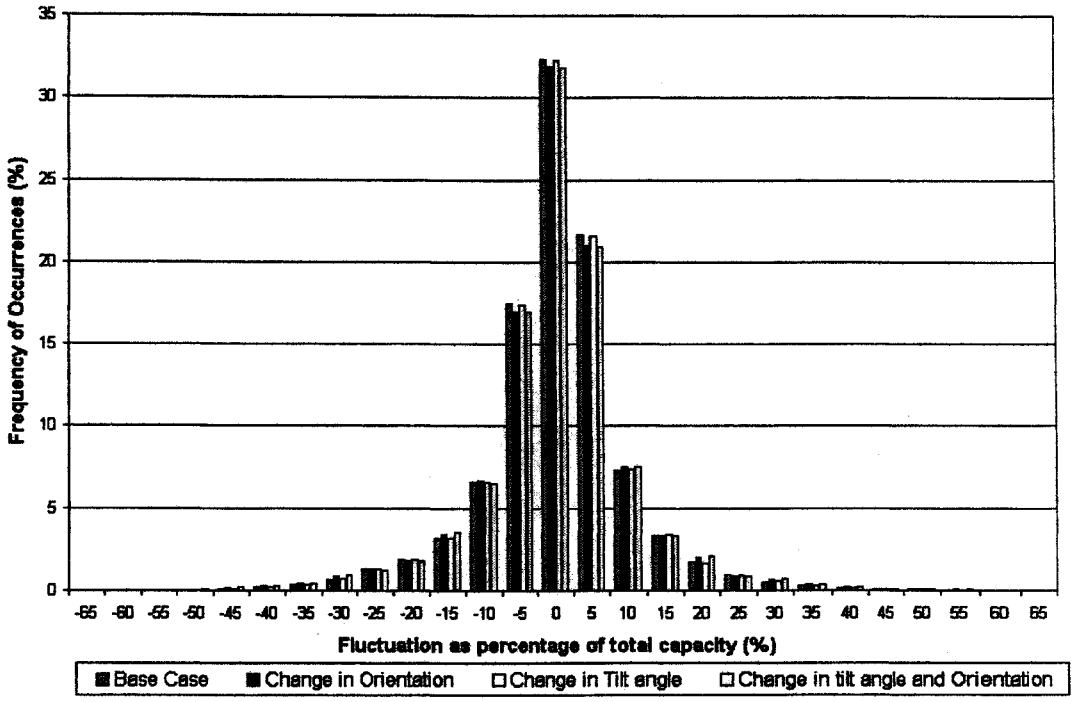

Figure 4-19 Power fluctuation pattern for the change in tilt angle and orientation

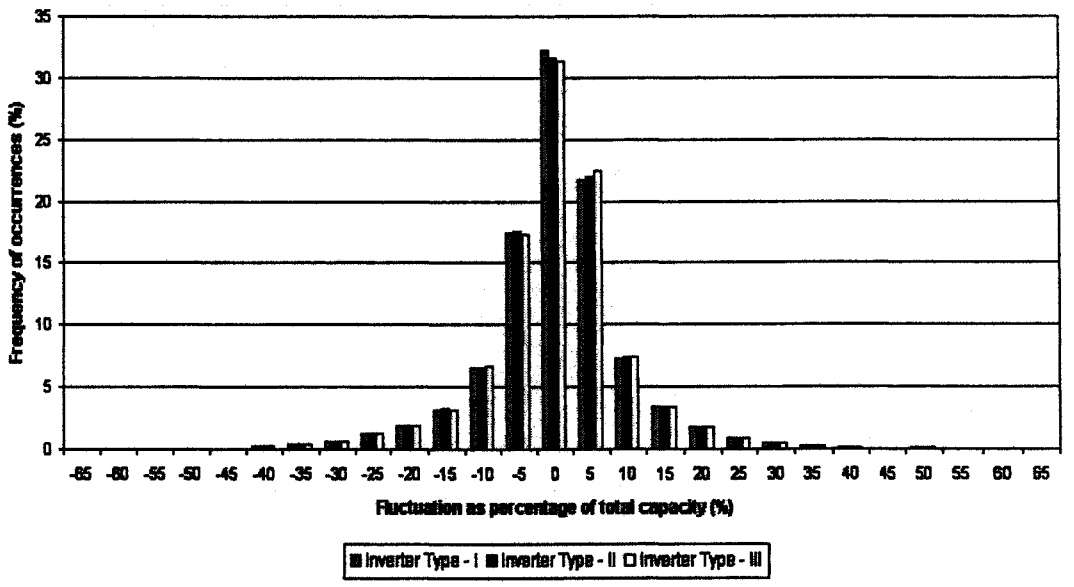

Figure 4-20 Power fluctuation pattern for different inverter type cases

4.7.3 Discussion

From the sensitivity analysis the following points were observed:

- For a single PV system, it was observed that there is no considerable change in energy output when tilt angle was changed from 25^0 to 40^0, with the same orientation. For the SMC it was observed that when the tilt angle is changed from case 1 to case 2, the change in energy output from the cluster was small. Similarly, there is no considerable change in power fluctuation pattern with the changes in the assumed tilt angles.
- For a single PV system it was observed that when the azimuth angle changed from 0^0 to -45^0 with tilt angle of 35^0, the maximum change in energy output was 5.94%. For the SMC it was observed that when the orientation changed from case 1 to case 2, the change in energy output was only 2.67% and there was a slightly higher number of occurrences of the higher magnitude of fluctuation.
- For a single PV system it was observed that when both tilt angle and orientation changed, the maximum change in energy output was 6.7%. For the SMC it was observed that when both tilt angle and orientation parameters were changed from case 1 to case 2, the maximum change in energy output was 2.86%. Also there was a slight change in the power fluctuation pattern. In practice not all PV systems are oriented in one direction and tilted at same angle. Hence it was decided that the assumed percentages in case 1 for each parameter can be used for SMC modelling.
- When the inverter type was changed from case 1 to case 3, the maximum change in energy output was only 2.3% and also there was a very small change in power fluctuation pattern. At present the transformerless inverter is not allowed by UK Standards. In the medium to long term there may be PV systems with transformerless inverters, so case 1 was assumed for the SMC modelling.

4.8 Projection To The Year 2030

The capacity of the installed grid connected PV systems in the UK was 5.189 MW in the year 2003 [34]. In the medium to long term, there will be a much higher number of PV systems connected to the utility grid. When the capacity of the installed PV systems is significant, the output power from these systems may have an impact on the grid. If PV is to displace a significant proportion of conventional electricity generation, at least another 25 years of aggressive market growth would be required [35]. During this time, there will be considerable changes in the PV system design. For an example the type of PV module, PV module efficiency and inverter efficiency will be different from the current scenario. So in order to analyse the impact of large-scale PV systems on the grid, these scenarios should be projected to the year 2030. The following sections explain the possible changes in PV system technologies by the year 2030.

4.8.1 PV module technology

Early R&D work in photovoltaics took place in 1950s and 1960s and was directed towards developing power sources for satellites. Only during the last 25 years R&D has been directed to developing PV for the large-scale power production usually associated with the terrestrial applications [36]. The PV market for terrestrial applications may be divided into 4 major segments; consumer application, remote industrial applications, application in developing countries and grid connected applications [37]. Whereas the market in the past basically developed from consumer products and remote industrial applications, the contribution of market segments have shifted towards grid connected systems and PV installations in developing countries [37]. The increase in the PV market and 25 years of research and development have led to the discovery of new materials, devices, fabrication approaches and continuing improvements in efficiency and reliability of PV cells and modules. The projection of PV module efficiency and their production by technologies for the year 2030 are discussed in this section.

PV module efficiency

PV cell and module efficiencies achieved in the production and in the laboratory for different technologies are given in Table 4-27 [35,38,39]. These values were used to project PV module efficiencies for the year 2030. One of the major R&D areas is the ability to produce products that possess higher solar conversion efficiencies demonstrated in the laboratory [40] and hence the following assumptions are made:

- Achieved cell efficiency in the production for the year 2000 will be taken as PV module efficiency for the year 2010.
- The maximum-recorded module efficiency in the lab will be taken as the PV module efficiency for the year 2020.
- The maximum cell efficiency in the laboratory will be taken as the PV module efficiency for the year 2030.

With these assumptions the PV module efficiency for the year 2030 was projected and results are given in Table 4-28.

Table 4-27 PV cell and module efficiency for different technologies

Technology	Achieved cell efficiency in 2000 (Production)	Maximum recorded cell/sub module efficiency in 2003 (Lab)	Achieved module efficiency in 2000 (Production)	Maximum recorded module efficiency in 2003 (Lab)
Single C-Si	15-17%	24.7%	12-15%	22.7%
Multi C-Si	13-15%	19.8%	11-14%	15.3%
Amorphous Silicon	---	12.7%	5-7%	10.4%
Cadmium Telluride	---	16.5%	---	10.7%
CIGS	---	18.9%	---	13.4%

Table 4-28 Projection of PV module efficiency for the year 2030

Technology	Year 2000	2010	2020	2030
Single C-Si	13%	17%	22.7%	24.7%
Multi C-Si	12%	14%	15.3%	19.8%
Amorphous Silicon	6%	8%	10.4%	12.7%
Cadmium Telluride	---	9%	10.7%	16.5%
CIGS	---	12%	13.4%	18.4%

PV cell production

PV cell production by technologies from the year 1999 to 2002 [41] is given in Table 4-29. In the year 2003 the world PV cell/module production by technologies is [35,41]

- Single crystalline silicon and multi crystalline silicon contributed 26.94% and 61.79% respectively.
- Amorphous silicon type contributed 3.4%
- Amorphous silicon on C_z slice type contributed 4%
- Micro crystalline silicon contributed 1.82%
- Crystal silicon concentrator and ribbon (silicon) types contributed 1%.
- CIS type PV module production contributed 0.54%
- Cadmium telluride based PV cell production contributed 0.4%

Table 4-29 PV cell/module production by technologies

Technology	1999	2000	2001	2002
Single C-Si	40.8%	37.4%	34.6%	36.4%
Multi C-Si	42.1%	48.2%	50.2%	51.6%
Cadmium Telluride	0.5%	0.3%	0.5%	0.7%
Amorphous silicon	12.3%	9.6%	8.9%	6.4%
CIS	0.2%	0.2%	0.2%	0.2%
Ribbon/ Sheet C-Si	4.1%	4.3%	5.6%	4.7%

The future contribution of the type of technologies in production depends upon many factors like efficiency, cost, resources etc. Different PV technologies in the present

market in terms of their research and manufacturing status, as well as issues and advantages they are facing in their future are discussed as follows:

- Crystalline silicon technology is well proven. Because crystalline silicon processes and costs are well understood, evolutionary improvements continue, along with increased automation and economies of scale [42].
- Single crystalline technology has consistently lost market share over the past years to multi-crystalline silicon technology. Even though Sharp have added a new single C-Si line and Sanyo's strong growth, it could increase the market by 1.8% [41].
- Thin film cell requires 1/10 to 1/100 of the expensive semiconductor material as that required by crystalline silicon for equal collection areas. Thin film cells are potentially cheaper than crystalline silicon because of their lower material costs and larger substrate size [36].
- Thin film technology offers different design options for the building integrated applications.
- BP closed its 10 MW of CdTe module productions in California [41].
- CIGS global share will increase, because [41]
    - Shell increased its CIGS productions from 600kW to 1MW.
    - Wurth solar GmbH planned to ramp up the CIGS production from 150kW to 450kW.
    - Global solar planned to increase the CIGS production from 200 kW to 2.2 MW.
- Efficiency of the CIGS modules has increased very reasonably. The maximum-recorded module efficiency is 13.4% while the multi crystalline silicon module efficiency is 15.3% [39].

Since there is considerable increase in the efficiency of CIGS type modules with low cost, the share of thin film type technology will increase. Also thin film technology offers different options for building integration application, so we can expect that there will be a higher share in BIPV systems. In spite of these changes, the market for crystalline silicon will be considerable because of well-proven technology and proved efficiency. Ribbon silicon products are proven and accepted in today's market but it faces competition from its ancestor and thin-film technologies. Concentrator systems essentially use only direct radiation and therefore their areas of

best applications require high intensity sunlight [42]. By considering these points the market share was projected to the year 2030 as

- Mono crystalline silicon 35%
- Multi crystalline silicon 35%
- Thin film cells 30%

A second scenario was assumed in which the growth of thin film PV module technologies is high because of their low cost, increasing efficiency (CIGS) and different design options for building integrated systems. In this case, the market share was projected to the year 2030 as

- Mono crystalline silicon 30%
- Multi crystalline silicon 30%
- Thin film cells 40%

It should be noted that emerging PV module technology might have considerable share by the year 2030. The exact mix of technologies is not important to calculate the average efficiency of PV modules for the year 2030. These two different scenarios of PV module production projection were used to estimate the average PV efficiency by the year 2030.

Average efficiency

The projected PV module efficiency for 2030 and projected PV market share by technologies were used to calculate the average efficiency of PV modules for 2030. The average efficiency was calculated as

Average efficiency = (0.35*24.7+0.35*19.8+0.3*18.4) = 21.095%

Similarly for the second scenario, the average efficiency was calculated as

Average efficiency = (0.30*24.7+0.30*19.8+0.4*18.4) = 20.71%

In both the cases, the average PV module efficiency was calculated as almost equal to 21%. This value was taken as the average PV module efficiency for the year 2030. This average efficiency can be used to calculate output power from the cluster for the year 2030. In the SMC modelling mono-crystalline silicon was used to estimate the PV system capacity and output power from the cluster. The projection of module efficiency and module production by different PV technologies can be implemented to study the output power from the cluster for the year 2030.

4.8.2 Inverter technology

The performance and quality of inverters have improved considerably in the last decade. The large-scale inverter market was stimulated by high-volume building systems. As explained in Chapter 2 before, at present the transformerless inverter is not recommended in the UK because of the issue of non-isolation of the grid from PV array and associated wiring. But in the future the transformerless inverter may be allowed in the UK [21]. Calais et al. [19] studied the efficiency of different single-phase inverter topologies for German market for the years 1994-2002. According to this study, the maximum efficiency of 96% was achieved through transformerless inverters and some of the inverter topologies have lower efficiency in order to reduce the cost.

According to the 1995 EUREC position paper [35], grid-connected inverters in the range 1-3 kW achieved a breakthrough in terms of costs, reliability, efficiency and safety. Large inverters >50 kW did not improve figures-of-merit to the same extent, probably because most of them are custom built and cannot profit from high volume production [35]. According to this paper, the achieved inverter efficiency in the year 2000 is 90% at 10% of load and 96% at 100% of load. As a medium term goal, the projected inverter efficiency for the year 2010 is greater than 95% at 10% of load and greater than 98% at 100% of load. Considering these points, for modelling the SMC, inverter types and their efficiencies were projected for the year 2030 and are given in Table 4-30.

Table 4-30 Projected inverter efficiency by types

Types	Percentage of PV systems	Efficiency at 10% of nominal rating	Efficiency at 100% of nominal rating
Inverter with line frequency transformer	50%	93%	95%
Inverter with high frequency transformer	25%	91%	94%
Inverter without transformer	25%	95%	98%

This inverter efficiency projection can be easily implemented in the cluster model and the output power from the dispersed PV systems can be calculated for the year 2030.

4.8.3 Dwelling stock

In order to model the SMC for the year 2030, the dwelling stock for England and Wales was projected. The government statistical release [10,11] provides the number of new dwellings completed from the year 1991 to 2001, in each region of England and Wales (Appendix C). These data were used to calculate the average number of dwellings completed in a year, which is 148,036. Also according to the recent English Housing Condition Survey 2001 [10] the average new-build dwellings per year are around 150,000, during the year 1996-2001. These two different sources result in similar values and this value was used to project the dwelling stock for the year 2030. The results are given in Table 4-31. The trend in increasing number of new dwellings may change, because of different issues like land area, cost etc. So this calculation assumes that the last 10-year trend will continue in the future.

Table 4-31 Projected dwelling stock for the year 2030

Region	Dwelling stock for the year 2000	Average number of new dwellings completed in a year	Dwelling stock for the year 2030
North East	1,127,000	6919	1,334,570
Yorkshire and Humber	2,144,000	13972	2,563,160
North West	2,956,000	19492	3,540,760
East Midlands	1,776,000	15081	2,228,430
West Midlands	2,206,000	15115	2,659,450
South West	2,128,000	16860	2,633,800
Eastern	2,285,000	20552	2,901,560
South East	3,333,000	25451	4,096,530
London	3,054,000	14594	3,491,820
Wales	1,267,000	9351	1,547,530

4.8.4 Non-Domestic building stock

Similar to the dwelling stock projection the non-domestic building stock was also projected for the year 2030. According to the BRE report on Non-Domestic building Energy Fact File the new build rate for non-domestic stock is 1% to 1.5% per annum [32]. The total number of non-domestic premises in which PV systems can be installed was calculated as 1,008,414 for the year 2000. Considering the new build rate as 1% per year, the total number of non-domestic premises in which PV systems can be installed was calculated as 1,359,190 for the year 2030.

4.9 Modelling of Multiple Cluster

In practice the deployment of PV systems in the UK will be a large number of small, geographically dispersed PV systems, which vary in their design parameters. In the SMC modelling the variation of system design parameters such as system size, tilt angle of PV array, orientation and balance of system design were taken into consideration. However the output power from the SMC was calculated by assuming solar radiation data for a single location. In practice the solar radiation will be different for geographically dispersed PV systems. Also the number of PV systems located in each region will be different depending on factors like solar radiation level, domestic and non-domestic buildings stock in the region etc. These factors are taken into account in the MC modelling. The output power from a very large number of small PV systems, dispersed geographically and connected to different points of the grid was calculated in the MC modelling.

In order to analyse the combined output power from dispersed PV systems, three locations in the UK, London 1, West Midlands 1 and a location in the South West region (South West 1) data were used. The dwelling stock in London, West Midland and South West regions are 14%, 10% and 10% of total England and Wales stocks respectively. The non-domestic building stocks in these regions are 17%, 10% and 9% of total stock in England and Wales respectively. In each region it was assumed that 2% of houses have PV on their roofs, 1% of non-domestic buildings have PV on their roofs and 1% of non-domestic buildings have PV on their façades. With this

assumption the total PV capacity installed in each region was calculated as 163.3 MW, 111.7 MW and 109.9 MW respectively and the total as 385 MW.

The output power from PV systems in a region was calculated using the measured horizontal radiation and ambient temperature data from a location in that region. The output power from each region was calculated, where the procedure was same as the SMC modelling. The output power from the MC was calculated by adding the PV output power from three regions. The fluctuation of PV output power for a single location was calculated and compared with the combined output power fluctuation and is shown in Figure 4-21. It was observed that the occurrences of high magnitude fluctuation were reduced for the combined output power from three locations compared with the single location. Further analysis on the combined output power is discussed in the next chapter.

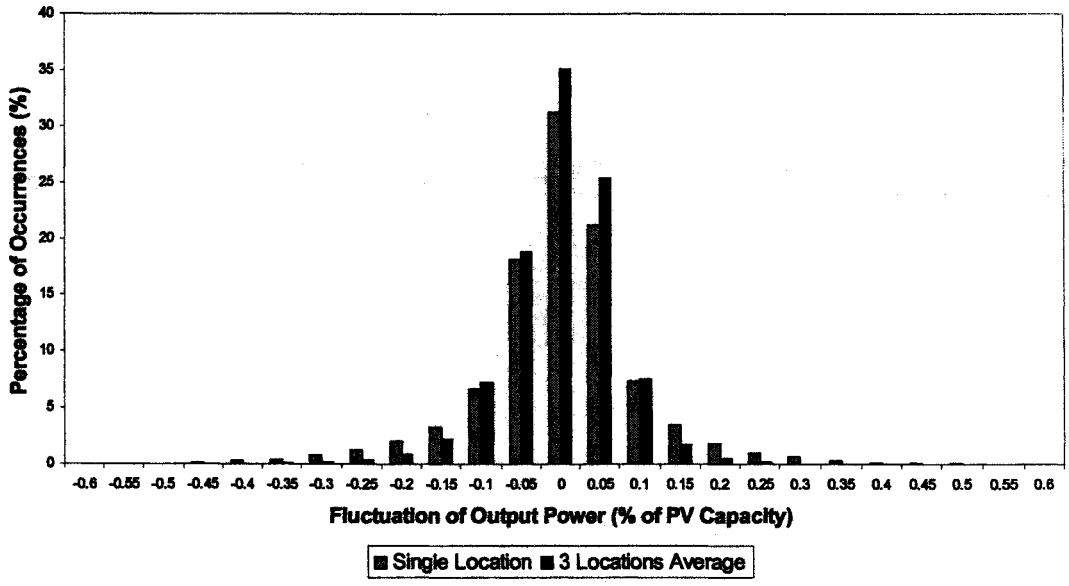

Figure 4-21 Comparison of output power fluctuation

4.10 Discussion

The aggregate output power from geographically dispersed PV systems is important to analyse the impact of dispersed PV systems on the grid. The BIPV systems design parameters such as the system size, tilt angle of PV arrays and orientation etc depend

upon the building envelope into which the system is to be integrated. Hence there will be range of different system designs and the assumption of a single PV system configuration will not be appropriate to analyse the combined output power from dispersed PV systems. In this study the methods to represent the dispersed PV systems, which vary in their design parameters, were considered.

In this study monocrystalline silicon PV module technology, which had a market share of 33% in 2003, was considered. This provides the highest output power per unit area and hence would have the highest impact on the network. However, the approach allows for simple modification to incorporate other technologies for all or some of the systems. Sensitivity analysis was carried out to determine the effect of assumptions made in the cluster modelling.

To define the system size in the SMC model, in this analysis the suitable roof area was calculated based on the criterion that the roof surface that can receive 90% or more of annual solar yield. If the suitability factor is calculated on the basis that the roof area that can receive 80% or more annual solar yield then the possible system size will be almost doubled. This calculation does not include any financial restriction. At present, in a three-bedroom house in the UK an average capacity of 1.5 kWp is being installed. This behaviour may change with the improvement in the reduction of PV system costs. In Japan most of the roof area in a domestic house is being used for PV installation. In this analysis the Performance Ratio (PR) of PV systems was varied from 0.76 to 0.86. This value is higher than the PR values obtained from installed PV systems, because in this analysis low loss systems were assumed. The low loss systems provide the highest output power and would have the highest impact on the network. However in the developed PV cluster model other losses can be included for all systems in the cluster or some of the systems.

In the medium to long term the PV penetration level is expected to be high. To analyse the impact of PV systems on the grid, the cluster model for the year 2030 was projected. It was assumed that the number of new dwellings per year in future would be same as now. There are many factors that could change these assumptions. Similarly, there may be change in bedroom classification, for an example there may

be an increase in three-bedroom type houses in the newly built houses. However these changes can be accommodated easily in the cluster model.

In this analysis the MC modelling was carried out on the basis of dwellings and non-domestic building stock. The percentage of buildings with PV was assumed the same for all regions in the MC modelling, which may be different in practice due to other factors like the irradiation level in the region, PV specialists in the region etc. However in the developed PV cluster model the percentage of buildings with PV in each region can be changed easily to analyse the output power for different scenarios. The change in output power behaviour by combining dispersed PV systems was observed. In the sixth chapter the behaviour of combined output power from dispersed PV systems is analysed in detail.

4.11 References for Chapter 4

1. A. Murata and K. Otani, "An analysis of time-dependent spatial distribution of output power from very many PV power systems installed on a nation-wide scale in Japan", Solar Energy Materials and Solar Cells, Vol. 47, pp. 197 – 202, 1997.
2. Photovoltaics in Buildings – A design handbook for architects and engineers, International Energy Agency, Paris, France, 1998.
3. C. M. Whitaker, H. J. Wenger, A. Iliceto, G. Chimento and F. Paletta, "Effects of irradiance and other factors on PV temperature coefficients", 22nd IEEE Photovoltaic Specialists Conference, Las Vegas, Vol. 1, pp. 608-613, 1991.
4. M. H. Macgnan and E. Lorenzo "On the optimal size of inverters for grid connected PV systems", 11th EC Photovoltaic Solar Energy Conference, Switzerland, pp. 1167-1170, October, 1992, Harwood Academic Publishers, Switzerland.
5. Crystalline silicon terrestrial photovoltaic (PV) modules – Design qualification and type approval – British Standard BS EN 61215:1995, IEC 61215:1995.

6. J. Schmid and H. Schmidt, "Inverters for photovoltaic systems", Proceedings of the fifth Contarctor's Meeting of the EC Photovoltaic Demonstration Projects, pp.122-132, Ispra, Italy, 1991.
7. A. Louche, G. Notton, P. Poggi and G. Peri, "Global approach for an optimal grid connected PV system sizing", 12th European Photovoltaic Solar Energy Conference, Vol.2, April 1994, pp.1638-1641, Published by H.S. Stephens & Associates, UK.
8. BP585F PV module data from the BP Solar company website, www.bpsolar.com
9. Sunny Boy 2500 type inverter data sheet obtained from company website www.sma.de
10. From the website of Office of the Deputy Prime Minster, UK, www.odpm.gov.uk
11. From the UK national statistics website, www.statistics.gov.uk
12. English House Condition Survey 1996, Published by Department of the Environment, UK.
13. From the National Assembly of Wales website, www.wales.gov.uk
14. Kerry Revell and Philip Leather, "The State of UK Housing", Chapter 1, The Policy Press, Second Edition, 2000.
15. English House Condition Survey 1991, Published by Department of the Environment, UK.
16. A Guide to Sustainable Roofing, Redland Roofing Systems Ltd., available from the website www.redland.co.uk
17. Potential for Building Integrated Photovoltaics, Photovoltaic Power System Programme, Technical Report IEA-PVPS T7-4, 2002, International Energy Agency.
18. From the website of the British Photovoltaics Association, www.pv-uk.org.uk
19. M. Calais, J. Myrzik, T. Spooner and V.G. Agelidis, "Inverters for single-phase grid connected photovoltaic systems - An overview", Proceedings of 33rd annual IEEE Power Electronics Specialist Conference, Vol.4, pp. 1995-2000, 2002.
20. Photovoltaics in Buildings – Guide to the installation of PV Systems, July 2002, Published by Department of Trade and Industry, UK available at www.dti.gov.uk/renewables

21. Low Voltage Grid Connection of Photovoltaic Power Systems, Published by Department of Trade and Industry, UK, ETSU Report No. S/P2/00215/REP available at www.dti.gov.uk/renewables
22. K. Peippo and P. D. Lund, "Optimal sizing of solar array and inverter in grid connected photovoltaic systems", Solar Energy Materials and Solar Cells, Vol.32, pp. 95-114, 1994.
23. R. Jayaraman, N.M. Pearsall and G.A. Putrus, "Optimal Sizing of Inverters for Grid-Connected PV Systems", 37th International Universities Power Engineering Conference, Staffordshire, UK, September 2002, Vol.2, pp 783-787.
24. J. Ramachandran, N.M. Pearsall and G.A. Putrus, "Impact of Inverter Size on PV System Energy Production and Cost", 38th International Universities Power Engineering Conference, Greece, September 2003, Vol.2, pp 573-576.
25. Data sheet for SINVERT inverter obtained from Siemens company website, www.ad.siemens.de
26. Data sheet for SUNMASTER 130S inverter from the Mastervolt company website, www.mastervoltsolar.com
27. C. W. G. Verhoeve, C.F.A. Fruman, E. de Held and W.C. Sinke, "Recent test results of AC-module inverters", 14th European Photovoltaic Solar Energy Conference, Barcelona, Vol. 3, pp. 2201 – 2203, July 1997, Published by H.S. Stephens & Associates, UK.
28. From the Valuation Office Agency, UK website, www.voa.gov.uk
29. Harry Bruhns, Philip Steadman and Horace Herring, "A database of modeling energy use in the non-domestic building stock of England and Wales", Applied Energy, Vol.66, pp. 277-297, 2000.
30. Philip Steadman, Harry Bruhns and Bratislav Gakovic, "Inferences about built form, Construction, and fabric in the nondomestic building stock of England and Wales", Environment and Planning B: Planning and Design, Vol.27, pp. 733-758, 2000.
31. P. Steadman, "Non-Domestic Building Stock Project: Development of a Database of Energy use in Non-Domestic Buildings: Inferences about Built Form, Construction and Fabric in the National Non-Domestic Building Stock", Phase 6, Final Report, June 1997, Department of the Environment, Transport and the Regions, UK.

32. Non-Domestic Building Energy Fact File, Published by Global Atmosphere Division of Department of Environment, Transport and the Regions, UK, January 1998.
33. Frank E. Brown, Peter A. Rickaby, Harry R. Bruhns and Philip Steadman, "Surveys on non-domestic buildings in four English towns", Environment and Planning B: Planning and Design, Vol.27, pp. 11-24, 2000.
34. "Trends in photovoltaic applications survey report of selected IEA countries between 1992 and 2003", Report IEA-PVPS T1-13: 2004, International Energy Agency, available from www.iea-pvpsuk.org.uk
35. The future for renewable energy - Prospects and Directions, EUREC Agency, James & James Ltd., 2002.
36. C. E. Witt, R.L. Mitchell, M. Symko-Davies and H.P. Thomas, "Terrestrial photovoltaics technologies – Recent progress in manufacturing R&D", 34th National Heat Transfer Conference, Pittsburgh, Pennsylvania, August 20-22, 2000.
37. W. Hoffmann, "PV solar electricity: One among the new millennium industries", 17th European Photovoltaic Solar Energy Conference and Exhibition, Munich, October 22-26, Vol. 1, pp. 851- 861, 2001, Published by WIP – Renewable Energies and ETA- Florence.
38. M. A. Green, K. Emery, D.L. King, S. Igari and W. Warta, "Solar cell efficiency tables (Version 20)", Progress in Photovoltaics: Research and Applications, Vol.10, pp. 355-360, 2002.
39. M. A. Green, K. Emery, D.L. King, S. Igari and W. Warta, "Solar cell efficiency tables (Version 21)", Progress in Photovoltaics: Research and Applications, Vol.11, pp. 39-45, 2003.
40. C.E. Witt, R.L. Mitchell, M. Symko-Davies, H.P. Thomas, R. King and D.S. Ruby, "Current status and future prospects for the PVMaT project", 11th International Photovoltaic Science and Engineering Conference, Sapporo, Japan, September 20-24, 1999.
41. M. Schmela, "Market survey on world cell production 2002", PHOTON International – Photovoltaic Magazine, March 2003, pp. 42-48.
42. R. D. McConnell, T. Surek and C.E. Witt, "Progress in PV manufacturing technologies", Renewable Energy, Vol.15, pp.502-505, 1998.

43. U. Jahn and W. Nasse, "Performance analysis and reliability of grid-connected PV systems in IEA countries", 3rd World Conference on Photovoltaic Energy Conversion, Osaka, Japan, May 2003.

5 SOLAR RADIATION FLUCTUATION

The output power from a PV system is mainly dependent on the solar radiation received by the PV array and therefore any study of the interaction of PV systems with the electricity network must take account of variation of solar radiation. The variation of solar radiation can be classified into two main categories. The first category is the diurnal variation in the value as a result of the position of the sun. This dominates on clear days with little cloud cover and is fully predictable. The second category is the short term variation resulting from the cloud cover which is less predictable. There are methods to forecast the short term solar radiation values [1]. However, this cloud cover will not occur in all locations at the same time. Because of this spatial in-homogeneity of the variations, the fluctuation of aggregated solar radiation values from different locations will be reduced. Hence aggregating output power from geographically dispersed PV systems would reduce the fluctuation of PV output power. For example, in an instant there may be a reduction of output power from PV systems in London due to cloud coverage. At the same instant there may be an increase in output power from PV systems in Newcastle due to cloud clearance. Therefore PV output power fluctuation in one location can be smoothed by aggregating the output power of geographically dispersed PV systems.

The change in output power from a PV system results in a change in net load demand to be met by the grid. Hence to analyse the impact of dispersed PV systems, connected to different points of the same grid, it is important to study the fluctuation of output power from geographically dispersed PV systems. In this work, the fluctuation of output power from dispersed PV systems connected to the UK national grid was analysed. In this chapter the fluctuation of solar radiation for different time intervals and the correlation of solar radiation with the distance of separation is analysed.

5.1 Background Theory

The PV output power mainly depends upon the solar radiation values. In BIPV systems, the PV arrays are tilted at some angle to the horizontal, depending upon the roof or façade angle. As an example, Figure 5-1 and Figure 5-2 show the comparison between horizontal radiation and tilted radiation values for the summer and winter seasons, corresponding to a PV system tilted at an angle of 30^0 to the horizontal surface and southwest oriented with an azimuth angle of 64^0. Tilted radiation values will vary with tilt angle and orientation of PV arrays as discussed in chapter 3. Geographically dispersed PV systems will vary in their tilt angle and orientation and hence to study the smoothing effect, tilted radiation values were used.

Figure 5-3 shows the measured minute tilted radiation values for a location in the London region, for a day in a summer month, which is an example of rapid changes in radiation caused by passing clouds. This type of cloud transition may not occur in all places at the same time, so the insolation at each location does not change simultaneously. By aggregating many locations the data fluctuation of tilted radiation will be reduced. This effect is known as a smoothing effect, which occurs due to spatial in-homogeneity in the variation of solar radiation.

In order to analyse the smoothing effect, hourly clearness index values calculated from the measured horizontal radiation values for the year 2001 from three different locations, London, South West and West Midlands regions, were used. These locations are separated by a maximum distance of 160 km. The number of occurrences of clearness index values in each interval was calculated for a single location (London region) and compared with the average of values from the three locations. The result is shown in Figure 5-4 and it illustrates that by adding locations, the numbers of clearness index occurrences in high and low magnitude were reduced. This result shows the reduction of rapid changes in radiation values, and hence the reduction in PV output power fluctuation by aggregating spatially distributed PV systems.

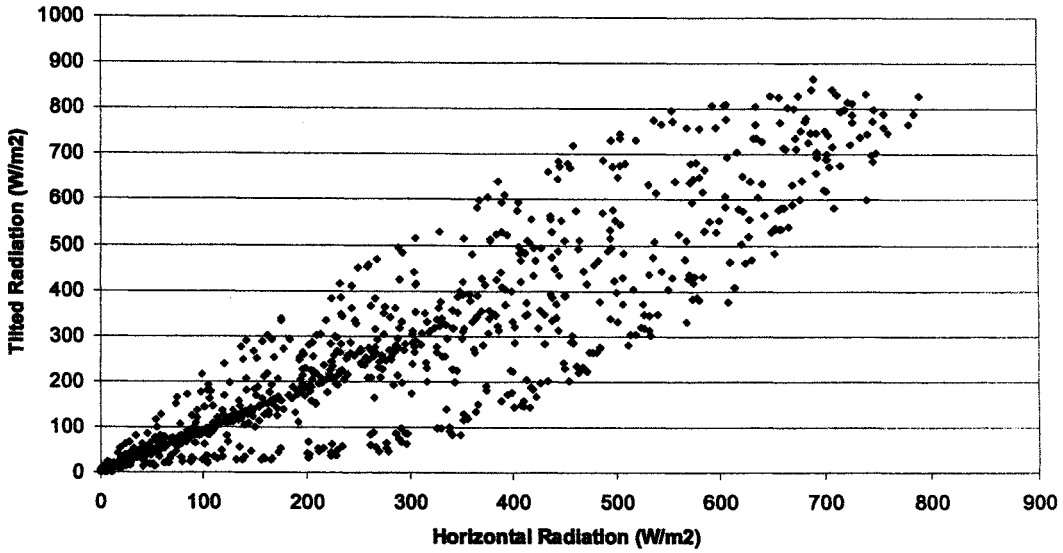

Figure 5-1 Comparison of horizontal and tilted radiation for a summer month (London location)

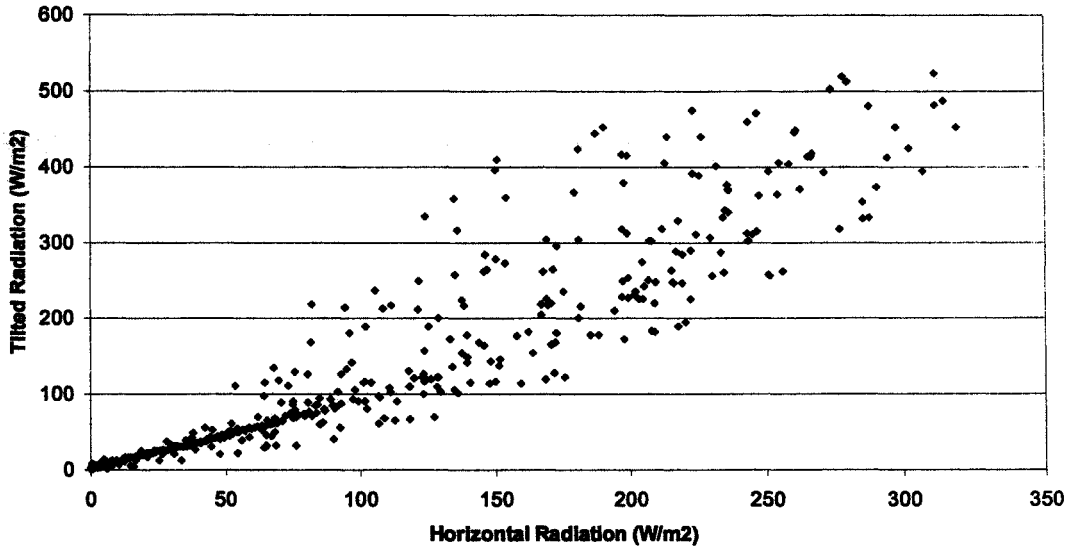

Figure 5-2 Comparison of horizontal and tilted radiation for a winter month (London location)

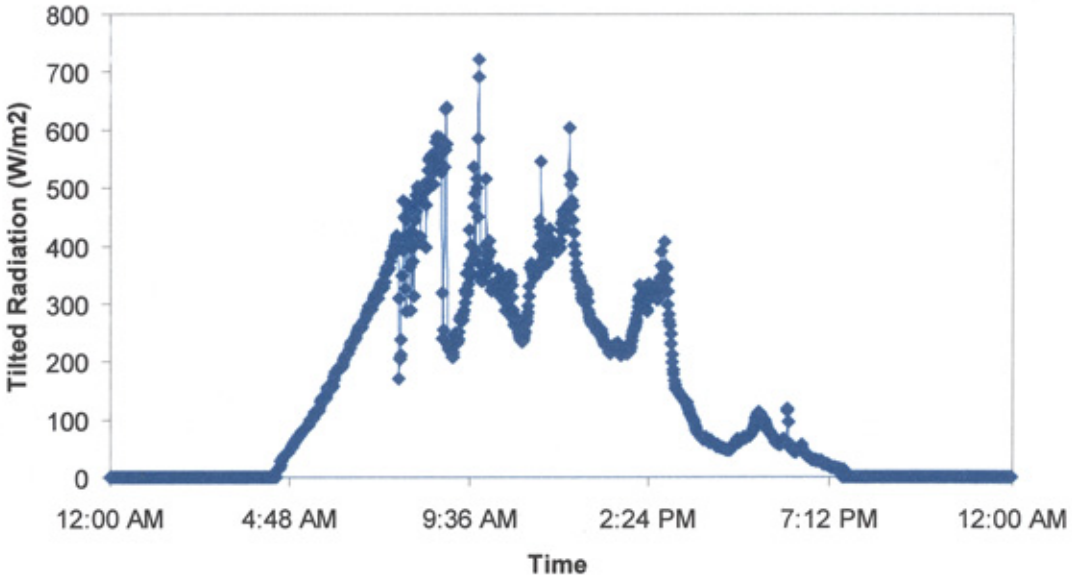

Figure 5-3 Example of short term variation in solar radiation values (London location)

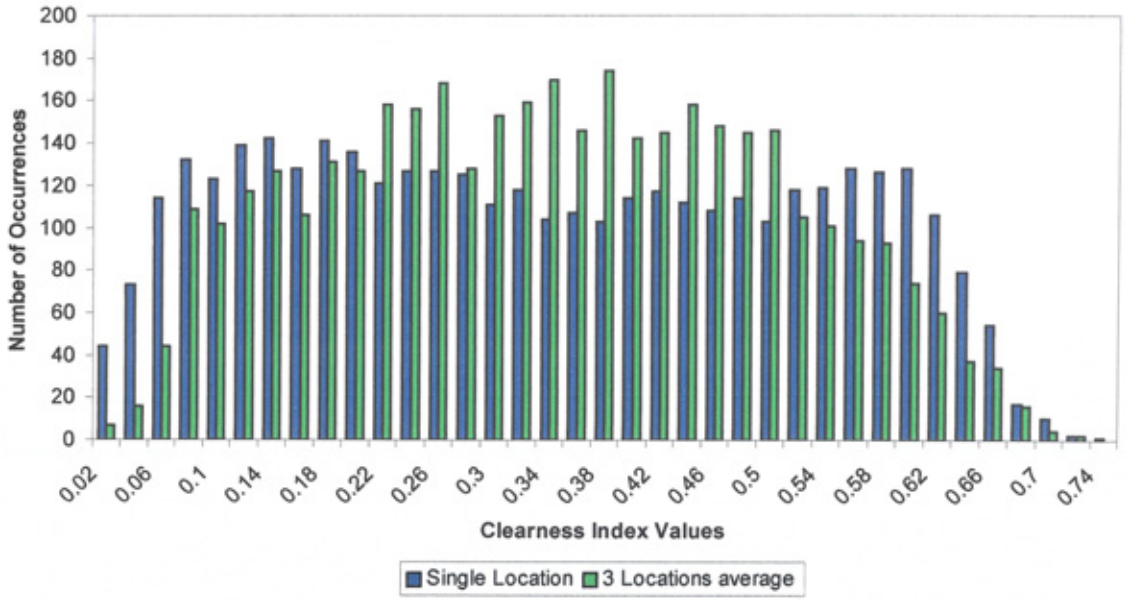

Figure 5-4 Comparison of annual occurrences of clearness index values - Single location: London, 3 locations: London, South West and West Midlands (There are no occurrences for clearness index above 0.74)

5.2 *Literature Review*

The spatial in-homogeneity of solar radiation may smooth the solar radiation fluctuation and could smooth the overall PV output power fed into the utility grid. Several researchers have investigated the reduction in fluctuation of solar radiation and hence the reduction in PV output power fluctuation from distributed PV systems, due to the spatial smoothing effect [2 - 8]. Travers et al. [2] have studied the impact of large PV systems and distributed PV systems on power systems, using data from Australian locations. The authors studied the reduction in the incremental value that can be achieved from a large penetration of PV systems due to the inflexibility of large power plant operations. The authors found that the fluctuation of output power from dispersed PV systems was reduced and had less impact on power systems compared with the large PV systems. They showed that this become apparent at 20% of PV penetration and significant at 30% of PV penetration. However, this study did not account for random fluctuations in the load. Kawasaki et al. [3] studied the radiation fluctuation in 4 locations in Japan, separated by a distance of approximately 185 km and showed that the smoothing effects were produced due to non-simultaneous variation of solar radiation. To study this variation behaviour in detail, the authors studied the correlation of radiation values between locations. They found that the time difference of variation of insolation between the locations separated by a distance of 20 km was 10 minutes.

Otani et al. [4] quantified the solar radiation fluctuation using fluctuation factor and power spectral density. They also investigated the cross-correlation of solar radiation between 9 different locations in Japan, within a distance of 6 km. They found that in a partly cloudy daytime, the fluctuation factor of the area total irradiance decreased to around 20 – 50% of each respective irradiance. However, they found that a considerable amount of fluctuation still remained under highly correlative irradiance fields. Therefore they suggested the optimum size of the area of the systems should be decided carefully by considering both the influence on the utility stability and their whole distribution loss. Otani et al. [5] have estimated the spatial smoothing effect using the correlation decay distance, which is a parameter indicating cloud size, within the radius of 2, 3 and 4 km. The authors found that the considerable

reduction of the fluctuation occurred, and the size of the area of PV output aggregation was an effective parameter to smooth the fluctuation. However, increasing the number of PV systems had little influence on the smoothing effect. The authors suggested that the smoothing effect also depends upon the time interval considered.

Wiemken et al. [6] analysed the combined power production of 100 grid connected PV systems in Germany and observed that the power characteristics are mainly determined by the large spatial distribution of the sites but not by the number. Authors studied the reduction of standard deviation of output power by aggregating many locations, using 5 minute measured data. They also studied the hourly cross correlation of solar radiation for 6 different locations in Germany, separated by the maximum distance of 700 km. Coppye et al. [8] investigated the reduction of output power fluctuation and the value of decentralised PV systems using data from 8 locations in Belgium. Murata et al. [7] investigated the smoothing of PV output power from many PV systems installed on a nation-wide scale in Japan, assuming 3 kW south oriented PV system was installed in detached houses. They observed that the PV output instability in power grids could be reduced by interconnection and the size of the smoothing effect by interconnection depends upon how much tie-line capacity is available to transfer PV power from one grid to the next.

In this work solar radiation fluctuation and reduction of radiation fluctuation due to spatial smoothing effect is analysed for UK sites. The analysis is carried out for different time periods: hourly, half-hourly and minute intervals. The correlation coefficient of the solar radiation field with respect to the distance was studied to define cluster size. Power output from dispersed PV systems was estimated using the cluster model, instead of assuming all identical systems. The output power pattern and standard deviation of output power with respect to the time of the day was studied for different seasons, with regard to the implications for reserve requirements.

5.3 Data Used

To analyse the variation of solar radiation and correlation of solar radiation, the following data were used.

Data Set I:

- Solar radiation data for the year 2001 from a location in the London region, a location in the South West region and a location in the West Midlands region. Hereafter in this thesis, these locations will be identified as London 1, South West 1 and West Midlands 1 respectively.
- Solar radiation data from Newcastle in the North East region for the months June and December 2001. This location will be identified as North East 1.
- Solar radiation data from a second location in the London region for the months June 2001 and December 2001. This location will be identified as London 2.
- Solar radiation data from the South West region for the month of June 2001. This location will be identified as South West 2.

Whenever the analysis was carried out for the whole year, London 1, South West 1 and West Midlands 1 locations data were used. When the analysis was carried out for the June month (summer month), data from six locations were used. When the analysis was carried out for the December month (winter month), data from five locations were used. The analysis that was carried out using the data set I is discussed in sections 5.4 and 5.5.

Data Set II:

At the starting of the analysis only data set I was available. Later for this project, Meteocontrol GmBh, Augsburg, Germany provided hourly horizontal radiation data from 12 different locations in the UK. These data were used to analyse the correlation of solar radiation for all seasons and for each month in detail. The correlation analysis that was carried out using data set II is discussed in section 5.6.

5.4 Tilted Radiation Fluctuation

Measured tilted radiation values from three locations; London 1, South West 1 and West Midlands 1, for the year 2001 were used in this analysis. Firstly hourly tilted radiation fluctuation for London 1 location was calculated. The magnitude of the

fluctuation of hourly tilted radiation values and the number of occurrences were calculated. Positive values indicate an increase in tilted radiation and negative values indicate a decrease in tilted radiation values. The maximum increase and decrease in tilted radiation values was observed as 0.64 kW/m^2 and 0.53 kW/m^2 respectively. Hourly tilted radiation fluctuation for the average of values for the three locations was calculated and compared with the single location (London 1) data and the result is shown in Figure 5-5. It was observed that the maximum tilted fluctuation was reduced to 0.44 kW/m^2 from 0.64 kW/m^2, by aggregating three locations. The fluctuation of tilted radiation behaviour will be different for different time horizons. Therefore the fluctuation of tilted radiation for hourly, half hourly and minute time periods was calculated for the combined data from the three locations. The magnitude of the tilted radiation fluctuation and the percentage of occurrences are shown in Figure 5-6. Occurrences at lower magnitude of fluctuation are increased for the minute time period compared with the hourly time period or half-hourly period. Therefore the standard deviation of the minute solar radiation fluctuation is lower and it is increased with the increase in time interval.

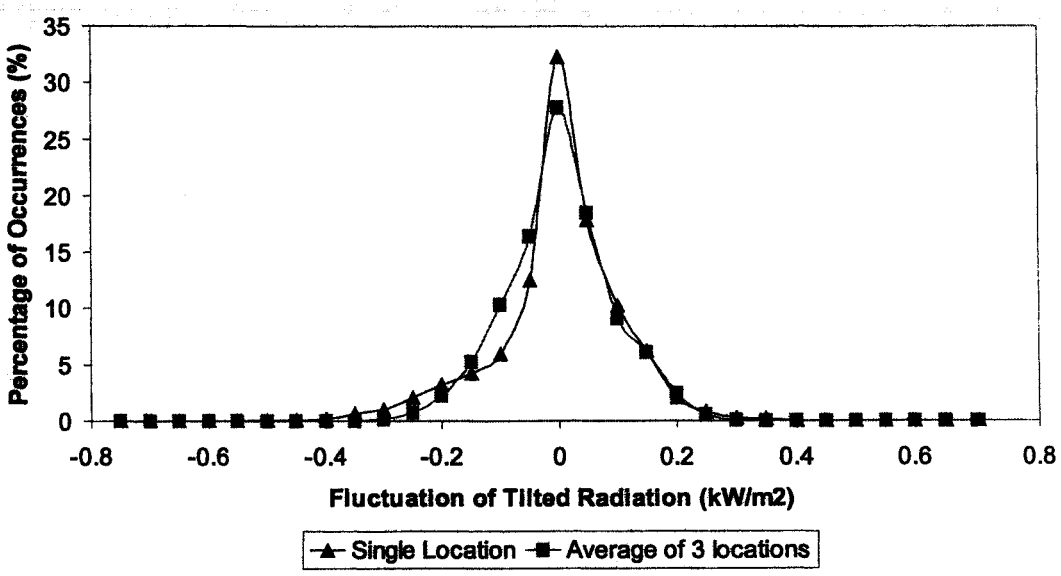

Figure 5-5 Hourly fluctuation of measured tilted radiation for the year 2001 – Single location: London 1, 3 locations: London 1, South West 1 and West Midlands 1)

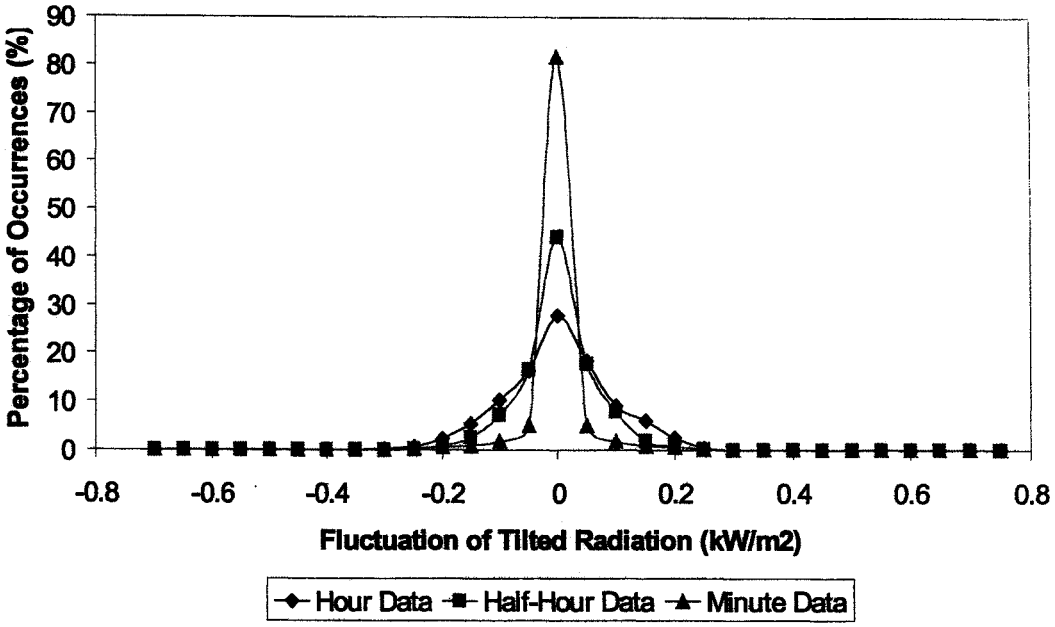

Figure 5-6 Fluctuation of tilted radiation as a function of time interval for the combined data from three locations (London 1, South West 1 and West Midlands 1)

5.5 Correlation Coefficient Analysis I

The above analysis shows that the fluctuation of tilted radiation will be reduced due to the inhomogeneity of solar radiation variation between different locations. In order to analyse this smoothing effect in detail, correlation coefficients of solar radiation values were analysed. The correlation of solar radiation values is used to understand the smoothing effect between locations and to choose the proper size of the cluster. This analysis was carried out for different seasons and for different time horizons.

5.5.1 Summer month

Measured horizontal radiation values for June from six different locations in the UK, London 1, South West 1, West Midlands 1, North East 1, London 2 and South West 2, were used. It was assumed that in all locations, PV arrays are tilted at an angle of 30^0 and south oriented. Measured horizontal radiation was translated to tilted

radiation using selected Hay's and Erbs model. Tilted radiation values between 9:00 to 15:00 for each location were used to calculate correlation coefficient values using the MATLAB software package. The distance of separation between the locations was calculated using latitude and longitude of the locations [9].

The distance of separation between different locations and their correlation coefficient values are tabulated in Table 5-1 and the result is shown in Figure 5-7. The correlation coefficient reduces with respect to the distance of separation between the stations. It can be observed that the correlation coefficient for minute tilted radiation dropped from 1.0 (corresponds to separation of 0 km) to 0.49 for locations separated by a distance of 17 km. For stations separated by between 50 km and 200 km, the correlation coefficient dropped to around 0.2. For stations separated by a distance greater than 300 km, the correlation coefficient dropped to around 0.1.

Similarly, correlation coefficient values with respect to the distance of separation between the locations were calculated for half-hour and hourly tilted radiation values. The correlation coefficient values for the different time horizons are shown in Figure 5-8. As explained before, the variation of solar radiation can be classified into diurnal variation and short term variation. The diurnal variation of solar radiation is fixed due to the sun and its spatial relationship to the earth (explained in section 3.1.1.). The short-term variation of solar radiation is due to the cloud cover movement that is random in nature. For longer time periods, the diurnal variation dominates the change in irradiance level whereas, for shorter time periods, the variation due to the cloud cover movement is influential. Hence for the same distance of separation, the correlation coefficient value is higher for longer time periods.

Table 5-1 Correlation of solar radiation with respect to distance for a summer month

Stations	Distance	Correlation Coefficient
	0	1.00
London 1 - London 2	17	0.49
South West 1 - South West 2	49	0.22
West Midlands 1 - South West 1	80	0.25
West Midlands 1 - South West 2	128	0.22
West Midlands 1 - London 2	133	0.25
London 1 - West Midlands 1	136	0.25
South West 1 - London 2	149	0.22
London 1 - South West 1	160	0.19
South West 2 - London 2	166	0.22
London 1 - South West 2	180	0.18
West Midlands 1 - North East 1	296	0.06
South West 1 - North East 1	360	0.05
London 1 - North East 1	395	0.02
North East 1 - London 2	402	0.05
North East 1 - South West 2	407	0.11

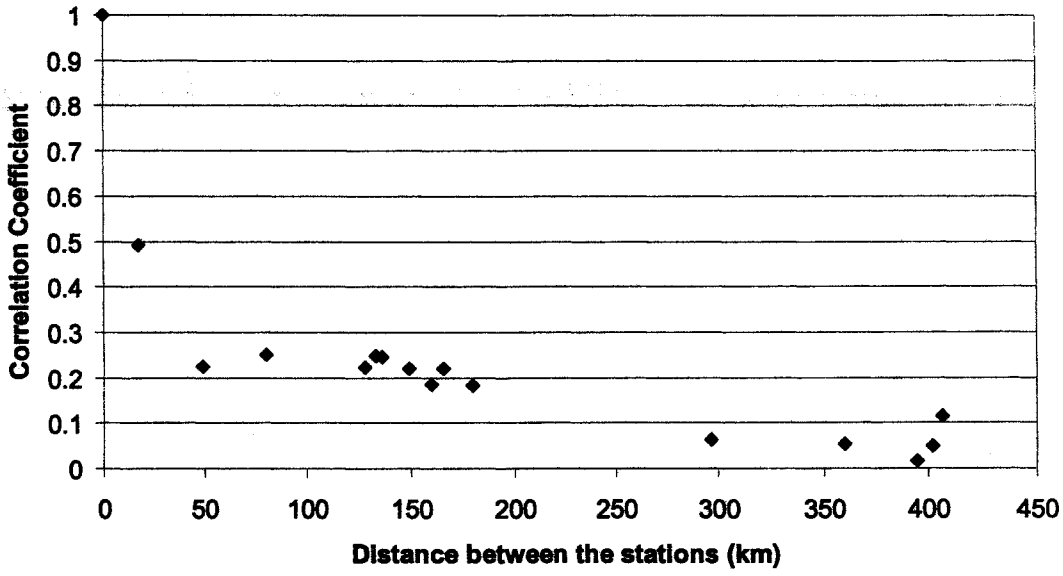

Figure 5-7 Correlation of minute tilted radiation with respect to distance for a summer month

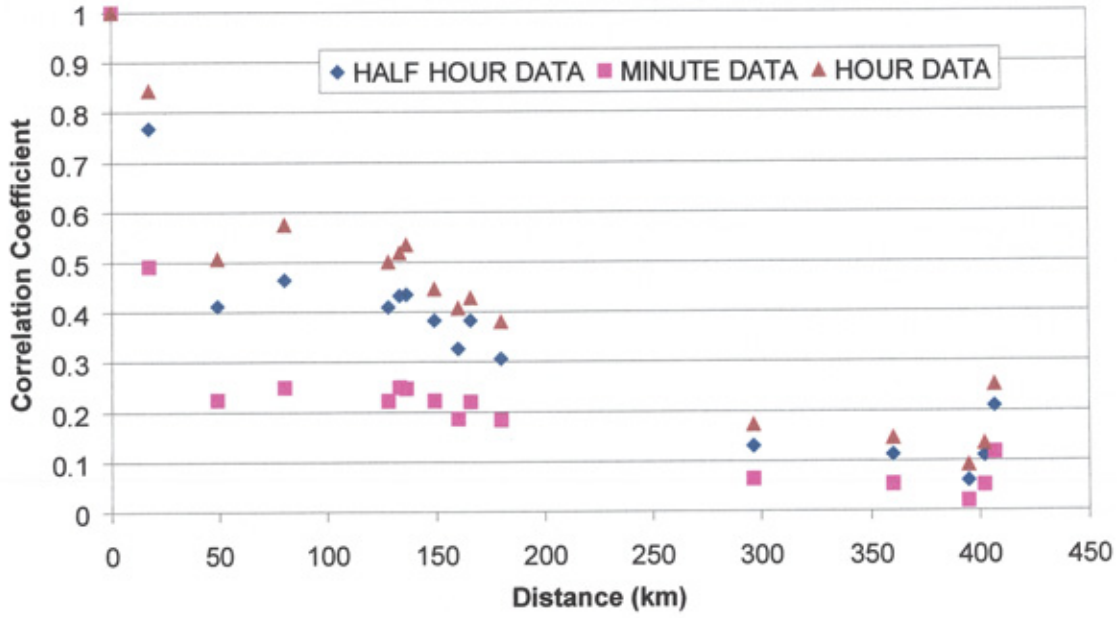

Figure 5-8 Correlation of tilted radiation with respect to distance for a summer month in terms of time interval

Analysis of the correlation coefficient values for three identified regions; below 50 km, 50 – 200 km, 300 – 400 km, was carried out in detail. Hourly correlation coefficient values between the London 1 and London 2 locations, separated by a distance of 17 km, were calculated for each day. Similarly for South West 1 and South West 2 locations, separated by a distance of 49 km and for London 2 and North East 1 locations, separated by a distance of 402 km, hourly correlation coefficients for each day were calculated. Correlation coefficient values for each day for these three cases are shown in Figure 5-9, Figure 5-10 and Figure 5-11.

In all the three cases, there are days with high correlation as well as days with low correlation. For the stations separated by 17 km distance, correlation coefficient values were high for many days and the number of days with correlation coefficient greater than 0.8 is 16. For the second region, it was reduced to 8 days and it was reduced to 2 days for the third region. Similarly for all three regions days with negative correlation values were compared. For stations separated by distance 17 km, there was only one day with negative correlation. For the second region, the number of days with negative correlation was increased to 6 days and it was increased to 12 days for the third region. With the increase in distance of separation between

locations, the number of days with higher correlation was decreased and the number of days with lower correlation was increased.

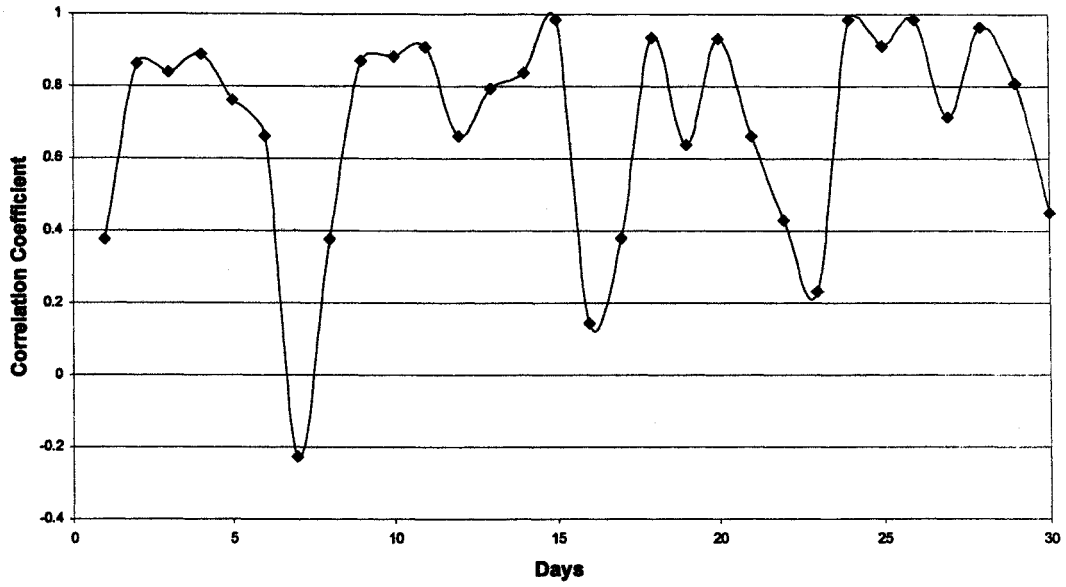

Figure 5-9 Correlation coefficient values for each day in a summer month between the London 1 and London 2 locations, separated by 17 km

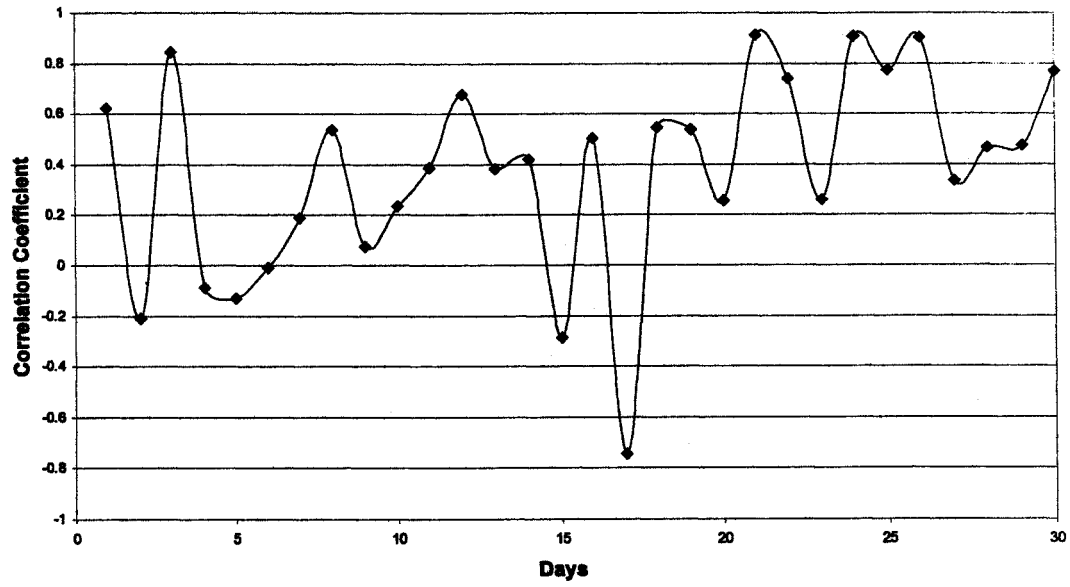

Figure 5-10 Correlation coefficient values for each day in a summer month between the South West 1 and South West 2 locations, separated by a distance of 49 km

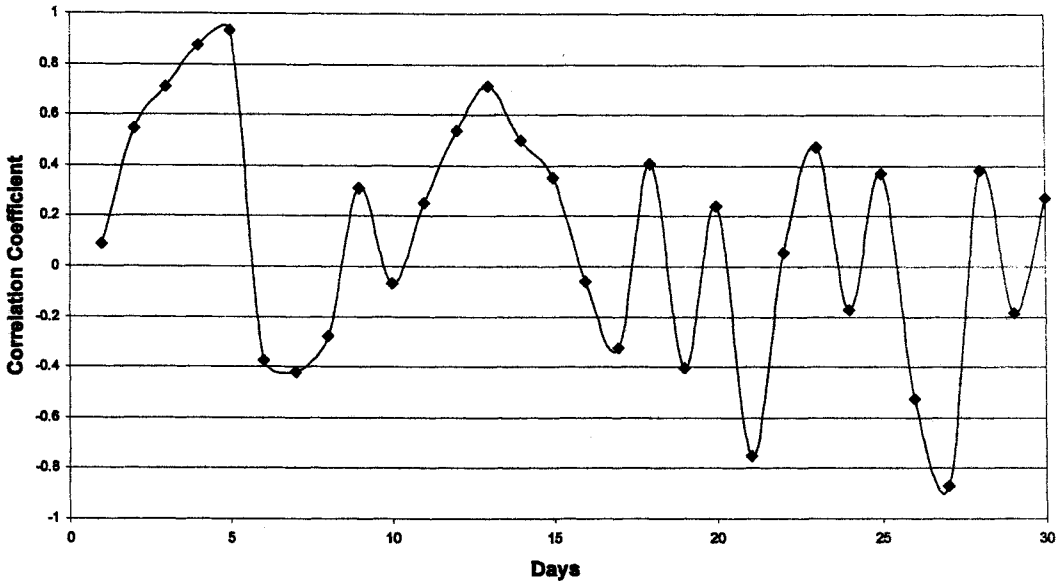

Figure 5-11 Correlation coefficient values for each day in a summer month between the London 2 and North East 1 locations, separated by a distance of 402 km

Even though the number of days with high correlation is lower for the second and third regions, correlation coefficient values on some days are high, greater than 0.8. Therefore further analysis was carried out for these regions. For the days with higher correlation and lower correlations, tilted radiation values were analysed. Tilted radiation values for the South West 1 and South West 2 locations were compared, for the days with high correlation values (24 to 26th), and are shown in Figure 5-12. Similarly tilted radiation values for the day with low correlation (7th) were compared as shown in Figure 5-13. For the days with high correlation, tilted radiation values were high and variation of tilted radiation is small and gradual. For the day with low correlation it can be noticed that in the morning time, when there was increase in tilted radiation for South West 2, the tilted radiation value decreased for the South West 1 location. Similarly during the afternoon when there was a decrease in tilted radiation for the South West 1 location, there was an increase in tilted radiation value for South West 2.

Similarly between the London 2 and North East 1 locations, tilted radiation values were compared for the days with high correlation (4th) and low correlation value (26th). The results of the comparison are shown in Figure 5-14 and Figure 5-15. It

can be observed that for the day with high correlation, tilted radiation values for North East 1 were higher than for the London 2 location. However, the shape of the curve is almost the same. From these results it was also observed that when the correlation was high, changes in tilted radiation values were small and gradual. When the correlation is low, the magnitude of the change in tilted radiation is high.

From this analysis, the following observations were made:

- For the locations separated by distance 17 km, a high correlation is obtained.
- For the locations separated by distance 50 – 200 km, smaller but still significant correlation values were obtained. Analysis of the correlation for each day in this region shows that high correlation values were obtained for stable days i.e., days with small and gradual variation in tilted radiation values.
- For the locations separated by distance over 300 km, correlation is low indicating that the weather conditions vary substantially across this range.
- By combining different locations with low correlation values, the fluctuation of tilted radiation will be reduced.

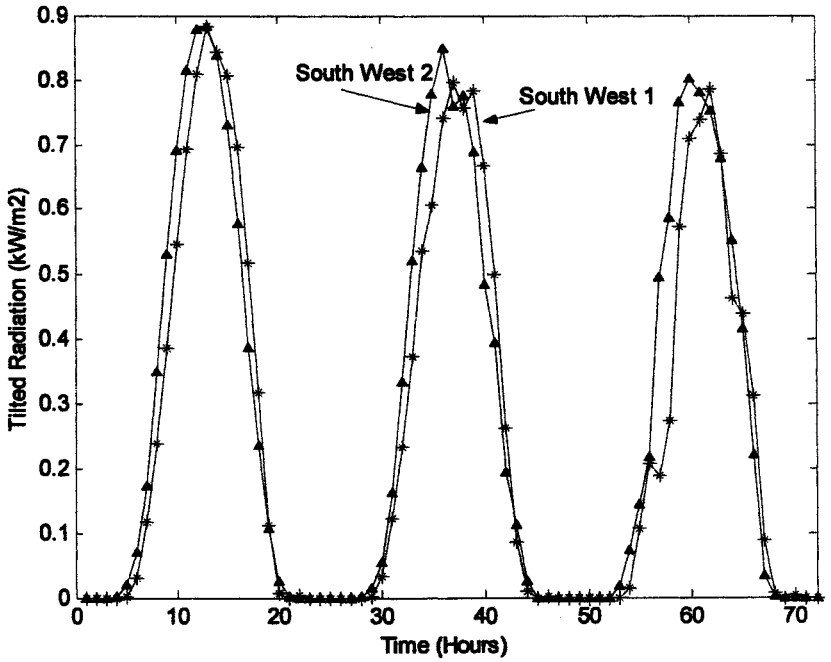

Figure 5-12 Comparison of tilted radiation values, between the South West 2 and South West 1 locations, for a day with high correlation in a summer month

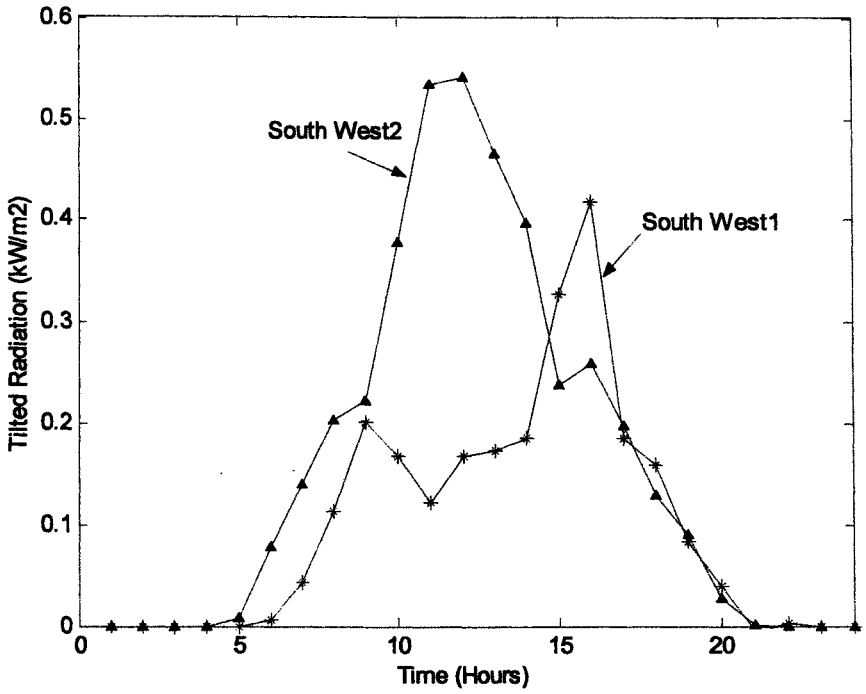

Figure 5-13 Comparison of tilted radiation values for a low correlation day in a summer between the South West 2 and South West 1 locations

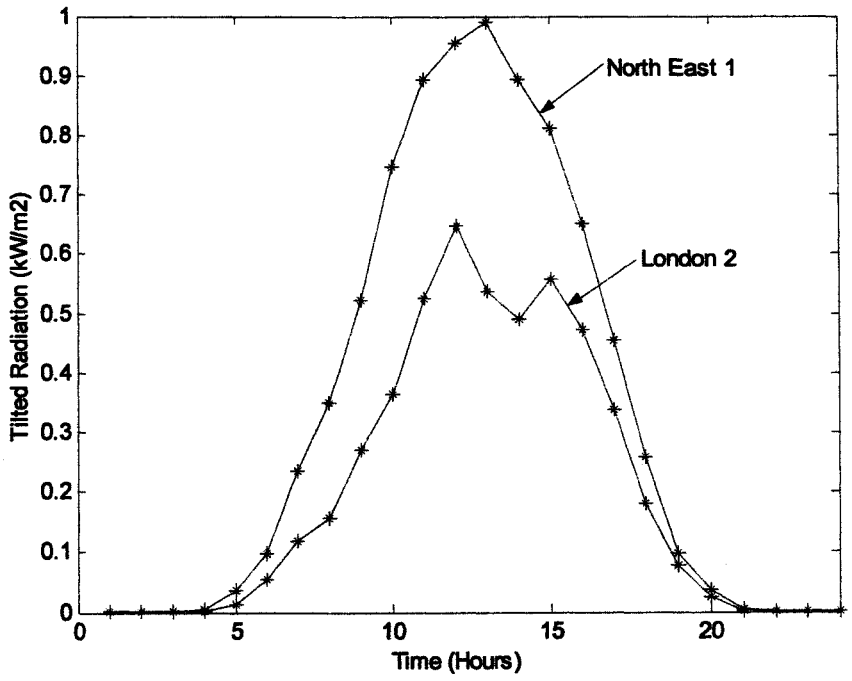

Figure 5-14 Comparison of tilted radiation values for a high correlated day in a summer month, between the North East 1 and London 2 locations

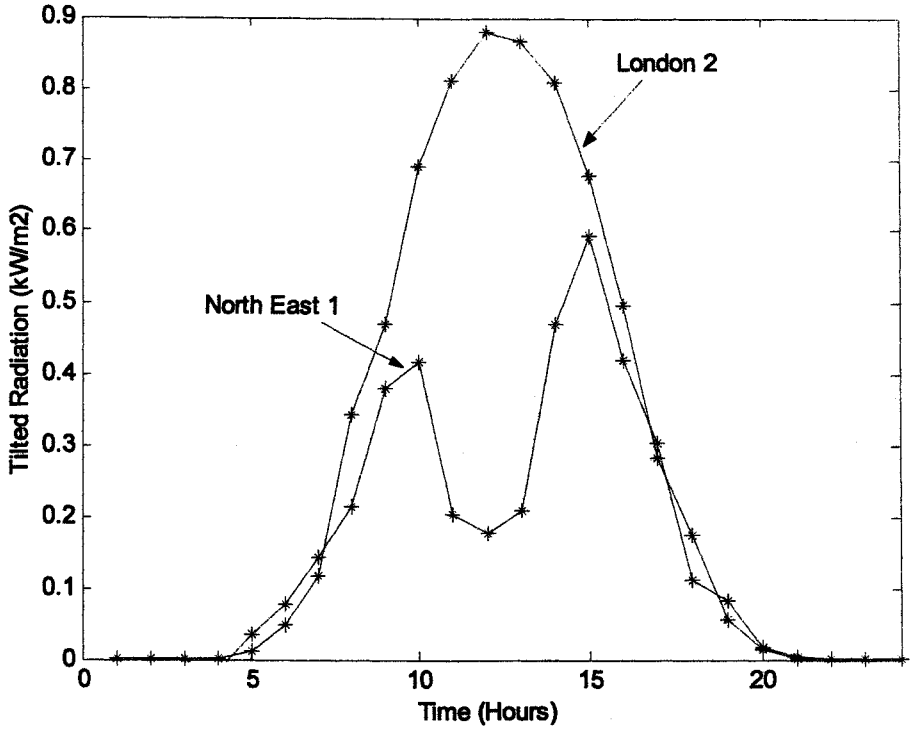

Figure 5-15 Comparison of tilted radiation values for a low correlation day in a summer month, between the North East 1 and London 2 locations

5.5.2 Winter month

Correlation coefficient analysis was carried out for a winter month (December), using measured horizontal radiation data from five[7] locations in the UK. Again, it was assumed that the PV arrays are tilted at an angle of 30^0 and south oriented. Tilted radiation values were calculated from measured horizontal radiation, using the selected Hay's model. Correlation coefficient values with respect to the distance of separation between locations were calculated for different time horizons and are shown in Figure 5-16. The correlation of minute tilted radiation values between different locations was compared with the summer month results as shown in Figure 5-17. For the same distance of separation, the correlation coefficient values were higher for the winter month compared with the summer month. Similar to the summer month, the correlation coefficient values were higher for longer time

[7] There are no data for South West 2 location.

periods, which is due to the influence of the sun position. The decrease in correlation coefficient values with respect to distance is similar to the summer month.

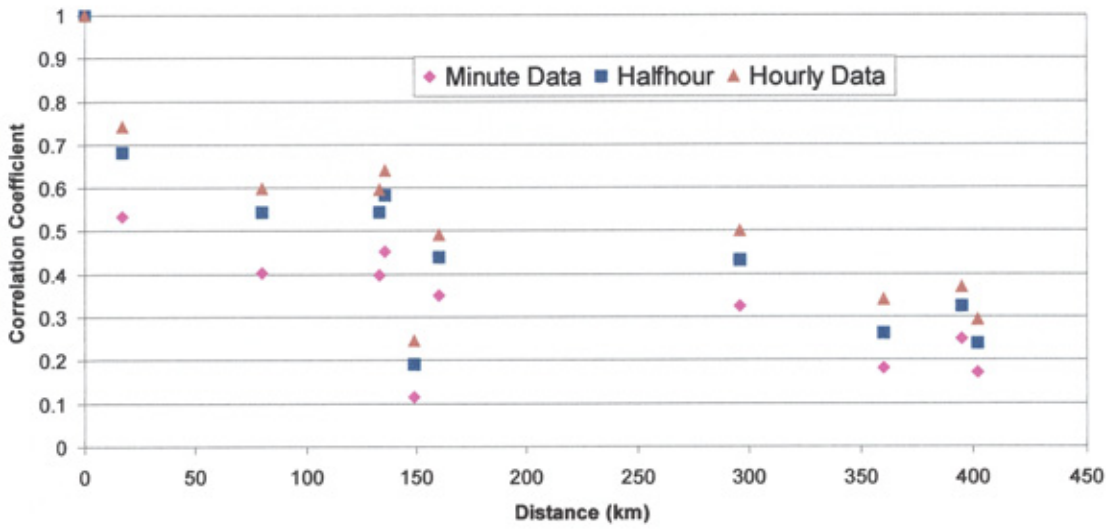

Figure 5-16 Correlation coefficient values with respect to separation between locations for a winter month

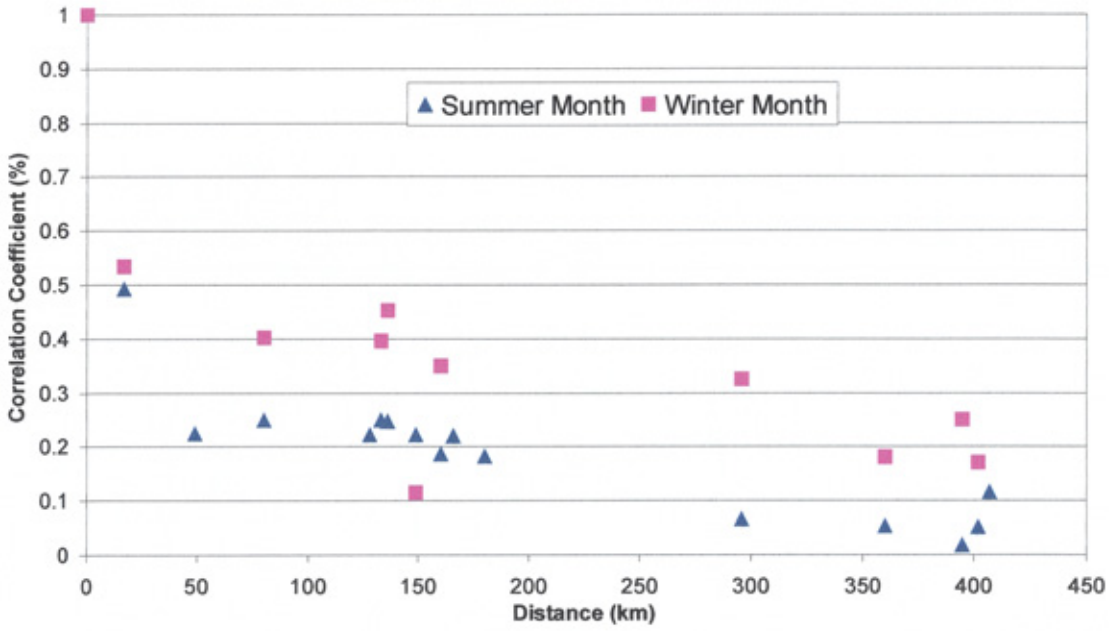

Figure 5-17 Comparison of correlation coefficient values between a summer month and a winter month

Similar to the summer month analysis, the correlation coefficient was further analysed for each day, for the three regions identified. The correlation coefficient values for each day were calculated for three different distances of separation between stations, 17 km, 80 km and 402 km. Correlation coefficient values for each day for these three cases are shown in Figure 5-18, Figure 5-19 and Figure 5-20.

Correlation coefficient values were higher for most of the days when the distance of separation is 17 km. In the winter season there are no days with correlation less than 0.5. In the summer season there are days with correlation less than 0.2, for the same distance of separation. When there was an increase in distance, the number of days with high correlation is decreased. It can be observed that in winter months there are no days with negative correlation values, even for locations separated by a distance 402 km. Since there were a higher number of stable days with high correlation in winter months, the monthly correlation values were higher compared with the summer month.

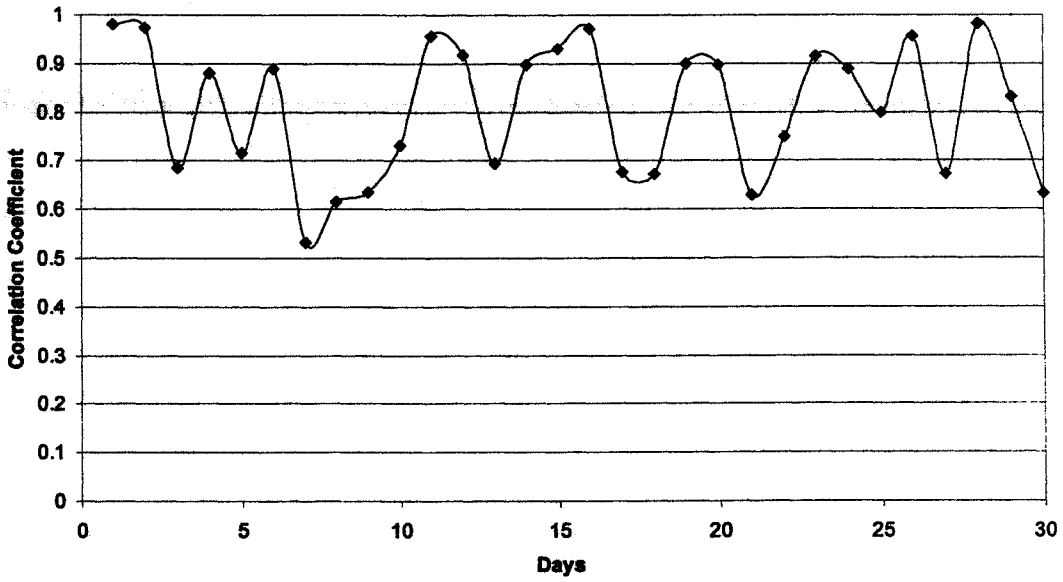

Figure 5-18 Correlation coefficient values for each day in a winter month, between the London 1 and London 2 locations

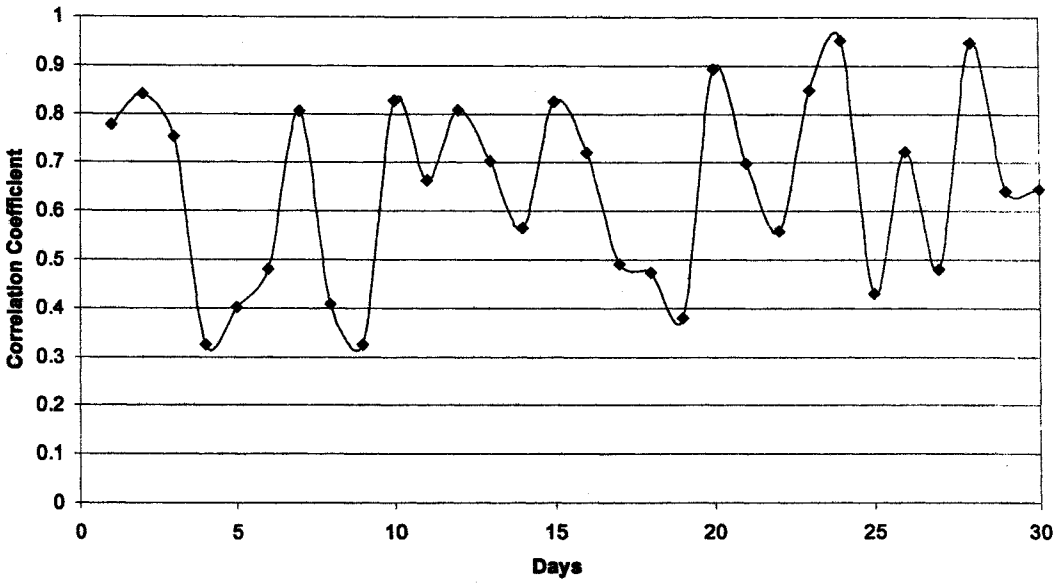

Figure 5-19 Correlation coefficient values for each day in a winter month, between the West Midlands 1 and South West 1 locations

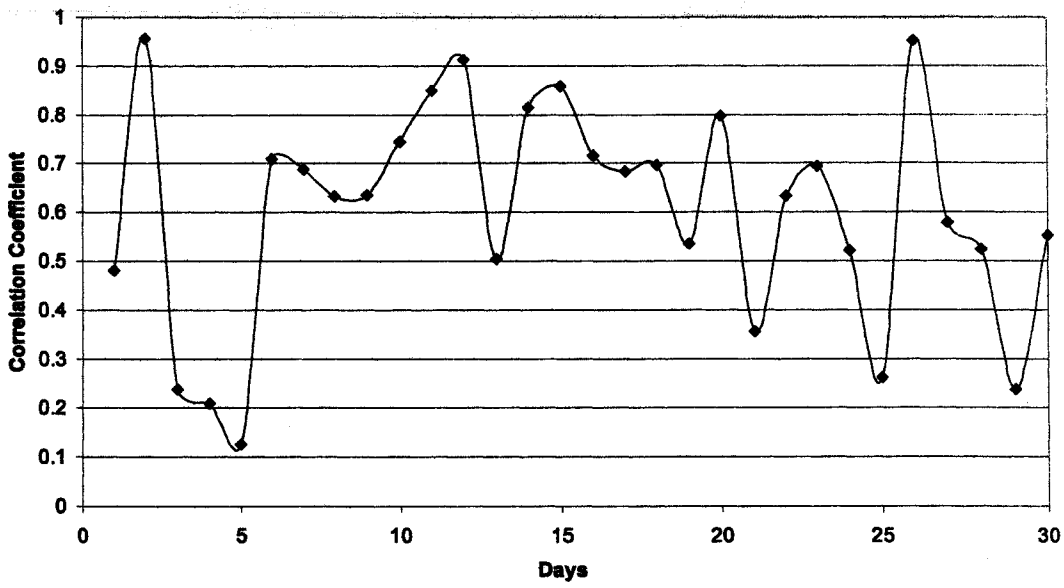

Figure 5-20 Correlation coefficient values for each day in a winter month, between the North East 1 and London 2 locations

Even though the number of days with high correlation is decreased with distance, correlation values are substantial for these days. Hence for the days with either high correlation or very low correlation values, tilted radiation values were compared, for the regions with distance of separation 50 – 200 km and 300 – 402 km. For the locations of West Midlands 1 and South West 1, separated by the distance of 80 km, for the day with high correlation (24th) and for the day with lower correlation (4th), the tilted radiation values were compared and shown in Figure 5-21 and Figure 5-22. Similarly for the North East 1 and London 2 locations, tilted radiation values were compared, for the days with high correlation (26th) and days with low correlation (3rd) as shown in Figure 5-23 and Figure 5-24. Similar to the summer month, days with high correlation have very stable weather conditions. When the days had variable weather conditions, the correlation values were lower.

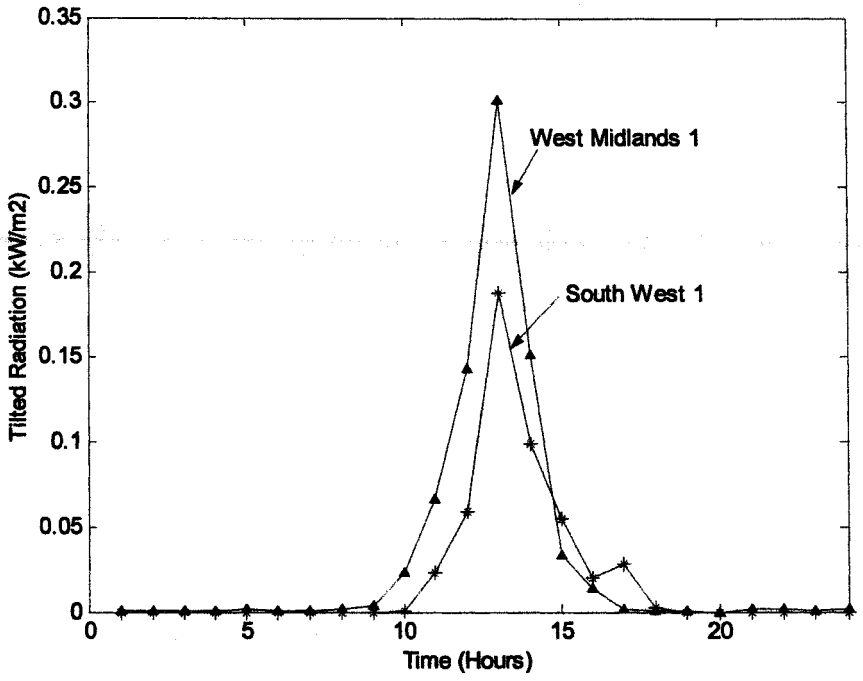

Figure 5-21 Comparison of tilted radiation values for a highly correlated day in a winter month, between the West Midlands 1 and South West 1 locations

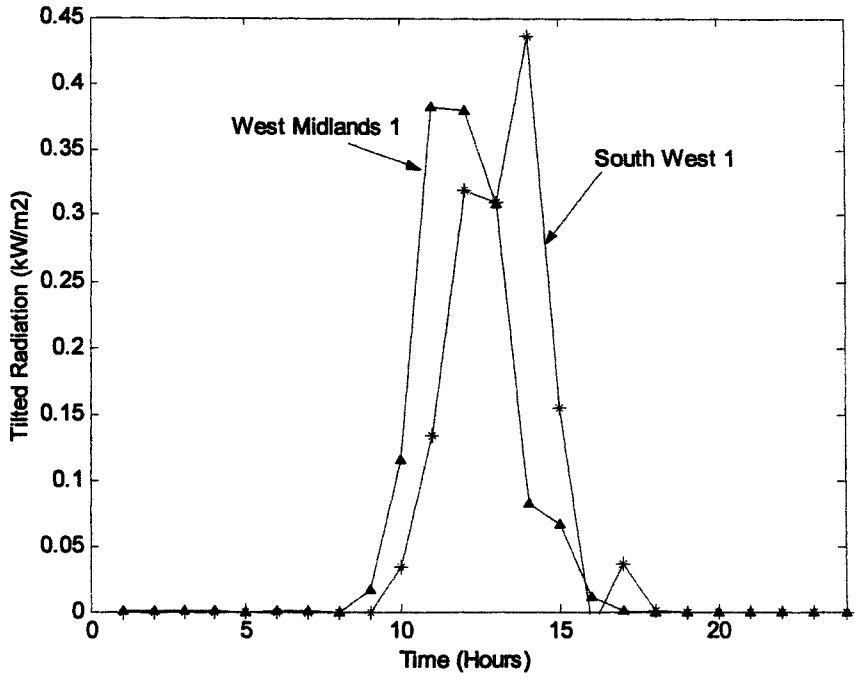

Figure 5-22 Comparison of tilted radiation values for a low correlated day, between the West Midlands 1 and South West 1 locations

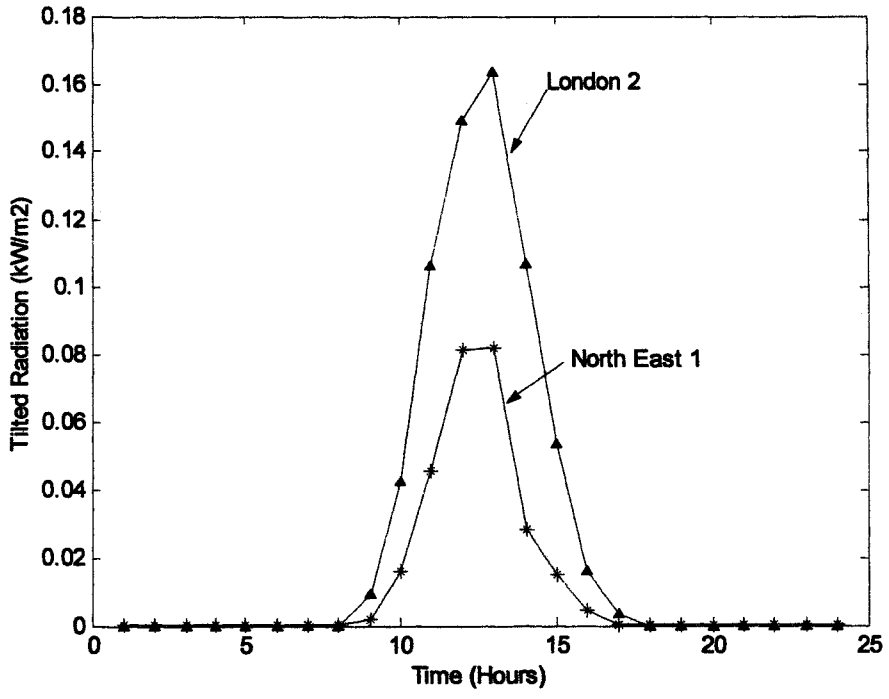

Figure 5-23 Comparison of tilted radiation values for a highly correlated day in a winter month, between the North East 1 and London 2 locations

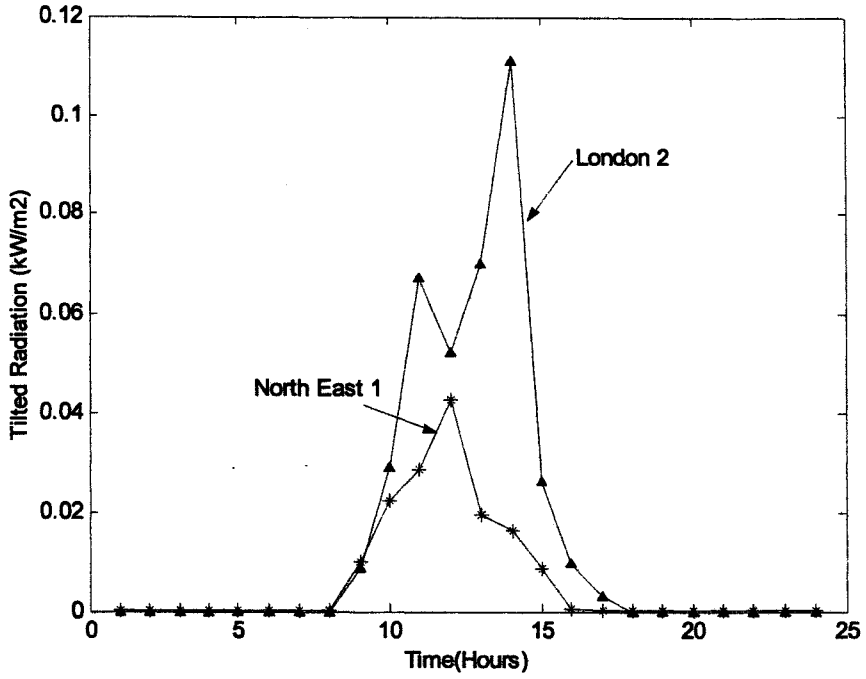

Figure 5-24 Comparison of tilted radiation values for a low correlated day in a winter month, between the North East 1 and London 2 locations

5.6 Correlation Coefficient Analysis II

In the previous analysis the correlation of solar radiation with the distance of separation was analysed for the summer and winter seasons using June and December radiation values from 6 different locations in the UK (Data set I). Using the data set I it was not possible to analyse the correlation coefficient values in detail for distances of separation below 50 km and between 200 and 250 km. It was also not possible to analyse the correlation coefficient values for different seasons. Hence to analyse the correlation coefficient of solar radiation values in detail the data set II were used. The data set II consists of hourly horizontal radiation values for October 2003 to September 2004 from 12 different UK locations, derived from satellite measurements, provided by Meteocontrol GmBh, Augsberg, Germany. These data were used to study the correlation of solar radiation values for each season and each month in detail. It was not possible to combine both data set I and data set II, to analyse the correlation coefficient of solar radiation, because these data sets

correspond to different years. Station name, latitude and longitude of 12 locations are given in Table 5-2. There are 66 different possible combinations from the 12 locations and the corresponding distances of separation (in km) are given in Table 5-3.

Table 5-2 Station name, latitude and longitude of selected 12 UK locations

Station Number	Station Name	Latitude	Longitude
1	Benson	51.37	1.05
2	Pembrey Sands	51.43	4.22
3	Hereford/Credenhill	52.05	2.48
4	Madley	52.02	2.51
5	Barbourne	52.12	2.13
6	Great Malvern	52.07	2.18
7	Skipton	53.58	2.02
8	Bingley	53.49	1.52
9	Emley Moor	53.37	1.4
10	Leeds	53.48	1.33
11	Leeming	54.18	1.32
12	Newcastle	54.59	1.36

Table 5-3 Distance of separation (in km) between the selected 12 locations

	Station 1	Station 2	Station 3	Station 4	Station 5	Station 6	Station 7	Station 8	Station 9	Station 10	Station 11	Station 12
Station 1	0.0	220.2	124.3	124.0	111.9	110.2	254.6	238.1	223.9	235.6	359.0	313.3
Station 2		0.0	138.4	135.0	163.2	157.6	281.9	293.4	288.6	300.8	400.5	363.0
Station 3			0.0	3.9	25.2	20.7	173.1	172.8	164.0	177.0	292.4	249.4
Station 4				0.0	28.3	23.3	176.8	176.7	167.9	180.9	296.1	253.2
Station 5					0.0	6.5	162.7	157.9	147.6	160.7	279.7	235.6
Station 6						0.0	168.4	164.2	154.0	167.1	285.8	241.8
Station 7							0.0	34.6	47.3	47.0	120.4	81.1
Station 8								0.0	15.5	12.6	122.9	77.9
Station 9									0.0	13.1	135.8	90.3
Station 10										0.0	123.6	77.9
Station 11											0.0	45.7
Station 12												0.0

5.6.1 Seasonal analysis

Measured hourly horizontal radiation values were translated to hourly tilted radiation values assuming that the PV arrays are tilted at an angle of 30^0 and south oriented for each location. Hourly tilted radiation values between 09:00 and 15:00 for each location were used to calculate correlation coefficient values. Hourly tilted radiation

values for June, July and August were used to calculate correlation values for the summer season. The correlation coefficient of tilted radiation values with the distance of separation between locations was calculated and is shown in Figure 5-25.

From these results it is possible to study the correlation coefficient of solar radiation values in detail for the distance of separation up to 400 km. It can be observed that the correlation dropped from 1 to 0.7 for locations separated by a distance of 100 km. The correlation value dropped to 0.4 for locations separated by a distance of 250 km. For locations separated by a distance greater than 250 km, the correlation values were low. Since 67 points are available, it was possible to obtain the suitable curve and function that fits the change in correlation coefficient with the distance of separation. In this case the Excel spreadsheet was used for curve fitting. The exponential curve and the corresponding function are indicated in Figure 5-25. The exponential function is in the form of $y = \exp(-a*x)$, where

y is the correlation coefficient

x is the distance of separation

a is the constant

By this function it is possible to study the correlation coefficient for different distances. As an example, the correlation coefficient was extrapolated up to 800 km and the result is shown in Figure 5-25.

Similarly the correlation coefficient values are calculated for spring (March, April and May), autumn (September, October and November) and winter seasons (December, January & February). Results from four seasons were compared as shown in Figure 5-26. The exponential curve and the corresponding function for each season are also shown in Figure 5-26. Similar to the previous analysis in this case also it was observed that for the same distance of separation, the correlation coefficient values were higher for the winter season compared with the summer season. The correlation coefficient values for spring and autumn seasons were higher compared with the summer season and lower compared with the winter season. The constant "a" in the exponential function was lower for the winter season and higher for summer season.

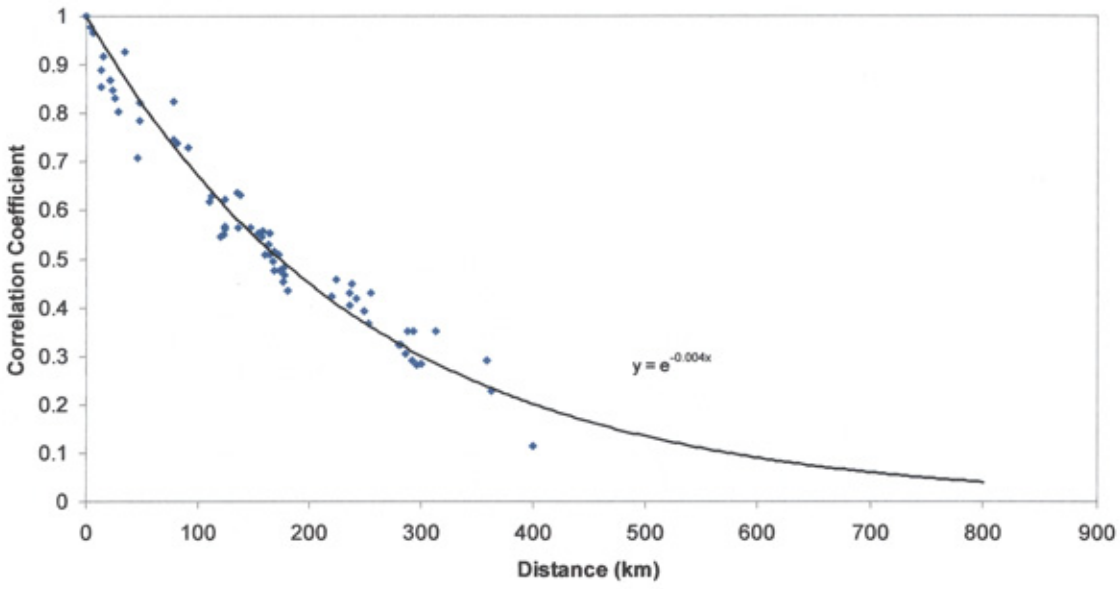

Figure 5-25 Correlation coefficient with the distance of separation for the summer season (values calculated for the distances up to 400 km and extrapolated up up to the distance of 800 km)

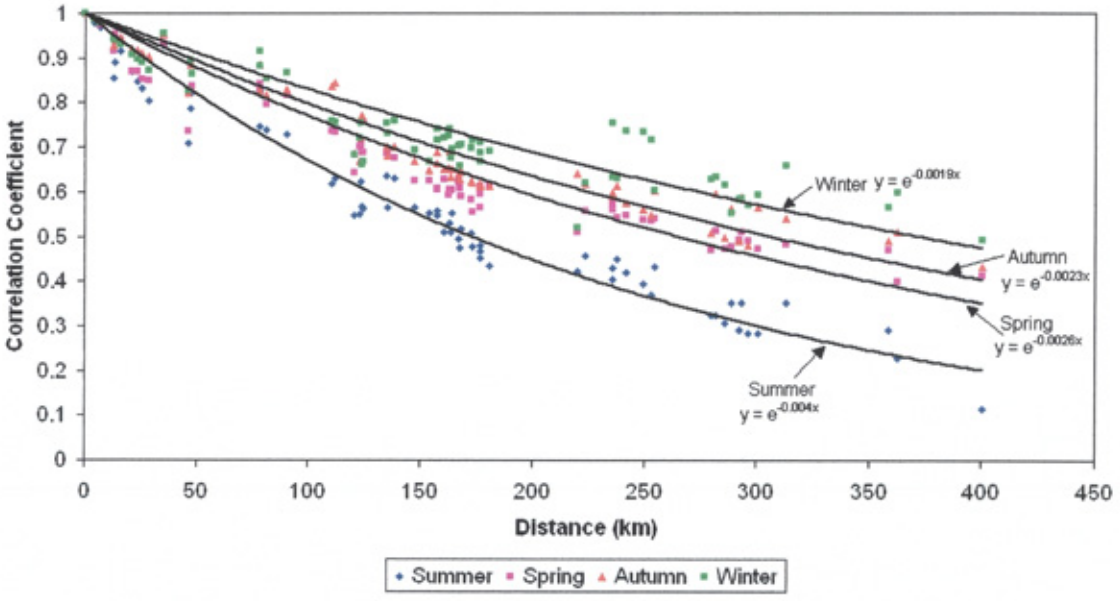

Figure 5-26 Correlation coefficient values with the distance of separation, for all seasons

5.6.2 Monthly analysis

In order to study the correlation coefficient values and the exponential function in detail, the analysis was carried out for each month. Similar to the seasonal analysis, tilted radiation values between 09:00 and 15:00 were used to calculate the correlation coefficient values for each month. The correlation coefficient values for each month

with the distance of separation are shown in Figure 5-27. For clarity, it was decided to plot the correlation values for four months in each graph. For the locations separated by a distance of 400 km, the correlation value was slightly negative for July and October (-0.020 and –0.023 respectively). In order to obtain the exponential function this point was neglected[8]. Hence the correlation values for July and October were plotted in a separate graph.

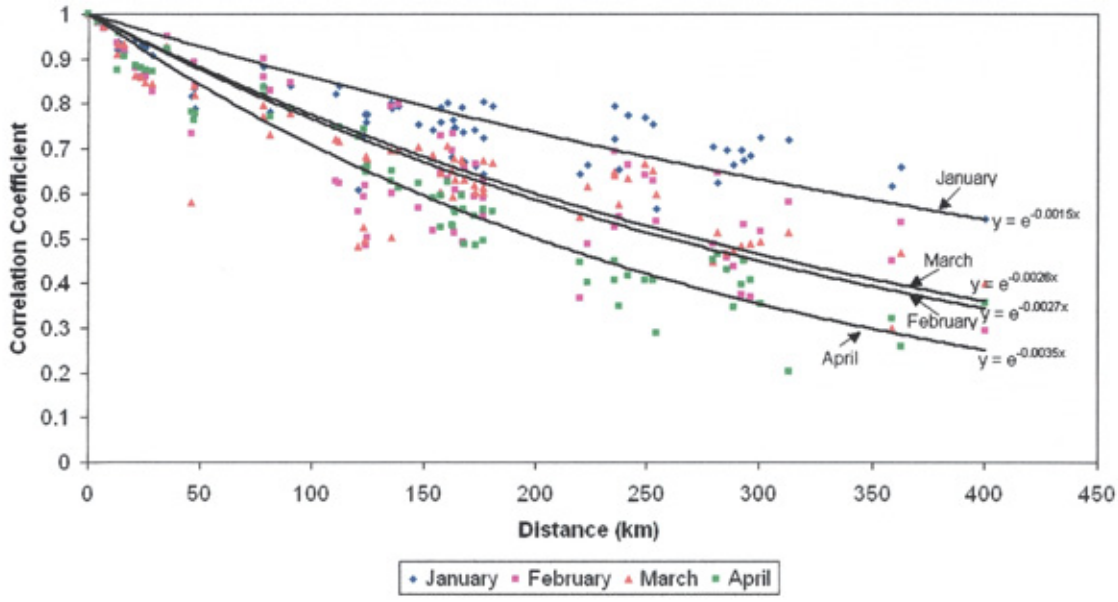

a) Correlation coefficient with the distance of separation for January, February, March and April

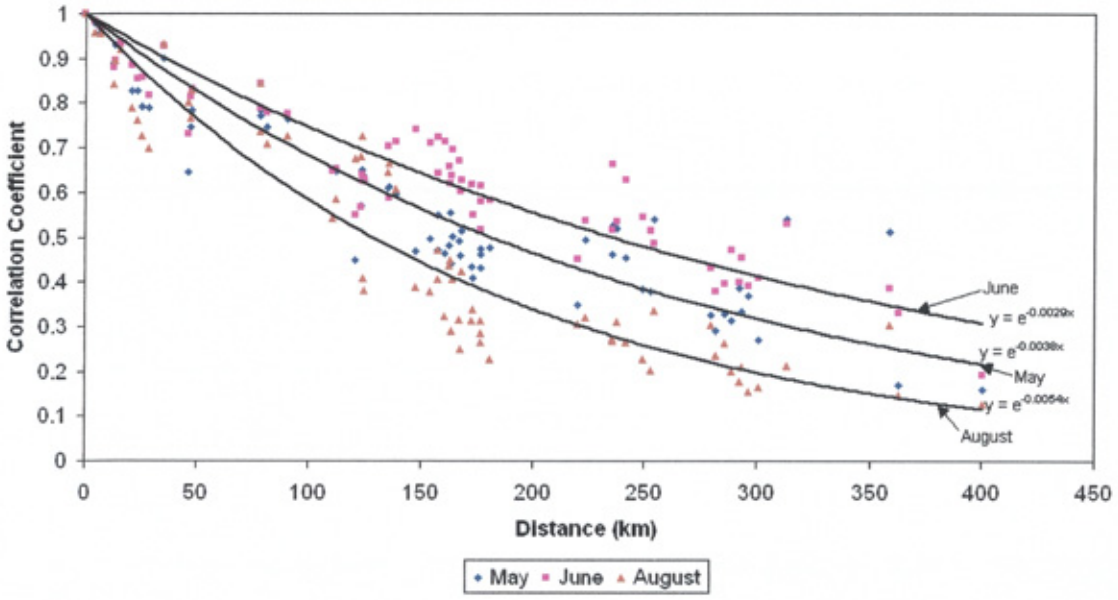

b) Correlation coefficient with the distance of separation for May, June and August

[8] If many years' data are used to calculate the correlation values, this problem may not occur.

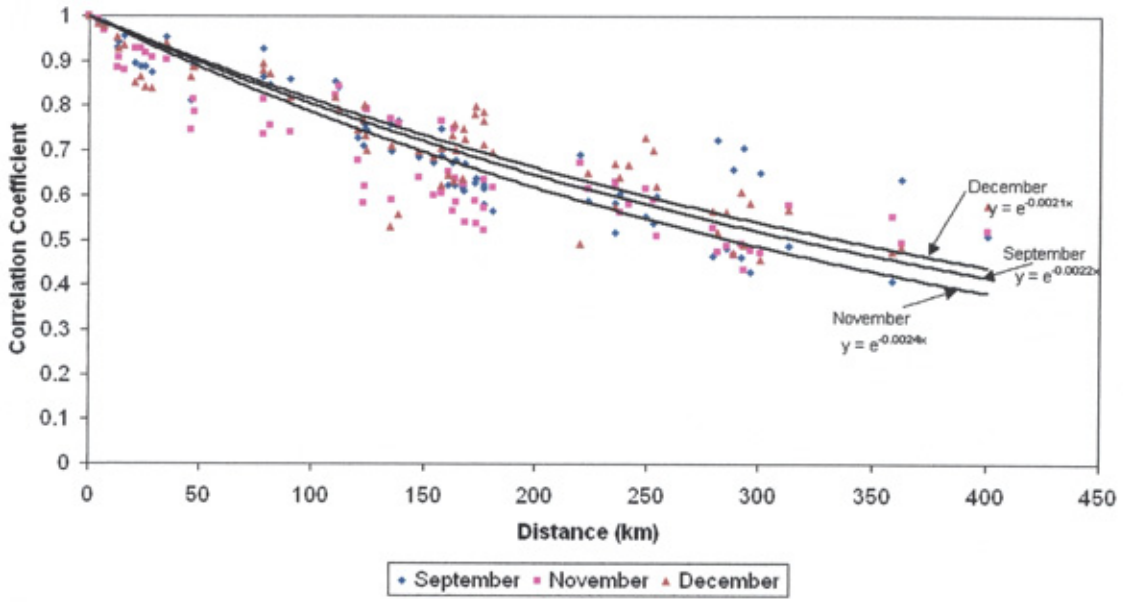

c) Correlation coefficient with the distance of separation for September, November and December

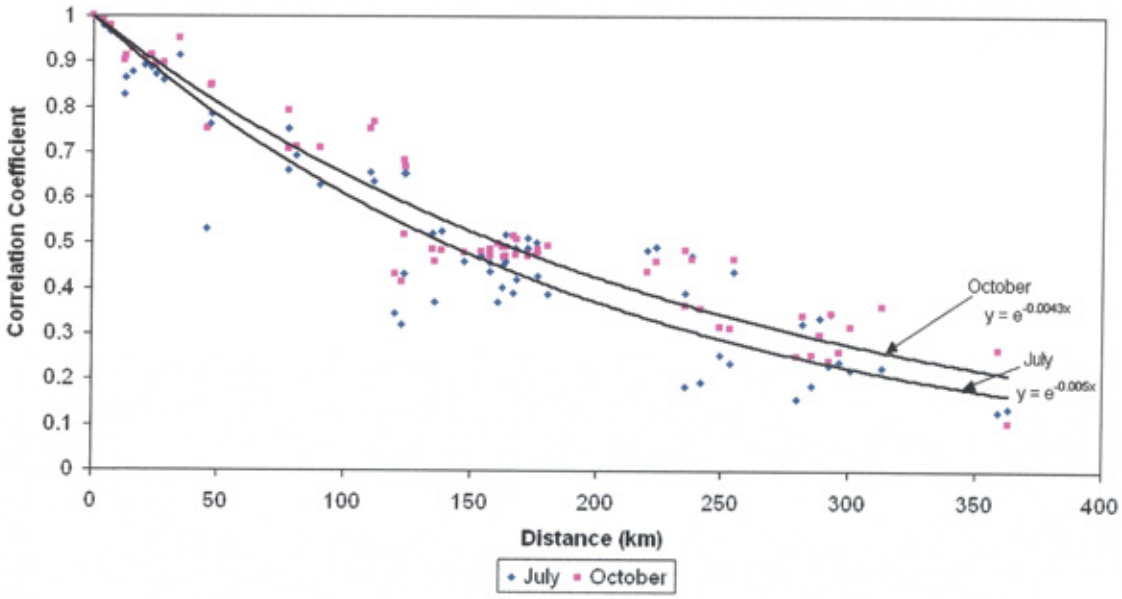

d) Correlation coefficient with the distance of separation for July and October

Figure 5-27 Correlation coefficient with the distance of separation for each month

In general, for the same distance of separation, the correlation coefficient values were lower for summer months (July & August) and higher in winter months (January & December). The correlation coefficient values in spring months (April & May) were higher than summer months and lower than autumn months (September

& November). The correlation coefficient values for autumn months (September & November) were lower than winter months (January & December). However the correlation coefficient values for June (Summer season) were greater than April and May (Spring season). Similarly the correlation coefficient values for March (Spring season) were greater than February (Winter season).

In order to analyse these results further, for the same distance of separation, the correlation coefficient values for each day was calculated for one month in each season (January, April, August, and September). Hourly correlation coefficient values between the Great Malvern and Emley Moor locations, separated by a distance of 154 km, were calculated for each day and compared as shown in Figure 5-28. It can be observed that for January the number of days with correlation coefficient values greater than 0.6 is 27 days whereas it is 8, 6 and 15 days for April, August and September respectively. There are no days with negative correlation in January whereas the number of days with the negative correlation is 8, 10 and 6 days for April, August and September.

For a day with higher correlation coefficient in August, hourly tilted radiation values were compared as shown in Figure 5-29 (a). Similarly for days with lower correlation, hourly tilted radiation values were compared as shown in Figure 5-29 (b&c). These results also indicate that the correlation values were high for the clear and stable days. When the days had variable weather condition, the correlation coefficient values were low. These results also indicate that the number of stable days was higher in January and lower for August. Hence for the same distance of separation, the correlation coefficient values were higher in January and lower in August.

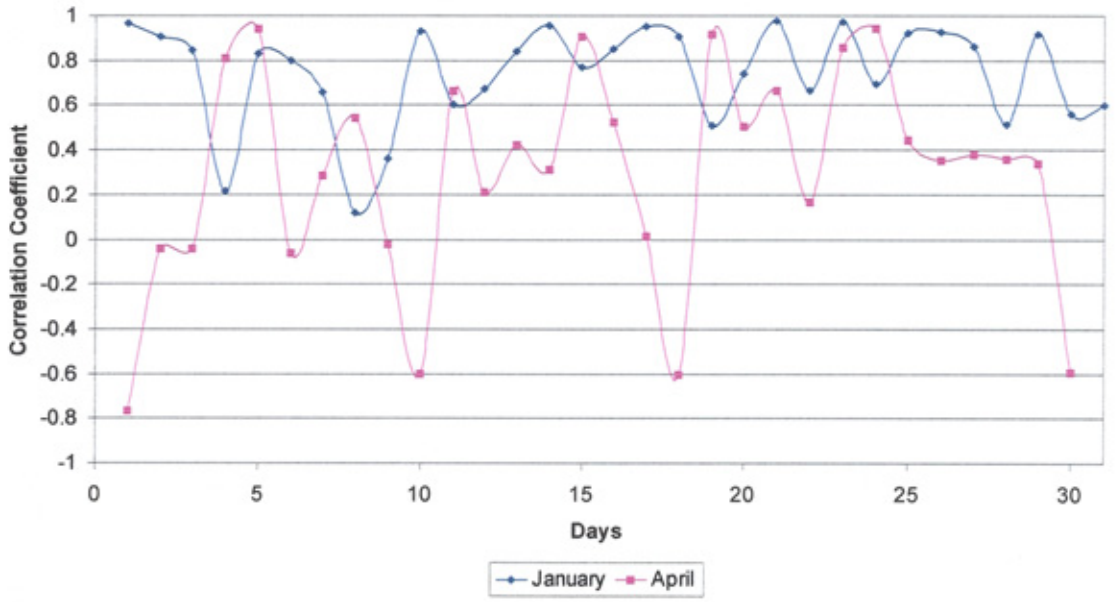

a) For January and April

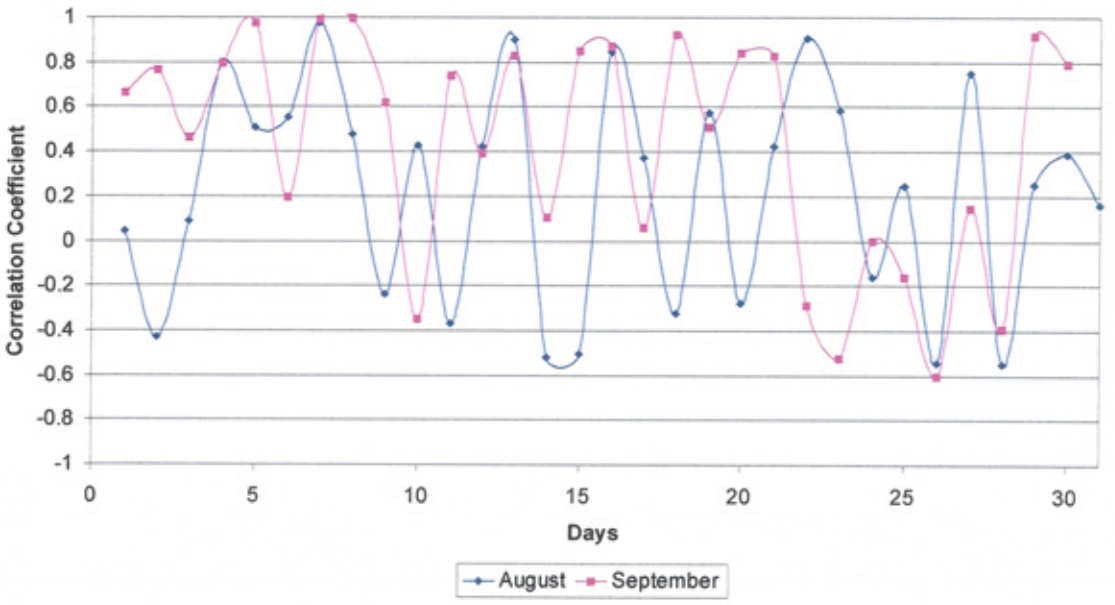

b) For August and September

Figure 5-28 Correlation coefficient values for each day, between the Great Malvern and Emley moor locations, separated by a distance of 154 km

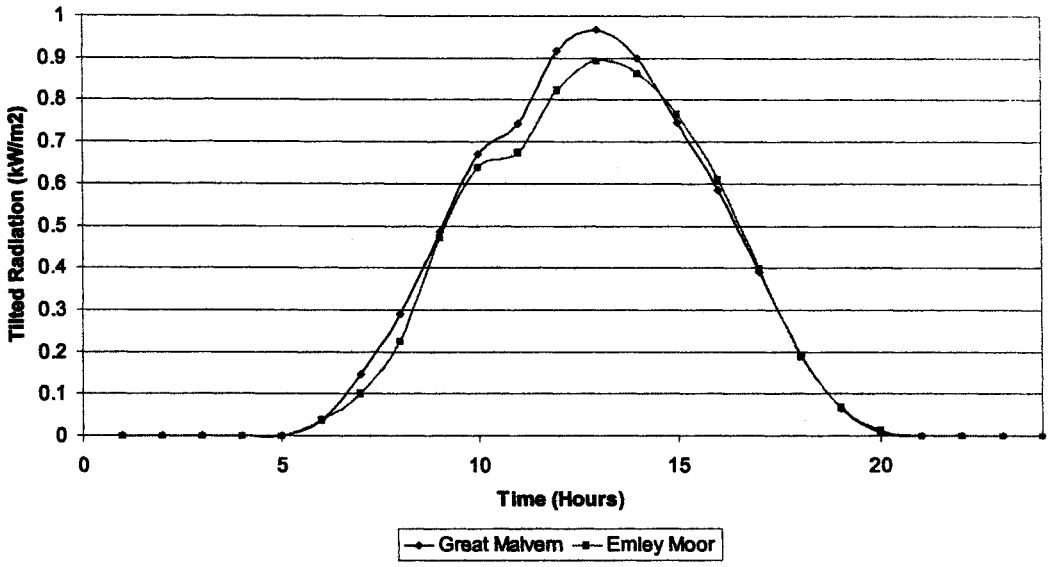

a) For a day with high correlation in August

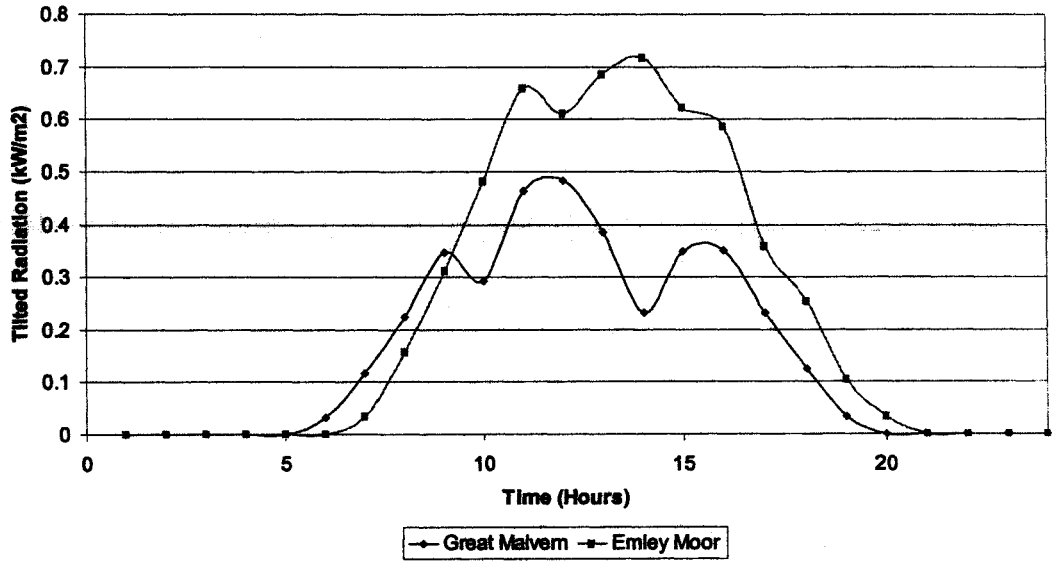

b) For a day with low correlation in August

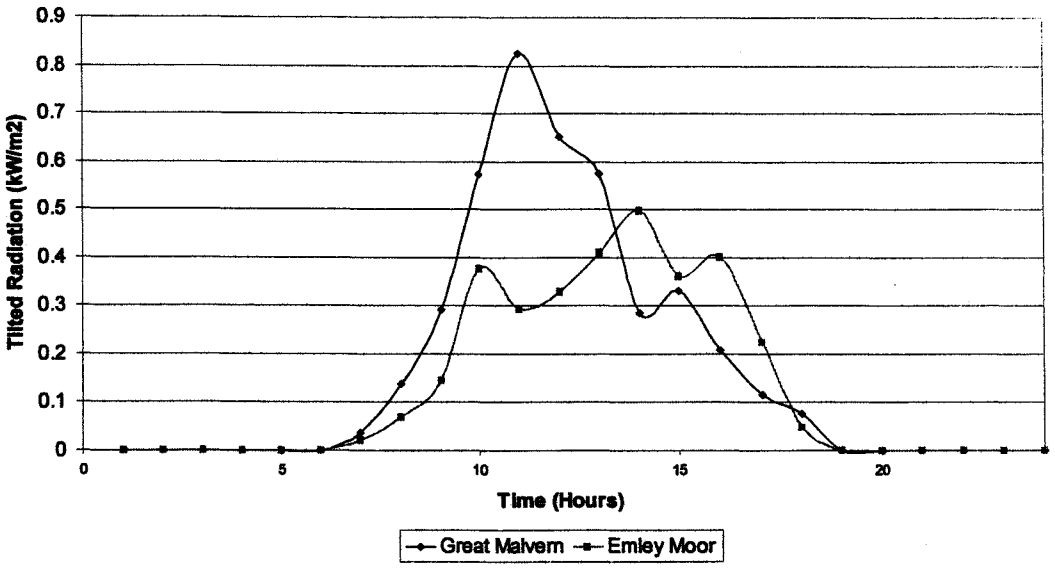

c) For a day with low correlation in April

Figure 5-29 Comparison of tilted radiation between the Great Malvern and Emley moor locations

As explained before, the correlation coefficient values for June (summer season) were higher than April and May (Spring season). Hourly correlation coefficient values between the Great Malvern and Emley Moor locations, separated by a distance of 154 km, were calculated for each day in April, May and June and are shown in Figure 5-30. It can be observed that the number of days with correlation coefficient greater than 0.8 was higher for June compared with April and May. For the days with higher and lower correlation in June, the tilted radiation values were compared as shown in Figure 5-31. These results also indicate that the correlation values were high for the clear and stable days. These results indicate that the number of stable days is higher in June compared with April and May. Hence for the same distance of separation, the correlation coefficient value for June (summer month) was higher than April and May (Spring Months).

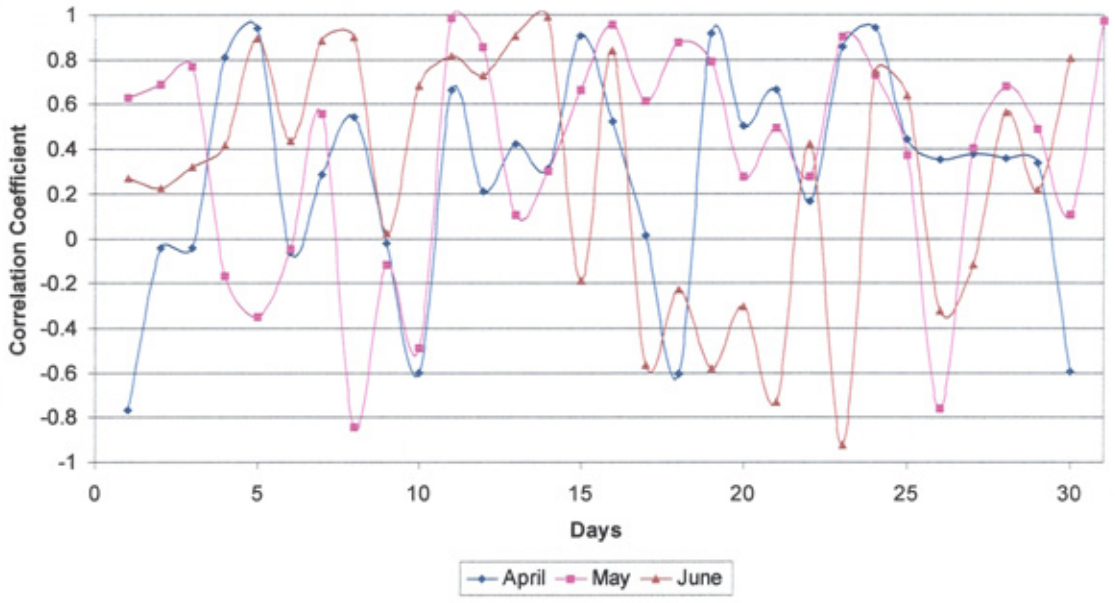

Figure 5-30 Correlation coefficient values for each day, between Great Malvern and Emley moor locations, separated by a distance of 154 km

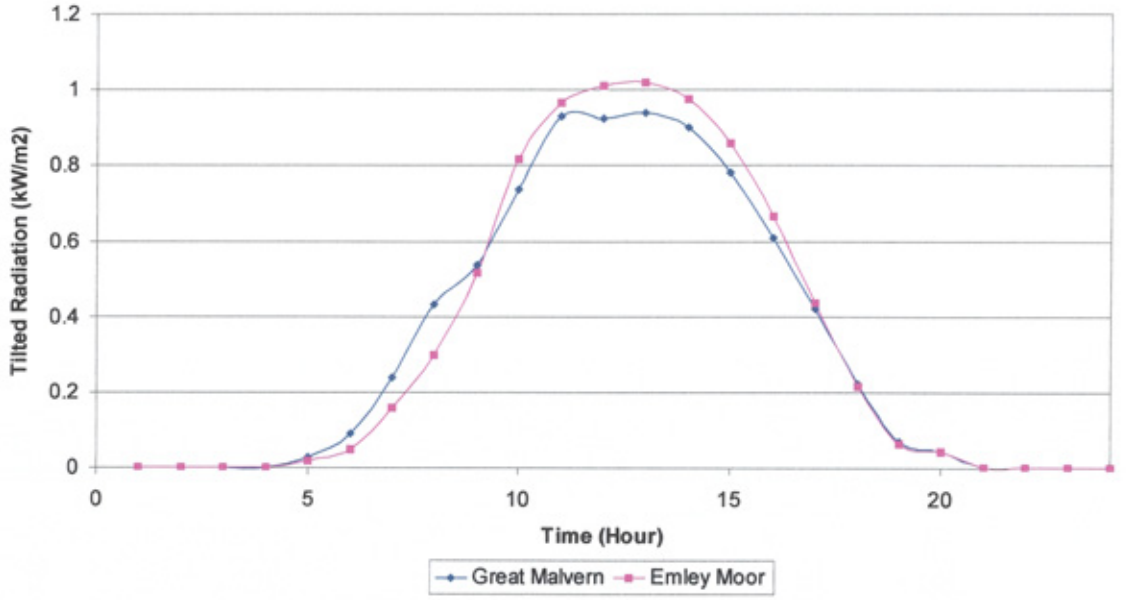

a) For a day with high correlation in June

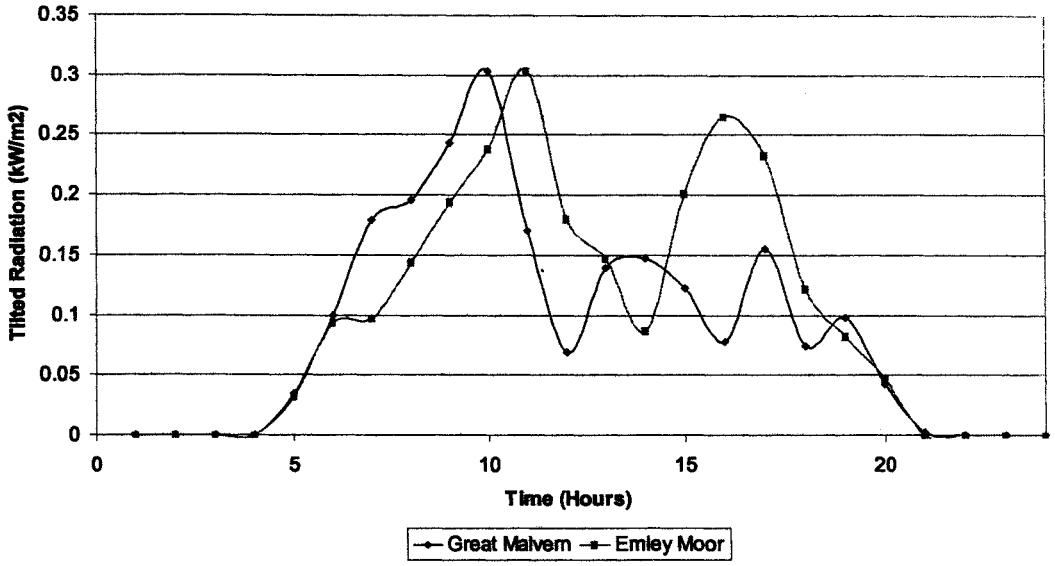

b) For a day with low correlation in June

Figure 5-31 Comparison of tilted radiation values, between the Great Malvern and Emley moor locations, separated by a distance of 154 km

The correlation coefficient values for each day in August were analysed for the locations separated by distances of 28.3 km, 176.8 km, 300.8 km and 400.5 km and compared as shown in Figure 5-32. For the locations separated by a distance of 28.3 km, the number of days with correlation coefficient greater than 0.8 was 9. For the locations separated by distances 176.8 km, 300.8 km and 400.5 km the number of days with correlation coefficient greater than 0.8 was 2, 3 and 3 respectively.

Similarly the correlation coefficient values for each day in January was analysed and is shown in Figure 5-33. For the locations separated by distances 28.3 km, 176.8 km, 300.8 km and 400.5 km the number of days with correlation coefficient greater than 0.8 was 25, 17, 23 and 21 respectively. All these results indicate that the number of stable days with higher correlation, decreased with increase in the distance of separation. This was less pronounced in the winter season compared with other seasons. The constant "a" in the exponential function indicates the decrease in the correlation coefficient and the number of stable days with the distance of separation.

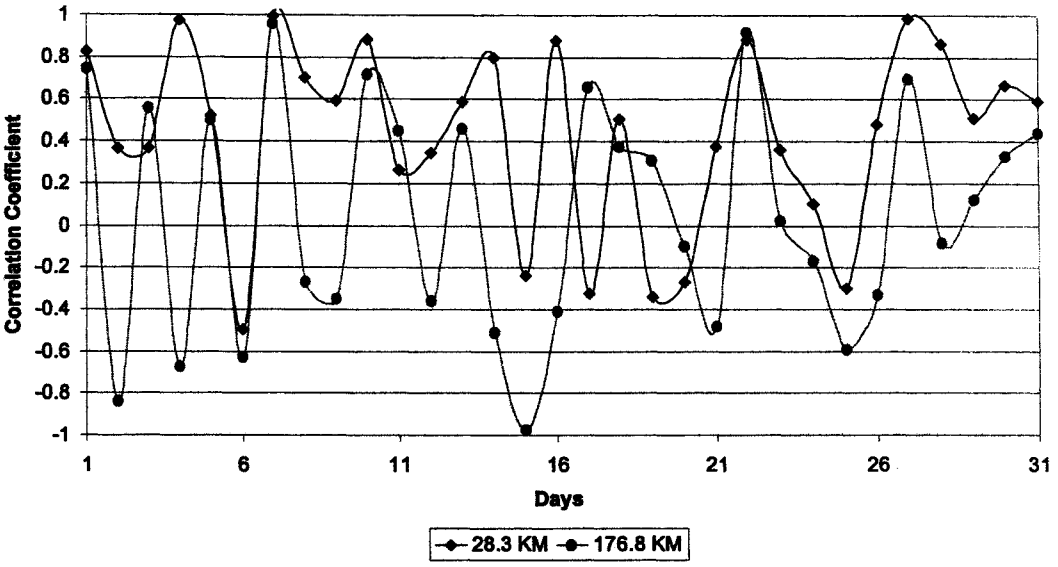

a) For the distance of separation 26.3 km and 176.8 km

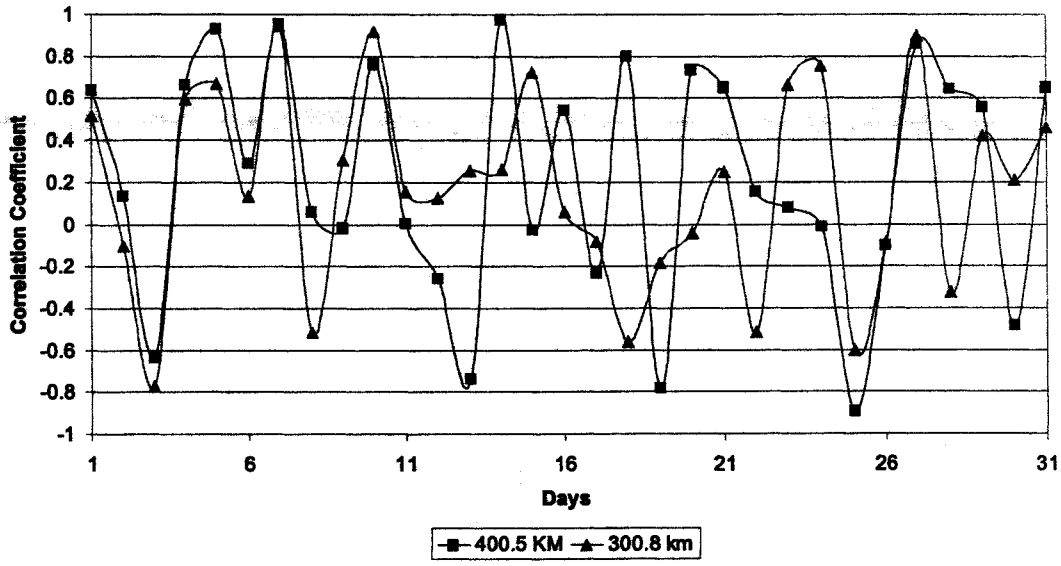

b) For the distance of separation 300.8 km and 400.5 km

Figure 5-32 Correlation coefficient values for each day in August

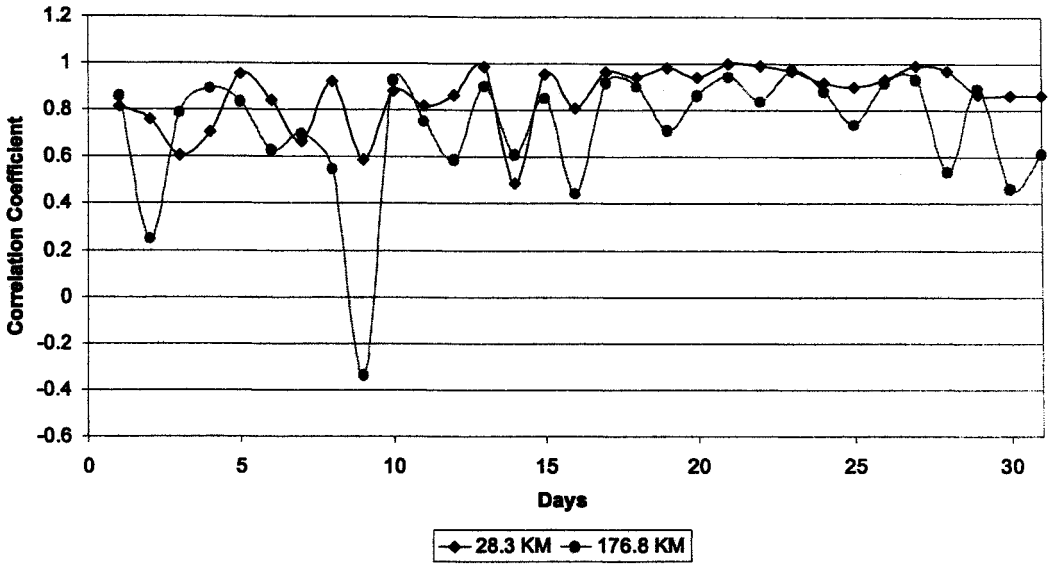

a) For the distance of separation 28.3 km and 176.8 km

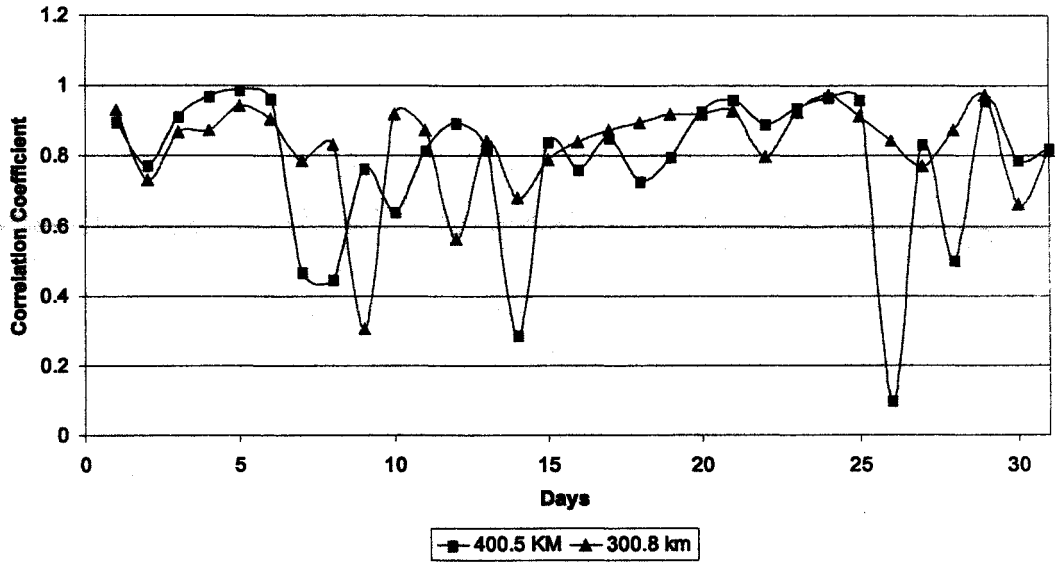

b) For the distance of separation 300.8 km and 400.5 km

Figure 5-33 Correlation coefficient values for each day in January

The correlation coefficient values for June from the data set II were compared with results obtained from the previous analysis (from the data set I) as shown in Figure 5-34. For the same distance of separation, the correlation coefficient values were lower for the data set I compared with the data set II. The correlation coefficient for each day was analysed using both data sets. From the data set I the South West 1 and South West 2 locations, separated by 49 km, were selected. From the data set II the

Newcastle and Leeming locations, separated by 45.7 km, were selected. The correlation coefficient values for each day, for both cases, were calculated and compared as shown in Figure 5-35. It can be observed that the number of days with higher correlation was in the data set II high compared with the data set I. It is worth to note that the data set I, data set II correspond to the years 2001, 2004 respectively. For the same month and for the same distance of separation, the number of days with high correlation is different for different years that may be due to the changes in weather pattern for each year.

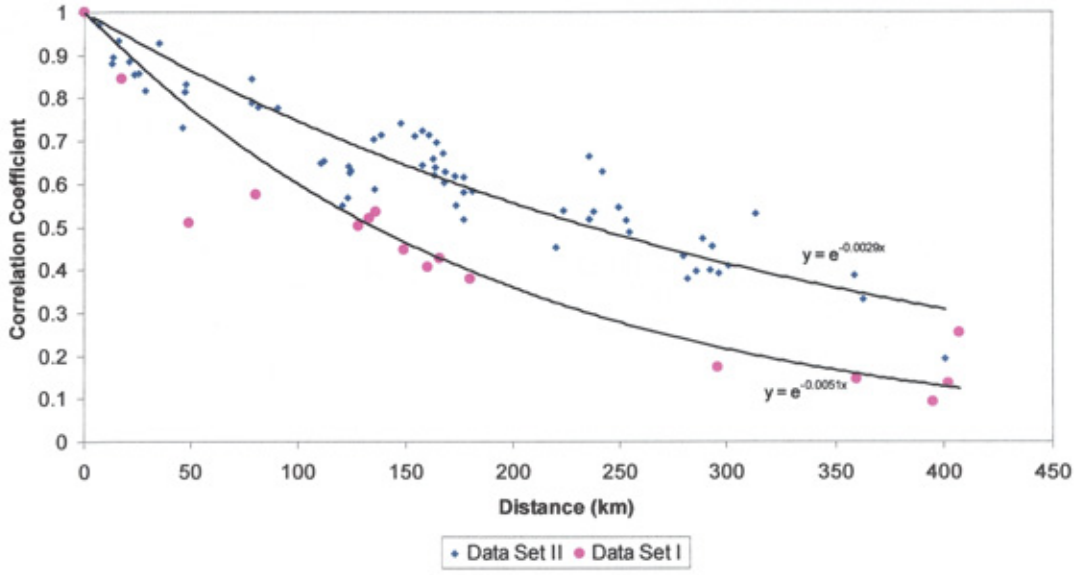

Figure 5-34 Correlation coefficient values with the distance of separation for June, using data set I and II

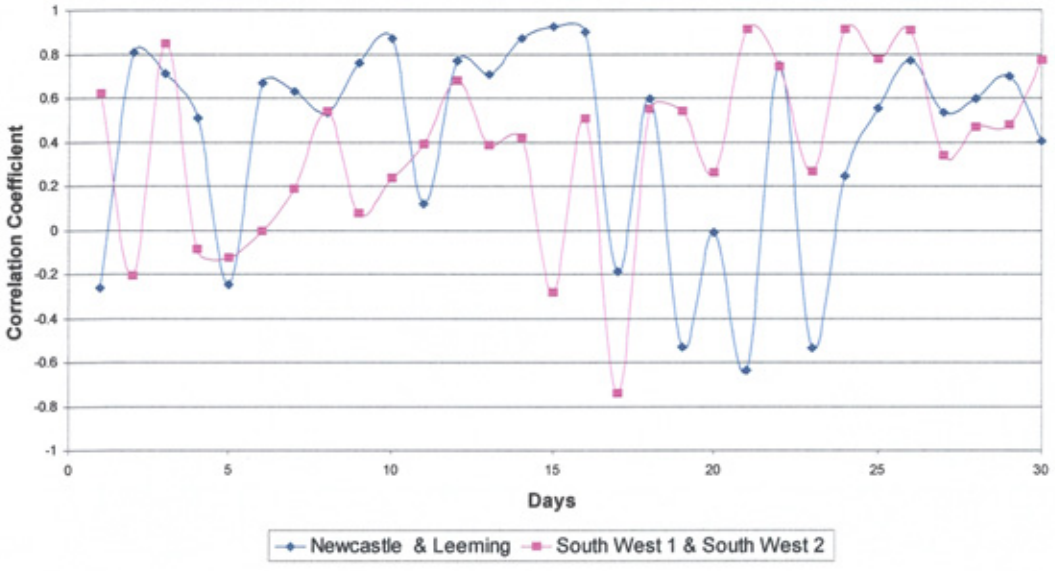

Figure 5-35 Correlation coefficient values for each day in June using data set I and II

5.7 Discussion

The fluctuation of solar radiation and the reduction in fluctuation by aggregating solar radiation values from different locations were analysed. In order to analyse the smoothing effect, the correlation coefficient of solar radiation values with respect to the distance was analysed. The correlation coefficient of solar radiation was analysed for different time intervals and seasons. From the analysis it was observed that for the same distance of separation, the correlation coefficient value was lower for shorter time intervals. The correlation coefficient values increase with the increase in time period considered. For longer time periods, the diurnal variation, which is fixed due to the sun and its spatial relationship, dominates the change in irradiance level. Whereas, for shorter time periods, the variation due to the cloud cover movement, which is random in nature, is influential. Hence for the same distance of separation, the correlation coefficient value is higher for longer time periods. This indicates that by combining solar radiation for different locations, smoothing effect will be more for lower time horizon compared with higher time horizon.

For the same distance of separation, the correlation coefficient of solar radiation was higher in the winter season and was lower in the summer season. The correlation coefficient values in spring and autumn seasons were lower than the winter season and higher than summer season. By analysing the correlation coefficient for each day it was observed that the number of stable days, days with higher correlation, were high in the winter season and low in the summer season. The correlation coefficient of solar radiation for each day in a month was analysed for different distance of separation. These results indicate that the number of stable days was decreased with the increase in the distance of separation. The exponential function that fits the correlation coefficient with the distance was obtained. The constant "a" in the function indicates the decrease in the correlation coefficient and the number of stable days with the distance of separation.

The change in correlation coefficient with the distance of separation can be divided into three main sections. They are the locations separated by a distance below 50 km, between 50 km to 250 km and distance greater than 250 km. For distances below

50 km, a high correlation is obtained. However in this region, there was a rapid decrease in correlation values. It is also indicating that the data from closely spaced sites can be used to predict relative performance of PV systems. From 50 – 250 km, smaller but still significant correlation values were obtained. Analysing the correlation for each day in this region shows that high correlation is obtained for stable days (good or poor). But for intermittent days, low correlation coefficient values were obtained. Thus prediction in this case is dependent on weather conditions and the results indicate that these tend to be similar in this range. For distance over 250 km, the correlation is low indicating that weather conditions tend to vary substantially across this range.

The correlation analysis showed that the correlation coefficient values were higher for the clear and stable days and when the days had variable weather conditions, the correlation coefficient values were low. This indicates that the fluctuation of PV power output by aggregating the output power from geographically dispersed PV systems would be reduced. The correlation of solar radiation values with the distance of separation can be used to study the standard deviation of output power of dispersed PV systems. The standard deviation of PV output power and the additional generation capacity required to keep the system balance is discussed in the next chapter.

5.8 References for Chapter 5

1. Eunan Martin Conway, "Stochastic modelling and forecasting of solar radiation", PhD thesis, University of Northumbria at Newcastle, UK, July 1998.
2. Dean L. Travers and R. John Kaye, "The impact of photovoltaic generation on electric power systems with thermal generating units", 14th European Photovoltaic Solar Energy Conference, Barcelona, Spain, Vol. 1, June 1997, pp. 1147-1150, Published by H.S. Stephens & Associates, Bedford, UK.
3. K. Kawasaki, T. Ohnishi and T. Suzuki, "Influence of a large amount of photovoltaic power generation systems upon utility power systems", 11th European Photovoltaic Solar Energy Conference, Switzerland, October 1992,

pp. 1199-1202, Published by Harwood Academic Publishers GmBH, Switzerland.

4. K. Otani, J. Minowa and K. Kurokawa "Study on areal solar irradiance for analysing areally-totalized PV systems", Solar Energy Materials and Solar Cells, Vol. 47, 1997, pp. 281-288.
5. K. Otani, A. Murata, K. Sakuta, J. Minowa and K. Kurokawa, "Statistical smoothing effect of power delivered to utilities by distributed PV systems", 2nd World Conference and Exhibition on Photovoltaic Solar Energy Conversion, Austria, Vol. 3, July 1998, pp. 2530 – 2533, Published by European Commission, Renewable Energies Unit.
6. E. Wiemken, H.G. Beyer, W. Heydenreich and K. Kiefer, "Power characteristics of PV ensembles: Experiences from the combined power production of 100 grid connected PV systems distributed over the area of Germany", Solar Energy, Vol. 70, No. 6, 2001, pp. 513-518.
7. A. Murata and K. Otani, "An analysis of time-dependent spatial distribution of output from very many PV power systems installed on a nation-wide scale in Japan", Solar Energy Materials and Solar Cells, Vol. 47, 1997, pp. 197-202.
8. W. Coppye, L. Geurts, A. Woyte, R. Belmans, J. Neyens and J. Nijis, "Determining the value of decentralised grid-connected photovoltaic electricity in Belgium", 17th European Photovoltaic Solar Energy Conference, Munich, Germany, October 2001, pp. 2418 – 2421, Published by WIP – Renewable Energies and ETA - Florence.
9. J. E. Hay, "Error associated with the spatial interpolation of mean solar irradiances", Solar Energy, Vol. 37, Issue 2, 1986, pp. 135-146.

6 RESERVE CAPACITY ANALYSIS

In chapter 5, the fluctuation of solar radiation for a single location and the reduction in fluctuation by aggregating solar radiation values from many locations were analysed. The fluctuation of solar radiation will result in the fluctuation of PV output power. The change in output power from PV systems results in a change in net load demand to be met by the grid. In order to maintain the system security, the system operator should balance the generation to the load demand and network power losses. In conventional grid management, additional generation levels known as reserve levels are brought to the operation to cover all the uncertainties, in order to balance the generation and demand. This can be in the short term, by holding appropriate level of response, or may be the long term, by holding appropriate operating reserve levels (detail explanation in section 6.1.2). If many PV systems are connected to the grid, the intermittency of output power from PV systems may affect the reserve requirement levels. In this chapter the fluctuation of PV output power for different time intervals was analysed with regards to the reserve requirement. As noted before, the UMIST group studied the fluctuation of output power using data from three locations to calculate the reserve requirement levels. In this work, in addition to the analysis using data from three locations, the implication of reserve requirement was analysed by combining data from many locations in the UK. Apart from this, factors that will affect the reserve requirement in the present UK network are discussed. The present UK network condition, the possible changes in the future and the different strategies to reduce the reserve requirement were analysed.

6.1 Background Theory

6.1.1 The UK grid network

The conventional arrangement of a modern large power system consists of

- Large Central Power Stations
- Transmission Network
- Distribution Network

Figure 6-1 is a single-line diagram, which represents the UK electricity network without renewable energy sources. The electrical power generated from large central generators is transmitted to the consumers through the network at certain pre-determined voltage levels. A complex power system may be characterised as operating at three voltage levels:

- Transmission Level: Over 132 kV (400 kV and 275 kV)
- Subtransmission Level: 132 kV, 66 kV and 33 kV
- Distribution Level: 11 kV, 400 V/ 230 V

The transmission network consisting of high voltage transmission lines is used for transmitting large quantities of power for large distances from central power stations. The distribution network consisting of lower voltage lines is used for distributing power to local areas over relatively shorter distance. The modern electricity system is an interconnected system, through which bulk electricity flows across the high voltage network [1]. Modern distribution systems were designed to accept the bulk power and to distribute it for the consumers. Thus the flow of power is always from higher to lower voltage levels in the conventional electric network [1].

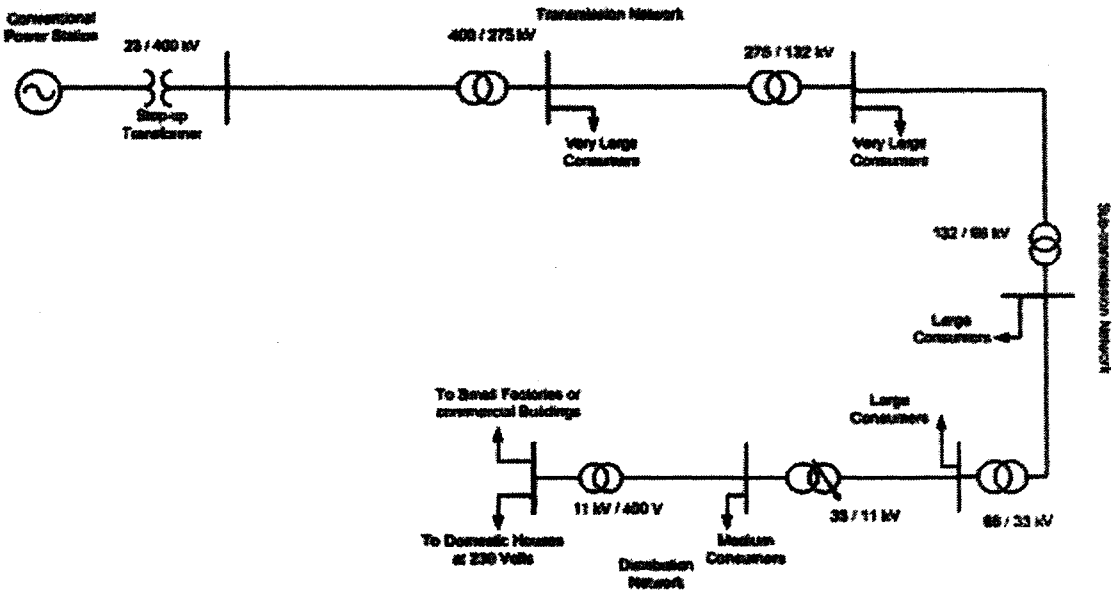

Figure 6-1 Representation of the UK Electric Supply Network

Electricity is supplied to the consumer at a given voltage and frequency, for example, for a domestic house at a voltage of 230 V and a frequency of 50 Hz. If unregulated, the voltage and frequency of electricity on the network vary when the demand on the system varies. System operators will respond to these variations and maintain the voltage and frequency within the acceptable limits to maintain the quality of supply. System operators ensure the matching of demand and generation by providing additional generation capacity to meet the failure of any generation plant and inaccuracy in demand forecast. There are four transmission systems in the UK, among these one in England and Wales, two in Scotland and another one in Northern Ireland. Each system is separately owned and operated. The largest system in terms of length and share of total transmission is the National Grid Company (NGC) system, covering England and Wales [1]. NGC also operates overhead lines connecting the transmission networks in England and Wales and Scotland, and an undersea link that connects France and England. NGC is a wholly owned subsidiary of National Grid Transco (NGT). There are 12 licensed Distribution Network Operators (DNOs) in England and Wales, two in Scotland and one in Northern Ireland [1].

6.1.2 Reserve requirements

An essential component in the operation of a power system is to balance the total generation to equal the load demand and power losses, in order to keep the system in security. The system operator, National Grid Company in the case of the UK, is responsible for this task. The system operator forecasts the load demand for one day in advance and they keep updating the forecast up to the real time. However, there is always some an error in forecasting the load demand in advance. In order to keep the supply and demand in balance, reserve generation systems are used. Reserve requirements are calculated based on the error in demand forecasting and this requirement will decrease as the time becomes closer to the operation point. This is due to the lower error in load demand forecasting when the time is closer to real time. However to start a coal generating unit from cold condition (OFF) and connect it to the network to generate the required power takes an average of 4 - 5 hours.

Hence, reserve levels delivered by these OFF line generators have to be notified at least 4 hours in advance to the system operators.

The different components of reserve capacity requirements are illustrated in Figure 6-2. There are mainly two components in the reserve categories, Contingency Reserve and Operating Reserve [2]. The contingency reserve is scheduled before the Final Plant Scheduling Stage (FPSS) in order to optimise the scheduling and to obtain the final solution at FPSS. FPSS is the instant that is 4 hours ahead of the real time. Contingency reserve requirements will be reduced as the real time approaches. The operating reserve requirement is scheduled at FPSS and is made up of short-term reserve and reserve for frequency response. Short-term reserve consists of two components, standing reserve and scheduled reserve. Both the scheduled and standing reserve are required to cover the changes in generation and demand that take place 4 hours ahead of the real time. These requirements are usually calculated from the statistical data on generation failures and shortfalls and the demand forecast error, by the system operators [2]. Reserve for frequency response provides a means of controlling the initial frequency drop if a certain amount of generation is lost.

Scheduled reserve is composed of all the generators able to react in the order of minutes and this includes [2]:

- Part-loaded generating plant
- Plants in hot standby
- Interconnections to neighbouring national electricity system

Generators that are able to generate with a short notice, about 20 minutes, provide **standing reserve** and this includes:

- Open Cycle Gas Turbine (OCGT) plant
- Pump storage plant
- Demand modification sources
- Industrial stand-by generation

In a competitive environment, NGC takes all the available measures to maintain system security at all time by balancing load demand and generation, with minimum cost. These measures includes:

- Acceptance of bid and offers submitted by the generation and demand
- Call off of ancillary services

When reserve is required, the system operator accepts or rejects the available bids and offers until reaching the desired reserve level. All bids and offers relate to generation already synchronised to the network. Therefore these generations are known as **spinning reserve**. If bids and offers are exhausted or economical condition occurred, the system operator makes use of ancillary services in order to balance demand and generation. These ancillary services represent the standing reserve agreements. The standing reserve units may not participate in the balancing mechanism.

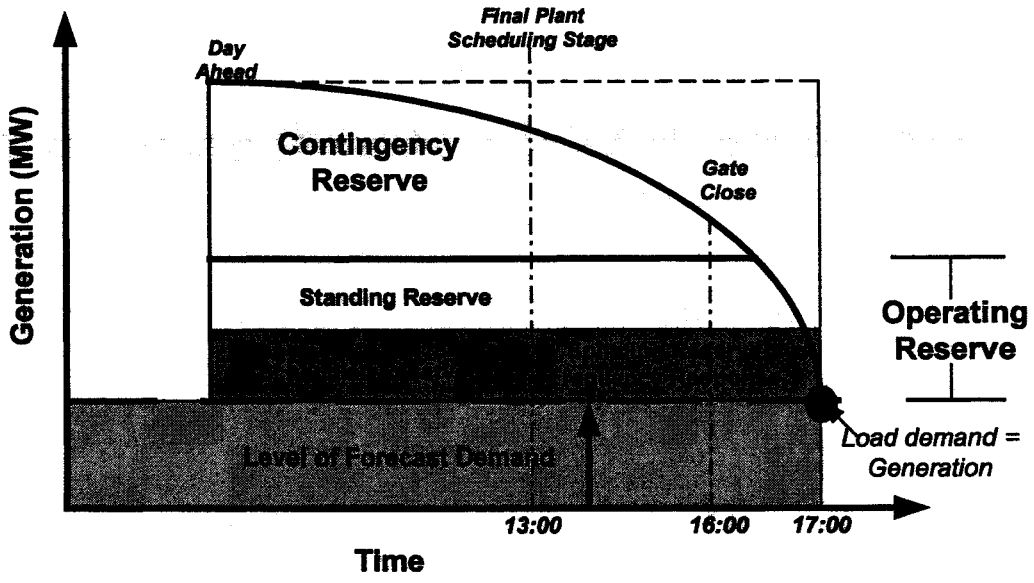

Figure 6-2 Representation of reserve requirement (Adopted from Ref. [2])

6.2 Output power Fluctuation

The fluctuation of PV output power was analysed using the measured horizontal radiation and ambient temperature values from three locations (London 1, West Midlands 1 and South West 1) in the UK. Measured horizontal radiation values were

translated into tilted radiation values using standard Hay's and Erbs models. Tilted radiation, ambient temperature and inverter efficiency were used to calculate the AC output power for the system defined. An installed capacity of 9.6 MWp in each location was assumed, representing a total of 3265 houses in each location. The developed cluster model was used to represent the systems, which vary in their design parameters. From the calculated values, the fluctuation of output power was analysed. In this analysis, half hour output power was used, since it is currently the period used for calculation of contributions to the electricity network in the UK and is thus important in terms of operation of the electricity market.

Fluctuation of output power was calculated as a percentage of PV capacity for a single location and compared with the ensemble (average of three locations) as shown in Figure 6-3. The maximum fluctuation for a single location was calculated as 60% of PV capacity but this was reduced to 35% of PV capacity for the ensemble. The standard deviation of the power fluctuation for a single location is 9% of PV capacity, whereas standard deviation for the ensemble power fluctuation is 6% of PV capacity. These results indicate that the aggregation of output power from geographically dispersed PV systems would reduce the output power fluctuation.

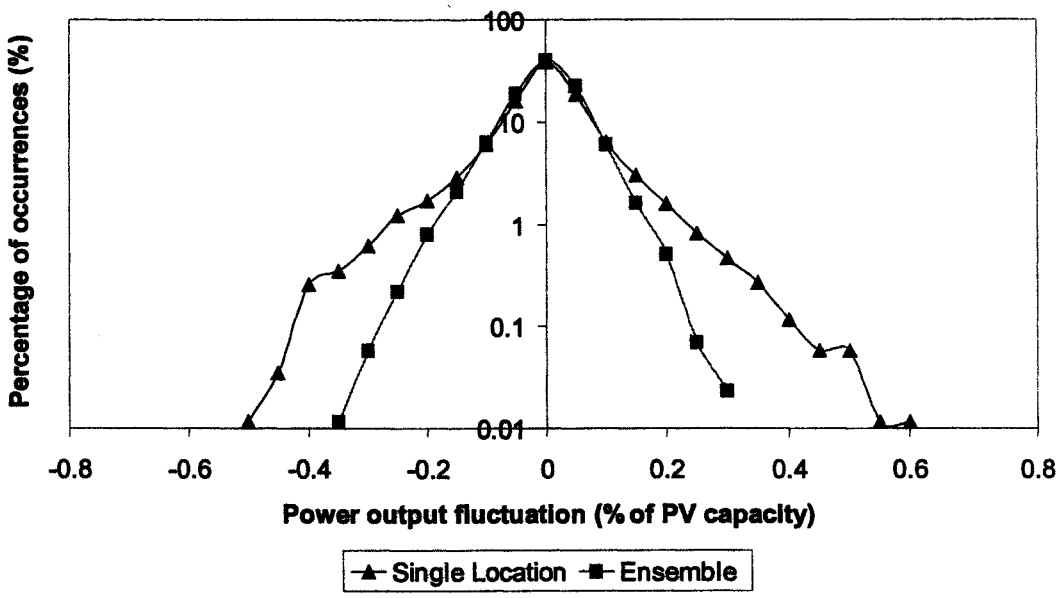

Figure 6-3 Fluctuation of half-hour output power (Single location: London 1, Ensemble: London 1, South West 1 and West Midlands 1)

6.2.1 Seasonal and time variation

The average power profile was calculated for each season: winter (January, February and December), spring (March, April and May), summer (June, July and August) and autumn (September, October and November) in terms of PV capacity and is shown in Figure 6-4. As expected, the output power is higher for summer months and lower for winter months. Since the power pattern is different for each season, the fluctuation of output power for each season needs to be analysed.

The average output power fluctuation was analysed with respect to time of the day for the summer season and the result is shown in Figure 6-5. In the morning, mean power fluctuations are positive because of increasing sunlight level and negative values occur in the afternoon because of decreasing sunlight level. Therefore, output power fluctuation will be different with respect to time of the day. Hence the standard deviation of output power also needs to be analysed with respect to the time of the day.

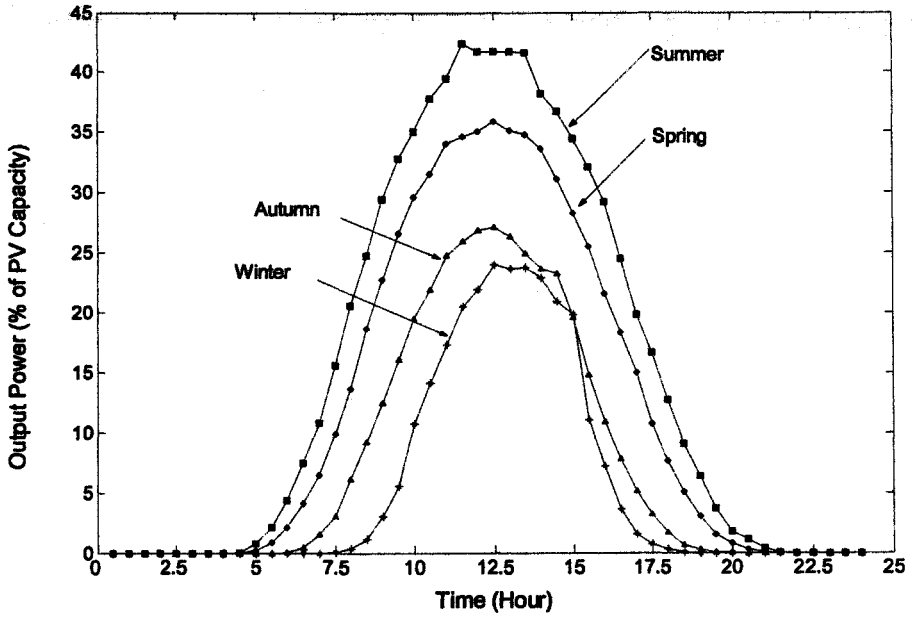

Figure 6-4 Average power profile by combining three locations (London 1, South West 1 and West Midlands 1), for different seasons

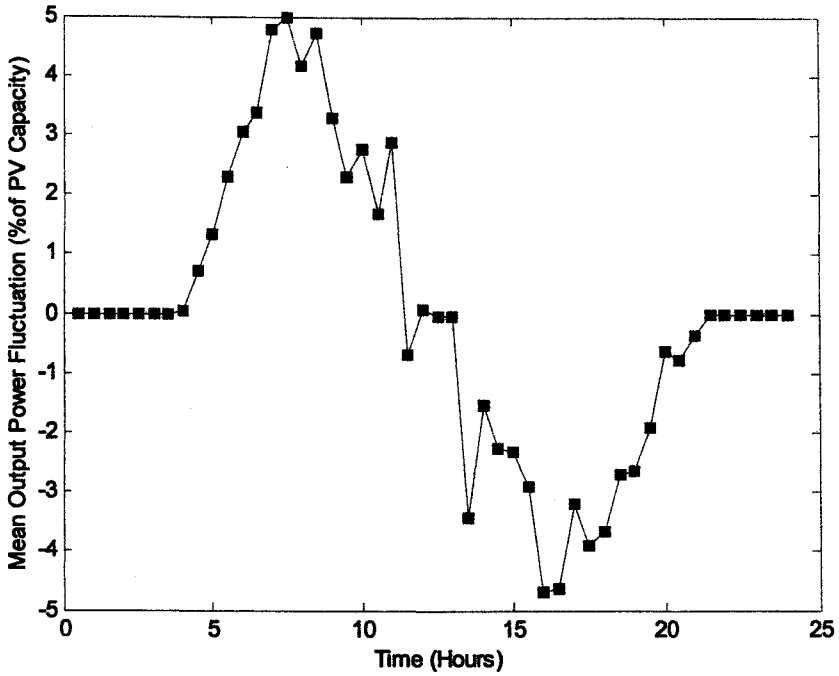

Figure 6-5 Mean output power fluctuation for the three locations average (London 1, South West 1 and West Midlands 1), for summer season

6.2.2 Standard deviation of output power

The output power fluctuation from one time interval to the next (e.g. 12:00 to 12:30 P.M.) was calculated for each day (30 days in June month). The output power fluctuation for each day will be used to calculate the standard deviation of output power for that time of the day. The standard deviation of output power calculated for the summer season is shown in Figure 6-6.

Figure 6-7 shows the magnitude of the half-hour output power fluctuation and the number of occurrences for noontime (12.00 to 12.30 P.M.) in the summer season, for the average of three locations. The distribution of power fluctuation is not exactly a normal distribution, however adding many years of data in the analysis will lead to a normal distribution. With these assumptions, for each season the standard deviation of output power fluctuation with respect to the time of the day was calculated and is shown in Figure 6-8. These results indicate that even though the output power pattern is different for each season, the standard deviation of half-hourly output power has a low seasonal dependence. The maximum standard deviation is 9.1%,

8.4%, 8.3% and 7.4% of PV capacity for winter, spring, summer and autumn seasons respectively. The standard deviation of output power is highest around the noontime for all seasons.

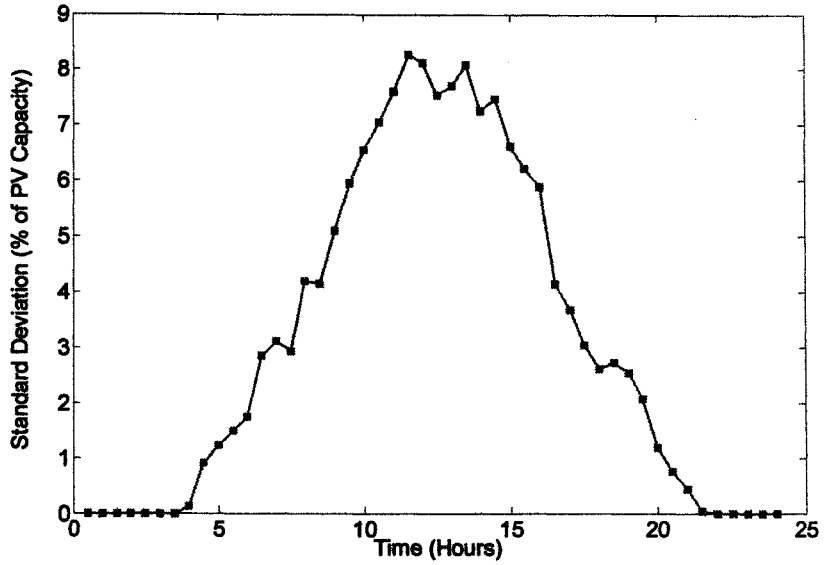

Figure 6-6 Standard deviation of output power for the summer season for the average of 3 locations (London 1, South West 1 and West Midlands 1)

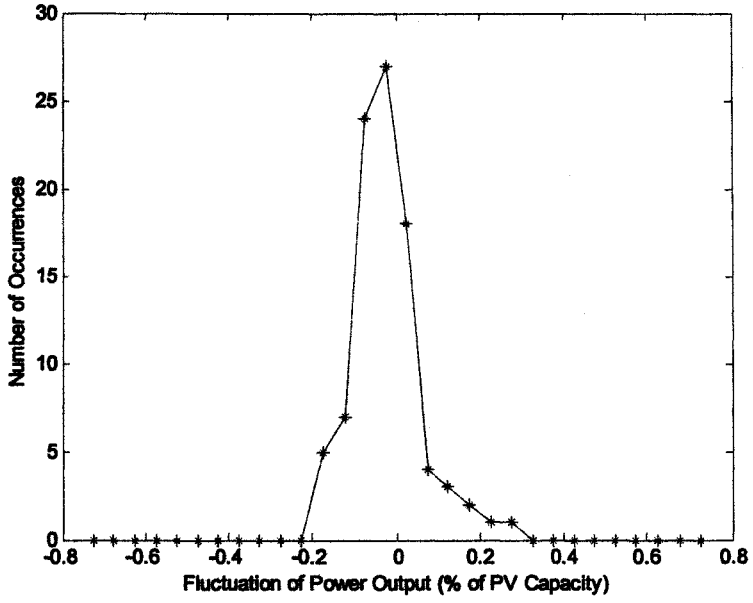

Figure 6-7 Distribution of half-hour output power fluctuation magnitude and occurrences, for the summer season at noontime, for the average of 3 locations

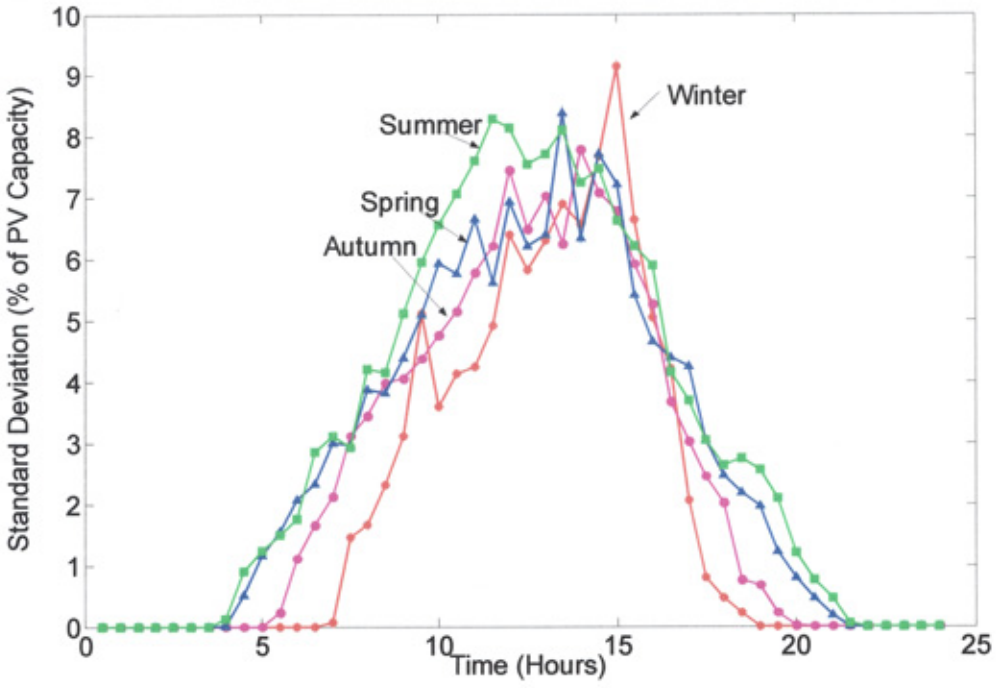

Figure 6-8 Standard deviation of half-hour output power with respect to time for different seasons, for the ensemble consisting of 3 locations (London 1, West Midlands 1 and South West 1)

6.2.3 Number of sites

The reduction of output power fluctuation was analysed using data from three locations, which are separated by a maximum distance of 160 km. However the addition of more locations, which have less correlation, will result in more smoothing of the output power. In order to illustrate this, the fluctuation of output power and standard deviation of output power for the June month was calculated using three locations. Adding two more locations, South West 2 and North East 1, further data fluctuation analysis was carried out. It was observed that maximum half-hour output power fluctuation for a single location was 41% of PV capacity, which is reduced to 26% of PV capacity for 3 locations, and reduced to 19% of PV capacity with all 5 locations. The corresponding standard deviation of output power with respect to time was also calculated and the result is shown in Figure 6-9. These results illustrate that addition of different locations data, which have less correlation, will result in more smoothing of PV output power.

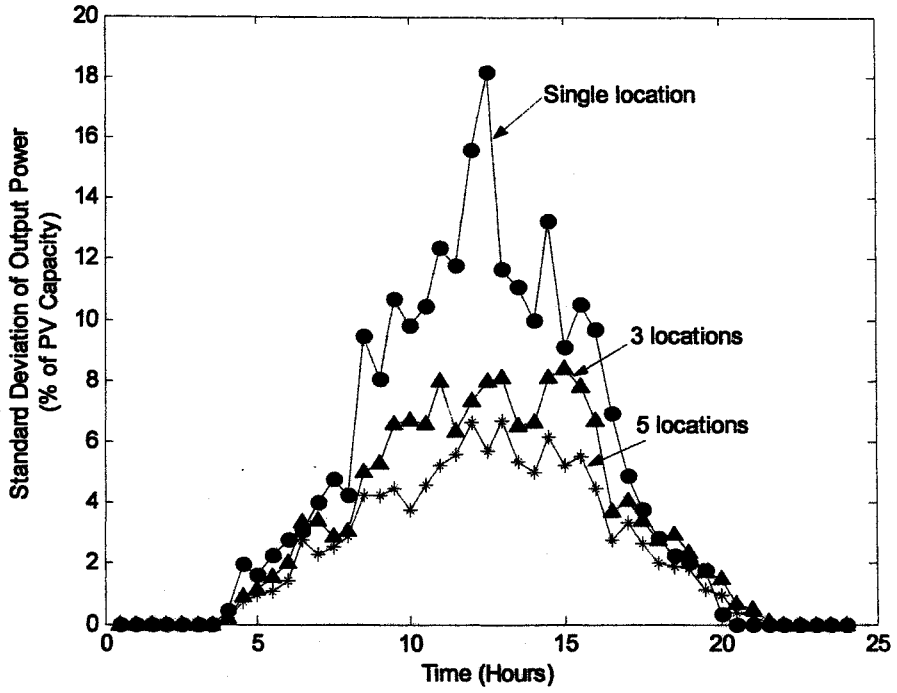

Figure 6-9 Comparison of standard deviation of half-hour output power with the number of locations (Single location: London 1; 3 locations: London 1, South West 1 and West Midlands 1; 5 Locations: London 1, South West 1 and 2, West Midlands 1 and North East 1)

6.2.4 Time horizons

In order to analyse reserve requirements needed to maintain load demand and supply balance, it is necessary to consider the fluctuation over longer time periods. Therefore, the behaviour of power fluctuation for longer time periods was analysed for the summer season. Figure 6-10 shows the standard deviation for half-hour, hour, two hour and four hour time period. The standard deviation of output power is increased with longer time periods. Figure 6-11 shows the standard deviation of output power for a 4-hour time period, which was studied for all seasons. The maximum standard deviation of output power for 4 hours time period is 16% of PV capacity, for the winter season.

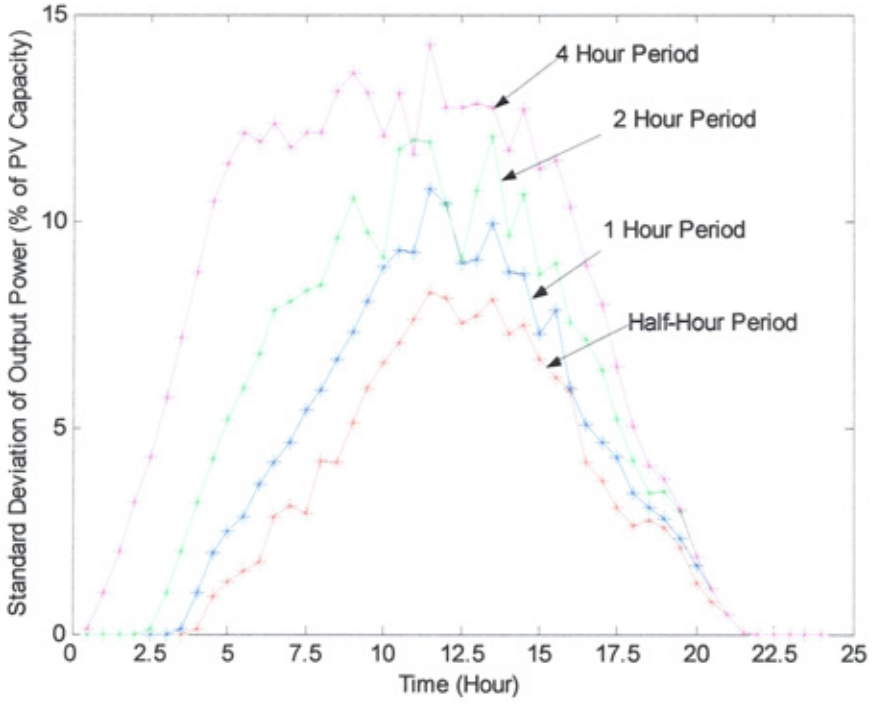

Figure 6-10 Comparison of standard deviation of output power for the summer season in terms of different time intervals

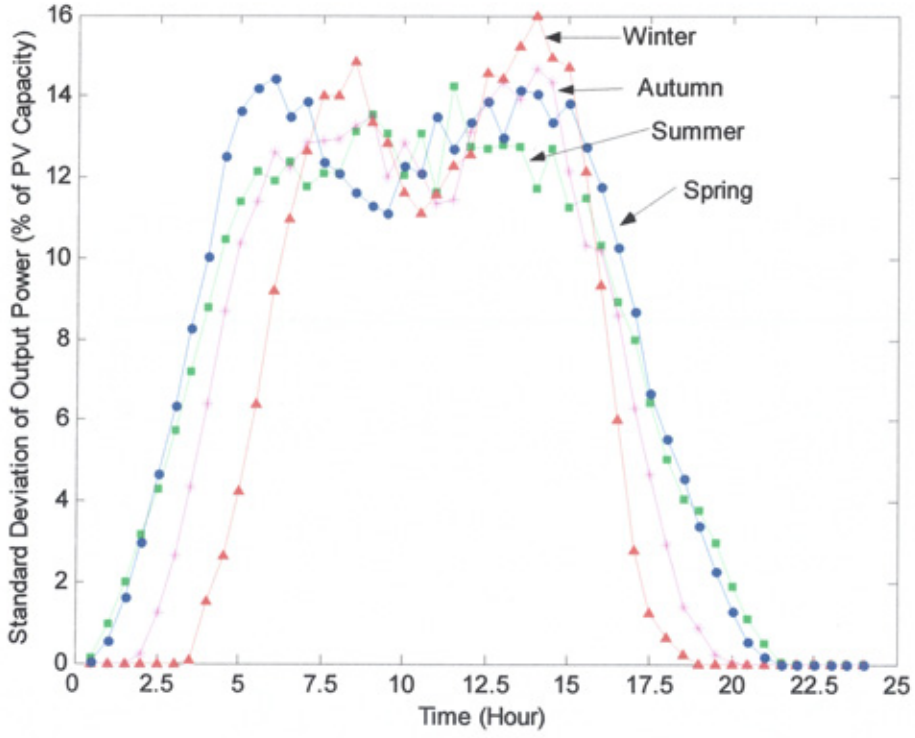

Figure 6-11 Comparison of standard deviation of output power, for 4 hour time interval, with respect to different seasons

6.3 Reserve Capacity Calculation

System operators should balance supply and demand to keep a balanced stable system. Supply and demand imbalance will occur due to different uncertainties, which include the error in load demand forecasting and sudden failure of large conventional generators. System operators provide reserve generation in order to meet these uncertainties. If many PV systems are added to the grid, it is possible that the fluctuation of PV output power may increase the level of reserve requirements. This section discusses the possible change in reserve requirement levels due to high penetration of PV systems in the network. This chapter also discusses different methods to overcome problems due to the intermittent nature of PV output power.

6.3.1 Demand forecast error

System operators predict load demand on a continuous basis and schedule generation and balance supply and demand to keep the system in security. The prediction of load demand depends on historical demand data, weather data (a sunny day will change the demand profile), the calendar day (holiday or working day) and other factors such as television guides etc. However there will be an error in forecasting load demand. Closer to the real time, the error in forecasting load demand will be reduced. The accuracy of forecasting the load demand and supply balance on the 4-hour time period is around 1.4% [3].

The Seven Year Statement (SYS) from National Grid Company, UK, provides details and key points regarding demand profiles. Typical load demand profiles for summer and winter, maximum load demand profile during winter and minimum load demand profile during summer for 2003 were collected from the SYS. Half-hour load demand profiles for these days are shown in Figure 6-12 [4]. Some of the key points regarding these demand profiles are:

1. The maximum and typical winter profiles are load demand profiles during weekdays.
    a. 00:00 h – 03:00 h: Operation of time switched and radio and tele-switched, storage heating and water heating equipment

b. 06:30 – 09:00 h: Build up to start of a working day
c. 09:00 – 16:00 h: Reflecting working day i.e., primarily commercial and industrial load demand
d. 16:30 – 17:30h: Rises to peak due to lighting load and increased domestic demand

2. The typical summer profile is the load demand profile for weekday
   a. As (1) above without effects of storage heating demand and with later onset of evening light load
3. The minimum summer profile is the load demand profile for Sunday
   a. As (2) above with increased lunchtime cooking demand

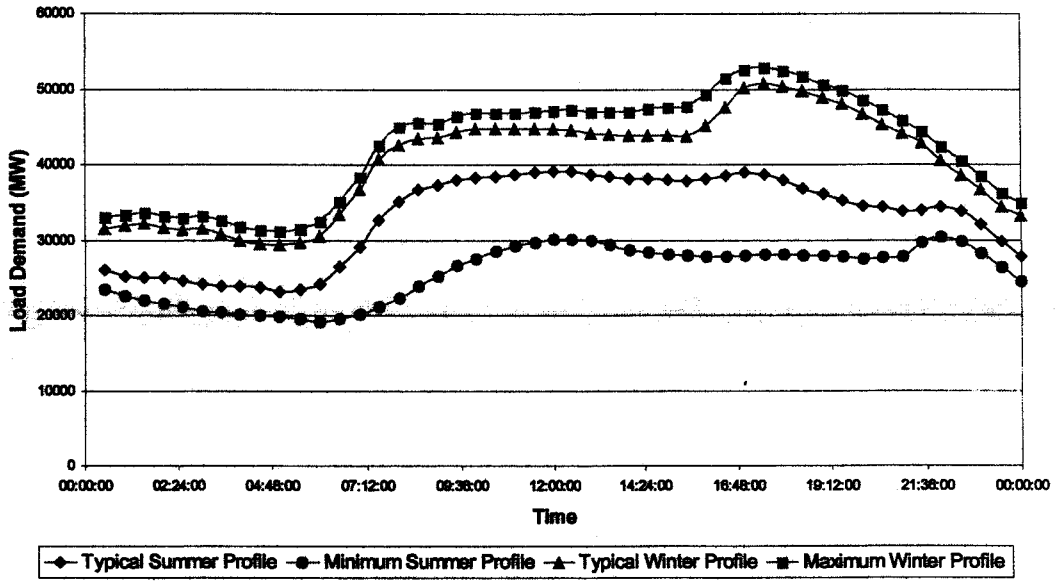

Figure 6-12 Load demand profile for England and Wales for typical days in the summer and winter seasons

It is worth noting that these demand profiles are an aggregation of all regional loads in the UK electricity network. Aggregation of generation and load demand is a powerful mechanism used by the electricity industry to simplify the operation of the utility network and to reduce the costs for consumers [5]. In this analysis, three locations in the UK, London 1, West Midlands 1 and South West 1 were considered. The dwelling stock in the London, West Midland and South West regions are 14%, 10% and 10% of the total England and Wales dwelling stock respectively. Non-

domestic building stocks in these regions are 17%, 10% and 9% of total stock in England and Wales respectively. The number of dwellings and non-domestic buildings in these regions are 35% of the total building stock in England and Wales. Therefore the total load demand for England and Wales is scaled down to 35%. Demand forecast error for 4 hours ahead was calculated by considering error of 1.4%.

6.3.2 Assumed scenarios

For two different scenarios, the output power from PV systems was calculated using the cluster model and data from three regions. From these values, the standard deviation of output power fluctuation was analysed. The assumed scenarios are:

Scenario 1: In each region PV is installed in 2% of house roofs, 1% of non-domestic building roofs, 1% of non-domestic façades. In this scenario, the total installed PV capacity is 385 MW.

Scenario 2: In each region PV installed in 6% of house roofs, 3% of non-domestic roofs and 3% of non-domestic facades. In this scenario, the total installed PV capacity is 1179 MW.

Half-hourly output power was calculated for these two scenarios by using the cluster model. The half-hour time series output power was used to calculate the power fluctuation for the 4-hour interval. The standard deviation of PV output power, for the 4-hour time interval, was calculated for summer and winter with respect to the time of the day, as shown in Figure 6-13 and Figure 6-14. An increase in the number of PV systems does not increase the percentage of standard deviation. The maximum standard deviation values vary from 165 MW to 190 MW with the seasons.

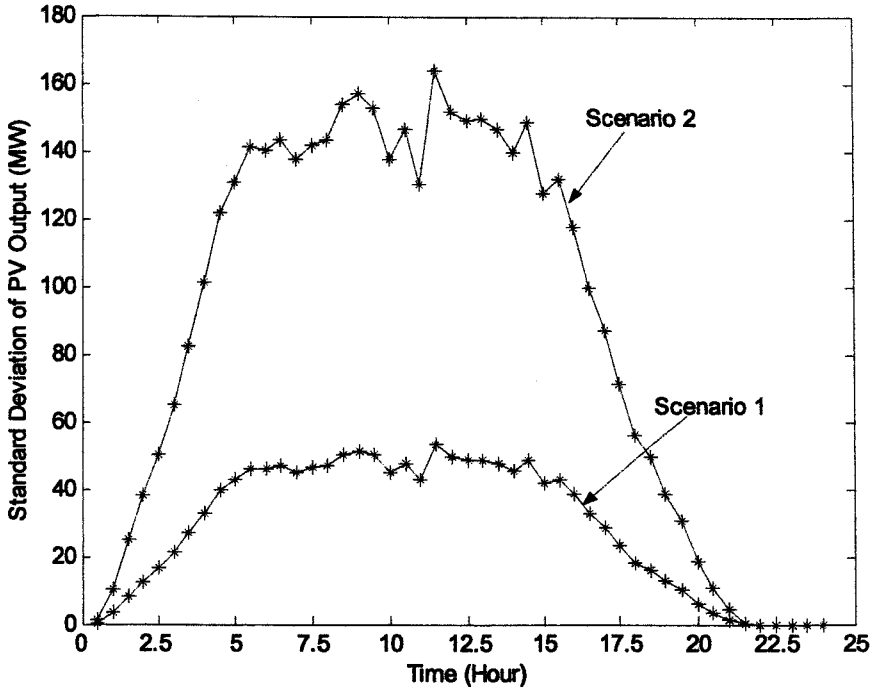

Figure 6-13 Standard deviation of PV output power for the summer season

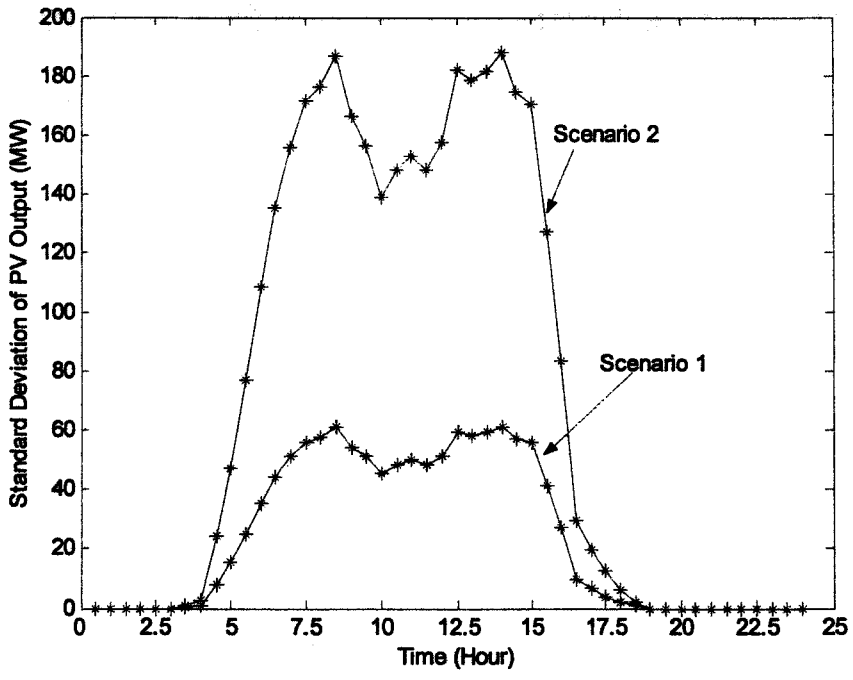

Figure 6-14 Standard deviation of PV output power for the winter season

6.3.3 Reserve capacity

The total standard deviation of the uncertainties (σ_{tot}) can be written as:

$$\sigma_{tot} = \sqrt{\left(\sigma^2_{DFE} + \sigma^2_{PV} + \sigma^2_{GF} - 2 * \rho_{DPV}\right)} \qquad 6.1$$

Where,

σ_{DFE} is the demand forecast error

σ_{PV} is the standard deviation of the PV output power fluctuation

ρ_{DPV} is the covariance between demand and PV output power

σ_{GF} is the standard deviation of conventional generation failure

In this analysis, only demand forecast error and standard deviation of PV output power were considered. Correlation between demand and PV output power and conventional generation failure were not taken into account. The standard deviation of supply and load demand balance will follow a normal distribution. Using a statistical approach, the probability of 99.7% of occurrence will be in the range $3*\sigma_{tot}$ and $-3*\sigma_{tot}$ [6]. Therefore by holding a spinning reserve of $3*\sigma_{tot}$, there is a probability of 99.7% of generation and demand mismatch can be covered[9] [7]. This is the standard method to calculate reserve requirement by statistical analysis followed by different authors [3,7]. These studies looked at the intermittency of wind power and additional reserve requirements for different wind penetration levels.

The amount of spinning reserve required to meet these uncertainties was calculated for the assumed two scenarios. The reserve required without PV systems and with PV systems was calculated for two typical days in the summer and winter seasons. In this study, only three locations data were used to analyse PV output power fluctuation. The reserve requirement levels for two typical days in the summer and winter seasons are shown in Figure 6-15 - Figure 6-18. From these results it can be observed that the increase in reserve requirement was less for smaller penetration of PV systems. The total reserve levels required were higher for the winter season.

[9] Standing reserve can cover the remaining percentage.

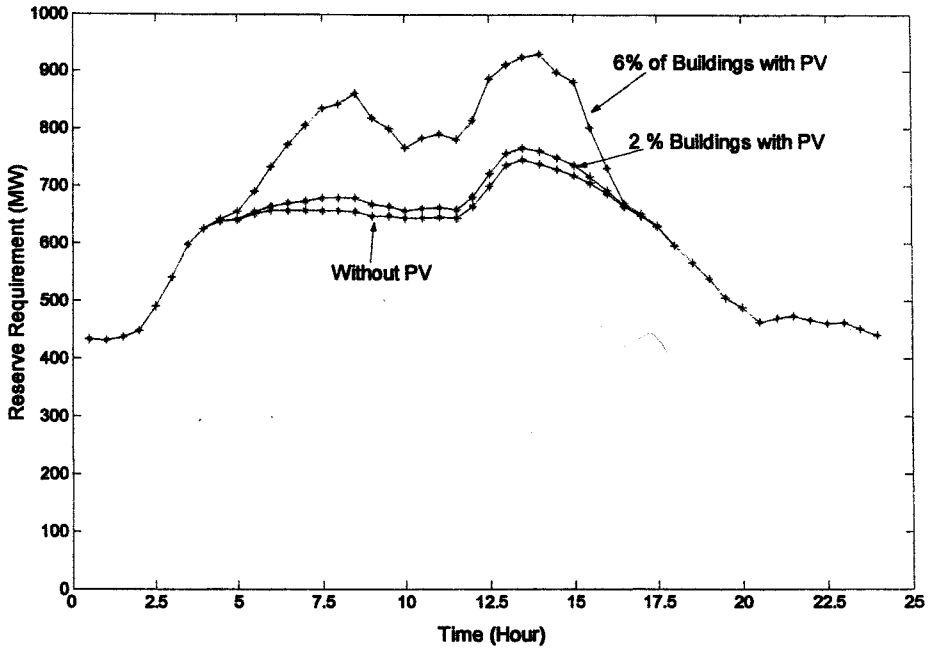

Figure 6-15 Reserve requirement for different PV penetration for a typical day in the winter season

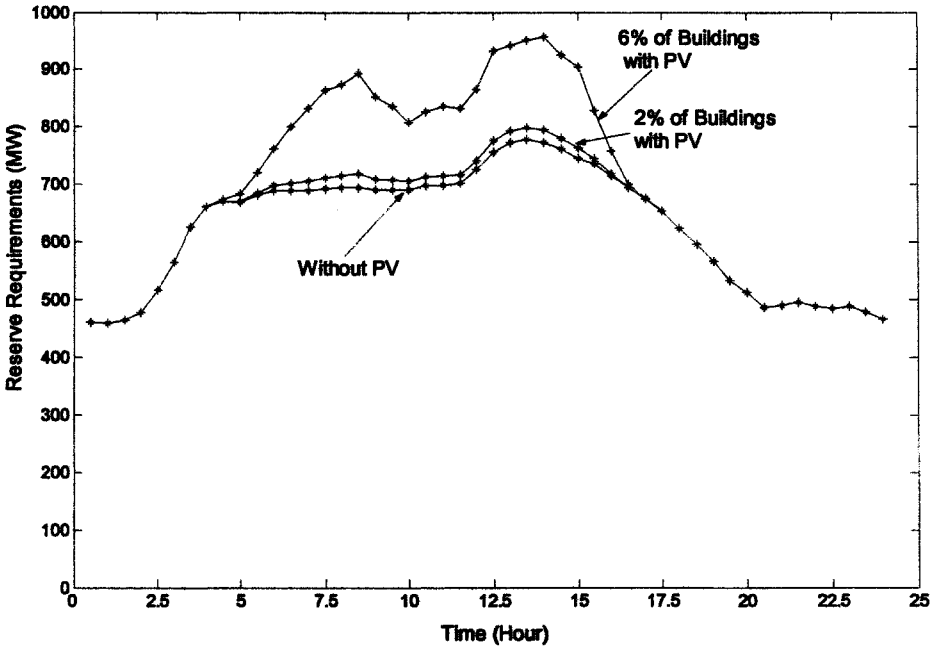

Figure 6-16 Reserve requirement for different PV penetration for the maximum winter season profile

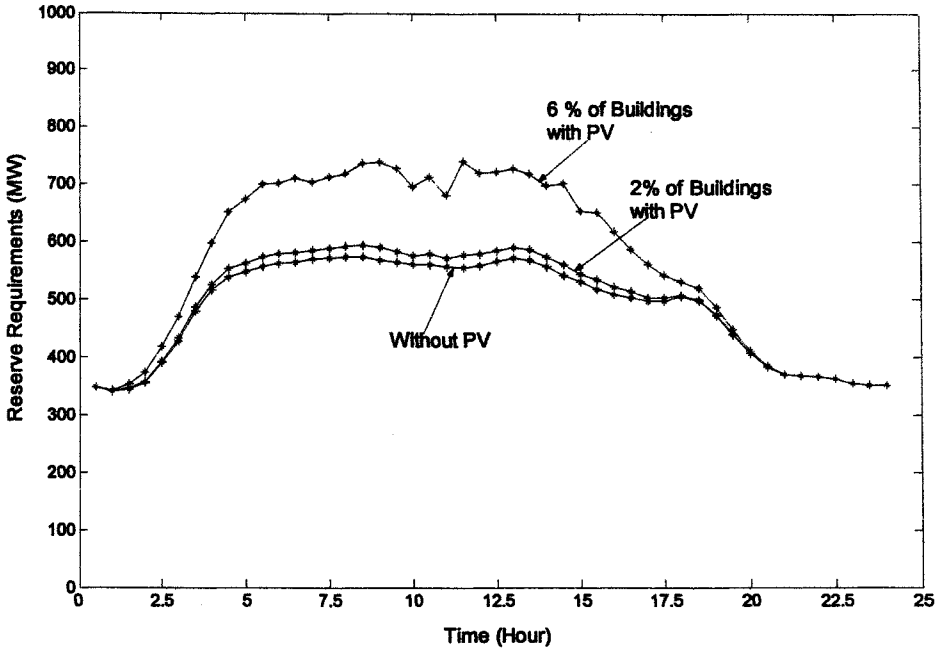

Figure 6-17 Reserve requirement for different PV penetration levels for a typical day in the summer season

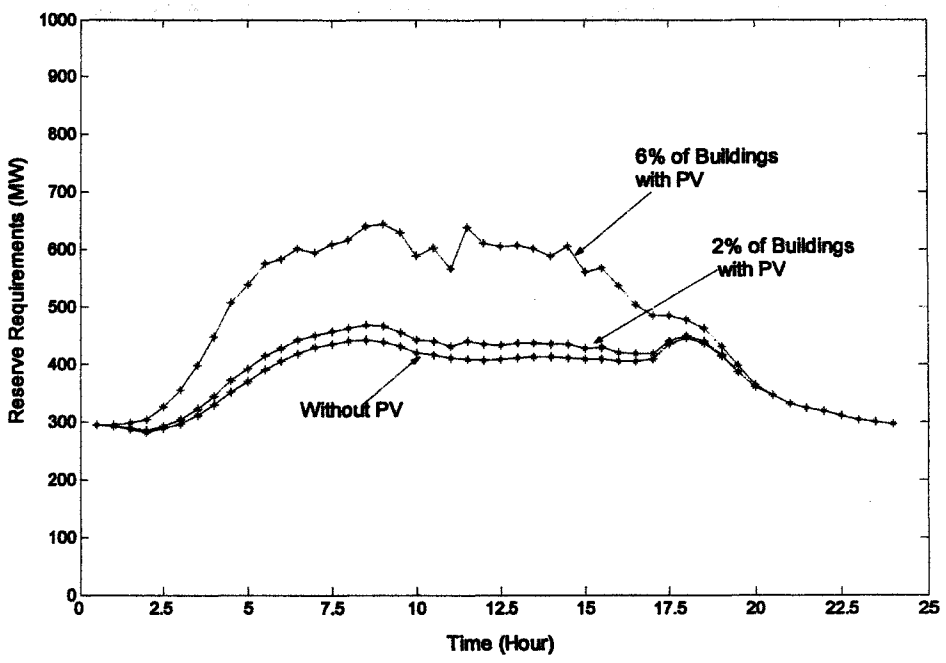

Figure 6-18 Reserve requirement for different PV penetration levels for the minimum summer season profile

Additional reserve levels required because of PV penetration were calculated for the scenario 2 and results are shown in Figure 6-19 and Figure 6-20. These results indicate that the amount of reserve required because of PV penetration is slightly lower for the winter season compared with the summer season. Even though the standard deviation of PV output power for the winter season is slightly higher than for the summer season, the additional reserve requirement was lower than for the summer season. This is because the load demand is high for the winter season and so the change in net standard deviation by introducing PV systems is less. For the same reason, the additional reserve required for the winter maximum profile day was slightly lower than the additional reserve required for the winter typical profile day. From these results it is also clear that duration of reserve required is less for the winter season. The additional reserve required was higher for the summer minimum profile day compared with other days. The additional reserve requirement calculations were based on the assumption that the network has reserve capacity only to meet the demand forecast error. In practice, the network will have more reserve (discussed in section 6.4.1) and hence the additional reserve requirement will be less than the calculated value. The implication of these statistical results and other factors that will affect the reserve requirement levels are discussed in the following sections.

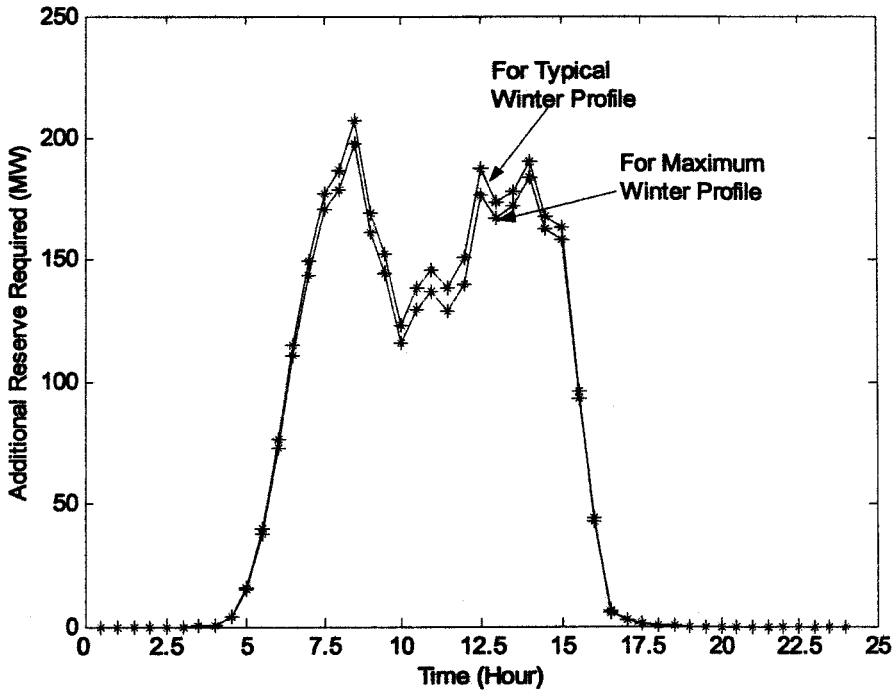

Figure 6-19 Additional reserve requirement for the winter season

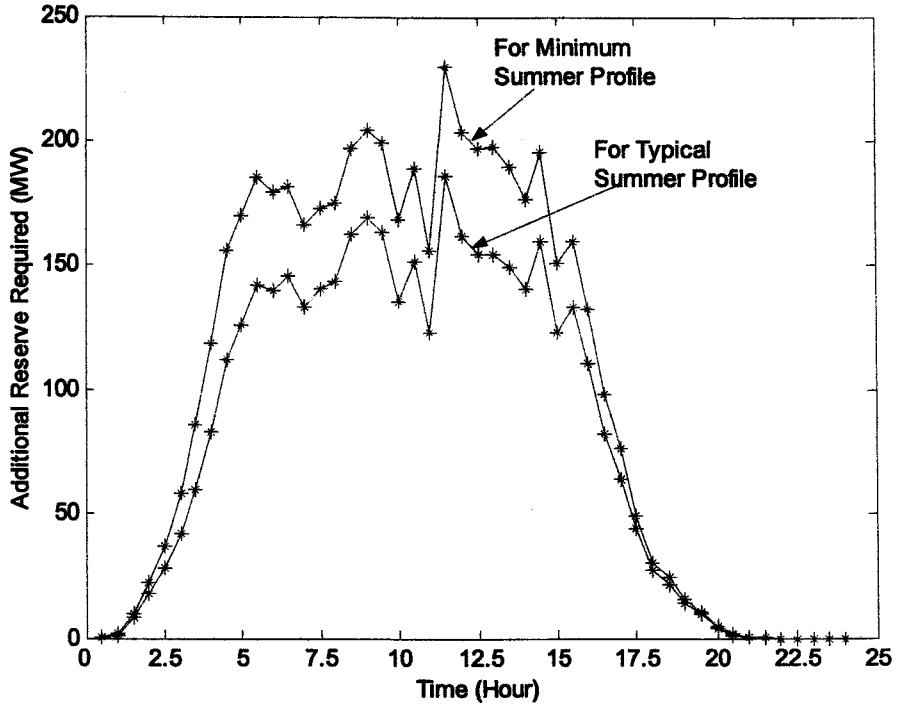

Figure 6-20 Additional reserve required for the summer season

6.4 Implication of Reserve Requirement

6.4.1 Present UK network condition

It is important to stress here that reserve requirements are assigned to back-up uncertainties due to the combined effect of fluctuations in demand, conventional generation and PV generation. In the above analysis only the demand forecast error and fluctuation of PV output power was used to calculate reserve requirements. As explained in equation 6.1, the correlation of load demand and PV output power may also affect the reserve requirements. Apart from these factors, another factor that has a strong influence on the reserve requirements is the sudden loss of a generating plant. The most dramatic loss of power in the UK would be the loss of one of the two 1000 MW cross-channel links that import electricity from France [3,8]. Similarly there are events that cause sudden changes in load demand. For example it has been reported that the conclusion of an episode of the BBC TV soap Eastenders created a sudden drop of 2,300 MW [8]. To keep power systems in balance during these types

of uncertainties, NGC already provides spinning reserve. Therefore with present electricity systems a significant amount of intermittent energy sources can be accommodated before additional reserve needs to be brought on line. NGC has criteria for absorbing additional intermittent generation. The threshold and mitigation options provided by NGC are given as [5,9]:

- The potential loss should be less than 3% of peak demand in an hour, which is approximately 1500 MW (assuming maximum demand of 50,000 MW). If it is greater than this threshold level, additional reserve services should be provided.
- The potential instant loss should be less than 2% of peak demand, which is approximately 1000 MW in one minute. If it is greater than this threshold level, additional frequency control measures should be provided.

Using the hourly fluctuation criteria, the amount of PV systems that can be added to the present network without additional reserve requirement was calculated. Using data from three locations, the maximum change in PV output for a one-hour period was calculated as 40% of PV capacity. Then the maximum PV systems that can be added without additional reserve required will be 3750 MW (7.5% of maximum demand), using data from only three locations. It is worth noting that the additional reserve capacity needed for the inclusion of 1179 MW was calculated as 200 MW, based on the assumption that the network has reserve capacity to meet only the demand forecast error. In practice, the network will have more reserve to meet sudden changes such as loss of a large generating plant. According to the NGC requirements, with the present reserve availability in the UK network, a PV capacity of 3750 MW can be added without additional reserves.

As explained before, the load demand profiles are an aggregation of load demand for all regions. This aggregation of load smoothes the total load demand in the network. Similarly, by combining PV systems in all regions, output fluctuation will be reduced and hence the reserve requirement will be reduced. In order to illustrate this, the output power for June[10] from 5 locations (London 1, West Midlands 1, South West 1, North East 1 and South West 2) was used. The maximum hourly output power fluctuation for three locations (London 1, West Midlands 1 and South West 1) was

[10] June month may not be representative of the maximum fluctuation in the year.

calculated as 26% of PV capacity. From this the maximum PV that can be added to the present network was calculated as 5770 MW. If all five regions were used, the maximum hourly fluctuation was calculated as 20% and PV capacity that can be added with the present network is calculated as 7500 MW. It must be noted that these thresholds represent the maximum PV capacity that can be added in the present network without additional reserve generation. Additional PV systems can be added but with increased additional reserve requirement and hence increase in system cost. NGC believes that sufficient response and reserve services will be available for a situation in which entire 2010 renewable target is met by wind-powered plant [8].

6.4.2 Aggregation of PV output and load demand

In the reserve requirement analysis, 6% of houses and non-domestic buildings in three different regions were assumed to have PV systems. This represents 332,385 houses with PV, 9940 non-domestic buildings with PV on roofs and 4070 non-domestic buildings with PV façade systems and represents a total PV capacity of 1179 MW. By including 1179 MW of PV in the network reserve requirement levels were calculated using the corresponding load demand profile for the three regions. The required maximum additional reserve requirement level was calculated as 230 MW. It is worth noting that load demand for these three regions is 35% of the total load demand in England and Wales. The total load demand is the aggregation of load demand in all regions and that represents reduction of load fluctuation in each region. Similarly aggregating PV output from different regions will reduce the fluctuation of PV output in each region. Therefore reserve requirement levels should ideally be calculated using the aggregated load demand profile and aggregated PV output power from all regions.

In order to illustrate this, the reserve requirement was analysed by the following three steps:

Step 1: Analysis of reserve requirement using PV output for three regions and aggregated total national load demand data. For this one-year data from London 1, West Midlands 1 and South West 1 locations PV data were used.

Step 2: Analysis of reserve requirement using different locations within a region and the regional load demand data. For this June month PV data from London 1 and London 2 locations in the London region was used.

Step 3: Analysis of reserve requirement using aggregated PV output from 5 different regions and aggregated total national load demand data. For this PV data for June from London 1, West Midlands 1, South West 1, South West 2 and North East 1 locations were used.

Step 1

By assuming that 1179 MW of PV systems was included in the national network, the additional reserve requirement level was calculated with national load demand data, instead of using load demand for three regions. The additional reserve requirement for the minimum summer load profile is shown in Figure 6-21 and for the maximum winter load profile is shown in Figure 6-22. When the total load demand was considered, additional reserve requirement is reduced at least by half compared with when three locations load demand data was used.

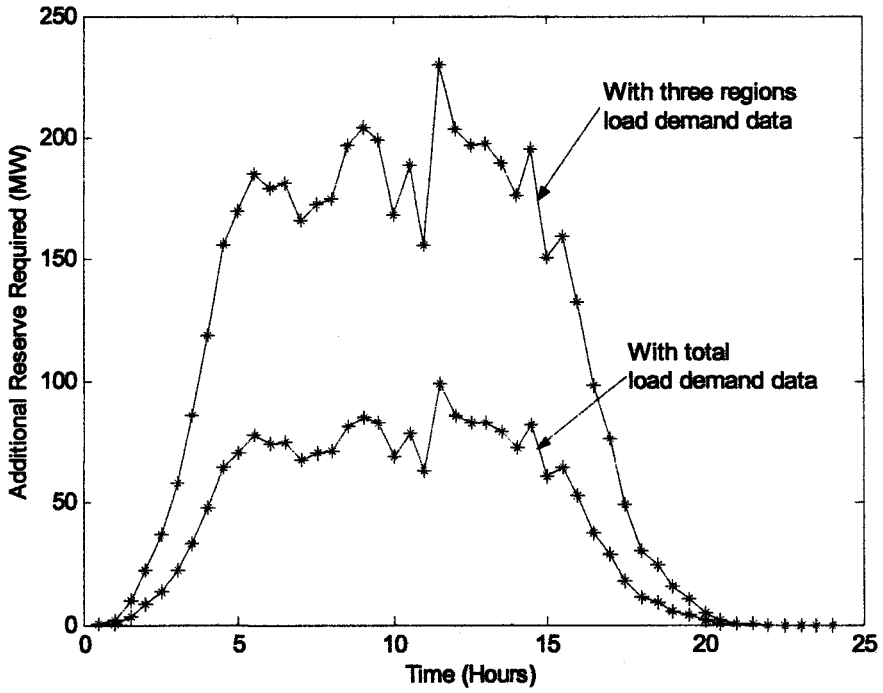

Figure 6-21 Change in additional reserve required for minimum summer load demand profile

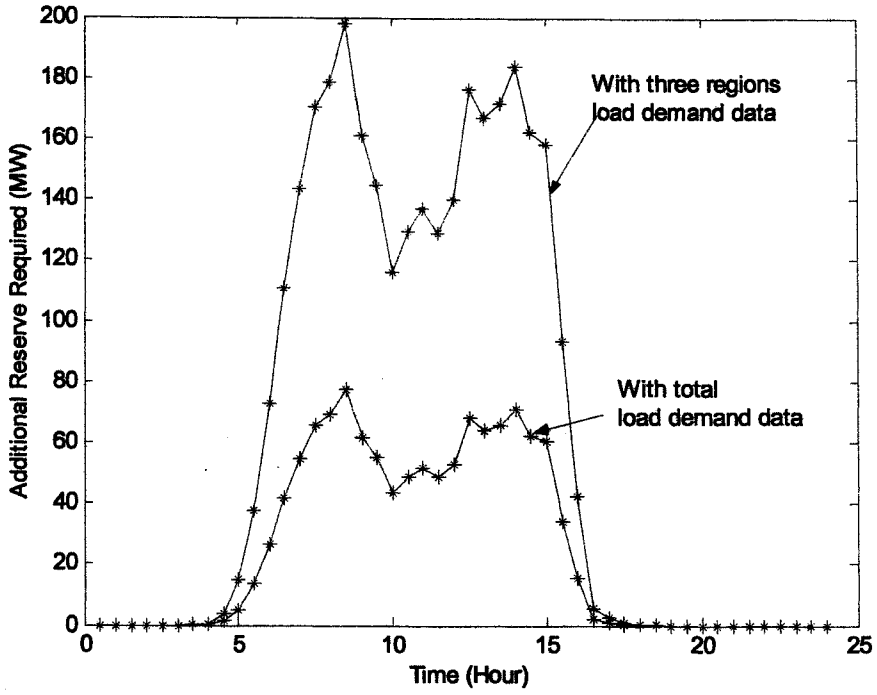

Figure 6-22 Change in additional reserve requirement for maximum winter load profile

Step 2

The above analysis shows the change in additional reserve requirement by considering the total load demand, but considering the PV output power from only three locations. By aggregating output power from different locations in the region, fluctuation and hence reserve requirement will be reduced. In the above analysis London region represents 136,855 houses with PV on roofs, 4745 non-domestic buildings with PV on roofs, 1920 non-domestic buildings with PV on facades. These systems represent a total land area of 15 km^2, assuming all PV systems are placed close to each other. In practise these systems will be dispersed and correlation will be decreased within these distances. But solar radiation data from only one location was used to calculate the standard deviation of PV output power for London region. By combining the PV output from different locations in the region, fluctuation of PV output and hence the reserve requirement will be reduced.

In order to illustrate this, June data from the London 1 and London 2 locations were used. The distance between the London 1 and London 2 locations is 17 km. It was considered that these two locations are in the same region (London). It is worth

noting that the correlation coefficient between these locations is high. It was assumed that 6% of houses and non-domestic buildings in the London region have PV systems. The load demand for the London region is 15% of the total load demand in the England and Wales. By using only the London 1 location, the additional reserve requirement for minimum summer load profile was calculated. Then, by assuming 3% of houses and non-domestic buildings in the region in the London 1 location and 3% of houses and non-domestic buildings in the London 2 location, the additional reserve requirement was calculated. These results were compared and shown in Figure 6-23 indicates that the reserve requirement was slightly reduced by combining different locations in the region.

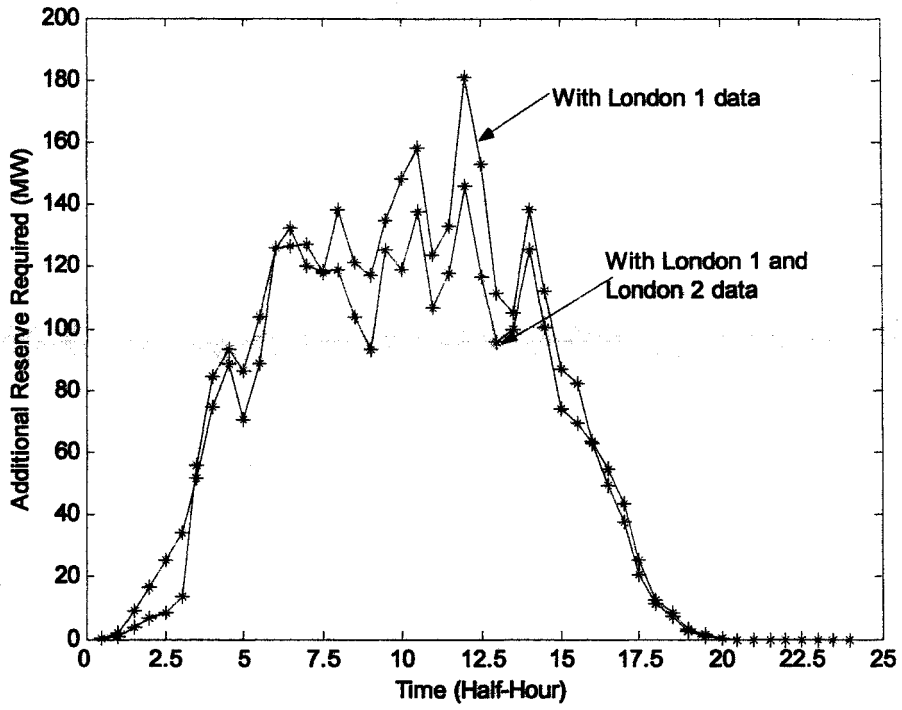

Figure 6-23 Additional Reserve Required for the London Region

Step 3

The above analysis was carried out to show the change in additional reserve requirement by combining different locations in the region, for which correlation is substantially high. The correlation of solar radiation for different regions will be less and hence by combining PV output power from all regions fluctuation will be reduced. Hence the additional reserve requirement by combining PV output from different regions PV output with the aggregated total load demand profile will be

reduced. To illustrate this June data from five locations (London 1, West Midlands 1, North East 1, South West 1 and South West 2) were used. It was assumed that in each region 1% of England and Wales dwellings are provided with PV, representing a total PV capacity of 2385 MW (5 times of 477 MW). The combined output power from all 5 regions was calculated and, from these values, the additional reserve required for summer load profiles was calculated and is shown in Figure 6-24. When the PV output from only three locations and the load demand from three regions were used, the maximum additional reserve required for the summer season by adding 1179 MW of PV capacity was calculated as 230 MW. When combining PV output for June for five different regions and the total load demand profile, the maximum additional reserve required for summer season by adding 2385 MW of PV capacity was calculated as 245 MW.

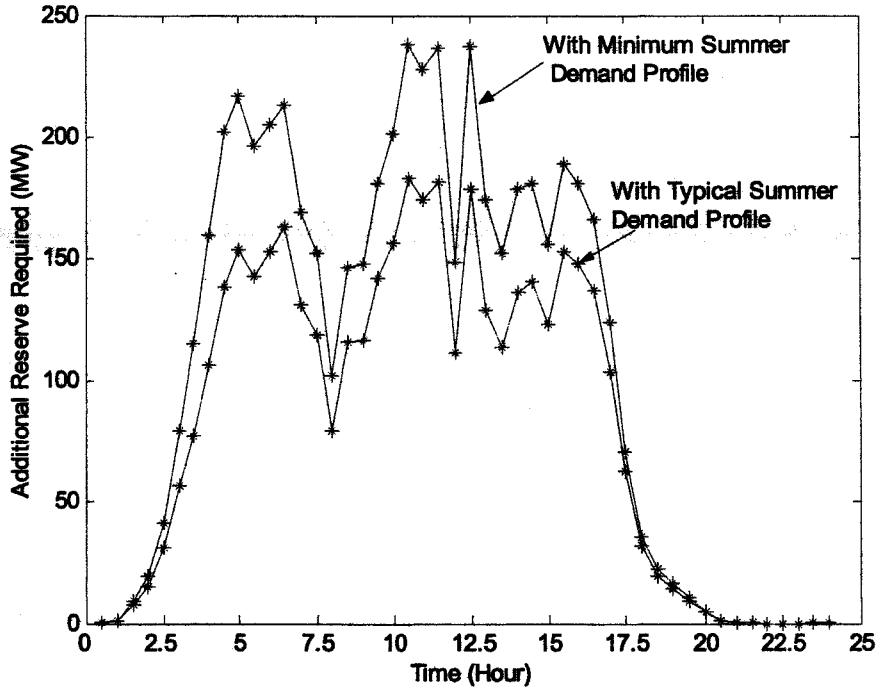

Figure 6-24 Additional reserve requirement for June, using data for five locations

Results from these analyses clearly indicate that reserve requirement is not "MW of reserve per MW of PV Capacity" rather it will be based on aggregated load demand and PV output from all regions [5].

6.4.3 Prediction of PV output power

As shown in Figure 6-19, the additional reserve requirement for the winter season was high at 08:00 and 14:00. This is due to the maximum change in output power from PV systems because of sunrise and sunset behaviour. By forecasting the weather for the day these changes can be easily predictable. In all the above analysis fluctuation of output power in four-hour time period was calculated from half hour power series assuming the weather profile for the day cannot be predicted. If it is predictable, the amount of additional reserve requirement can be reduced. It is worth noting that NGC already uses the weather profile to forecast the load demand for the next day [4]. The following explanation illustrates the reduction in reserve requirement by predicting the weather pattern of the day. If the weather pattern of the day is predictable a different approach can be applied which is illustrated in Figure 6-25.

Using data from all the clear days in the summer season an average power profile for clear days can be calculated. In this analysis, data for 18 clear days were used to construct the average power profile for clear days. From this average profile, for a clear day, an expected change in output power from 07:00 to 11:00 can be calculated. The difference between actual power fluctuation and expected change in output power will be the error in predicting PV output. This can be carried out for different times of the day and for all clear days. These values can be used to calculate the reserve requirement. It is worth noting that the magnitude of the average profile for whole summer season is lower compared with the average profile for clear days shown in Figure 6-26. Hence the calculation of output power fluctuation from the average profile for all days for the summer season will have more errors. In this analysis the average profile for clear days was used to calculate the error in predicting PV output.

The reserve requirement by adding 1179 MW of PV capacity (radiation data from three locations and load demand profile from three regions) was calculated for clear days in the summer season. These results are compared with the additional reserve required for the summer season when the weather pattern of the day is not predictable and shown in Figure 6-27 (a) and Figure 6-27 (b). This clearly indicates

that reserve requirement levels are reduced considerably during the morning and evening periods compared with the additional reserve required when the weather pattern is not predictable. It can be observed that the additional reserve requirements are high during the noon period only.

Similar analysis was carried out for poor days in the winter season. In this analysis data for 9 poor days in the winter season were used to construct the average power profile. If the day is predictable as a poor day, the additional reserve requirement for the winter season was calculated and is shown in Figure 6-28 (a). When the weather profile is not predictable, the additional reserve requirement for winter season is shown in Figure 6-28 (b). This clearly indicates that additional reserve requirement levels were very low for poor weather days. These results indicate that reserve requirement levels and the duration of reserve requirement will be reduced if the day is predictable. There is no much change in the additional reserve requirement between the maximum and typical winter profiles. It should be noted that, in this analysis, profiles for only 18 clear days and 9 poor days were used. This issue should be studied with data from more years to improve the accuracy of the results.

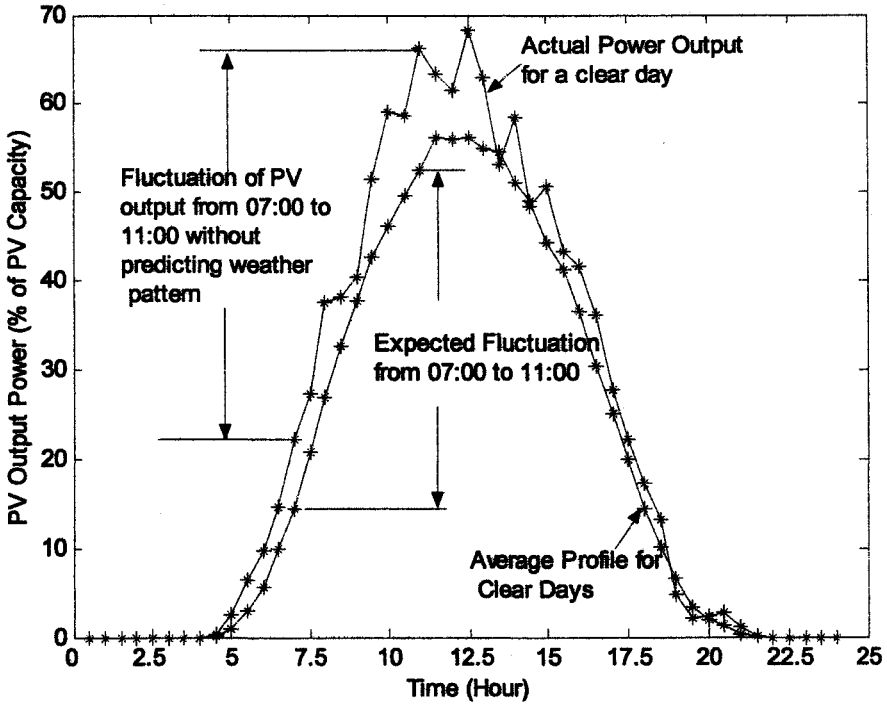

Figure 6-25 Illustration of error in predicting PV output power fluctuation

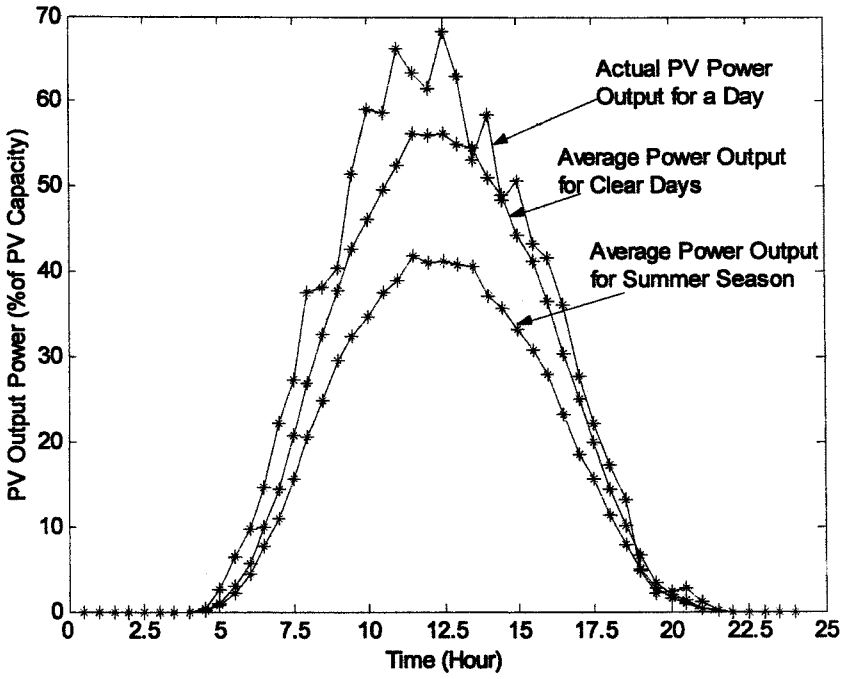

Figure 6-26 Comparison of average PV output for summer season with average PV profile for clear days

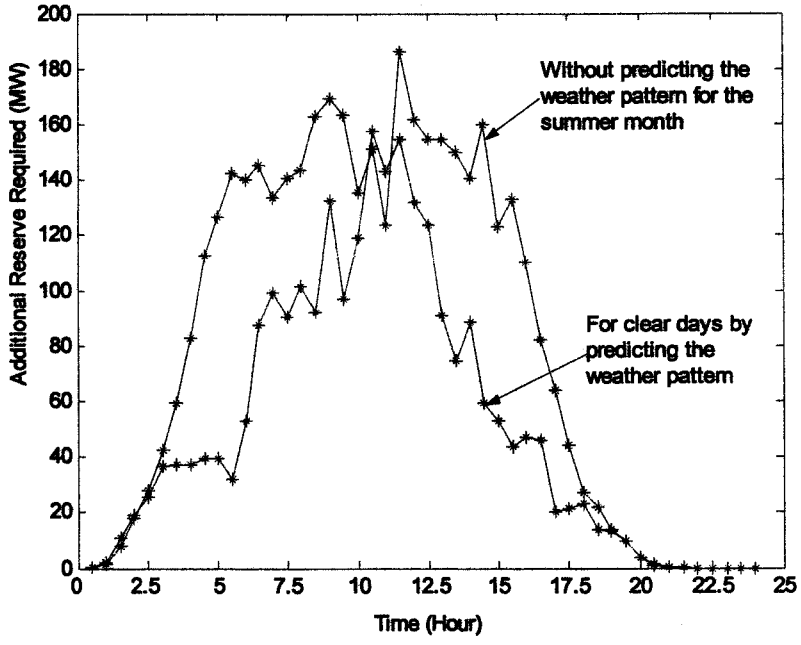

a) Additional reserve requirement for the typical load demand profile in the summer season

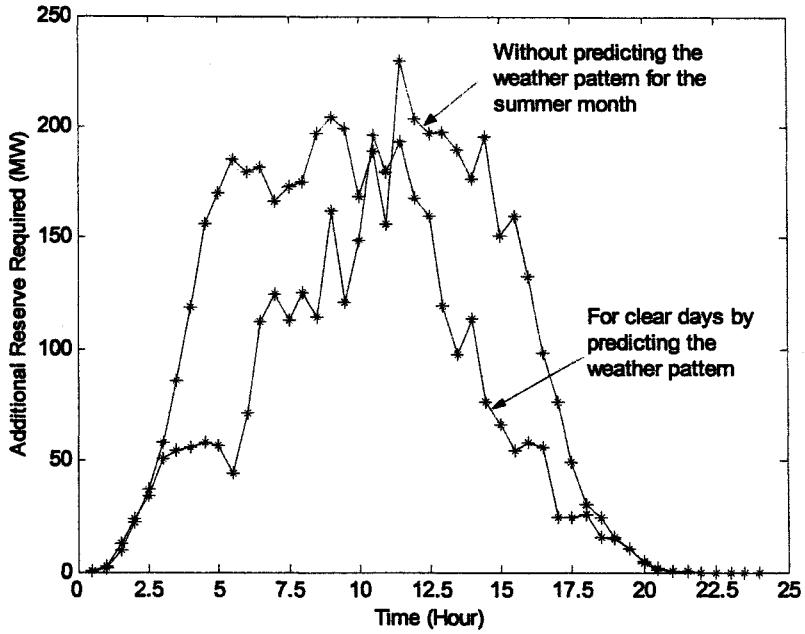

b) Additional reserve requirement for the minimum load profile in the summer season

Figure 6-27 Change in additional reserve requirement by predicting weather pattern of the day

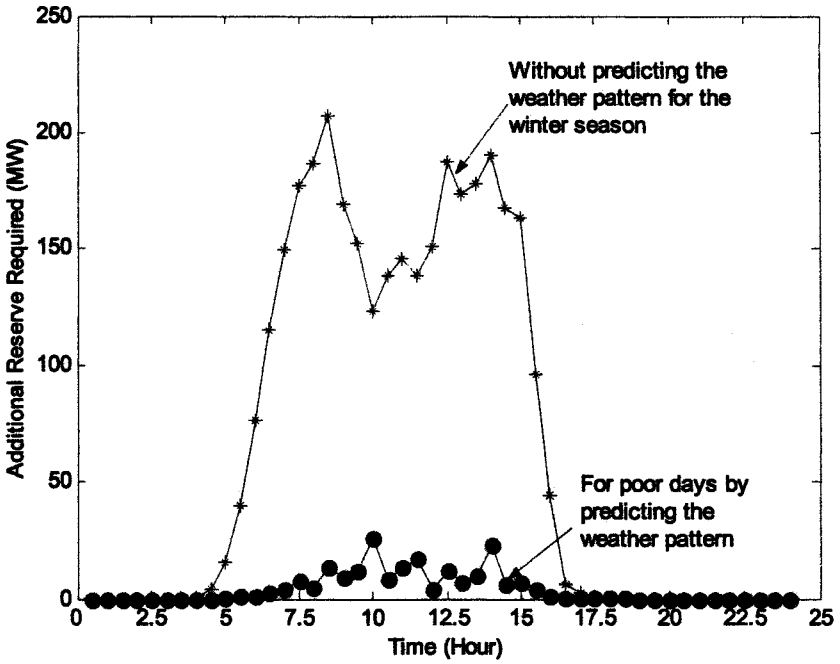

a) Additional reserve requirement for the typical load demand profile in the winter season

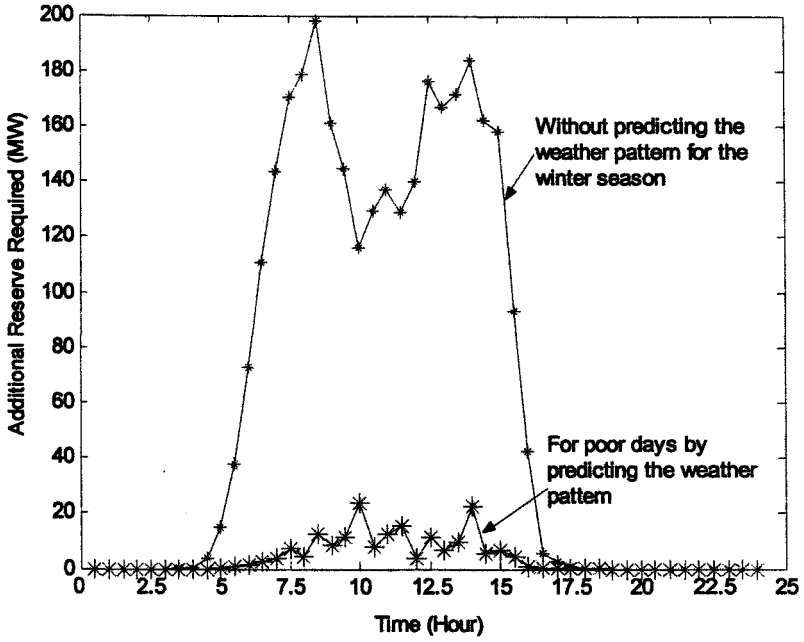

b) Additional reserve requirement for the maximum load demand profile in the winter season

Figure 6-28 Change in additional reserve requirement for poor day in winter season, by predicting weather pattern of the day

6.4.4 Correlation of demand and PV generation

The above analysis considered demand forecast error and PV output power fluctuation, but correlation between PV output power and load demand was not considered. If the correlation of demand and PV output power is positive, i.e., if there is a probability of PV output power and load demand increases at the same instant, the net total standard deviation value will be reduced.

Figure 6-29 shows typical load demand profile and average PV output power for the summer season. During morning hours in the summer season, demand and PV output power increases and hence the correlation between the demand and PV output power exists. But in the afternoon the correlation between demand and PV output power is reduced. Figure 6-30 shows load demand profile and average PV output power profile for the winter season. Correlation between demand and PV generation is low in the winter season. The correlation value will change with time of the day and may vary for each day. Hence, since the load demand profile for each day is not available,

it was not possible to carry out this study in detail. If these values are known, the reserve requirement can be calculated using the equation 6.1.

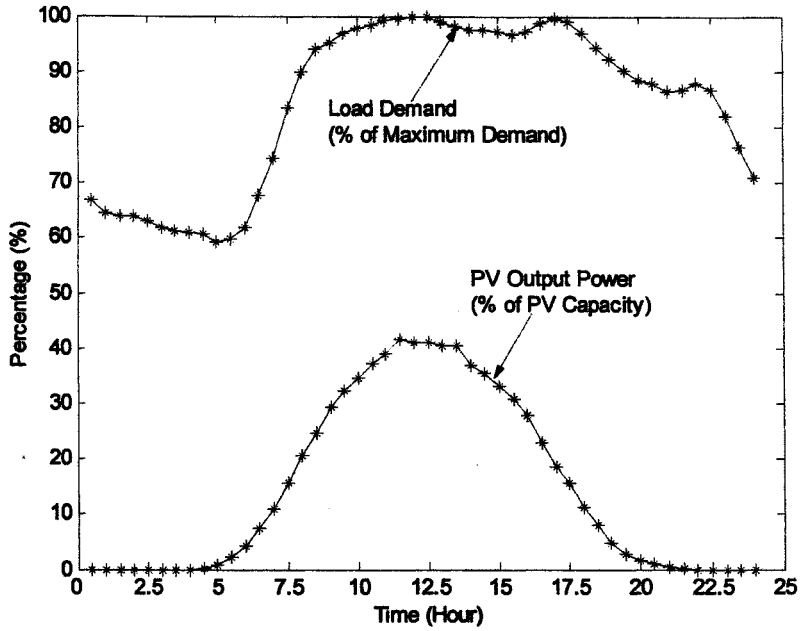

Figure 6-29 Comparison of load demand profile and average PV output power profile for the summer season

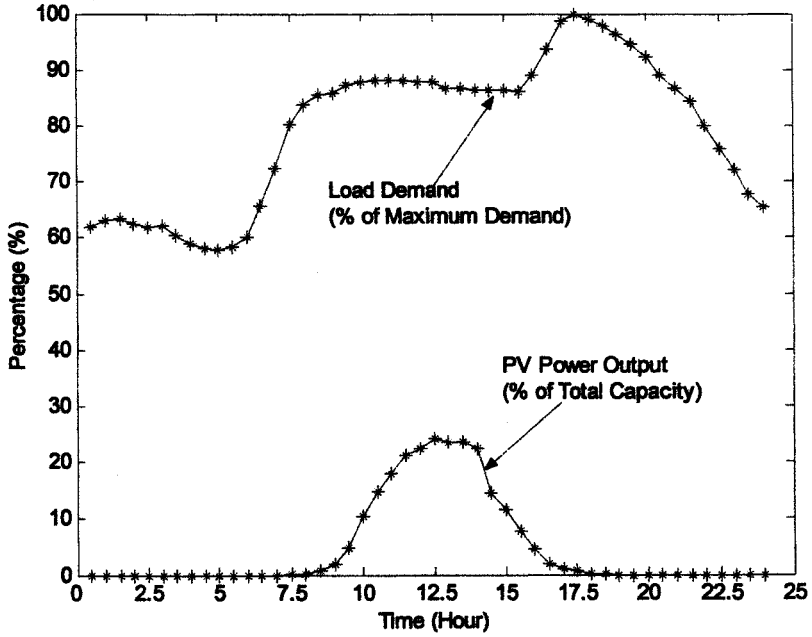

Figure 6-30 Comparison of load demand profile and average PV output power profile for the winter season

In all the above analysis (section 6.4.1 to 6.4.4) factors that will affect the reserve requirement level in the present network were analysed. The penetration of PV systems in the network will increase in the medium to long term. During this period there will be changes in load profile and operation strategies in the present network that will affect the reserve requirements. These factors and their influence on reserve requirements are discussed in the following section.

6.4.5 Future network

Different Energy Sources

In practise there will be different renewable sources like PV, wind, biomass energy, wave and tidal added to the grid. Some of these energy sources like PV, wind and tidal are intermittent power sources. By combining the output from all these renewable sources, the intermittency of output power may be reduced or increased depending on the correlation between the sources. For example, there is the probability that wind output power is lower in summer while PV output is higher in the summer. Hence there may be a decrease in the output power fluctuation by combining output from PV and wind systems. There are energy sources like biomass energy from crops that can be controllable and dispatched and which can help to smooth the output power. The UK government has a target for Combined Heat and Power (CHP) generation of at least 10,000 MW by 2010 [10]. In the winter the heat demand will be high and hence electricity production from a CHP system will be high. In the winter PV systems will produce less output. In the summer, the average household uses less heating and hence electricity production will be less. PV systems can produce high output power during summer periods. Hence combined CHP and PV systems may match the load demand throughout the year. These conditions will reduce the reserve requirements. The Royal Commission on Environmental Pollution (RCEP) recommended the government to study the policy to promote the use of Combined Heat and Power (CHP) as a spinning reserve to back-up intermittent renewable energy sources [10]. Therefore by selecting a proper energy mix from different sources, the power flow can be smoothed.

Change in Load Demand

Energy is often wasted because of poorly insulated buildings or where heating and lighting are poorly controlled. For example, energy saving light bulbs use less than a quarter of the energy of ordinary light bulbs [11]. Therefore UK government has programmes to improve the energy efficiency by providing efficient boiler types, insulating walls and installing energy saving lights [11]. Because of these energy efficiency programmes, the load profile on the future network will be different. For example, energy consumption due to thermal load will be reduced by energy efficiency programmes along with usage of micro-CHP and small-scale renewable heat such as solar water heating etc. Therefore, demand for thermal energy in the buildings will no longer grow substantially in the future [12].

According to the National Grid, there has been a growth of 5% in air conditioning in the commercial sector in the last five years. It expects to see a further 6% growth in the period to 2010 [13]. There is likely to be a rise in the residential market, but this is speculative at the moment as it also depends on complex socio-economic factors. These changes will change the load demand profile. Historical and projected changes in the minimum load demand profile on the UK electricity system are shown in Figure 6-31. This clearly indicates that in long term minimum load demand is expected to increase. This will affect the additional reserve required for the summer season. The amount of reduction in reserve requirement depends upon the magnitude of the minimum load demand. It is also worth noting that if the load requirement by air conditioning units has good correlation with PV output profile, reserve requirement levels will be further reduced.

Different Strategies

As noted before, NGC believes that sufficient response and reserve services will be available for a situation in which the entire 2010 renewable target is met by wind-powered plant. However, an increase in penetration level will require additional reserve levels. At present the electricity network is a passive network, where the power flow is always from high voltage to low voltage levels. However the extensive penetration of PV systems will result in an active network, where the power flow will

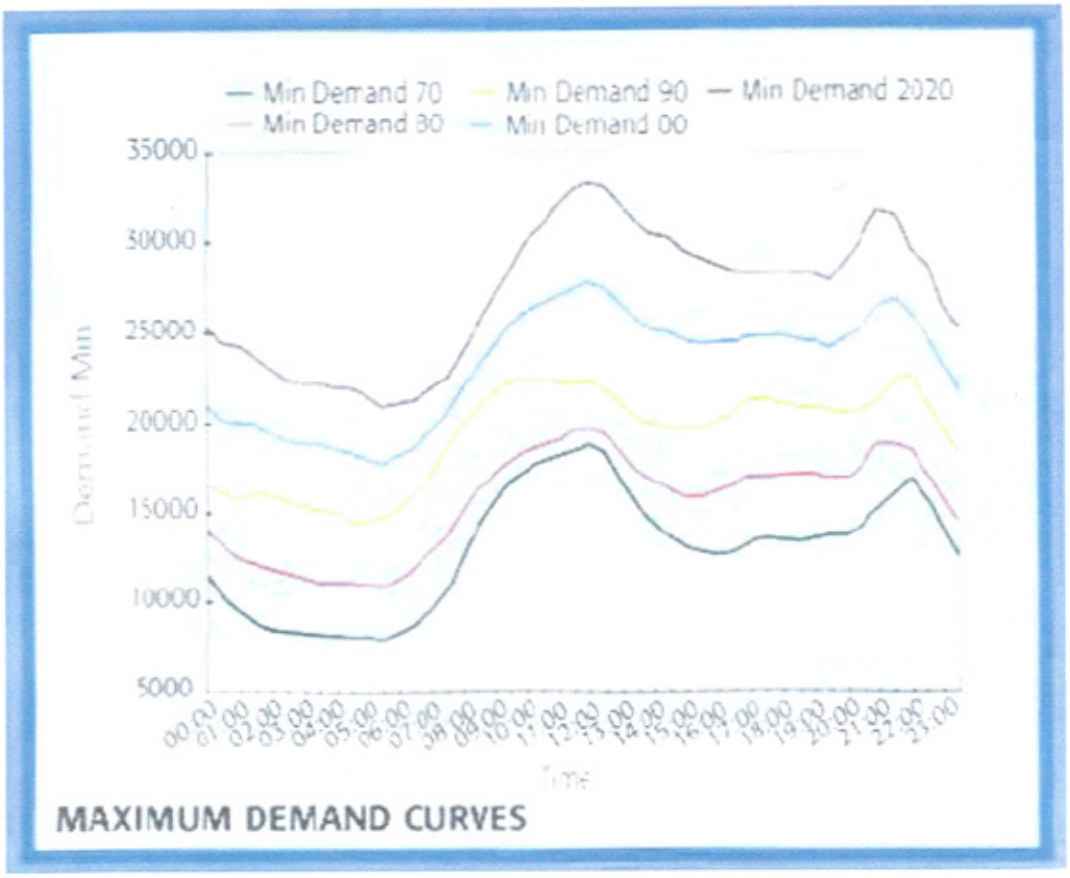

Figure 6-31 Changes in minimum load demand in the UK electricity network (Source: IEE Power Engineer Magazine [12])

become bidirectional. When the network is active there may be changes in the way that the system is secured.

In this work, the requirement for conventional generators as reserve to keep the system in balance was discussed. In this method system balance will be maintained by controlling power flow in the network by adjusting generation. The most likely reserve in the short term will be coal plant, but Combined Cycle Gas Turbine (CCGT) will be increasingly used for this purpose [5]. Apart from this method there are two more possible methods, Demand Side Management (DSM) and storage [5,7], which can be used to balance demand and generation. By the DSM method, the balance of demand and generation is obtained by controlling load demand on the network. Load management could reduce the power fluctuation on the grid and can be used to reduce the magnitude of reserve requirements. As explained before, load

shedding is already a reserve service for which NGC contract and which can compete with reserve offered by generators.

Using storage methods, power produced during an off-peak period will be stored and it can be used during a peak demand period or during the shortage of generation. There are short term (seconds to minutes) storage devices such as flywheels, ultra capacitors and medium term storage devices (minutes to hours) like pumped hydro storage and long-term storage methods (days) like hydrogen storage. In the UK, 2800 MW of pumped storage plants are used for load levelling, peak lopping and also used as fast response spinning reserve [5]. Recent improvements in storage technologies show that these methods may be a viable solution for intermittency. For example improvement in hydrogen and regenerative fuel cells technologies present exciting possibilities for the storage of energy. Similarly Kinetic Energy Storage System (KESS) developed by Urenco Power Technologies stores 14 MJ of energy, of which up to 11MJ of energy can be usefully used depending upon the application [14]. This flywheel system can provide maximum power in less than 5 milliseconds.

A NGC report on the future network suggests that energy storage methods would considerably ease the problems of incorporating intermittent renewable energy sources [8]. Woyte et al. [15] have investigated the fluctuation of solar radiation and indicated the suitability of storage methods to control the voltage on a theoretical basis. Small autonomous PV/Diesel/Battery hybrid systems and autonomous PV/Electrolyser/ Fuel cells hybrid systems have been explored, but effective implementation on larger systems has not yet been accomplished. At present providing the reserve requirement by conventional power generation and DSM are considered as the most economical [5,7]. The system balance by matching load demand and generation can be obtained by the methods explained. Selecting a suitable method depends upon the magnitude, duration and frequency of the intermittency. By selecting a suitable method, a balance of load demand and generation can be achieved and the level of PV penetration on the grid can be increased.

6.5 Discussion

The fluctuation of solar radiation and hence PV output power fluctuation was analysed. Output power fluctuation from a PV system depends upon the variation in solar radiation, which occurs due to cloud transients. This variation in solar radiation does not occur simultaneously in all locations. Hence by combining spatially dispersed PV systems, the fluctuation of PV output power can be reduced. The correlation of tilted radiation values depends upon distance between locations, time period considered and season. Therefore the smoothing effect also depends upon the size of the area (distance of separation between locations) and the time interval considered.

The standard deviation of PV output power fluctuation was calculated for each season with respect to time of the day using half-hour time interval data. Even though the average output power is lower for winter season, the standard deviation of half-hour output power fluctuation was similar for all seasons. The standard deviation of half-hour output power fluctuation is high around noontime. Standard deviation values increased with the increase in time period. By adding data for many locations, for which correlation values are low, standard deviation values were reduced.

The electricity network operators should balance the supply and demand to keep the system in security. There are uncertainties that cause imbalance, which are error in predicting load demand, error in conventional power generation, sudden failure of generators etc. If PV systems are added to the network, the fluctuation of PV output power will provide an additional uncertainty to the system. Therefore the penetration of PV systems may increase the reserve requirement levels. From the reserve requirement analysis, the following points were observed:

- With the present network, 3750 MW of PV capacity can be included without additional reserve requirements. This value was calculated based on PV output power from three locations. NGC has reported that present network has sufficient reserves for a situation in which the entire 2010 target is met by wind.

- Since the correlation of solar radiation between different regions is reduced compared to a single region, the aggregated PV output power from different regions will be smoothed. Therefore reserve requirement levels will be reduced. Hence the additional reserve requirement is not on the basis of "MW of reserve per MW of PV capacity". It is based upon the aggregation of load demand and of PV output from all regions.

- It was observed that the additional reserve requirement because of the PV penetration was highest for summer minimum load condition. It was also observed that for winter season, the duration for which the reserve is required was reduced.

- The prediction of the weather profile of the day will reduce the magnitude and duration of the reserve requirement. This was illustrated for clear days in the summer season and poor days in the winter season. However for a variable day, short-term prediction of PV output power may be necessary. Therefore developing prediction methods will help to increase the penetration of PV sources.

In practise different renewable energy sources and Combined Heat and Power (CHP) energy sources will be added in the network. The combined output power from all these sources may reduce the intermittency. In this analysis load demand profile for the year 2003 was used. In future the load demand profile may change due to implementation of energy efficiency programmes or usage of air-conditioning units etc. These changes will influence the reserve requirement levels due to PV penetration. For example, an increase in air conditioning units will increase the minimum load demand and hence the additional reserve required for the summer season will be reduced.

The RCEP report [10] suggested that by 2050 some 15 million houses might each have a 4 kW PV system installed, representing 60,000 MW. Therefore, in the medium to long term, there will be a substantial increase in PV sources. When the penetration level of PV increases, the network will become more active. In this case

it will be necessary to adopt novel approaches to achieve satisfactory operation. Demand Side Management (DSM) and energy storage methods are viable options to control variability. At present providing conventional generators or the DSM method appear to be the most cost effective routes. In the future, storage methods, such as hydrogen and fuel cell technologies may ease the intermittent problems and may help to increase the value of PV sources. Selecting a suitable method depends upon the duration, frequency and magnitude of intermittency. Selecting suitable methods and control strategies can increase the penetration of PV systems.

6.6 References for Chapter 6

1. "UK Electricity Networks", Post note from Parliamentary Office of Science and Technology, Number 163, October 2001.
2. Andrew Ryan, "NGT's Role in Securing Reserve", National Grid Transco, UK, available from www.nationalgrid.com.
3. G. Hartnell, "Wind on the system – Grid integration of wind power", Renewable Energy World, Vol. 3, No. 2, March – April 2000, pp. 60 – 64.
4. "2004 Seven Year Statement", National Grid Company, UK available at www.nationalgrid.com/uk.
5. "Renewables Network Impact Study Annex 4: Intermittency Literature Survey", The Carbon Trust & DTI, UK, November 2003 available at www.carbontrust.co.uk.
6. Morris Hamburg and Peg Young, "Statistical Analysis for Decision Making", Chapter 5, Sixth Edition, 1994, The Dryden Press, Fort Worth.
7. Ilex Energy Consulting Ltd and Goran Strbac, "Quantifying the system cost of additional renewables in 2020", report submitted to the Department of Trade and Industry, UK, 2002 available at www.dti.gov.uk.
8. "National grid and distributed generation – Facilitating the future", National Grid, UK, September 2001 available at website www.nationalgrid.com.uk.
9. David Milborrow, "The real costs and problems of integrating wind", Blowing Workshop, Belfast, 2001 available at website http://www.ee.qub.ac.uk/blowing/activity/belfast/main.htm.

10. "Biomass as a Renewable Energy Source", Published by the Royal Commission on Environmental Pollution, UK, 2004 available at www.rcep.org.uk.
11. Energy White Paper, "Our Energy Future – creating low carbon economy", HMSO, 2003 available at www.dti.gov.uk.
12. "Renewable energies for sustainable development: Impulses for renewables 2004", Policy paper, German Advisory Council on Global Change, 2004, available at www.wbgu.de.
13. Janet Wood, "The effect of one degree", The IEE Power Engineer Magazine, The Institution of Electrical Engineers, UK, June/July 2003, pp 6-8.
14. Colin Tarrant, "A new move in energy recapture", The IEE Power Engineer Magazine, The Institution of Electrical Engineers, December/January 2003/04, pp. 26-30.
15. A. Woyte, R. Belmans and J. Nijis, "Analysing short-time irradiance fluctuation by their characteristic time scales", 3rd World Conference on Photovoltaic Energy Conversion, Japan 2003.

7 CONCLUSIONS

This is the first study to have developed suitable methods to represent the PV resource and output power from dispersed PV systems, in order to analyse the impact of multiple PV systems on the UK transmission network. In this work, the Markov Transition Matrix (MTM) method was used to generate the synthetic solar radiation. By this method, for the given daily total irradiance values, the different probabilistic distributions of hourly and half-hourly solar radiation values were generated. To represent dispersed PV systems, a detailed PV cluster model was developed instead of using a single optimised PV system to calculate the output power. Solar radiation values were generated for different locations in the UK, to study the combined output power from dispersed PV systems connected to different points on the same network. This method resulted in an approach to determine the probability of variation in the output power from a large number of dispersed PV systems.

Since the output power from a PV system is variable, the inclusion of a high penetration of PV systems may affect the demand and generation balance in the network. This imbalance will affect the system frequency and hence the stability of the system. To ensure system stability, additional reserve generation is needed to balance the demand and generation. This work has studied the change in reserve requirements by the implementation of different PV penetration levels, using the developed cluster model to estimate the output power for different cases. The following section reviews the work carried out.

7.1 Review of the Work

In this work it was found that a single MTM could be used to generate the solar radiation values for four different locations in the UK, instead of constructing a matrix for each location. This is a simpler solution than the construction of a new matrix for each location, because of the low availability of measured data for short time intervals. It was found that the MTM was suitable for representing actual data in terms of both absolute values and variability. In this work, the single yearly MTM was constructed using data from four locations in the UK. The robustness of the

matrix can be improved by adding more data from different locations. To generate the hourly or half-hourly radiation values, the daily total irradiation values are given as an input for each location and the correlation of solar radiation between locations was not considered (possible further work in this area is outlined in section 7.2).

The standard Hay model was validated to translate the horizontal radiation to tilted radiation values. The calculated tilted radiation values from the model gave good fit with the measured values for all months except winter months. The error in calculating tilted radiation values is high in winter months, particularly for the systems with high tilt angles. However, the output power from the winter season will be low and hence the impact on the grid will be reduced.

To calculate the output power from multiple PV systems, assuming a single optimised PV system does not represent the variation of design parameters in the dispersed PV systems. In this work, a detailed PV cluster model was developed, and the model considered the possible changes in the system design parameters to the year 2030, to analyse the impact of large-scale assimilation of PV systems. Whilst the model was developed using the national statistics, regional characteristics can be incorporated to calculate the regional output. The cluster model can be used to obtain the output power from dispersed PV systems in each region and for different PV penetration levels.

The output power calculated from the cluster model was used to study the fluctuation of PV output power. The maximum half-hourly output power fluctuation was observed as 60% of PV capacity for a single location and it was reduced to 35% of PV capacity for the ensemble (consists of 3 locations). The correlation of solar radiation values between different locations was low for days with variable weather conditions. The correlation of solar radiation was high for stable days but the fluctuation of radiation values were low. These results indicate that by combining the output power from different locations, the fluctuation will be reduced and hence it will have less impact on the system stability.

In this work, the requirement of additional reserve generation to ensure system stability for large-scale penetration of PV systems was analysed. From the statistical

analysis it was found that for the inclusion of 1179 MW of PV systems, the additional reserve required for the winter season was calculated as 200 MW. That is 17% of PV capacity and this is slightly higher for the summer season. These calculations were based on the assumption that the network has reserve capacity only to meet the demand forecast error. In practice, the network will have more reserve to meet sudden changes such as loss of a large generating plant. According to the NGC, with the present reserve availability in the UK network, intermittent generators with a capacity such that the potential loss is less than 1500MW in an hour can be added without additional reserves. Using this criterion, it was found that 3750 MW of PV systems could be installed in the present network without additional reserve requirement. The increase in the penetration level above this limit will increase the reserve requirement in the absence of other measures. But the increase is not on the basis of "MW of reserve per MW of PV capacity", rather it is based on the aggregation of load demand and of PV output from all regions. By predicting the weather pattern of the day, the additional reserve required in the winter season was calculated as 2% of PV capacity. Thus the reserve requirement was reduced by a factor of 8, by forecasting the weather pattern of the day.

By predicting the weather pattern of the day, for the summer season, the duration for which the additional reserve required will also be reduced. The additional reserve required was found to be high only during the noontime. There are methods existing to forecast the short-term solar radiation values, which can also be implemented to estimate the expected change in fluctuation, and the reserve requirement will be reduced. In the summer season, the output power from PV systems is high and the load on the system is low. This leads to high reserve requirement levels in the noontime. But there is an increasing trend in the usage of air conditioning that will increase the minimum load level and thus reduce the reserve level. The amount of reduction in the reserve level depends on the change in load demand profile.

The output power produced during minimum load conditions can be stored and can be used during peak load periods or when there is no generation from PV systems. Recent developments in hydrogen storage and fuel cell technologies will help to reduce the reserve requirement levels in the summer season. Apart from controlling the generation, load also can be controlled to balance the generation and demand

(known as Demand Side Management DSM). The penetration level of PV systems can be increased, by selecting suitable methods to balance the demand and generation.

7.2 Further Work

As explained before, the aggregation of output power from many locations and regions will reduce the fluctuation of PV output power. To study the reserve requirement, knowledge of the combined output power of dispersed PV systems is necessary. But the measured short term solar radiation data are not available for many locations. From the correlation analysis, it was found that the correlation coefficient values from closely spaced sites, less than 50 km, are high. Hence, if the solar radiation values are available for only one location in the cluster, the correlation of solar radiation values can be used to extrapolate the solar radiation values for other locations in the cluster. These values can be used to study the combined output power from the cluster.

In this work, the solar radiation data was generated for different locations by providing the daily total irradiance values for each location. The solar radiation values for one cluster can be correlated to other neighbouring clusters using the correlation coefficient values. Then, the combined output power from all the locations and clusters can be used to study the variation of PV output power. This analysis was not carried out in this work due to data unavailability and time limitations. Thus, further work on generating solar radiation data should include the development of data for different locations by the MTM method by considering the correlation between locations.

In this work, it was illustrated that if the weather pattern of the day is predictable then the reserve requirement can be reduced. However, for a day with variable weather conditions, prediction of PV output power for shorter time intervals may be necessary. Therefore, developing or adopting methods to predict the weather pattern of the day and predicting output power from PV systems for short time intervals will be an important study. The prediction of combined output power from many PV

systems distributed in a large geographical area is necessary. If the weather pattern is predicted for few sites then it can be extrapolated to different sites by the MTM approach, using the correlation values. By predicting the combined output power, the penetration of PV systems can be increased with minimum increase in system cost. To summarise, further work on the reserve requirement analysis should include the development or adoption of existing methods to forecast the solar radiation values and extrapolate them to different locations by the MTM approach. This will help to increase the PV penetration level with less reserve requirement.

7.3 Summary

Using data from 3 locations in the UK, the maximum hourly PV output power fluctuation was calculated as 40% of PV capacity. Using this value, the PV capacity that can be added to the existing network was calculated as 3750 MW (7.5% of maximum demand of 50,000) without additional reserve requirements. For a typical PV system in the UK, the amount of energy that can be produced in a year is 800 kWh/kW PV capacity. Using this value, the amount of energy that can be produced from a PV capacity of 3750 MW is 3 TWh. This is equivalent to almost 1% of the total electricity demand for the UK (350 TWh).

Using the June data from 5 locations (data set I) the maximum change in the output power was calculated as 20% of PV capacity. Using the data from 12 locations in the UK (data set II) the maximum increase in the output power was calculated as 21% of PV capacity and the maximum decrease in the output power was calculated as 36% of PV capacity. Even though there are 12 locations providing data, these locations represent 6 regions only. The change in output power above 30% occurred only 10 times in the year. Also, the maximum decrease in the output power occurred during the sunset period of the winter month. This transition is fully predictable and the system operators can schedule the generation and hence this transition does not need any reserve.

If the output power values from many regions are added the maximum fluctuation will be lower than these values. Considering the maximum fluctuation of 20% of PV capacity, the PV capacity that can be added to the present systems without additional reserve requirement is 7500 MW (15% of maximum demand of 50,000). The amount of energy that can be produced from these systems is equivalent to almost 2% of the total UK electricity demand.

If the capacity of PV systems is increased, additional reserve requirements are needed to keep the system in balance. The additional reserve requirement was calculated as 17% of PV capacity for the inclusion of 1179 MW. This value will increase with the increase in PV system capacity. For the inclusion of an additional 15,000 MW of PV systems in the system (7,500+15,000 =22,500 MW) and assuming the reserve requirement as 30% of PV capacity, the reserve requirement is 4500 MW.

For the winter season, if the weather pattern of the day is predictable, the additional reserve requirement will be reduced by a factor of 8. Then the reserve requirement for the winter season (= 4500/8) is 562.5 MW. This reserve level is also required only for a short time, particularly for the noontime. In the summer season, if the weather pattern of the day is predictable, 4500 MW of reserve is needed only during the noontime. Methods to forecast the short term variation of solar radiation can be applied and the amount of additional reserve level required will be reduced. The amount of reduction in the reserve requirement by forecasting the short term variation needs to be quantified. The growing air conditioning usage will increase the load demand in the summer season and this will reduce the required reserve level.

The combination of available pumped storage plus spinning reserve must be sufficient to keep the system frequency within acceptable limits and to maintain the system stability. As noted before, in the UK, 2800 MW of pumped storage plants are used for load levelling and also used as fast response spinning reserves. These existing pumped storage plants are operating at low load factor and hence these plants can be utilised to facilitate the PV penetration levels and the additional reserve requirement will be reduced. In addition to this, system operators can exploit the existing HVDC link with France (2000 MW) and the proposed link with Norway (1200 MW) and Netherlands (1000 MW) to trade the power. In power systems with

large hydro generation, more intermittent energy sources can be added because they can deliver back-up power more rapidly. Hence, PV output power can be traded with systems having substantial hydro plant such as Norway that generates around 99% of electricity from hydro plants.

Hence, a PV capacity of 22,500 MW that can generate a little over 5% of the UK electricity demand can be added to the grid with minimum increase in the system cost. The penetration of PV systems can be further increased by using the storage methods and Demand Side Management method, with minimum increase in the reserve requirement. Therefore, the variation of PV output is unlikely to be a threat to the system security.

APPENDIX A – MARKOV TRANSITION MATRIX

A1 Yearly Instantaneous MTM Method

The Transition Number Matrix constructed by using hourly instantaneous data is given in Table A- 1. From the number of transitions in each event, the transition probability was calculated and the resulting yearly instantaneous MTM is given in Table A- 2. The Limiting Transition Matrix (LTM) from the yearly instantaneous MTM is given in Table A- 3. Limiting state probabilities from LTM and Marginal Probability values from measured data were compared and are given in Table A- 4.

A2 Monthly Instantaneous MTM Method

The instantaneous MTM for the month of June and the resulting Limiting Transition Matrix are shown in Table A- 5 and Table A- 6 respectively.

A3 Yearly Average MTM Method

The Transition Number Matrix and the resulting yearly average MTM are shown in Table A- 7 and Table A- 8 respectively. The Limiting Transition Matrix obtained from the yearly average MTM is given in Table A- 9.

A4 Yearly average UK MTM

Using hourly average data from four different locations in the UK, the yearly average UK MTM was constructed and is shown in Table A- 10. The resulting Limiting State Transition Matrix from the yearly average UK MTM is shown in Table A- 11.

A5 Yearly half-hour average UK MTM

Using half-hour average data from four different locations in the UK, the yearly half-hour average UK MTM was constructed and is shown in Table A- 12. The resulting Limiting Transition Matrix from the yearly half-hour average UK MTM is shown in Table A- 13.

Table A- 1 Transition Number Matrix using yearly instantaneous data

	State 1	State 2	State 3	State 4	State 5	State 6	State 7	State 8	State 9	State 10	State 11	State 12	State 13	State 14	State 15	State 16	State 17	State 18	State 19	State 20	State 21	State 22	State 23	State 24	State 25
State 1	218	121	37	22	9	9	2	2	4	2	0	1	1	0	1	0	0	0	1	0	0	0	0	0	0
State 2	287	405	242	128	49	38	21	17	7	4	2	3	3	2	1	3	0	3	2	3	2	1	1	0	0
State 3	107	372	345	222	115	64	50	35	33	15	11	9	5	6	6	2	2	3	3	1	3	2	0	1	2
State 4	64	225	303	251	193	128	95	53	36	31	25	8	11	6	6	6	7	8	7	5	7	6	2	3	1
State 5	38	157	235	219	212	167	107	89	57	33	26	19	23	13	14	10	12	9	11	9	10	2	5	2	4
State 6	24	90	136	185	189	162	138	98	57	54	39	20	19	17	12	12	18	14	9	11	9	12	5	9	4
State 7	15	57	84	141	165	164	134	101	77	46	41	37	24	18	17	13	19	18	17	11	15	11	10	3	4
State 8	9	44	60	108	104	119	131	102	87	80	33	23	25	19	22	19	17	12	24	15	15	7	13	4	2
State 9	7	29	60	65	79	83	86	85	56	58	37	27	21	22	23	19	17	17	13	16	12	9	7	6	8
State 10	4	16	47	69	69	80	74	59	49	50	37	25	18	14	20	20	15	16	15	17	12	11	7	7	5
State 11	2	15	31	32	46	59	49	61	46	38	23	25	18	21	13	9	15	14	20	11	9	8	5	3	2
State 12	1	6	20	27	34	37	47	46	53	45	24	22	25	18	26	14	14	16	10	18	12	7	4	3	1
State 13	2	7	17	19	34	30	35	36	43	62	40	39	16	13	16	14	10	16	10	8	2	2	3	3	2
State 14	0	5	14	24	26	18	20	28	30	34	48	46	42	23	18	12	13	12	11	8	6	2	2	0	0
State 15	2	3	10	20	19	27	27	28	24	23	29	37	62	65	31	31	16	20	19	8	6	2	5	4	1
State 16	2	4	9	18	26	18	22	21	13	14	14	25	32	57	76	49	32	25	10	11	8	6	2	4	2
State 17	1	2	8	9	17	24	28	20	16	17	10	16	12	26	70	97	65	37	16	15	5	5	4	3	1
State 18	2	4	6	10	22	20	21	20	14	28	15	16	16	19	27	48	103	141	72	27	12	8	3	6	1
State 19	0	3	7	11	13	17	29	23	24	12	14	9	14	15	17	30	30	114	182	60	20	16	11	4	2
State 20	1	0	7	5	14	19	23	21	24	14	7	10	13	4	18	15	16	35	75	53	29	16	11	4	2
State 21	0	2	2	4	26	19	19	13	12	8	10	8	8	6	5	9	12	39	30	26	21	12	6	3	9
State 22	0	2	3	3	10	18	9	17	11	10	11	9	5	6	11	8	17	13	26	17	9	3	3	3	2
State 23	0	1	1	4	12	5	10	13	10	6	6	9	6	7	6	2	2	7	12	9	7	11	9	5	3
State 24	0	2	2	3	7	8	13	6	5	5	4	4	2	4	7	2	4	5	7	8	9	8	4	4	2
State 25	0	1	1	1	6	3	9	13	3	2	0	6	1	3	3	2	2	8	6	6	4	1	1	3	2

Table A- 2 Yearly instantaneous Markov Transition Matrix

	State 1	State 2	State 3	State 4	State 5	State 6	State 7	State 8	State 9	State 10	State 11	State 12	State 13	State 14	State 15	State 16	State 17	State 18	State 19	State 20	State 21	State 22	State 23	State 24	State 25
State 1	0.5070	0.2814	0.0980	0.0512	0.0309	0.0209	0.0047	0.0047	0.0093	0.0047	0.0000	0.0023	0.0023	0.0000	0.0023	0.0000	0.0000	0.0000	0.0023	0.0000	0.0000	0.0000	0.0000	0.0000	0.0000
State 2	0.2360	0.3331	0.1990	0.0997	0.0403	0.0313	0.0173	0.0140	0.0069	0.0033	0.0016	0.0025	0.0025	0.0016	0.0009	0.0025	0.0000	0.0025	0.0016	0.0025	0.0016	0.0009	0.0009	0.0000	0.0000
State 3	0.0757	0.2631	0.2440	0.1570	0.0913	0.0453	0.0354	0.0249	0.0233	0.0106	0.0078	0.0064	0.0035	0.0042	0.0042	0.0014	0.0014	0.0021	0.0021	0.0007	0.0021	0.0014	0.0000	0.0007	0.0014
State 4	0.0430	0.1513	0.2038	0.1688	0.1298	0.0861	0.0639	0.0366	0.0242	0.0208	0.0168	0.0064	0.0074	0.0040	0.0040	0.0040	0.0047	0.0054	0.0047	0.0034	0.0047	0.0040	0.0013	0.0020	0.0007
State 5	0.0256	0.1059	0.1685	0.1477	0.1430	0.1126	0.0722	0.0600	0.0384	0.0223	0.0175	0.0128	0.0155	0.0088	0.0094	0.0067	0.0081	0.0061	0.0074	0.0061	0.0067	0.0013	0.0034	0.0013	0.0027
State 6	0.0179	0.0670	0.1013	0.1378	0.1407	0.1206	0.1028	0.0739	0.0424	0.0402	0.0290	0.0149	0.0141	0.0127	0.0089	0.0089	0.0134	0.0104	0.0067	0.0082	0.0067	0.0089	0.0037	0.0067	0.0030
State 7	0.0121	0.0459	0.0676	0.1134	0.1335	0.1319	0.1078	0.0813	0.0619	0.0370	0.0330	0.0289	0.0193	0.0145	0.0137	0.0105	0.0153	0.0145	0.0137	0.0088	0.0121	0.0088	0.0080	0.0024	0.0032
State 8	0.0084	0.0410	0.0659	0.1006	0.0988	0.1108	0.1220	0.0959	0.0810	0.0569	0.0307	0.0214	0.0233	0.0177	0.0205	0.0177	0.0158	0.0112	0.0223	0.0140	0.0140	0.0065	0.0121	0.0037	0.0019
State 9	0.0081	0.0336	0.0696	0.0764	0.0916	0.0963	0.0998	0.0866	0.0660	0.0673	0.0429	0.0313	0.0244	0.0255	0.0267	0.0220	0.0197	0.0197	0.0151	0.0166	0.0139	0.0104	0.0081	0.0070	0.0093
State 10	0.0054	0.0214	0.0630	0.0791	0.0925	0.1072	0.0992	0.0791	0.0657	0.0570	0.0498	0.0335	0.0241	0.0188	0.0268	0.0268	0.0201	0.0214	0.0201	0.0228	0.0161	0.0147	0.0094	0.0094	0.0067
State 11	0.0035	0.0260	0.0537	0.0655	0.0832	0.1023	0.0849	0.1057	0.0797	0.0659	0.0399	0.0433	0.0312	0.0364	0.0225	0.0156	0.0260	0.0243	0.0347	0.0191	0.0156	0.0139	0.0087	0.0052	0.0035
State 12	0.0019	0.0095	0.0378	0.0510	0.0643	0.0899	0.0888	0.0870	0.1002	0.0851	0.0454	0.0416	0.0473	0.0340	0.0491	0.0265	0.0265	0.0302	0.0189	0.0340	0.0227	0.0132	0.0076	0.0057	0.0019
State 13	0.0042	0.0146	0.0354	0.0396	0.0708	0.0625	0.0760	0.0760	0.0896	0.1282	0.0833	0.0813	0.0333	0.0271	0.0333	0.0292	0.0208	0.0333	0.0208	0.0167	0.0042	0.0042	0.0063	0.0063	0.0042
State 14	0.0000	0.0113	0.0317	0.0543	0.0588	0.0407	0.0452	0.0633	0.0679	0.0769	0.1086	0.1041	0.0950	0.0520	0.0407	0.0271	0.0294	0.0271	0.0249	0.0181	0.0136	0.0045	0.0045	0.0000	0.0000
State 15	0.0039	0.0058	0.0193	0.0385	0.0366	0.0520	0.0520	0.0539	0.0462	0.0443	0.0559	0.0713	0.1195	0.1252	0.0597	0.0597	0.0308	0.0385	0.0366	0.0154	0.0116	0.0039	0.0096	0.0077	0.0019
State 16	0.0040	0.0080	0.0160	0.0360	0.0520	0.0360	0.0440	0.0420	0.0260	0.0260	0.0260	0.0500	0.0640	0.1140	0.1520	0.0980	0.0640	0.0500	0.0200	0.0220	0.0160	0.0120	0.0040	0.0080	0.0040
State 17	0.0019	0.0038	0.0153	0.0172	0.0324	0.0498	0.0534	0.0382	0.0305	0.0324	0.0191	0.0305	0.0229	0.0496	0.1336	0.1851	0.1240	0.0706	0.0305	0.0286	0.0095	0.0095	0.0076	0.0057	0.0019
State 18	0.0030	0.0061	0.0091	0.0151	0.0333	0.0303	0.0318	0.0303	0.0212	0.0424	0.0227	0.0242	0.0242	0.0287	0.0408	0.0726	0.1568	0.2139	0.1089	0.0408	0.0182	0.0121	0.0045	0.0091	0.0015
State 19	0.0000	0.0044	0.0103	0.0162	0.0192	0.0251	0.0428	0.0340	0.0355	0.0177	0.0207	0.0133	0.0207	0.0222	0.0251	0.0443	0.0443	0.1684	0.2688	0.0886	0.0295	0.0236	0.0162	0.0059	0.0030
State 20	0.0022	0.0000	0.0157	0.0112	0.0314	0.0426	0.0516	0.0471	0.0538	0.0314	0.0157	0.0224	0.0291	0.0090	0.0404	0.0336	0.0359	0.0785	0.1682	0.1413	0.0650	0.0359	0.0247	0.0090	0.0045
State 21	0.0000	0.0065	0.0065	0.0129	0.0841	0.0515	0.0515	0.0421	0.0388	0.0259	0.0324	0.0259	0.0259	0.0194	0.0162	0.0291	0.0388	0.1262	0.0971	0.0841	0.0650	0.0388	0.0194	0.0097	0.0291
State 22	0.0000	0.0088	0.0133	0.0133	0.0442	0.0796	0.0398	0.0752	0.0487	0.0442	0.0487	0.0398	0.0221	0.0265	0.0487	0.0354	0.0752	0.0575	0.1150	0.0752	0.0398	0.0133	0.0133	0.0133	0.0088
State 23	0.0000	0.0061	0.0061	0.0245	0.0736	0.0307	0.0613	0.0798	0.0613	0.0368	0.0368	0.0552	0.0368	0.0429	0.0368	0.0123	0.0123	0.0429	0.0736	0.0552	0.0429	0.0675	0.0552	0.0307	0.0184
State 24	0.0000	0.0160	0.0160	0.0240	0.0560	0.0640	0.1040	0.0480	0.0400	0.0400	0.0320	0.0320	0.0160	0.0320	0.0560	0.0160	0.0320	0.0400	0.0960	0.0640	0.0720	0.0640	0.0320	0.0320	0.0160
State 25	0.0000	0.0118	0.0118	0.0118	0.0706	0.0353	0.1059	0.1529	0.0353	0.0235	0.0000	0.0706	0.0118	0.0353	0.0353	0.0235	0.0235	0.0706	0.0706	0.0706	0.0471	0.0118	0.0118	0.0353	0.0235

Table A- 3 Limiting Transition Matrix from yearly instantaneous MTM

	State 1	State 2	State 3	State 4	State 5	State 6	State 7	State 8	State 9	State 10	State 11	State 12	State 13	State 14	State 15	State 16	State 17	State 18	State 19	State 20	State 21	State 22	State 23	State 24	State 25
State 1	0.1107	0.1507	0.1254	0.1005	0.0806	0.0679	0.0563	0.0455	0.0352	0.0262	0.0208	0.0179	0.0165	0.0150	0.0169	0.0157	0.0160	0.0205	0.0207	0.0133	0.0091	0.0063	0.0046	0.0033	0.0024
State 2	0.1107	0.1507	0.1254	0.1005	0.0806	0.0679	0.0563	0.0455	0.0352	0.0262	0.0208	0.0179	0.0165	0.0150	0.0169	0.0157	0.0160	0.0205	0.0207	0.0133	0.0091	0.0063	0.0046	0.0033	0.0024
State 3	0.1107	0.1507	0.1254	0.1005	0.0806	0.0679	0.0563	0.0455	0.0352	0.0262	0.0208	0.0179	0.0165	0.0150	0.0169	0.0157	0.0160	0.0205	0.0207	0.0133	0.0091	0.0063	0.0046	0.0033	0.0024
State 4	0.1107	0.1507	0.1254	0.1005	0.0806	0.0679	0.0563	0.0455	0.0352	0.0262	0.0208	0.0179	0.0165	0.0150	0.0169	0.0157	0.0160	0.0205	0.0207	0.0133	0.0091	0.0063	0.0046	0.0033	0.0024
State 5	0.1107	0.1507	0.1254	0.1005	0.0806	0.0679	0.0563	0.0455	0.0352	0.0262	0.0208	0.0179	0.0165	0.0150	0.0169	0.0157	0.0160	0.0205	0.0207	0.0133	0.0091	0.0063	0.0046	0.0033	0.0024
State 6	0.1107	0.1507	0.1254	0.1005	0.0806	0.0679	0.0563	0.0455	0.0352	0.0262	0.0208	0.0179	0.0165	0.0150	0.0169	0.0157	0.0160	0.0205	0.0207	0.0133	0.0091	0.0063	0.0046	0.0033	0.0024
State 7	0.1107	0.1507	0.1254	0.1005	0.0806	0.0679	0.0563	0.0455	0.0352	0.0262	0.0208	0.0179	0.0165	0.0150	0.0169	0.0157	0.0160	0.0205	0.0207	0.0133	0.0091	0.0063	0.0046	0.0033	0.0024
State 8	0.1107	0.1507	0.1254	0.1005	0.0806	0.0679	0.0563	0.0455	0.0352	0.0262	0.0208	0.0179	0.0165	0.0150	0.0169	0.0157	0.0160	0.0205	0.0207	0.0133	0.0091	0.0063	0.0046	0.0033	0.0024
State 9	0.1107	0.1507	0.1254	0.1005	0.0806	0.0679	0.0563	0.0455	0.0352	0.0262	0.0208	0.0179	0.0165	0.0150	0.0169	0.0157	0.0160	0.0205	0.0207	0.0133	0.0091	0.0063	0.0046	0.0033	0.0024
State 10	0.1107	0.1507	0.1254	0.1005	0.0806	0.0679	0.0563	0.0455	0.0352	0.0262	0.0208	0.0179	0.0165	0.0150	0.0169	0.0157	0.0160	0.0205	0.0207	0.0133	0.0091	0.0063	0.0046	0.0033	0.0024
State 11	0.1107	0.1507	0.1254	0.1005	0.0806	0.0679	0.0563	0.0455	0.0352	0.0262	0.0208	0.0179	0.0165	0.0150	0.0169	0.0157	0.0160	0.0205	0.0207	0.0133	0.0091	0.0063	0.0046	0.0033	0.0024
State 12	0.1107	0.1507	0.1254	0.1005	0.0806	0.0679	0.0563	0.0455	0.0352	0.0262	0.0208	0.0179	0.0165	0.0150	0.0169	0.0157	0.0160	0.0205	0.0207	0.0133	0.0091	0.0063	0.0046	0.0033	0.0024
State 13	0.1107	0.1507	0.1254	0.1005	0.0806	0.0679	0.0563	0.0455	0.0352	0.0262	0.0208	0.0179	0.0165	0.0150	0.0169	0.0157	0.0160	0.0205	0.0207	0.0133	0.0091	0.0063	0.0046	0.0033	0.0024
State 14	0.1107	0.1507	0.1254	0.1005	0.0806	0.0679	0.0563	0.0455	0.0352	0.0262	0.0208	0.0179	0.0165	0.0150	0.0169	0.0157	0.0160	0.0205	0.0207	0.0133	0.0091	0.0063	0.0046	0.0033	0.0024
State 15	0.1107	0.1507	0.1254	0.1005	0.0806	0.0679	0.0563	0.0455	0.0352	0.0262	0.0208	0.0179	0.0165	0.0150	0.0169	0.0157	0.0160	0.0205	0.0207	0.0133	0.0091	0.0063	0.0046	0.0033	0.0024
State 16	0.1107	0.1507	0.1254	0.1005	0.0806	0.0679	0.0563	0.0455	0.0352	0.0262	0.0208	0.0179	0.0165	0.0150	0.0169	0.0157	0.0160	0.0205	0.0207	0.0133	0.0091	0.0063	0.0046	0.0033	0.0024
State 17	0.1107	0.1507	0.1254	0.1005	0.0806	0.0679	0.0563	0.0455	0.0352	0.0262	0.0208	0.0179	0.0165	0.0150	0.0169	0.0157	0.0160	0.0205	0.0207	0.0133	0.0091	0.0063	0.0046	0.0033	0.0024
State 18	0.1107	0.1507	0.1254	0.1005	0.0806	0.0679	0.0563	0.0455	0.0352	0.0262	0.0208	0.0179	0.0165	0.0150	0.0169	0.0157	0.0160	0.0205	0.0207	0.0133	0.0091	0.0063	0.0046	0.0033	0.0024
State 19	0.1107	0.1507	0.1254	0.1005	0.0806	0.0679	0.0563	0.0455	0.0352	0.0262	0.0208	0.0179	0.0165	0.0150	0.0169	0.0157	0.0160	0.0205	0.0207	0.0133	0.0091	0.0063	0.0046	0.0033	0.0024
State 20	0.1107	0.1507	0.1254	0.1005	0.0806	0.0679	0.0563	0.0455	0.0352	0.0262	0.0208	0.0179	0.0165	0.0150	0.0169	0.0157	0.0160	0.0205	0.0207	0.0133	0.0091	0.0063	0.0046	0.0033	0.0024
State 21	0.1107	0.1507	0.1254	0.1005	0.0806	0.0679	0.0563	0.0455	0.0352	0.0262	0.0208	0.0179	0.0165	0.0150	0.0169	0.0157	0.0160	0.0205	0.0207	0.0133	0.0091	0.0063	0.0046	0.0033	0.0024
State 22	0.1107	0.1507	0.1254	0.1005	0.0806	0.0679	0.0563	0.0455	0.0352	0.0262	0.0208	0.0179	0.0165	0.0150	0.0169	0.0157	0.0160	0.0205	0.0207	0.0133	0.0091	0.0063	0.0046	0.0033	0.0024
State 23	0.1107	0.1507	0.1254	0.1005	0.0806	0.0679	0.0563	0.0455	0.0352	0.0262	0.0208	0.0179	0.0165	0.0150	0.0169	0.0157	0.0160	0.0205	0.0207	0.0133	0.0091	0.0063	0.0046	0.0033	0.0024
State 24	0.1107	0.1507	0.1254	0.1005	0.0806	0.0679	0.0563	0.0455	0.0352	0.0262	0.0208	0.0179	0.0165	0.0150	0.0169	0.0157	0.0160	0.0205	0.0207	0.0133	0.0091	0.0063	0.0046	0.0033	0.0024
State 25	0.1107	0.1507	0.1254	0.1005	0.0806	0.0679	0.0563	0.0455	0.0352	0.0262	0.0208	0.0179	0.0165	0.0150	0.0169	0.0157	0.0160	0.0205	0.0207	0.0133	0.0091	0.0063	0.0046	0.0033	0.0024

Table A- 4 Comparison between MP and LSP from yearly instantaneous MTM

States	State 1	State 2	State 3	State 4	State 5	State 6	State 7	State 8	State 9	State 10	State 11	State 12	State 13	State 14	State 15	State 16	State 17	State 18	State 19	State 20	State 21	State 22	State 23	State 24	State 25
MP	0.0419	0.0847	0.0921	0.0975	0.0835	0.0736	0.0671	0.0579	0.0457	0.0394	0.0305	0.0277	0.0251	0.0230	0.0269	0.0259	0.0271	0.0344	0.0352	0.0232	0.0161	0.0119	0.0085	0.0066	0.0045
LSP	0.1107	0.1507	0.1254	0.1005	0.0806	0.0679	0.0563	0.0455	0.0362	0.0262	0.0208	0.0179	0.0165	0.0150	0.0169	0.0157	0.0160	0.0205	0.0207	0.0133	0.0091	0.0063	0.0046	0.0033	0.0024

Table A- 5 June month instantaneous MTM

	State 1	State 2	State 3	State 4	State 5	State 6	State 7	State 8	State 9	State 10	State 11	State 12	State 13	State 14	State 15	State 16	State 17	State 18	State 19	State 20	State 21	State 22	State 23	State 24	State 25
State 1	0.4868	0.3684	0.0526	0.0132	0.0526	0.0132	0.0000	0.0000	0.0132	0.0000	0.0000	0.0000	0.0000	0.0000	0.0000	0.0000	0.0000	0.0000	0.0000	0.0000	0.0000	0.0000	0.0000	0.0000	0.0000
State 2	0.2299	0.3797	0.1672	0.0956	0.0481	0.0160	0.0214	0.0053	0.0000	0.0053	0.0000	0.0000	0.0000	0.0000	0.0000	0.0053	0.0000	0.0107	0.0053	0.0000	0.0000	0.0000	0.0000	0.0000	0.0000
State 3	0.0579	0.2158	0.2842	0.1628	0.1316	0.0316	0.0211	0.0316	0.0211	0.0053	0.0105	0.0105	0.0000	0.0053	0.0053	0.0053	0.0053	0.0000	0.0053	0.0000	0.0000	0.0000	0.0000	0.0000	0.0000
State 4	0.0440	0.1099	0.1813	0.1758	0.1319	0.0934	0.0714	0.0495	0.0385	0.0275	0.0220	0.0000	0.0000	0.0000	0.0110	0.0055	0.0055	0.0055	0.0055	0.0055	0.0055	0.0000	0.0055	0.0055	0.0000
State 5	0.0347	0.0841	0.1931	0.1535	0.1337	0.0792	0.0644	0.0644	0.0149	0.0198	0.0297	0.0149	0.0149	0.0149	0.0149	0.0050	0.0050	0.0050	0.0149	0.0000	0.0198	0.0000	0.0000	0.0000	0.0099
State 6	0.0063	0.0252	0.1195	0.1195	0.1761	0.1447	0.0881	0.0629	0.0755	0.0314	0.0314	0.0252	0.0000	0.0126	0.0000	0.0063	0.0126	0.0126	0.0063	0.0063	0.0189	0.0126	0.0000	0.0000	0.0063
State 7	0.0000	0.0588	0.0515	0.1544	0.1324	0.1250	0.1250	0.0294	0.0294	0.0588	0.0515	0.0588	0.0000	0.0074	0.0000	0.0074	0.0074	0.0074	0.0074	0.0074	0.0221	0.0221	0.0294	0.0000	0.0074
State 8	0.0147	0.0074	0.0588	0.0809	0.0662	0.1250	0.1029	0.1250	0.0735	0.0662	0.0368	0.0147	0.0221	0.0221	0.0294	0.0147	0.0368	0.0147	0.0147	0.0221	0.0147	0.0147	0.0000	0.0000	0.0000
State 9	0.0093	0.0278	0.0463	0.0926	0.0926	0.0833	0.0648	0.0833	0.0741	0.0833	0.0185	0.0648	0.0370	0.0278	0.0278	0.0093	0.0370	0.0000	0.0093	0.0185	0.0278	0.0185	0.0093	0.0093	0.0278
State 10	0.0000	0.0000	0.0667	0.0667	0.1444	0.0778	0.0778	0.1000	0.0778	0.0889	0.0444	0.0222	0.0333	0.0222	0.0222	0.0333	0.0111	0.0000	0.0222	0.0222	0.0111	0.0222	0.0111	0.0111	0.0111
State 11	0.0000	0.0317	0.0317	0.0635	0.0794	0.1270	0.0635	0.1270	0.0635	0.1111	0.0317	0.0635	0.0159	0.0317	0.0000	0.0317	0.0000	0.0000	0.0317	0.0317	0.0159	0.0317	0.0159	0.0000	0.0000
State 12	0.0000	0.0169	0.0169	0.0339	0.0847	0.0508	0.0678	0.0169	0.1017	0.0847	0.0339	0.0508	0.0339	0.0169	0.0847	0.0169	0.0169	0.0339	0.0678	0.0508	0.0339	0.0000	0.0000	0.0000	0.0000
State 13	0.0000	0.0000	0.0244	0.0000	0.0488	0.1220	0.0488	0.0732	0.1220	0.2195	0.0732	0.0976	0.0000	0.0244	0.0244	0.0000	0.0244	0.0244	0.0000	0.0000	0.0244	0.0000	0.0000	0.0488	0.0000
State 14	0.0000	0.0000	0.0270	0.0270	0.0811	0.0811	0.0270	0.0811	0.1081	0.1351	0.0541	0.0270	0.0541	0.0270	0.1081	0.0270	0.0270	0.0541	0.0000	0.0541	0.0000	0.0000	0.0000	0.0000	0.0000
State 15	0.0000	0.0000	0.0345	0.0172	0.0517	0.1034	0.0345	0.0345	0.0517	0.0690	0.0345	0.0345	0.2069	0.0345	0.0345	0.0345	0.0345	0.0690	0.0517	0.0172	0.0000	0.0000	0.0172	0.0345	0.0000
State 16	0.0256	0.0000	0.0256	0.0256	0.0513	0.0256	0.0256	0.1026	0.0256	0.0000	0.0000	0.1026	0.0513	0.1282	0.1538	0.0256	0.0513	0.1026	0.0513	0.0000	0.0000	0.0256	0.0000	0.0000	0.0000
State 17	0.0000	0.0189	0.0189	0.0000	0.0377	0.0189	0.0755	0.0377	0.0189	0.0189	0.0377	0.0377	0.0377	0.0566	0.1698	0.0943	0.0755	0.1132	0.0377	0.0755	0.0189	0.0000	0.0000	0.0000	0.0000
State 18	0.0000	0.0000	0.0000	0.0139	0.0417	0.0417	0.0139	0.0556	0.0278	0.0139	0.0000	0.0139	0.0278	0.0417	0.0278	0.0694	0.1111	0.2361	0.1667	0.0556	0.0278	0.0000	0.0139	0.0000	0.0000
State 19	0.0000	0.0294	0.0147	0.0147	0.0147	0.0000	0.0294	0.0441	0.0294	0.0147	0.0000	0.0147	0.0147	0.0147	0.0441	0.0588	0.0735	0.1029	0.2647	0.0882	0.0441	0.0147	0.0294	0.0441	0.0000
State 20	0.0000	0.0000	0.0182	0.0000	0.0000	0.0545	0.1091	0.0727	0.0545	0.0000	0.0182	0.0000	0.0000	0.0000	0.0545	0.0364	0.0000	0.1091	0.1091	0.2000	0.0545	0.0364	0.0545	0.0182	0.0000
State 21	0.0000	0.0000	0.0000	0.0000	0.0682	0.0909	0.1136	0.0455	0.0682	0.0000	0.0909	0.0682	0.0227	0.0000	0.0455	0.0000	0.0227	0.0455	0.0682	0.0682	0.1136	0.0455	0.0000	0.0000	0.0227
State 22	0.0000	0.0769	0.0385	0.0385	0.0000	0.1154	0.0000	0.0769	0.0385	0.0385	0.0385	0.0385	0.0000	0.0000	0.0385	0.0000	0.0769	0.1154	0.0769	0.1154	0.0385	0.0000	0.0385	0.0000	0.0000
State 23	0.0000	0.0000	0.0000	0.0400	0.1200	0.0400	0.0800	0.1600	0.0400	0.0000	0.0800	0.0400	0.0000	0.0000	0.0400	0.0000	0.0000	0.0000	0.0000	0.0400	0.0400	0.0800	0.0800	0.0800	0.0400
State 24	0.0000	0.0000	0.0000	0.0000	0.0000	0.0833	0.0000	0.1667	0.0833	0.0833	0.2500	0.0000	0.0000	0.0000	0.1667	0.0000	0.0000	0.0833	0.0000	0.0000	0.0833	0.0000	0.0000	0.0000	0.0000
State 25	0.0000	0.0000	0.0000	0.0000	0.1000	0.1000	0.2000	0.2000	0.2000	0.0000	0.0000	0.0000	0.0000	0.0000	0.0000	0.0000	0.0000	0.1000	0.0000	0.0000	0.0000	0.0000	0.1000	0.0000	0.0000

Table A- 6 Limiting Transition Matrix from June month instantaneous MTM

	State 1	State 2	State 3	State 4	State 5	State 6	State 7	State 8	State 9	State 10	State 11	State 12	State 13	State 14	State 15	State 16	State 17	State 18	State 19	State 20	State 21	State 22	State 23	State 24	State 25
State 1	0.0970	0.1455	0.1237	0.0931	0.0947	0.0652	0.0521	0.0462	0.0368	0.0317	0.0226	0.0200	0.0129	0.0128	0.0183	0.0125	0.0161	0.0216	0.0219	0.0159	0.0142	0.0082	0.0072	0.0043	0.0037
State 2	0.0970	0.1455	0.1237	0.0931	0.0947	0.0652	0.0521	0.0462	0.0368	0.0317	0.0226	0.0200	0.0129	0.0128	0.0183	0.0125	0.0161	0.0216	0.0219	0.0159	0.0142	0.0082	0.0072	0.0043	0.0037
State 3	0.0970	0.1455	0.1237	0.0931	0.0947	0.0652	0.0521	0.0462	0.0368	0.0317	0.0226	0.0200	0.0129	0.0128	0.0183	0.0125	0.0161	0.0216	0.0219	0.0159	0.0142	0.0082	0.0072	0.0043	0.0037
State 4	0.0970	0.1455	0.1237	0.0931	0.0947	0.0652	0.0521	0.0462	0.0368	0.0317	0.0226	0.0200	0.0129	0.0128	0.0183	0.0125	0.0161	0.0216	0.0219	0.0159	0.0142	0.0082	0.0072	0.0043	0.0037
State 5	0.0970	0.1455	0.1237	0.0931	0.0947	0.0652	0.0521	0.0462	0.0368	0.0317	0.0226	0.0200	0.0129	0.0128	0.0183	0.0125	0.0161	0.0216	0.0219	0.0159	0.0142	0.0082	0.0072	0.0043	0.0037
State 6	0.0970	0.1455	0.1237	0.0931	0.0947	0.0652	0.0521	0.0462	0.0368	0.0317	0.0226	0.0200	0.0129	0.0128	0.0183	0.0125	0.0161	0.0216	0.0219	0.0159	0.0142	0.0082	0.0072	0.0043	0.0037
State 7	0.0970	0.1455	0.1237	0.0931	0.0947	0.0652	0.0521	0.0462	0.0368	0.0317	0.0226	0.0200	0.0129	0.0128	0.0183	0.0125	0.0161	0.0216	0.0219	0.0159	0.0142	0.0082	0.0072	0.0043	0.0037
State 8	0.0970	0.1455	0.1237	0.0931	0.0947	0.0652	0.0521	0.0462	0.0368	0.0317	0.0226	0.0200	0.0129	0.0128	0.0183	0.0125	0.0161	0.0216	0.0219	0.0159	0.0142	0.0082	0.0072	0.0043	0.0037
State 9	0.0970	0.1455	0.1237	0.0931	0.0947	0.0652	0.0521	0.0462	0.0368	0.0317	0.0226	0.0200	0.0129	0.0128	0.0183	0.0125	0.0161	0.0216	0.0219	0.0159	0.0142	0.0082	0.0072	0.0043	0.0037
State 10	0.0970	0.1455	0.1237	0.0931	0.0947	0.0652	0.0521	0.0462	0.0368	0.0317	0.0226	0.0200	0.0129	0.0128	0.0183	0.0125	0.0161	0.0216	0.0219	0.0159	0.0142	0.0082	0.0072	0.0043	0.0037
State 11	0.0970	0.1455	0.1237	0.0931	0.0947	0.0652	0.0521	0.0462	0.0368	0.0317	0.0226	0.0200	0.0129	0.0128	0.0183	0.0125	0.0161	0.0216	0.0219	0.0159	0.0142	0.0082	0.0072	0.0043	0.0037
State 12	0.0970	0.1455	0.1237	0.0931	0.0947	0.0652	0.0521	0.0462	0.0368	0.0317	0.0226	0.0200	0.0129	0.0128	0.0183	0.0125	0.0161	0.0216	0.0219	0.0159	0.0142	0.0082	0.0072	0.0043	0.0037
State 13	0.0970	0.1455	0.1237	0.0931	0.0947	0.0652	0.0521	0.0462	0.0368	0.0317	0.0226	0.0200	0.0129	0.0128	0.0183	0.0125	0.0161	0.0216	0.0219	0.0159	0.0142	0.0082	0.0072	0.0043	0.0037
State 14	0.0970	0.1455	0.1237	0.0931	0.0947	0.0652	0.0521	0.0462	0.0368	0.0317	0.0226	0.0200	0.0129	0.0128	0.0183	0.0125	0.0161	0.0216	0.0219	0.0159	0.0142	0.0082	0.0072	0.0043	0.0037
State 15	0.0970	0.1455	0.1237	0.0931	0.0947	0.0652	0.0521	0.0462	0.0368	0.0317	0.0226	0.0200	0.0129	0.0128	0.0183	0.0125	0.0161	0.0216	0.0219	0.0159	0.0142	0.0082	0.0072	0.0043	0.0037
State 16	0.0970	0.1455	0.1237	0.0931	0.0947	0.0652	0.0521	0.0462	0.0368	0.0317	0.0226	0.0200	0.0129	0.0128	0.0183	0.0125	0.0161	0.0216	0.0219	0.0159	0.0142	0.0082	0.0072	0.0043	0.0037
State 17	0.0970	0.1455	0.1237	0.0931	0.0947	0.0652	0.0521	0.0462	0.0368	0.0317	0.0226	0.0200	0.0129	0.0128	0.0183	0.0125	0.0161	0.0216	0.0219	0.0159	0.0142	0.0082	0.0072	0.0043	0.0037
State 18	0.0970	0.1455	0.1237	0.0931	0.0947	0.0652	0.0521	0.0462	0.0368	0.0317	0.0226	0.0200	0.0129	0.0128	0.0183	0.0125	0.0161	0.0216	0.0219	0.0159	0.0142	0.0082	0.0072	0.0043	0.0037
State 19	0.0970	0.1455	0.1237	0.0931	0.0947	0.0652	0.0521	0.0462	0.0368	0.0317	0.0226	0.0200	0.0129	0.0128	0.0183	0.0125	0.0161	0.0216	0.0219	0.0159	0.0142	0.0082	0.0072	0.0043	0.0037
State 20	0.0970	0.1455	0.1237	0.0931	0.0947	0.0652	0.0521	0.0462	0.0368	0.0317	0.0226	0.0200	0.0129	0.0128	0.0183	0.0125	0.0161	0.0216	0.0219	0.0159	0.0142	0.0082	0.0072	0.0043	0.0037
State 21	0.0970	0.1455	0.1237	0.0931	0.0947	0.0652	0.0521	0.0462	0.0368	0.0317	0.0226	0.0200	0.0129	0.0128	0.0183	0.0125	0.0161	0.0216	0.0219	0.0159	0.0142	0.0082	0.0072	0.0043	0.0037
State 22	0.0970	0.1455	0.1237	0.0931	0.0947	0.0652	0.0521	0.0462	0.0368	0.0317	0.0226	0.0200	0.0129	0.0128	0.0183	0.0125	0.0161	0.0216	0.0219	0.0159	0.0142	0.0082	0.0072	0.0043	0.0037
State 23	0.0970	0.1455	0.1237	0.0931	0.0947	0.0652	0.0521	0.0462	0.0368	0.0317	0.0226	0.0200	0.0129	0.0128	0.0183	0.0125	0.0161	0.0216	0.0219	0.0159	0.0142	0.0082	0.0072	0.0043	0.0037
State 24	0.0970	0.1455	0.1237	0.0931	0.0947	0.0652	0.0521	0.0462	0.0368	0.0317	0.0226	0.0200	0.0129	0.0128	0.0183	0.0125	0.0161	0.0216	0.0219	0.0159	0.0142	0.0082	0.0072	0.0043	0.0037
State 25	0.0970	0.1455	0.1237	0.0931	0.0947	0.0652	0.0521	0.0462	0.0368	0.0317	0.0226	0.0200	0.0129	0.0128	0.0183	0.0125	0.0161	0.0216	0.0219	0.0159	0.0142	0.0082	0.0072	0.0043	0.0037

Table A- 7 Transition Number Matrix using yearly average data

	State 1	State 2	State 3	State 4	State 5	State 6	State 7	State 8	State 9	State 10	State 11	State 12	State 13	State 14	State 15	State 16	State 17	State 18	State 19	State 20	State 21	State 22	State 23	State 24	State 25
State 1	133	111	22	9	7	3	2	1	0	0	0	1	0	0	1	0	0	0	1	0	0	0	0	0	0
State 2	108	536	303	111	48	24	18	10	5	4	1	2	2	1	3	0	1	1	0	0	1	0	0	0	0
State 3	21	291	622	353	158	89	43	24	12	13	3	4	4	3	0	0	2	2	0	0	0	3	1	1	1
State 4	8	102	306	378	241	181	115	63	37	23	18	10	7	15	7	1	0	1	1	0	0	2	1	1	0
State 5	4	50	153	228	285	240	160	100	46	45	31	26	18	13	4	3	1	4	1	2	0	0	0	2	0
State 6	7	25	79	154	214	242	193	151	92	76	45	38	23	13	10	5	6	2	1	1	1	1	1	1	2
State 7	1	20	44	84	156	177	197	154	113	100	78	60	46	21	14	6	9	4	2	1	1	0	2	2	1
State 8	0	4	35	69	86	136	147	144	133	119	85	55	57	40	24	25	16	5	1	0	3	1	2	1	0
State 9	0	4	19	38	61	86	119	119	87	82	115	61	82	49	31	24	10	5	1	1	0	1	0	0	1
State 10	0	1	7	19	39	66	86	109	91	101	107	109	72	78	60	21	16	4	3	2	1	0	0	0	0
State 11	0	1	5	21	26	66	76	89	103	93	108	106	103	74	51	31	23	11	6	6	1	1	1	1	0
State 12	0	2	3	10	19	47	37	74	79	72	91	83	97	123	69	48	33	15	3	4	0	0	0	0	0
State 13	0	2	3	12	16	25	65	57	78	74	80	83	90	114	112	63	41	15	8	3	0	0	0	0	0
State 14	0	2	3	3	9	17	28	39	49	71	92	95	105	104	140	120	45	23	8	3	1	0	1	0	0
State 15	0	0	2	3	8	13	10	27	35	57	63	64	102	116	114	128	89	38	9	1	0	0	0	0	0
State 16	0	1	0	3	6	9	14	25	12	30	33	40	83	122	109	123	146	52	11	5	1	0	0	0	0
State 17	0	2	0	3	0	10	8	10	17	16	35	32	42	54	82	121	129	126	27	8	1	0	0	0	0
State 18	0	0	0	0	1	1	3	2	9	10	12	18	25	26	37	45	124	159	44	5	0	0	0	0	0
State 19	0	0	0	0	0	0	0	3	3	5	3	10	12	8	6	11	22	48	76	9	0	0	0	0	0
State 20	0	0	0	0	0	0	0	0	3	1	3	5	3	5	5	3	2	9	14	6	0	0	0	0	0
State 21	0	0	0	1	1	0	0	1	0	1	2	0	0	0	1	2	0	0	0	1	1	0	0	0	0
State 22	0	0	0	1	0	0	0	0	0	0	0	1	0	0	0	0	1	0	0	1	0	0	0	0	0
State 23	0	0	0	0	0	0	0	0	1	0	0	0	0	0	1	1	0	0	0	0	0	0	0	0	0
State 24	0	0	0	0	1	1	0	0	1	0	0	0	0	0	0	0	0	0	0	0	0	0	0	0	0
State 25	0	0	0	0	0	0	0	0	0	0	1	1	0	1	0	0	0	0	0	1	0	0	0	0	0

Table A- 8 Yearly average Markov Transition Matrix

	State 1	State 2	State 3	State 4	State 5	State 6	State 7	State 8	State 9	State 10	State 11	State 12	State 13	State 14	State 15	State 16	State 17	State 18	State 19	State 20	State 21	State 22	State 23	State 24	State 25
State 1	0.4570	0.3914	0.0756	0.0309	0.0241	0.0103	0.0069	0.0034	0.0000	0.0000	0.0060	0.0034	0.0000	0.0000	0.0034	0.0000	0.0000	0.0000	0.0034	0.0000	0.0000	0.0000	0.0000	0.0000	0.0000
State 2	0.0919	0.4682	0.2579	0.0945	0.0391	0.0204	0.0136	0.0085	0.0043	0.0034	0.0009	0.0017	0.0017	0.0009	0.0026	0.0009	0.0009	0.0009	0.0000	0.0000	0.0009	0.0000	0.0000	0.0000	0.0000
State 3	0.0137	0.1902	0.3412	0.2307	0.1039	0.0461	0.0281	0.0157	0.0078	0.0095	0.0020	0.0026	0.0026	0.0020	0.0000	0.0000	0.0013	0.0013	0.0000	0.0000	0.0000	0.0020	0.0007	0.0007	0.0007
State 4	0.0053	0.0676	0.2029	0.2597	0.1699	0.1208	0.0763	0.0351	0.0245	0.0163	0.0119	0.0066	0.0046	0.0099	0.0046	0.0007	0.0000	0.0007	0.0007	0.0000	0.0000	0.0013	0.0007	0.0007	0.0000
State 5	0.0028	0.0353	0.1081	0.1618	0.2013	0.1695	0.1130	0.0705	0.0325	0.0318	0.0219	0.0184	0.0127	0.0092	0.0028	0.0021	0.0007	0.0028	0.0007	0.0014	0.0000	0.0000	0.0000	0.0014	0.0000
State 6	0.0051	0.0181	0.0571	0.1114	0.1547	0.1759	0.1396	0.1092	0.0695	0.0550	0.0325	0.0275	0.0165	0.0094	0.0072	0.0036	0.0043	0.0014	0.0007	0.0007	0.0007	0.0007	0.0007	0.0007	0.0014
State 7	0.0008	0.0165	0.0341	0.0690	0.1207	0.1370	0.1525	0.1192	0.0975	0.0774	0.0604	0.0464	0.0346	0.0163	0.0108	0.0046	0.0070	0.0031	0.0015	0.0008	0.0008	0.0000	0.0015	0.0015	0.0008
State 8	0.0000	0.0034	0.0295	0.0691	0.0724	0.1145	0.1237	0.1212	0.1120	0.1002	0.0715	0.0463	0.0480	0.0337	0.0262	0.0210	0.0135	0.0042	0.0008	0.0000	0.0025	0.0008	0.0017	0.0008	0.0000
State 9	0.0000	0.0040	0.0191	0.0382	0.0612	0.0863	0.1195	0.1195	0.0973	0.0823	0.1155	0.0612	0.0823	0.0492	0.0311	0.0241	0.0100	0.0050	0.0010	0.0010	0.0000	0.0010	0.0000	0.0000	0.0010
State 10	0.0000	0.0010	0.0071	0.0192	0.0393	0.0686	0.0957	0.1099	0.0917	0.1016	0.1079	0.1099	0.0726	0.0786	0.0605	0.0212	0.0161	0.0040	0.0030	0.0020	0.0010	0.0000	0.0000	0.0000	0.0000
State 11	0.0000	0.0010	0.0050	0.0210	0.0269	0.0659	0.0768	0.0988	0.1028	0.0928	0.1078	0.1648	0.1028	0.0739	0.0509	0.0309	0.0230	0.0110	0.0060	0.0060	0.0010	0.0010	0.0010	0.0010	0.0000
State 12	0.0000	0.0022	0.0033	0.0110	0.0209	0.0517	0.0497	0.0814	0.0868	0.0792	0.1001	0.0913	0.1067	0.1353	0.0759	0.0528	0.0363	0.0165	0.0033	0.0044	0.0000	0.0000	0.0000	0.0000	0.0000
State 13	0.0000	0.0021	0.0032	0.0129	0.0172	0.0289	0.0591	0.0612	0.0858	0.0795	0.0999	0.0892	0.0997	0.1224	0.1203	0.0977	0.0440	0.0161	0.0086	0.0032	0.0000	0.0000	0.0000	0.0000	0.0000
State 14	0.0000	0.0021	0.0031	0.0031	0.0094	0.0177	0.0292	0.0406	0.0500	0.0740	0.0958	0.0998	0.1125	0.1083	0.1468	0.1250	0.0469	0.0240	0.0083	0.0031	0.0010	0.0000	0.0010	0.0000	0.0000
State 15	0.0000	0.0000	0.0023	0.0034	0.0091	0.0149	0.0114	0.0309	0.0400	0.0651	0.0720	0.0731	0.1166	0.1326	0.1303	0.1440	0.1017	0.0411	0.0103	0.0011	0.0000	0.0000	0.0000	0.0000	0.0000
State 16	0.0000	0.0012	0.0000	0.0037	0.0075	0.0112	0.0174	0.0311	0.0149	0.0373	0.0410	0.0497	0.0709	0.1616	0.1364	0.1528	0.1814	0.0646	0.0137	0.0062	0.0012	0.0000	0.0000	0.0000	0.0000
State 17	0.0000	0.0028	0.0000	0.0042	0.0000	0.0139	0.0111	0.0139	0.0236	0.0222	0.0486	0.0444	0.0583	0.0749	0.1137	0.1676	0.1789	0.1748	0.0374	0.0069	0.0014	0.0000	0.0000	0.0000	0.0000
State 18	0.0000	0.0000	0.0000	0.0000	0.0019	0.0019	0.0058	0.0038	0.0173	0.0192	0.0230	0.0345	0.0460	0.0499	0.0710	0.0864	0.2360	0.3052	0.0845	0.0096	0.0000	0.0000	0.0000	0.0000	0.0000
State 19	0.0000	0.0000	0.0000	0.0000	0.0000	0.0000	0.0000	0.0140	0.0140	0.0233	0.0140	0.0465	0.0698	0.0372	0.0279	0.0512	0.1023	0.2233	0.3535	0.0372	0.0000	0.0000	0.0000	0.0000	0.0000
State 20	0.0000	0.0000	0.0000	0.0000	0.0000	0.0000	0.0000	0.0000	0.0508	0.0169	0.0508	0.0847	0.0508	0.0847	0.0847	0.0508	0.0339	0.1525	0.2373	0.1017	0.0000	0.0000	0.0000	0.0000	0.0000
State 21	0.0000	0.0000	0.0000	0.0909	0.0909	0.0000	0.0000	0.0909	0.0000	0.0909	0.1818	0.0000	0.0000	0.0000	0.0909	0.1818	0.0909	0.0000	0.0000	0.0909	0.0909	0.0000	0.0000	0.0000	0.0000
State 22	0.0000	0.0000	0.0000	0.2500	0.0000	0.0000	0.0000	0.0000	0.0000	0.0000	0.0000	0.2500	0.0000	0.0000	0.0000	0.0000	0.2500	0.0000	0.0000	0.2500	0.0000	0.0000	0.0000	0.0000	0.0000
State 23	0.0000	0.0000	0.0000	0.0000	0.0000	0.0000	0.0000	0.0000	0.3333	0.0000	0.0000	0.0000	0.0000	0.0000	0.3333	0.3333	0.0000	0.0000	0.0000	0.0000	0.0000	0.0000	0.0000	0.0000	0.0000
State 24	0.0000	0.0000	0.0000	0.0000	0.3333	0.3333	0.0000	0.0000	0.3333	0.0000	0.0000	0.0000	0.0000	0.0000	0.0000	0.0000	0.0000	0.0000	0.0000	0.0000	0.0000	0.0000	0.0000	0.0000	0.0000
State 25	0.0000	0.0000	0.0000	0.0000	0.0000	0.0000	0.0000	0.0000	0.0000	0.0000	0.2500	0.2500	0.0000	0.2500	0.0000	0.0000	0.0000	0.0000	0.0000	0.2500	0.0000	0.0000	0.0000	0.0000	0.0000

Table A- 9 Limiting Transition Matrix from yearly average MTM

	State 1	State 2	State 3	State 4	State 5	State 6	State 7	State 8	State 9	State 10	State 11	State 12	State 13	State 14	State 15	State 16	State 17	State 18	State 19	State 20	State 21	State 22	State 23	State 24	State 25
State 1	0.0135	0.0568	0.0760	0.0774	0.0725	0.0752	0.0702	0.0644	0.0548	0.0540	0.0549	0.0493	0.0522	0.0535	0.0483	0.0426	0.0390	0.0284	0.0118	0.0032	0.0007	0.0005	0.0005	0.0005	0.0003
State 2	0.0135	0.0568	0.0760	0.0774	0.0725	0.0752	0.0702	0.0644	0.0548	0.0540	0.0549	0.0493	0.0522	0.0535	0.0483	0.0426	0.0390	0.0284	0.0118	0.0032	0.0007	0.0005	0.0005	0.0005	0.0003
State 3	0.0135	0.0568	0.0760	0.0774	0.0725	0.0752	0.0702	0.0644	0.0548	0.0540	0.0549	0.0493	0.0522	0.0535	0.0483	0.0426	0.0390	0.0284	0.0118	0.0032	0.0007	0.0005	0.0005	0.0005	0.0003
State 4	0.0135	0.0568	0.0760	0.0774	0.0725	0.0752	0.0702	0.0644	0.0548	0.0540	0.0549	0.0493	0.0522	0.0535	0.0483	0.0426	0.0390	0.0284	0.0118	0.0032	0.0007	0.0005	0.0005	0.0005	0.0003
State 5	0.0135	0.0568	0.0760	0.0774	0.0725	0.0752	0.0702	0.0644	0.0548	0.0540	0.0549	0.0493	0.0522	0.0535	0.0483	0.0426	0.0390	0.0284	0.0118	0.0032	0.0007	0.0005	0.0005	0.0005	0.0003
State 6	0.0135	0.0568	0.0760	0.0774	0.0725	0.0752	0.0702	0.0644	0.0548	0.0540	0.0549	0.0493	0.0522	0.0535	0.0483	0.0426	0.0390	0.0284	0.0118	0.0032	0.0007	0.0005	0.0005	0.0005	0.0003
State 7	0.0135	0.0568	0.0760	0.0774	0.0725	0.0752	0.0702	0.0644	0.0548	0.0540	0.0549	0.0493	0.0522	0.0535	0.0483	0.0426	0.0390	0.0284	0.0118	0.0032	0.0007	0.0005	0.0005	0.0005	0.0003
State 8	0.0135	0.0568	0.0760	0.0774	0.0725	0.0752	0.0702	0.0644	0.0548	0.0540	0.0549	0.0493	0.0522	0.0535	0.0483	0.0426	0.0390	0.0284	0.0118	0.0032	0.0007	0.0005	0.0005	0.0005	0.0003
State 9	0.0135	0.0568	0.0760	0.0774	0.0725	0.0752	0.0702	0.0644	0.0548	0.0540	0.0549	0.0493	0.0522	0.0535	0.0483	0.0426	0.0390	0.0284	0.0118	0.0032	0.0007	0.0005	0.0005	0.0005	0.0003
State 10	0.0135	0.0568	0.0760	0.0774	0.0725	0.0752	0.0702	0.0644	0.0548	0.0540	0.0549	0.0493	0.0522	0.0535	0.0483	0.0426	0.0390	0.0284	0.0118	0.0032	0.0007	0.0005	0.0005	0.0005	0.0003
State 11	0.0135	0.0568	0.0760	0.0774	0.0725	0.0752	0.0702	0.0644	0.0548	0.0540	0.0549	0.0493	0.0522	0.0535	0.0483	0.0426	0.0390	0.0284	0.0118	0.0032	0.0007	0.0005	0.0005	0.0005	0.0003
State 12	0.0135	0.0568	0.0760	0.0774	0.0725	0.0752	0.0702	0.0644	0.0548	0.0540	0.0549	0.0493	0.0522	0.0535	0.0483	0.0426	0.0390	0.0284	0.0118	0.0032	0.0007	0.0005	0.0005	0.0005	0.0003
State 13	0.0135	0.0568	0.0760	0.0774	0.0725	0.0752	0.0702	0.0644	0.0548	0.0540	0.0549	0.0493	0.0522	0.0535	0.0483	0.0426	0.0390	0.0284	0.0118	0.0032	0.0007	0.0005	0.0005	0.0005	0.0003
State 14	0.0135	0.0568	0.0760	0.0774	0.0725	0.0752	0.0702	0.0644	0.0548	0.0540	0.0549	0.0493	0.0522	0.0535	0.0483	0.0426	0.0390	0.0284	0.0118	0.0032	0.0007	0.0005	0.0005	0.0005	0.0003
State 15	0.0135	0.0568	0.0760	0.0774	0.0725	0.0752	0.0702	0.0644	0.0548	0.0540	0.0549	0.0493	0.0522	0.0535	0.0483	0.0426	0.0390	0.0284	0.0118	0.0032	0.0007	0.0005	0.0005	0.0005	0.0003
State 16	0.0135	0.0568	0.0760	0.0774	0.0725	0.0752	0.0702	0.0644	0.0548	0.0540	0.0549	0.0493	0.0522	0.0535	0.0483	0.0426	0.0390	0.0284	0.0118	0.0032	0.0007	0.0005	0.0005	0.0005	0.0003
State 17	0.0135	0.0568	0.0760	0.0774	0.0725	0.0752	0.0702	0.0644	0.0548	0.0540	0.0549	0.0493	0.0522	0.0535	0.0483	0.0426	0.0390	0.0284	0.0118	0.0032	0.0007	0.0005	0.0005	0.0005	0.0003
State 18	0.0135	0.0568	0.0760	0.0774	0.0725	0.0752	0.0702	0.0644	0.0548	0.0540	0.0549	0.0493	0.0522	0.0535	0.0483	0.0426	0.0390	0.0284	0.0118	0.0032	0.0007	0.0005	0.0005	0.0005	0.0003
State 19	0.0135	0.0568	0.0760	0.0774	0.0725	0.0752	0.0702	0.0644	0.0548	0.0540	0.0549	0.0493	0.0522	0.0535	0.0483	0.0426	0.0390	0.0284	0.0118	0.0032	0.0007	0.0005	0.0005	0.0005	0.0003
State 20	0.0135	0.0568	0.0760	0.0774	0.0725	0.0752	0.0702	0.0644	0.0548	0.0540	0.0549	0.0493	0.0522	0.0535	0.0483	0.0426	0.0390	0.0284	0.0118	0.0032	0.0007	0.0005	0.0005	0.0005	0.0003
State 21	0.0135	0.0568	0.0760	0.0774	0.0725	0.0752	0.0702	0.0644	0.0548	0.0540	0.0549	0.0493	0.0522	0.0535	0.0483	0.0426	0.0390	0.0284	0.0118	0.0032	0.0007	0.0005	0.0005	0.0005	0.0003
State 22	0.0135	0.0568	0.0760	0.0774	0.0725	0.0752	0.0702	0.0644	0.0548	0.0540	0.0549	0.0493	0.0522	0.0535	0.0483	0.0426	0.0390	0.0284	0.0118	0.0032	0.0007	0.0005	0.0005	0.0005	0.0003
State 23	0.0135	0.0568	0.0760	0.0774	0.0725	0.0752	0.0702	0.0644	0.0548	0.0540	0.0549	0.0493	0.0522	0.0535	0.0483	0.0426	0.0390	0.0284	0.0118	0.0032	0.0007	0.0005	0.0005	0.0005	0.0003
State 24	0.0135	0.0568	0.0760	0.0774	0.0725	0.0752	0.0702	0.0644	0.0548	0.0540	0.0549	0.0493	0.0522	0.0535	0.0483	0.0426	0.0390	0.0284	0.0118	0.0032	0.0007	0.0005	0.0005	0.0005	0.0003
State 25	0.0135	0.0568	0.0760	0.0774	0.0725	0.0752	0.0702	0.0644	0.0548	0.0540	0.0549	0.0493	0.0522	0.0535	0.0483	0.0426	0.0390	0.0284	0.0118	0.0032	0.0007	0.0005	0.0005	0.0005	0.0003

Table A- 10 Yearly average UK MTM

	State 1	State 2	State 3	State 4	State 5	State 6	State 7	State 8	State 9	State 10	State 11	State 12	State 13	State 14	State 15	State 16	State 17	State 18	State 19	State 20	State 21	State 22	State 23	State 24	State 25
State 1	0.3537	0.3959	0.1262	0.0593	0.0325	0.0153	0.0057	0.0036	0.0000	0.0038	0.0000	0.0019	0.0000	0.0000	0.0019	0.0000	0.0000	0.0000	0.0019	0.0000	0.0000	0.0000	0.0000	0.0000	0.0000
State 2	0.0945	0.4186	0.2698	0.1078	0.0461	0.0222	0.0166	0.0100	0.0039	0.0072	0.0006	0.0011	0.0011	0.0006	0.0017	0.0000	0.0006	0.0006	0.0000	0.0000	0.0006	0.0006	0.0000	0.0000	0.0000
State 3	0.0222	0.1808	0.3319	0.2263	0.1169	0.0610	0.0289	0.0182	0.0103	0.0071	0.0016	0.0032	0.0024	0.0012	0.0000	0.0004	0.0008	0.0008	0.0000	0.0000	0.0000	0.0012	0.0004	0.0004	0.0004
State 4	0.0098	0.0723	0.1935	0.2417	0.1671	0.1239	0.0727	0.0362	0.0279	0.0164	0.0111	0.0089	0.0046	0.0089	0.0034	0.0004	0.0000	0.0009	0.0004	0.0000	0.0004	0.0009	0.0004	0.0004	0.0000
State 5	0.0084	0.0297	0.1058	0.1635	0.1980	0.1683	0.1168	0.0739	0.0417	0.0325	0.0208	0.0148	0.0108	0.0096	0.0036	0.0024	0.0004	0.0016	0.0008	0.0008	0.0000	0.0004	0.0000	0.0008	0.0000
State 6	0.0077	0.0160	0.0655	0.1093	0.1445	0.1749	0.1486	0.1113	0.0753	0.0534	0.0332	0.0275	0.0154	0.0101	0.0069	0.0040	0.0028	0.0012	0.0004	0.0004	0.0004	0.0004	0.0004	0.0004	0.0008
State 7	0.0012	0.0099	0.0338	0.0622	0.1119	0.1287	0.1571	0.1286	0.0941	0.0846	0.0693	0.0472	0.0332	0.0170	0.0112	0.0070	0.0062	0.0017	0.0008	0.0004	0.0008	0.0000	0.0008	0.0008	0.0008
State 8	0.0000	0.0078	0.0266	0.0535	0.0779	0.1005	0.1327	0.1230	0.1138	0.0995	0.0728	0.0521	0.0512	0.0323	0.0203	0.0161	0.0115	0.0061	0.0005	0.0005	0.0014	0.0005	0.0009	0.0005	0.0000
State 9	0.0000	0.0041	0.0137	0.0344	0.0523	0.0770	0.1099	0.1125	0.1120	0.1028	0.1049	0.0811	0.0719	0.0466	0.0309	0.0187	0.0096	0.0041	0.0005	0.0005	0.0005	0.0005	0.0005	0.0005	0.0005
State 10	0.0000	0.0016	0.0073	0.0199	0.0376	0.0700	0.0925	0.0993	0.1066	0.1619	0.1051	0.1061	0.0795	0.0711	0.0549	0.0240	0.0136	0.0042	0.0028	0.0016	0.0005	0.0000	0.0000	0.0000	0.0000
State 11	0.0000	0.0016	0.0054	0.0189	0.0226	0.0539	0.0717	0.0900	0.1013	0.1019	0.1154	0.1078	0.1073	0.0776	0.0518	0.0313	0.0218	0.0097	0.0038	0.0032	0.0011	0.0011	0.0005	0.0005	0.0000
State 12	0.0006	0.0017	0.0035	0.0117	0.0204	0.0449	0.0408	0.0758	0.0927	0.0866	0.1073	0.0939	0.1102	0.1329	0.0741	0.0484	0.0327	0.0146	0.0023	0.0023	0.0000	0.0000	0.0000	0.0006	0.0000
State 13	0.0000	0.0017	0.0023	0.0104	0.0161	0.0253	0.0541	0.0495	0.0789	0.0910	0.1071	0.1002	0.0950	0.1313	0.1192	0.0651	0.0334	0.0109	0.0058	0.0017	0.0012	0.0000	0.0000	0.0000	0.0000
State 14	0.0000	0.0011	0.0017	0.0039	0.0078	0.0173	0.0279	0.0334	0.0535	0.0713	0.0836	0.0986	0.1176	0.1298	0.1621	0.1226	0.0507	0.0178	0.0066	0.0017	0.0006	0.0006	0.0006	0.0006	0.0000
State 15	0.0006	0.0000	0.0018	0.0042	0.0071	0.0172	0.0166	0.0279	0.0366	0.0528	0.0652	0.0718	0.1168	0.1406	0.1560	0.1595	0.0872	0.0265	0.0065	0.0006	0.0000	0.0006	0.0000	0.0000	0.0000
State 16	0.0000	0.0006	0.0013	0.0026	0.0051	0.0084	0.0135	0.0231	0.0199	0.0315	0.0450	0.0553	0.0739	0.1253	0.1620	0.2102	0.1597	0.0450	0.0129	0.0045	0.0013	0.0000	0.0000	0.0000	0.0000
State 17	0.0000	0.0016	0.0000	0.0023	0.0008	0.0094	0.0094	0.0117	0.0164	0.0203	0.0391	0.0383	0.0571	0.0735	0.1071	0.1806	0.2598	0.1400	0.0235	0.0055	0.0039	0.0000	0.0000	0.0000	0.0000
State 18	0.0000	0.0000	0.0000	0.0014	0.0041	0.0027	0.0082	0.0082	0.0137	0.0205	0.0274	0.0369	0.0492	0.0508	0.0643	0.0848	0.2339	0.3119	0.0725	0.0068	0.0027	0.0000	0.0000	0.0000	0.0000
State 19	0.0000	0.0000	0.0000	0.0000	0.0000	0.0076	0.0038	0.0115	0.0191	0.0229	0.0267	0.0382	0.0496	0.0382	0.0344	0.0534	0.1145	0.2252	0.3206	0.0305	0.0000	0.0000	0.0000	0.0038	0.0000
State 20	0.0000	0.0000	0.0000	0.0000	0.0000	0.0152	0.0000	0.0000	0.0606	0.0303	0.0455	0.0909	0.0606	0.0758	0.0758	0.0455	0.0606	0.1364	0.2121	0.0909	0.0000	0.0000	0.0000	0.0000	0.0000
State 21	0.0000	0.0000	0.0000	0.0500	0.0500	0.0500	0.0500	0.1000	0.0000	0.0500	0.2000	0.0000	0.0000	0.0500	0.1500	0.1000	0.0500	0.0000	0.0000	0.0500	0.0500	0.0000	0.0000	0.0000	0.0000
State 22	0.0000	0.0000	0.0000	0.1429	0.0000	0.0000	0.0000	0.0000	0.0000	0.0000	0.0000	0.1429	0.1429	0.1429	0.0000	0.0000	0.1429	0.0000	0.1429	0.1429	0.0000	0.0000	0.0000	0.0000	0.0000
State 23	0.0000	0.0000	0.0000	0.0000	0.1250	0.0000	0.1250	0.0000	0.1250	0.0000	0.1250	0.2500	0.0000	0.0000	0.1250	0.1250	0.0000	0.0000	0.0000	0.0000	0.0000	0.0000	0.0000	0.0000	0.0000
State 24	0.0000	0.0000	0.0000	0.0000	0.2000	0.2000	0.0000	0.0000	0.2000	0.0000	0.0000	0.0000	0.0000	0.0000	0.0000	0.0000	0.2000	0.0000	0.0000	0.0000	0.0000	0.0000	0.2000	0.0000	0.0000
State 25	0.0000	0.0000	0.0000	0.0000	0.0000	0.0000	0.0000	0.0000	0.0000	0.0000	0.2000	0.2000	0.0000	0.2000	0.0000	0.0000	0.0000	0.0000	0.0000	0.2000	0.2000	0.0000	0.0000	0.0000	0.0000

Table A- 11 Limiting Transition Matrix from yearly average UK MTM

	State 1	State 2	State 3	State 4	State 5	State 6	State 7	State 8	State 9	State 10	State 11	State 12	State 13	State 14	State 15	State 16	State 17	State 18	State 19	State 20	State 21	State 22	State 23	State 24	State 25
State 1	0.0123	0.0479	0.0693	0.0731	0.0709	0.0730	0.0724	0.0651	0.0612	0.0586	0.0577	0.0535	0.0547	0.0564	0.0525	0.0475	0.0394	0.0224	0.0079	0.0019	0.0008	0.0005	0.0003	0.0004	0.0002
State 2	0.0123	0.0479	0.0693	0.0731	0.0709	0.0730	0.0724	0.0651	0.0612	0.0586	0.0577	0.0535	0.0547	0.0564	0.0525	0.0475	0.0394	0.0224	0.0079	0.0019	0.0008	0.0005	0.0003	0.0004	0.0002
State 3	0.0123	0.0479	0.0693	0.0731	0.0709	0.0730	0.0724	0.0651	0.0612	0.0586	0.0577	0.0535	0.0547	0.0564	0.0525	0.0475	0.0394	0.0224	0.0079	0.0019	0.0008	0.0005	0.0003	0.0004	0.0002
State 4	0.0123	0.0479	0.0693	0.0731	0.0709	0.0730	0.0724	0.0651	0.0612	0.0586	0.0577	0.0535	0.0547	0.0564	0.0525	0.0475	0.0394	0.0224	0.0079	0.0019	0.0008	0.0005	0.0003	0.0004	0.0002
State 5	0.0123	0.0479	0.0693	0.0731	0.0709	0.0730	0.0724	0.0651	0.0612	0.0586	0.0577	0.0535	0.0547	0.0564	0.0525	0.0475	0.0394	0.0224	0.0079	0.0019	0.0008	0.0005	0.0003	0.0004	0.0002
State 6	0.0123	0.0479	0.0693	0.0731	0.0709	0.0730	0.0724	0.0651	0.0612	0.0586	0.0577	0.0535	0.0547	0.0564	0.0525	0.0475	0.0394	0.0224	0.0079	0.0019	0.0008	0.0005	0.0003	0.0004	0.0002
State 7	0.0123	0.0479	0.0693	0.0731	0.0709	0.0730	0.0724	0.0651	0.0612	0.0586	0.0577	0.0535	0.0547	0.0564	0.0525	0.0475	0.0394	0.0224	0.0079	0.0019	0.0008	0.0005	0.0003	0.0004	0.0002
State 8	0.0123	0.0479	0.0693	0.0731	0.0709	0.0730	0.0724	0.0651	0.0612	0.0586	0.0577	0.0535	0.0547	0.0564	0.0525	0.0475	0.0394	0.0224	0.0079	0.0019	0.0008	0.0005	0.0003	0.0004	0.0002
State 9	0.0123	0.0479	0.0693	0.0731	0.0709	0.0730	0.0724	0.0651	0.0612	0.0586	0.0577	0.0535	0.0547	0.0564	0.0525	0.0475	0.0394	0.0224	0.0079	0.0019	0.0008	0.0005	0.0003	0.0004	0.0002
State 10	0.0123	0.0479	0.0693	0.0731	0.0709	0.0730	0.0724	0.0651	0.0612	0.0586	0.0577	0.0535	0.0547	0.0564	0.0525	0.0475	0.0394	0.0224	0.0079	0.0019	0.0008	0.0005	0.0003	0.0004	0.0002
State 11	0.0123	0.0479	0.0693	0.0731	0.0709	0.0730	0.0724	0.0651	0.0612	0.0586	0.0577	0.0535	0.0547	0.0564	0.0525	0.0475	0.0394	0.0224	0.0079	0.0019	0.0008	0.0005	0.0003	0.0004	0.0002
State 12	0.0123	0.0479	0.0693	0.0731	0.0709	0.0730	0.0724	0.0651	0.0612	0.0586	0.0577	0.0535	0.0547	0.0564	0.0525	0.0475	0.0394	0.0224	0.0079	0.0019	0.0008	0.0005	0.0003	0.0004	0.0002
State 13	0.0123	0.0479	0.0693	0.0731	0.0709	0.0730	0.0724	0.0651	0.0612	0.0586	0.0577	0.0535	0.0547	0.0564	0.0525	0.0475	0.0394	0.0224	0.0079	0.0019	0.0008	0.0005	0.0003	0.0004	0.0002
State 14	0.0123	0.0479	0.0693	0.0731	0.0709	0.0730	0.0724	0.0651	0.0612	0.0586	0.0577	0.0535	0.0547	0.0564	0.0525	0.0475	0.0394	0.0224	0.0079	0.0019	0.0008	0.0005	0.0003	0.0004	0.0002
State 15	0.0123	0.0479	0.0693	0.0731	0.0709	0.0730	0.0724	0.0651	0.0612	0.0586	0.0577	0.0535	0.0547	0.0564	0.0525	0.0475	0.0394	0.0224	0.0079	0.0019	0.0008	0.0005	0.0003	0.0004	0.0002
State 16	0.0123	0.0479	0.0693	0.0731	0.0709	0.0730	0.0724	0.0651	0.0612	0.0586	0.0577	0.0535	0.0547	0.0564	0.0525	0.0475	0.0394	0.0224	0.0079	0.0019	0.0008	0.0005	0.0003	0.0004	0.0002
State 17	0.0123	0.0479	0.0693	0.0731	0.0709	0.0730	0.0724	0.0651	0.0612	0.0586	0.0577	0.0535	0.0547	0.0564	0.0525	0.0475	0.0394	0.0224	0.0079	0.0019	0.0008	0.0005	0.0003	0.0004	0.0002
State 18	0.0123	0.0479	0.0693	0.0731	0.0709	0.0730	0.0724	0.0651	0.0612	0.0586	0.0577	0.0535	0.0547	0.0564	0.0525	0.0475	0.0394	0.0224	0.0079	0.0019	0.0008	0.0005	0.0003	0.0004	0.0002
State 19	0.0123	0.0479	0.0693	0.0731	0.0709	0.0730	0.0724	0.0651	0.0612	0.0586	0.0577	0.0535	0.0547	0.0564	0.0525	0.0475	0.0394	0.0224	0.0079	0.0019	0.0008	0.0005	0.0003	0.0004	0.0002
State 20	0.0123	0.0479	0.0693	0.0731	0.0709	0.0730	0.0724	0.0651	0.0612	0.0586	0.0577	0.0535	0.0547	0.0564	0.0525	0.0475	0.0394	0.0224	0.0079	0.0019	0.0008	0.0005	0.0003	0.0004	0.0002
State 21	0.0123	0.0479	0.0693	0.0731	0.0709	0.0730	0.0724	0.0651	0.0612	0.0586	0.0577	0.0535	0.0547	0.0564	0.0525	0.0475	0.0394	0.0224	0.0079	0.0019	0.0008	0.0005	0.0003	0.0004	0.0002
State 22	0.0123	0.0479	0.0693	0.0731	0.0709	0.0730	0.0724	0.0651	0.0612	0.0586	0.0577	0.0535	0.0547	0.0564	0.0525	0.0475	0.0394	0.0224	0.0079	0.0019	0.0008	0.0005	0.0003	0.0004	0.0002
State 23	0.0123	0.0479	0.0693	0.0731	0.0709	0.0730	0.0724	0.0651	0.0612	0.0586	0.0577	0.0535	0.0547	0.0564	0.0525	0.0475	0.0394	0.0224	0.0079	0.0019	0.0008	0.0005	0.0003	0.0004	0.0002
State 24	0.0123	0.0479	0.0693	0.0731	0.0709	0.0730	0.0724	0.0651	0.0612	0.0586	0.0577	0.0535	0.0547	0.0564	0.0525	0.0475	0.0394	0.0224	0.0079	0.0019	0.0008	0.0005	0.0003	0.0004	0.0002
State 25	0.0123	0.0479	0.0693	0.0731	0.0709	0.0730	0.0724	0.0651	0.0612	0.0586	0.0577	0.0535	0.0547	0.0564	0.0525	0.0475	0.0394	0.0224	0.0079	0.0019	0.0008	0.0005	0.0003	0.0004	0.0002

Table A- 12 Yearly half-hour average UK MTM

	State 1	State 2	State 3	State 4	State 5	State 6	State 7	State 8	State 9	State 10	State 11	State 12	State 13	State 14	State 15	State 16	State 17	State 18	State 19	State 20	State 21	State 22	State 23	State 24	State 25
State 1	0.5129	0.3259	0.0810	0.0454	0.0116	0.0045	0.0053	0.0000	0.0027	0.0036	0.0027	0.0000	0.0000	0.0018	0.0000	0.0009	0.0009	0.0009	0.0000	0.0000	0.0000	0.0000	0.0000	0.0000	0.0000
State 2	0.1037	0.4982	0.2448	0.0863	0.0340	0.0193	0.0109	0.0049	0.0022	0.0011	0.0005	0.0014	0.0011	0.0003	0.0000	0.0005	0.0000	0.0000	0.0003	0.0000	0.0000	0.0000	0.0000	0.0003	0.0003
State 3	0.0188	0.1929	0.3839	0.2222	0.0896	0.0362	0.0209	0.0112	0.0067	0.0051	0.0034	0.0030	0.0030	0.0008	0.0019	0.0006	0.0000	0.0006	0.0000	0.0000	0.0000	0.0002	0.0000	0.0000	0.0000
State 4	0.0096	0.0701	0.2079	0.3007	0.1629	0.0965	0.0506	0.0260	0.0178	0.0096	0.0090	0.0051	0.0041	0.0020	0.0016	0.0012	0.0010	0.0010	0.0004	0.0004	0.0002	0.0000	0.0000	0.0000	0.0000
State 5	0.0031	0.0247	0.0860	0.1852	0.2365	0.1852	0.1109	0.0534	0.0353	0.0238	0.0184	0.0098	0.0059	0.0033	0.0022	0.0026	0.0020	0.0015	0.0000	0.0000	0.0002	0.0000	0.0000	0.0000	0.0000
State 6	0.0028	0.0134	0.0428	0.1070	0.1741	0.2069	0.1676	0.1036	0.0547	0.0406	0.0272	0.0203	0.0136	0.0067	0.0052	0.0052	0.0032	0.0026	0.0011	0.0004	0.0002	0.0002	0.0002	0.0002	0.0000
State 7	0.0011	0.0103	0.0244	0.0573	0.1099	0.1608	0.1920	0.1405	0.1033	0.0809	0.0464	0.0298	0.0217	0.0128	0.0114	0.0076	0.0038	0.0043	0.0011	0.0007	0.0004	0.0000	0.0000	0.0000	0.0002
State 8	0.0008	0.0060	0.0156	0.0321	0.0709	0.1241	0.1635	0.1530	0.1176	0.0896	0.0704	0.0469	0.0401	0.0263	0.0182	0.0117	0.0078	0.0029	0.0021	0.0005	0.0003	0.0009	0.0000	0.0003	0.0000
State 9	0.0000	0.0045	0.0122	0.0217	0.0427	0.0787	0.1190	0.1336	0.1306	0.1217	0.1003	0.0706	0.0543	0.0401	0.0252	0.0220	0.0066	0.0083	0.0027	0.0009	0.0009	0.0003	0.0006	0.0006	0.0000
State 10	0.0003	0.0029	0.0068	0.0190	0.0370	0.0666	0.0865	0.1070	0.1128	0.1240	0.1154	0.1041	0.0710	0.0543	0.0431	0.0286	0.0151	0.0087	0.0039	0.0029	0.0013	0.0000	0.0009	0.0006	0.0000
State 11	0.0017	0.0020	0.0051	0.0139	0.0240	0.0450	0.0690	0.0917	0.1099	0.1160	0.1133	0.1127	0.0988	0.0734	0.0457	0.0335	0.0237	0.0132	0.0054	0.0020	0.0024	0.0000	0.0000	0.0003	0.0003
State 12	0.0000	0.0004	0.0054	0.0105	0.0181	0.0366	0.0504	0.0867	0.0873	0.1072	0.1123	0.1018	0.1478	0.0942	0.0620	0.0399	0.0254	0.0149	0.0098	0.0036	0.0025	0.0018	0.0011	0.0000	0.0004
State 13	0.0003	0.0010	0.0020	0.0044	0.0166	0.0244	0.0338	0.0536	0.0687	0.0873	0.0968	0.1134	0.1350	0.1641	0.0873	0.0596	0.0372	0.0183	0.0095	0.0037	0.0024	0.0007	0.0009	0.0003	0.0000
State 14	0.0000	0.0010	0.0010	0.0037	0.0088	0.0173	0.0248	0.0421	0.0466	0.0551	0.0636	0.0935	0.1339	0.1547	0.1808	0.0809	0.0428	0.0265	0.0122	0.0088	0.0014	0.0010	0.0000	0.0000	0.0003
State 15	0.0000	0.0010	0.0007	0.0034	0.0044	0.0106	0.0160	0.0263	0.0239	0.0444	0.0447	0.0708	0.0877	0.1468	0.2028	0.1905	0.0731	0.0311	0.0137	0.0048	0.0020	0.0010	0.0003	0.0007	0.0000
State 16	0.0000	0.0000	0.0014	0.0014	0.0048	0.0069	0.0131	0.0152	0.0203	0.0307	0.0376	0.0393	0.0551	0.0861	0.1671	0.2829	0.1523	0.0562	0.0183	0.0089	0.0038	0.0007	0.0000	0.0000	0.0000
State 17	0.0000	0.0000	0.0009	0.0013	0.0047	0.0055	0.0108	0.0140	0.0170	0.0221	0.0277	0.0374	0.0477	0.0638	0.0791	0.1617	0.3953	0.1272	0.0323	0.0081	0.0021	0.0013	0.0000	0.0000	0.0000
State 18	0.0000	0.0000	0.0006	0.0012	0.0024	0.0072	0.0113	0.0084	0.0125	0.0268	0.0298	0.0263	0.0495	0.0471	0.0515	0.0794	0.1677	0.3663	0.0911	0.0161	0.0030	0.0012	0.0000	0.0000	0.0006
State 19	0.0000	0.0000	0.0026	0.0026	0.0039	0.0013	0.0105	0.0118	0.0105	0.0236	0.0249	0.0327	0.0484	0.0406	0.0599	0.0654	0.0825	0.1924	0.3233	0.0445	0.0170	0.0026	0.0000	0.0000	0.0000
State 20	0.0000	0.0000	0.0000	0.0000	0.0000	0.0046	0.0183	0.0046	0.0411	0.0411	0.0411	0.0411	0.0602	0.0776	0.0594	0.1142	0.1142	0.0959	0.1644	0.1096	0.0137	0.0046	0.0046	0.0000	0.0000
State 21	0.0000	0.0000	0.0000	0.0208	0.0104	0.0104	0.0104	0.0104	0.0000	0.0313	0.0313	0.0208	0.0833	0.1042	0.0625	0.0625	0.0521	0.1042	0.1563	0.1146	0.0833	0.0208	0.0104	0.0000	0.0000
State 22	0.0294	0.0000	0.0000	0.0000	0.0588	0.0000	0.0000	0.0000	0.0588	0.0294	0.1176	0.0294	0.0588	0.0000	0.0882	0.0882	0.1176	0.0588	0.1176	0.0882	0.0588	0.0000	0.0000	0.0000	0.0000
State 23	0.0000	0.0500	0.1000	0.0000	0.1000	0.0000	0.1500	0.0000	0.0000	0.0500	0.1000	0.0500	0.1000	0.0000	0.0500	0.0000	0.1000	0.1000	0.0000	0.0000	0.0500	0.0000	0.0000	0.0000	0.0000
State 24	0.0000	0.0000	0.0000	0.1000	0.0000	0.1000	0.0000	0.1000	0.1000	0.1000	0.0000	0.0000	0.1000	0.0000	0.0000	0.1000	0.0000	0.0000	0.1000	0.0000	0.0000	0.1000	0.0000	0.1000	0.0000
State 25	0.0000	0.0000	0.0000	0.0000	0.1111	0.0000	0.1111	0.1111	0.0000	0.1111	0.1111	0.0000	0.1111	0.0000	0.0000	0.0000	0.0000	0.1111	0.0000	0.0000	0.1111	0.0000	0.0000	0.1111	0.0000

Table A- 13 Limiting Transition Matrix from yearly half-hour average UK MTM

	State 1	State 2	State 3	State 4	State 5	State 6	State 7	State 8	State 9	State 10	State 11	State 12	State 13	State 14	State 15	State 16	State 17	State 18	State 19	State 20	State 21	State 22	State 23	State 24	State 25
State 1	0.0193	0.0622	0.0789	0.0804	0.0758	0.0756	0.0736	0.0628	0.0550	0.0512	0.0482	0.0451	0.0479	0.0471	0.0472	0.0467	0.0379	0.0269	0.0121	0.0035	0.0015	0.0005	0.0002	0.0002	0.0001
State 2	0.0193	0.0622	0.0789	0.0804	0.0758	0.0756	0.0736	0.0628	0.0550	0.0512	0.0482	0.0451	0.0479	0.0471	0.0472	0.0467	0.0379	0.0269	0.0121	0.0035	0.0015	0.0005	0.0002	0.0002	0.0001
State 3	0.0193	0.0622	0.0789	0.0804	0.0758	0.0756	0.0736	0.0628	0.0550	0.0512	0.0482	0.0451	0.0479	0.0471	0.0472	0.0467	0.0379	0.0269	0.0121	0.0035	0.0015	0.0005	0.0002	0.0002	0.0001
State 4	0.0193	0.0622	0.0789	0.0804	0.0758	0.0756	0.0736	0.0628	0.0550	0.0512	0.0482	0.0451	0.0479	0.0471	0.0472	0.0467	0.0379	0.0269	0.0121	0.0035	0.0015	0.0005	0.0002	0.0002	0.0001
State 5	0.0193	0.0622	0.0789	0.0804	0.0758	0.0756	0.0736	0.0628	0.0550	0.0512	0.0482	0.0451	0.0479	0.0471	0.0472	0.0467	0.0379	0.0269	0.0121	0.0035	0.0015	0.0005	0.0002	0.0002	0.0001
State 6	0.0193	0.0622	0.0789	0.0804	0.0758	0.0756	0.0736	0.0628	0.0550	0.0512	0.0482	0.0451	0.0479	0.0471	0.0472	0.0467	0.0379	0.0269	0.0121	0.0035	0.0015	0.0005	0.0002	0.0002	0.0001
State 7	0.0193	0.0622	0.0789	0.0804	0.0758	0.0756	0.0736	0.0628	0.0550	0.0512	0.0482	0.0451	0.0479	0.0471	0.0472	0.0467	0.0379	0.0269	0.0121	0.0035	0.0015	0.0005	0.0002	0.0002	0.0001
State 8	0.0193	0.0622	0.0789	0.0804	0.0758	0.0756	0.0736	0.0628	0.0550	0.0512	0.0482	0.0451	0.0479	0.0471	0.0472	0.0467	0.0379	0.0269	0.0121	0.0035	0.0015	0.0005	0.0002	0.0002	0.0001
State 9	0.0193	0.0622	0.0789	0.0804	0.0758	0.0756	0.0736	0.0628	0.0550	0.0512	0.0482	0.0451	0.0479	0.0471	0.0472	0.0467	0.0379	0.0269	0.0121	0.0035	0.0015	0.0005	0.0002	0.0002	0.0001
State 10	0.0193	0.0622	0.0789	0.0804	0.0758	0.0756	0.0736	0.0628	0.0550	0.0512	0.0482	0.0451	0.0479	0.0471	0.0472	0.0467	0.0379	0.0269	0.0121	0.0035	0.0015	0.0005	0.0002	0.0002	0.0001
State 11	0.0193	0.0622	0.0789	0.0804	0.0758	0.0756	0.0736	0.0628	0.0550	0.0512	0.0482	0.0451	0.0479	0.0471	0.0472	0.0467	0.0379	0.0269	0.0121	0.0035	0.0015	0.0005	0.0002	0.0002	0.0001
State 12	0.0193	0.0622	0.0789	0.0804	0.0758	0.0756	0.0736	0.0628	0.0550	0.0512	0.0482	0.0451	0.0479	0.0471	0.0472	0.0467	0.0379	0.0269	0.0121	0.0035	0.0015	0.0005	0.0002	0.0002	0.0001
State 13	0.0193	0.0622	0.0789	0.0804	0.0758	0.0756	0.0736	0.0628	0.0550	0.0512	0.0482	0.0451	0.0479	0.0471	0.0472	0.0467	0.0379	0.0269	0.0121	0.0035	0.0015	0.0005	0.0002	0.0002	0.0001
State 14	0.0193	0.0622	0.0789	0.0804	0.0758	0.0756	0.0736	0.0628	0.0550	0.0512	0.0482	0.0451	0.0479	0.0471	0.0472	0.0467	0.0379	0.0269	0.0121	0.0035	0.0015	0.0005	0.0002	0.0002	0.0001
State 15	0.0193	0.0622	0.0789	0.0804	0.0758	0.0756	0.0736	0.0628	0.0550	0.0512	0.0482	0.0451	0.0479	0.0471	0.0472	0.0467	0.0379	0.0269	0.0121	0.0035	0.0015	0.0005	0.0002	0.0002	0.0001
State 16	0.0193	0.0622	0.0789	0.0804	0.0758	0.0756	0.0736	0.0628	0.0550	0.0512	0.0482	0.0451	0.0479	0.0471	0.0472	0.0467	0.0379	0.0269	0.0121	0.0035	0.0015	0.0005	0.0002	0.0002	0.0001
State 17	0.0193	0.0622	0.0789	0.0804	0.0758	0.0756	0.0736	0.0628	0.0550	0.0512	0.0482	0.0451	0.0479	0.0471	0.0472	0.0467	0.0379	0.0269	0.0121	0.0035	0.0015	0.0005	0.0002	0.0002	0.0001
State 18	0.0193	0.0622	0.0789	0.0804	0.0758	0.0756	0.0736	0.0628	0.0550	0.0512	0.0482	0.0451	0.0479	0.0471	0.0472	0.0467	0.0379	0.0269	0.0121	0.0035	0.0015	0.0005	0.0002	0.0002	0.0001
State 19	0.0193	0.0622	0.0789	0.0804	0.0758	0.0756	0.0736	0.0628	0.0550	0.0512	0.0482	0.0451	0.0479	0.0471	0.0472	0.0467	0.0379	0.0269	0.0121	0.0035	0.0015	0.0005	0.0002	0.0002	0.0001
State 20	0.0193	0.0622	0.0789	0.0804	0.0758	0.0756	0.0736	0.0628	0.0550	0.0512	0.0482	0.0451	0.0479	0.0471	0.0472	0.0467	0.0379	0.0269	0.0121	0.0035	0.0015	0.0005	0.0002	0.0002	0.0001
State 21	0.0193	0.0622	0.0789	0.0804	0.0758	0.0756	0.0736	0.0628	0.0550	0.0512	0.0482	0.0451	0.0479	0.0471	0.0472	0.0467	0.0379	0.0269	0.0121	0.0035	0.0015	0.0005	0.0002	0.0002	0.0001
State 22	0.0193	0.0622	0.0789	0.0804	0.0758	0.0756	0.0736	0.0628	0.0550	0.0512	0.0482	0.0451	0.0479	0.0471	0.0472	0.0467	0.0379	0.0269	0.0121	0.0035	0.0015	0.0005	0.0002	0.0002	0.0001
State 23	0.0193	0.0622	0.0789	0.0804	0.0758	0.0756	0.0736	0.0628	0.0550	0.0512	0.0482	0.0451	0.0479	0.0471	0.0472	0.0467	0.0379	0.0269	0.0121	0.0035	0.0015	0.0005	0.0002	0.0002	0.0001
State 24	0.0193	0.0622	0.0789	0.0804	0.0758	0.0756	0.0736	0.0628	0.0550	0.0512	0.0482	0.0451	0.0479	0.0471	0.0472	0.0467	0.0379	0.0269	0.0121	0.0035	0.0015	0.0005	0.0002	0.0002	0.0001
State 25	0.0193	0.0622	0.0789	0.0804	0.0758	0.0756	0.0736	0.0628	0.0550	0.0512	0.0482	0.0451	0.0479	0.0471	0.0472	0.0467	0.0379	0.0269	0.0121	0.0035	0.0015	0.0005	0.0002	0.0002	0.0001

APPENDIX B – NON-DOMESTIC BUILDING STOCK DATA

In the NDBS report[11], non-domestic buildings were divided into 14 activity groups and six major built form groups and details are given in Table B- 1 and Table B- 2. Figure B- 1 shows the classification of non-domestic premises by different built form groups.

Table B- 1 Classification of non-domestic premises by activity groups

Activity Group	*Contains*
Office	Commercial offices, Local government offices, Surgeries, Adult education, Police Stations, Law-courts
Retail	Smaller shops, Financial and Commercial services, Personal services, Eating places (Restaurants, Cafes)
Large shops	
Commercial residential	Boarding houses and guest houses, Hotels, Public houses, homes and hotels
Performance halls	Theatres, Cinemas and Bingo halls
Leisure halls	Scout and guide huts, Village and church halls, Leisure centres, Sport halls, Swimming pools, Museums and Art galleries
Clubs	Clubhouses including sports clubhouses, night clubs and discotheques
Manufacturing	Factories, Works, Mills, Workshops, Garages, Vehicle showrooms and Telephone exchanges
Storage	Warehouses and stores
Depots	Storage depots, road haulage depots, bus or coach depots
Parking	Parking buildings
Education	Nursery schools and kindergartens, Primary schools, Secondary schools, Special schools
Churches	Churches and other places of worship
Hospitals	

[11] P. Steadman et al., "Inferences about built form, construction and fabric in the nondomestic building stock of England and Wales", Environment and Planning B: Planning and Design, Vol. 27, pp. 733-758, 2000.

Table B- 2 Grouping of non-domestic premises by built forms

Built Form Grouping		Contains
Side-lit (CSX)	CS4	Cellular side-lit strip, 1-4 storeys
	CS5	Cellular side-lit strip, more than 4 storeys
	OD4	Open-plan side-lit strip, 1-4 storeys
	OD5	Open plan side-lit strip, more than 4 storeys
Deep Plan (CDOX)	CD0	Cellular side-lit around deep-plan artificially fit
	CDH	Cellular side-lit around hall
	OA	Open-plan multi-storey artificially fit
Sheds (OSX)	OS	Open plan single shed
	CDS	Shed with cellular day-lit strip inside
	OC1	Open-plan continuous single storey
	AI	Monopitch aisle to hall or shed
Halls (Hall)	HA	Artificially lit hall
	HD	Day-lit hall
Extensions (EX)	EX	Small single storey extension
Circulation (CIRC)	CB	Circulation bridge
	CL	Ground level circulation link
	CT	Attached circulation tower
	PO	Porch
Other (MISC)	CT1	Cellular top-lit single storey
	OG	Open plan car parking, Trucking deck
	PR	Roof level plant room
	RA	Railway arch
	SR	Single room form
	SSR	String of single room forms plus all other parasitic forms

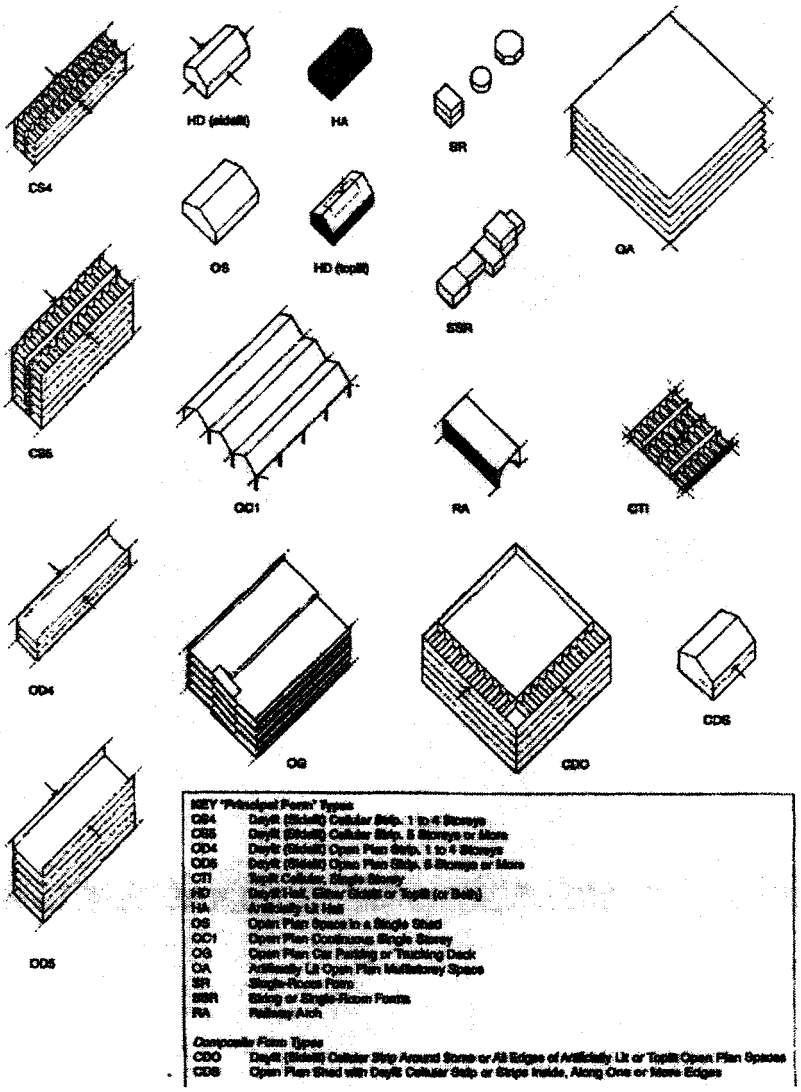

Figure B- 1 Representation of different built form groups (Source: NDBS Report)

In the NDBS report, the number of premises in each activity group by eight different size distributions is given in Table B- 3. After neglecting the number of premises which are not suitable for PV installation, the number of premises in each activity group is given in Table B- 4. The mean floor area for each activity group by eight different size distributions is given in Table B-5. From this the mean floor area for non-domestic buildings in each size band was calculated and results are given in Table B- 6. These data were used to model the non-domestic PV systems.

Table B- 3 Number of non-domestic premises in each activity groups

Premises Size Band (m^2)	Schools	Offices	Retail	Large shops	Commercial/ Residential	Performance Halls	Leisure Hall	Clubs	Manufacturing	Storage	Depot	Parking	Hospitals	Churches	All
0-30	0	40830	77365	40	829	0	1437	0	13746	18021	2430	0	0	956	155654
30-100	0	106462	313321	23	3315	88	7186	1330	78176	41206	2275	3740	2	956	558080
100-300	562	84610	154093	112	18231	88	12648	13740	101690	50048	3481	5440	22	18401	463166
300-1000	5776	32720	34433	3686	63252	350	5174	25486	65016	41121	4781	6800	197	21029	309821
1000-3000	17359	7897	2783	5066	3596	800	1437	3324	23384	16370	2817	510	382	6452	92177
3k-10k	4098	2445	528	2598	3018	536	575	443	8684	5154	1223	170	502	0	29974
10k-30k	1050	377	29	172	145	88	287	0	2198	889	236	340	336	0	6147
30k-100k	0	35	4	24	0	0	0	0	462	83	35	0	368	0	1011
	28845	275376	582556	11721	92386	1950	28744	44323	293356	172892	17278	17000	1809	47794	1616030

Table B- 4 Potential non-domestic premises for PV installation in each activity groups

Premises Size Band (m^2)	Schools	Offices	Retail	Large shops	Commercial/ Residential	Performance Halls	Leisure Hall	Clubs	Manufacturing	Storage	Depot	Parking	Hospitals	Churches	All
0-30	0	40830	0	40	829	0	1437	0	13746	18021	2430	0	0	0	77333
30-100	0	106462	0	23	3315	88	7186	0	78176	41206	2275	3740	2	0	242473
100-300	562	84610	0	112	18231	88	12648	0	101690	50048	3481	5440	22	0	276932
300-1000	5776	32720	34433	3686	63252	350	5174	25486	65016	41121	4781	6800	197	0	288792
1000-3000	17359	7897	2783	5066	3596	800	1437	3324	23384	16370	2817	510	382	0	85725
3k-10k	4098	2445	528	2598	3018	536	575	443	8684	5154	1223	170	502	0	29974
10k-30k	1050	377	29	172	145	88	287	0	2198	889	236	340	336	0	6147
30k-100k	0	35	4	24	0	0	0	0	462	83	35	0	368	0	1011
	28845	275376	582556	11721	92386	1950	28744	44323	293356	172892	17278	17000	1809	0	1008387

Table B- 5 Mean floor area by premises size group

Premises Size Band (m^2)	Schools	Offices	Retail	Large shops	Commercial/ Residential	Performance Halls	Leisure Hall	Clubs	Manufacturing	Storage	Depot	Parking	Hospitals	Churches
0-30	0	24	0	3	20	0	20	0	22	19	9	0	0	0
30-100	0	80	0	84	50	65	65	0	71	68	69	65	65	0
100-300	135	222	0	244	128	200	200	0	195	198	207	200	201	0
300-1000	519	660	605	982	484	650	650	540	582	599	632	650	701	0
1000-3000	1702	2136	2084	1997	1755	2000	2000	1670	1822	1830	1882	2000	1905	0
3k-10k	5729	6517	5733	5860	5000	6500	6500	4700	5629	5469	5486	6500	5866	0
10k-30k	12066	19117	18896	17012	15840	20000	20000	0	17453	16897	17238	20000	17882	0
30k-100k	0	53515	79104	64706	0	0	0	0	58917	49963	61877	0	58608	0

Table B- 6 Mean floor area by premises size band

Premises Size band (m^2)	Number of Premises	Total Floor Area (m^2)	Mean Floor Area (m^2)	Percentage (%)
0-30	77333	1692041	22	7.67
30-100	242473	17910161	74	24.05
100-300	276932	55319429	200	27.46
300-1000	288792	167062049	578	28.64
1000-3000	85725	158277696	1846	8.50
3k-10k	29974	169884983	5668	2.97
10k-30k	6174	103406904	16822	0.61
30k-100k	1011	58842407	58202	0.10

APPENDIX C – NUMBER OF NEW DWELLINGS

This Table C- 1 shows the number of new dwellings for different regions in England and Wales, from 1991 to 2001. These values were used to estimate the average number of new dwellings completed for a year and were used to project the dwelling stock for the year 2030.

Table C- 1 Number of new dwellings completed in England and Wales, from 1991 to 2001

Year	Number of New Dwellings started and completed										
	1990	1991	1992	1993	1994	1995	1996	1997	1998	1999	2000
North East	6,876	6,620	6,497	6,304	7,408	6,818	7,151	7,581	6,665	7,428	6,760
North West	18,951	18,764	19,081	19,831	21,036	20,496	19,447	19,201	18,969	18,922	19,716
Yorkshire & the Humber	12,244	13,944	13,018	14,211	14,882	14,910	15,159	15,464	13,085	13,418	13,361
East Midlands	14,730	15,522	14,205	15,148	16,700	16,213	14,067	14,549	14,755	16,378	13,619
West Midlands	16,697	15,611	16,528	14,803	17,220	14,792	14,292	13,392	14,301	15,297	13,871
East	22,838	21,599	20,056	21,817	21,871	21,203	21,408	21,301	18,986	18,745	16,243
London	17,232	17,077	14,433	14,632	15,122	16,291	12,577	13,623	12,864	12,480	14,205
South East	29,867	27,373	24,040	25,797	26,955	26,992	24,981	25,441	23,346	23,175	21,995
South West	20,597	18,622	14,873	15,171	16,772	16,884	16,775	19,003	15,929	15,912	14,969

APPENDIX D – LIST OF PUBLICATIONS

1. R. Jayaraman, N.M. Pearsall and G.A. Putrus, "Optimal sizing of inverters for grid-connected PV systems", 37th International Universities Power Engineering Conference, Staffordshire, UK, September 2002, Vol.2, pp 783-787.

2. J. Ramachandran, N.M. Pearsall, "Synthetic generation of solar radiation for different locations in the UK", Conference C79 of the Solar Energy Society, Loughborough, UK, April 2003, pp 31-36.

3. J. Ramachandran, N.M. Pearsall and G.A. Putrus, "Impact of inverter size on PV system energy production and cost", 38th International Universities Power Engineering Conference, Greece, September 2003, Vol.2, pp 573-576.

4. J. Ramachandran and N.M. Pearsall, "Synthetic generation of solar radiation data for different locations in the UK", The International Journal of Ambient Energy, Vol. 25, No.1, January 2004, pp. 33 – 38.

5. J. Ramachandran, N.M. Pearsall and G.A. Putrus, "Reduction in solar radiation fluctuation by spatial smoothing effect", 19th European Photovoltaic Solar Energy Conference and Exhibition, Paris, 7 – 11 June 2004, Vol. 3, pp. 2900-2903.